Universidad Autónoma de Madrid

Faculty of Science

Department of Biology

EFFECTS OF MICROGRAVITY AND PARTIAL GRAVITY AND THE INFLUENCE OF PHOTOSTIMULATION ON PLANT ADAPTATION TO SPACEFLIGHT

Memory presented by

Alicia Villacampa Calvo

to obtain the PhD degree in Biology at Universidad Autónoma de Madrid

Thesis Director

Dr. Francisco Javier Medina Díaz

Thesis Co-director

Dr. Malgorzata Ciska

Thesis Tutor

Dr. Marta Martín Basanta

Centro de Investigaciones Biológicas Margarita Salas
Madrid 2021

Index

AGRADECIMIENTOS

En primer lugar, me gustaría agradecer al Centro de Investigaciones Biológicas Margarita Salas la disponibilidad de recursos para la realización de la tesis. También a la Universidad Autónoma de Madrid, en especial a mi tutora Marta Martín Basanta por facilitarme siempre los trámites y aclararme dudas.

Quiero agradecer su apoyo a mis directores de tesis, el Dr. Francisco Javier Medina Díaz y la Dr. Malgorzata Ciska. Gracias por vuestra dedicación y ayuda durante todo el desarrollo de este trabajo. Gosia, tu amistad es una de las mejores cosas que saco de estos años.

A mis compañeros de laboratorio Arantxa y Raúl por los buenos momentos en el laboratorio. He aprendido mucho de vosotros y esta tesis no sería lo mismo sin vosotros. También a los estudiantes que han pasado por el laboratorio durante mi tesis, en especial Ana, Ludo, Adela e Iris.

A todos los compañeros del CIB, Emmanuel, Laura, Edu, Yolanda, Elena, Fran e Irene. Irene, gracias por aguantarme mis rollos al final de las tardes, creo que habrías terminado antes tu tesis sin mí.

A mis compañeros del CBM, Patri y Rubén, por todo lo que aprendí con vosotros y todo lo que aguantamos juntos. Creo que oficialmente, dejo de ser pollito.

I want to thank also Dr. Simon Gilroy and Dr. Richard Barker for my short stay in the University of Wisconsin in Madison. Thank you for the welcoming environment and all the help in the RNA-seq analysis. I wish it could have been longer.

I also want to thank the Seedling Growth experiment team, including Dr. John Z. Kiss and Dr. Joshua Vandenbrink, and also Dr. Gwo-shing Sun from NASA Ames research center and Mona Schiefloe from the N-USOC for their help in the ground control experiment.

También quiero agradecer su apoyo a mis padres por su apoyo en general y en especial en mis estudios. Quién iba a decir que haría una tesis sobre plantas. También a mi hermano, con quien he podido compartir la experiencia de hacer una tesis al mismo tiempo y creo que me entiende mejor que nadie.

Por último, dar las gracias a Tomás, por estar ahí en todos los momentos, y entenderme y apoyarme siempre.

ABSTRACT

ABSTRACT

Space exploration will need the use of plants as part of bioregenerative life support systems to provide oxygen and nutrients, and also as a part of the waste recycling system. How the spatial environment affects plant growth and development is still under study. Exposure to microgravity has been reported to affect the functions of plants at different levels, such as cell growth and proliferation, or ribosome biogenesis, or the alterations found in oxidative state, or heat shock proteins expression. A considerable reprogramming of gene expression takes place in response to the environmental change.

The Seedling Growth (SG) space experiment was performed in three different launches, with different *Arabidopsis thaliana* ecotypes and genotypes. They were exposed to different gravity levels for 2 (SG1-2) or 6 days (SG2-3) and different light conditions, including blue and red light lateral illumination to analyze the effects of these wavelengths on plant development in space.

The results proved *A. thaliana* seedlings respond to partial gravity levels differently than to microgravity. The transcriptomic analysis showed microgravity produced a downregulation in photosynthesis function and an increase in plastid and mitochondrial genome expression in comparison to 1 *g* control. Different levels of partial gravity also had a differential effect on *A. thaliana* seedlings transcriptome. We tested 5 different gravity levels in SG1-2, namely microgravity, low *g* (0.09 *g*), Moon gravity (0.18 *g*), Mars gravity (0.36 *g*) and reduced *g* (0.57 *g*) for the last two days of the experiment. Surprisingly, low *g* was the condition which had the highest impact on transcriptomic expression compared to the 1 *g* control. However, higher gravity levels (0.18-0.57 *g*) showed fewer differences with the control, being almost non-existent at reduced gravity level (0.57 *g*).

On the other hand, Mars gravity level produced an adaptive response to the space environment, as shown in SG2-3, where seedlings were exposed to altered gravity levels throughout the experiment. This adaptive response was observed in the transcriptomic data, where abscisic acid (ABA), ethylene and salicylic acid (SA) signaling pathways were activated. In addition, we analyzed possible enrichment of transcripts encoding different transcription factor (TF) families at different gravity levels and found WRKY and ATAF1/2 CUC2 (cup-shaped cotyledon) (NAC) TF were significantly enriched in Mars condition. These TFs are known targets for genetic crops improvement and this strategy could be used to produce crops better adapted to the space environment.

Moreover, we included two mutants, *nuc1-2* and *nuc2-2*, deficient in the two variants of the nucleolar protein nucleolin, into the SG2-3 experiment in order to study how ribosome biogenesis is affected in space. As an additional advantage, NUC2 protein is known to participate in the general stress response of plants. First, we analyzed the response of these mutant lines to the space experiment growth conditions in the ground control. We found a differential response of *nuc1-2* and *nuc2-2* to red light photostimulation compared to WT seedlings, which suggests NUC2 is involved in the response to red light. In addition, the results suggest NUC2 overexpression and red light photostimulation could be beneficial to plants in space. This analysis will help us to understand how the space environment influences ribosome biogenesis in space.

Space research is very scarce due to high cost and complex logistics. This has enforced the use of microgravity simulation as a tool to further explore microgravity effects and validate results from the space experiments. The simplest and most accessible device for microgravity simulation is the 2D-

clinostat. However, the variability in the use of clinostats for microgravity simulation complicates the comparison between different experiments, and some results obtained may not reflect the response to microgravity itself. We studied the most common clinorotation speeds and two orientations of the sample in respect to the rotation axis to analyze different outcomes. We demonstrate the limitations of fast clinorotation, which is effective only at a very small distance from the center of rotation. In addition, we found a stress response in horizontally clinorotated seedlings which was not connected to the response to microgravity. These results make slow vertical clinorotation the most proper setting in our system.

RESUMEN

RESUMEN

La exploración espacial necesitará el uso de plantas como parte de los sistemas de soporte vital biorregenerativos para proporcionar oxígeno y nutrientes, y también como parte del sistema de reciclaje de desechos. Aún se está estudiando cómo el ambiente espacial afecta el crecimiento y desarrollo de las plantas. La exposición a la microgravedad afecta las funciones de las plantas a diferentes niveles, como el crecimiento y la proliferación celular, la biogénesis de ribosomas, alteraciones en el estado oxidativo, o la expresión de proteínas de choque térmico. Se produce una reprogramación considerable de la expresión génica en respuesta al cambio ambiental.

El experimento espacial Seedling Growth (SG) se realizó en tres lanzamientos diferentes, con diferentes ecotipos y genotipos de *Arabidopsis thaliana*. Las plántulas fueron expuestas a diferentes niveles de gravedad durante 2 (SG1-2) o 6 días (SG2-3) y diferentes condiciones de luz, incluida la iluminación lateral de luz azul y roja para analizar los efectos de estas longitudes de onda en el desarrollo de las plantas en el espacio.

Los resultados demostraron que las plántulas de *A. thaliana* responden a los niveles de gravedad parcial de manera diferente que a la microgravedad. El análisis transcriptómico mostró que la microgravedad producía una bajada en la transcripción de genes relacionados con la fotosíntesis y un aumento en la expresión del genoma mitocondrial y de los plástidos en comparación con el control 1 *g*. Los diferentes niveles de gravedad parcial también tuvieron un efecto diferencial en el transcriptoma de las plántulas de *A. thaliana*. Probamos 5 niveles de gravedad diferentes en SG1-2, microgravedad, gravedad baja (0,09 *g*), gravedad lunar (0,18 *g*), gravedad de Marte (0,36 *g*) y gravedad reducida (0,57 *g*) durante los dos últimos días del experimento. Sorprendentemente, la gravedad baja fue la condición que tuvo el mayor impacto en la expresión transcriptómica en comparación con el control de 1 *g*. Sin embargo, los niveles de gravedad más altos (0,18-0,57 *g*) mostraron menos diferencias con el control, siendo casi inexistentes a nivel de gravedad reducido (0,57 *g*).

Por otro lado, el nivel de gravedad de Marte produjo una respuesta adaptativa al entorno espacial, como se muestra en SG2-3, donde las plántulas fueron expuestas a niveles de gravedad alterados durante todo el experimento. Esta respuesta adaptativa se observó en los datos transcriptómicos, donde se activaron las vías de señalización del ácido abscísico (ABA), etileno y ácido salicílico (SA). Además, analizamos el posible enriquecimiento en la transcripción de diferentes familias de factores de transcripción (TF) en diferentes niveles de gravedad y encontramos que WRKY y ATAF1/2 CUC2 (*cup-shaped cotyledon*) (NAC) TF se enriquecieron significativamente en el nivel de gravedad de Marte. Estos TF son objetivos conocidos para la mejora genética de cultivos y esta estrategia podría usarse para producir cultivos mejor adaptados al ambiente espacial.

Además, incluimos dos mutantes, *nuc1-2* y *nuc2-2*, deficientes en las dos variantes de la proteína nucleolar nucleolina, en el experimento SG2-3 para estudiar cómo se ve afectada la biogénesis de los ribosomas en el espacio. Como ventaja adicional, se sabe que la proteína NUC2 participa en la respuesta general al estrés de las plantas. Primero, analizamos la respuesta de estas líneas mutantes a las condiciones de crecimiento del experimento espacial en el control en Tierra. Encontramos una respuesta diferencial de *nuc1-2* y *nuc2-2* a la fotoestimulación con luz roja en comparación con las plántulas WT, lo que sugiere que NUC2 está involucrado en la respuesta a la luz roja. Además, los resultados sugieren que la sobreexpresión de NUC2 y la fotoestimulación de la luz roja podrían ser

beneficiosas para las plantas en el espacio. Este análisis nos ayudará a comprender cómo el entorno espacial influye en la biogénesis de los ribosomas en el espacio.

La investigación espacial es muy escasa debido al alto coste y la compleja logística. Esto ha reforzado el uso de la simulación de microgravedad como herramienta para explorar más a fondo los efectos de la microgravedad y validar los resultados de los experimentos espaciales. El dispositivo más simple y accesible para la simulación de microgravedad es el clinostato 2D. Sin embargo, la variabilidad en el uso de clinostatos para la simulación de microgravedad complica la comparación entre diferentes experimentos, y algunos resultados obtenidos pueden no reflejar la respuesta a la microgravedad en sí. Estudiamos dos de las velocidades de clinorrotación más comunes y dos orientaciones de la muestra con respecto al eje de rotación para analizar diferentes resultados. Demostramos las limitaciones de la clinorrotación rápida, que es efectiva solo a una distancia muy pequeña del centro de rotación. Además, encontramos una respuesta al estrés en las plántulas con clinorrotación horizontal que no estaba relacionada con la respuesta a la microgravedad. Estos resultados muestran que la clinorrotación vertical lenta es la más adecuada para la simulación de la microgravedad en nuestro sistema.

INTRODUCTION

INTRODUCTION

Space exploration has always fascinated humankind but the visions of travel to the outer space rarely involved plants. However, plants will be required as the source of nutrients and oxygen, as well as waste recycling systems for long space exploration missions (Fu et al., 2016; Zabel et al., 2016). Thus, it is important to study how to cultivate plants in space efficiently. The most difficult parameter to overcome in the space environment is altered gravity level, since all other parameters such as breathable air, nutrient levels, humidity, temperature or light conditions can be adjusted. Only cosmic radiation represents a challenge comparable to gravity due to the lack of 100% effective protective shields. On the other hand, plants and every organism on Earth have evolved under a constant gravity level and its modification or absence may be a difficult challenge to overcome for an organism.

There are different ways to study the effect of microgravity on an organism (Böhmer and Schleiff, 2019). Real microgravity research onboard the International Space Station (ISS) provides the most valuable information (Vandenbrink and Kiss, 2016), but involves high cost and the access to it is very limited. Drop-towers are other facilities for real microgravity research but the period of time for which the microgravity condition is generated is limited to just a few seconds (Schmidt, 2010). Parabolic flights also provide real microgravity for experimentation, but it is preceded by a period of hypergravity (Pletser, 2016) which may alter the way an organism respond to microgravity. Simulation is an alternative for real microgravity experiments and can be achieved in Ground Based Facilities (GBFs) that include clinostats and Random Positioning Machines (RPM). These do not eliminate the gravity vector, but average the gravity force by rotating the samples and impeding the gravity perception (van Loon, 2007; Herranz et al., 2013).

1. Gravitropism

Plants are sessile organisms that respond to external stimuli by tropic responses, positive tropism if the growth is towards a stimulus or negative tropism if its direction is away from a stimulus. Tropisms enable plants to grow their shoots towards the light and direct the roots towards water (reviewed in Muthert et al., 2020). Gravity is one of the most important factors that orient plant growth through a positive root gravitropism and a negative shoot gravitropism. **Gravitropism** is fulfilled in three steps: gravity perception, signal transduction and differential growth (Sato et al., 2015; Swarup and Bennett, 2018). There are two models for gravity perception, the first and most accepted takes place in statocytes, specialized cells which contain starch-rich plastids called statoliths (Sack et al., 1986). In the shoot, statoliths are found in endodermal cells (Toyota et al., 2013) and in the root in the root tip, in the columella. The statoliths sediment according to the gravity vector and trigger a signaling cascade leading to the gravitropic response (Morita, 2010; Sato et al., 2015; Swarup and Bennett, 2018). In the root columella, there are three to four layers of statocytes, also called stories (S1-S4). The root cap stem cells (CSC) are located directly under the quiescent center (QC) and above the first statocytes layer (S1). CSC are responsible for constant regeneration of the root columella (Hong et al., 2015). The layers of statocytes assume first gravity perception (S1-S2) and then secretory functions (S3-S4) to protect the root tip (Kiss et al., 1989). The statoliths of layers S3 and S4 do not always sediment. In addition, the central cells of columella are the most responsive ones (Sack, 1991; Baum and Rost,

1996) and therefore are thought to be the most implicated in gravitropism, as confirmed by removing individual cells of columella with laser (Blancaflor et al., 1998). The statocytes that are the most important for gravity perception are highlighted in red in the Fig. 1a-b.
Another model for gravity perception is the protoplast pressure model which is based on studies on internodal cells of algae, *Nitellopsis* and *Chara*, which do not contain statoliths but respond to gravitropic stimuli (Wayne et al., 1990; Staves et al., 1992). The model is based on the fact that the gravity vector, acting on the cytoplasm mass, causes tension and pressure, which is detected by unknown receptors at the plasma membrane. This model is also supported by the fact that starchless *A. thaliana* mutants respond to gravitational stimuli, although the response is diminished (Kiss et al., 1989).

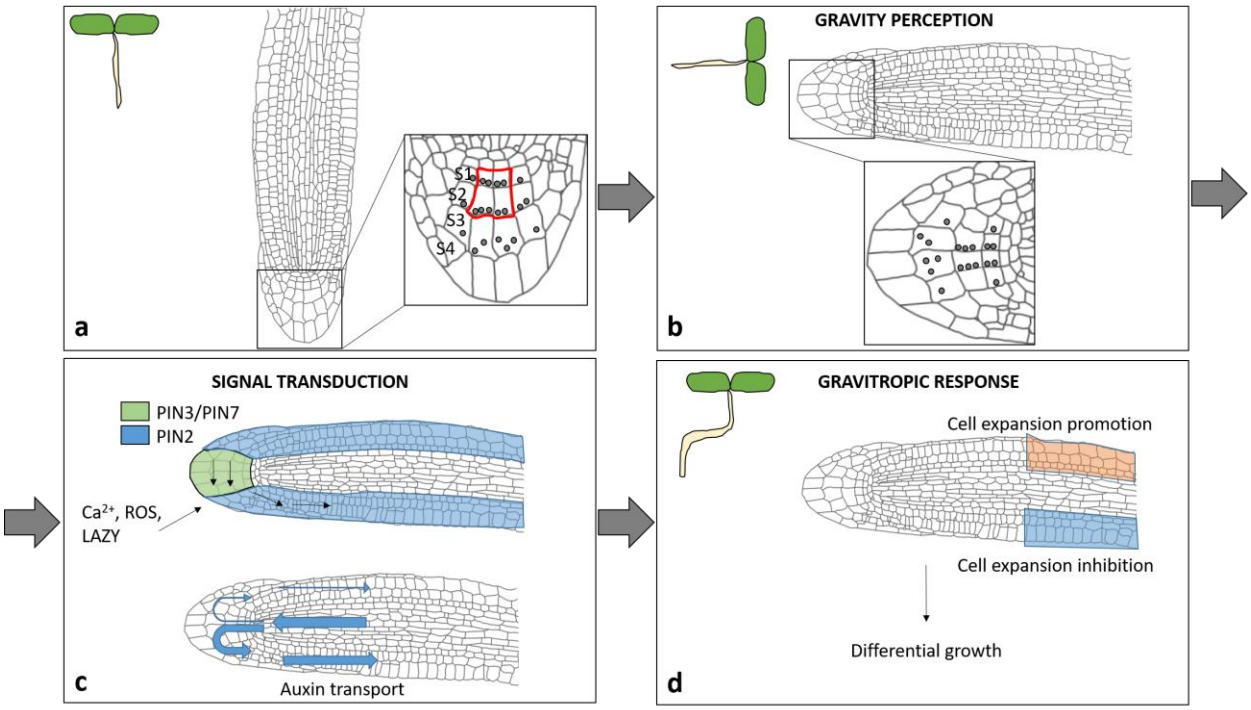

Figure 1. Gravitropic signaling. a) Root meristem. Highlighted in red the most responsive statocytes to gravitropic stimuli of the columella. b) Gravity perception according to the statolith model after the gravitropic stimulus. c) Gravitropic signal transduction with PIN2, PIN3 and PIN7 localization in the root meristem. d) Gravitropic response.

The steps that follow gravity perception are still under study, and some steps in this signaling cascade are still unknown. Nevertheless, concerning the statolith sedimentation model, it has been established that the sedimentation of the statoliths, with the participation of actin microfilaments, leads to calcium ion waves. It is assumed that **Ca^{2+} channels** in the cortical **Endoplasmic Reticulum** (**ER**) open when statoliths sediment onto the ER (Leitz et al., 2009). These Ca^{2+} waves inside the cell most probably cause asymmetrical distribution of **PIN-FORMED (PIN**) transporters (Zhang et al., 2011). Recent studies show that **LAZY** proteins are also involved in the early steps of gravity signal transduction (Yoshihara and Spalding, 2017; Nakamura et al., 2019; Furutani et al., 2020). LAZY proteins were proven to promote polar auxin transport, probably through regulation of PIN3 polar distribution in the root columella (Taniguchi et al., 2017). PIN3 is the first PIN protein involved in the

gravity signal transduction. RCC1-like domain (RLD) proteins were recently discovered as LAZY interactors, that could be the link between LAZY and PIN proteins in gravity signal transduction (Furutani et al., 2020). After PIN3 relocalization in the root columella (Friml et al., 2002; Ottenschläger et al., 2003; Kleine-Vehn et al., 2010), PIN7, which also localizes in the columella, changes its polarity (Kleine-Vehn et al., 2010). Both, PIN3 and PIN7, localize in the cell membrane at the lower part of the cells according to the gravity vector direction upon reorientation. Then, PIN2 transports auxin through the epidermis to the elongation zone (Fig. 1c). PIN2 polar distribution causes **auxin** accumulation at the lower side of the root, according to the gravity vector, where it inhibits cell expansion (Swarup et al., 2005). On the other hand, cell elongation is promoted at the upper side of the root with lower auxin levels. This differential growth between the upper and the lower side of the root causes bending towards the direction of gravity upon reorientation (Luschnig et al., 1998; Swarup et al., 2005; Abas et al., 2006) (Fig. 1c-d).

Reactive Oxygen Species (ROS) also play an essential role in gravitropic signaling and other tropisms (Joo et al., 2001; Krieger et al., 2016). An asymmetric distribution of hydrogen peroxide has been found in gravitropic response (Krieger et al., 2016). This asymmetric distribution of ROS after gravistimulation depends on auxin and calcium signaling (Monshausen et al., 2011). In addition, ROS are involved in lateral root formation and root growth (Tsukagoshi et al., 2010; Manzano et al., 2014; Passaia et al., 2014).

2. Phototropism

Phototropism is the orientation of the plant growth according to the position of a light source. Under normal conditions of plant growth in the Earth, the major source of light is the Sun and the phototropic axis coincides with the gravitropic axis, with opposite directions. In these conditions, phototropism and gravitropism are cooperative and interacting processes. As in gravitropism, phototropism can be divided into three steps: light perception, signal transduction and asymmetric growth. Light perception is fulfilled by various photoreceptors: cryptochromes, phototropins and phytochromes (reviewed in Fankhauser and Staiger, (2002); Mo et al., (2015)). Cryptochromes and phototropins are responsible for blue light perception (Cashmore et al., 1999; Briggs and Christie, 2002), whereas phytochromes perceive red and far red light (Quail, 2002). Moreover, UVR8 protein is responsible for UVB light perception (Brown and Jenkins, 2008; Rizzini et al., 2011). In addition to sensitivity to different spectrums of light, these photoreceptors have also differential spatial expression. In the root, although this organ is usually buried under ground, photoreceptors are differentially expressed (Mo et al., 2015). Phytochromes are mainly expressed in the root cap (Somers and Quail, 1995a, 1995b), whereas phototropin1 (phot1) is expressed in the upper part of the root, close to the surface (Galen et al., 2006). Cryptochromes are only expressed in the shoot, however, they affect root elongation by inhibiting rootward auxin transport (Canamero et al., 2006; Mao et al., 2014).

The routes involved in signal transduction in gravi- and phototropisms are interconnected. The third phase of phototropism, the asymmetric growth is mediated by differential auxin distribution, as in gravitropism. In this case, auxin accumulates in the illuminated side of the roots (Zhang et al., 2013). However, asymmetrical auxin distribution requirement for phototropic response has been questioned (Kimura et al., 2018).

Phototropism orients plant growth and can provide a direction cue in the absence of gravity in space. Plants display positive shoot phototropism and negative root phototropism. Nevertheless, these tropisms have to be revised in the space environment. During the TROPI and **Seedling Growth** (**SG**) series of space experiments, new red and blue light root positive phototropisms have been discovered (Millar et al., 2010; Kiss et al., 2012; Vandenbrink et al., 2016). Different light wavelengths influence plant growth differently (Silva-Navas et al., 2015) and specific light spectra can be applied to overcome deleterious effects of space environment (Sullivan and Deng, 2003; Lin et al., 2013). Red light was reported to stimulate ribosome biogenesis and cell proliferation (Reichler et al., 2001), which are known to be affected during spaceflight (Matía et al., 2010). In fact, red light photostimulation has been used to overcome the spaceflight effects in the SG experiment and in simulated microgravity experiments (Valbuena et al., 2018). On the other hand, blue light has been reported to be involved in the lateral root growth (Moni et al., 2015). Also, blue light exposure reduced root growth compared to the roots exposed to red light or kept darkness (Silva-Navas et al., 2015). Etiolation (the growth of the plant in the absence of light) has also a significant impact on plant growth and development. Cell cycle arrest in the apical meristem has been reported in plants grown in the dark (Lopez-Juez et al., 2008; Mohammed et al., 2018). However, light can be also a stress factor for the root development, as it reduces cell proliferation in the root meristem (Silva-Navas et al., 2015, 2016). This is the reason why some researchers have developed methods for growing seedlings *in vitro*, keeping the root in the dark while shoots are illuminated, in order to recreate a more natural plant environment (Yokawa et al., 2014; Silva-Navas et al., 2015).

3. Other tropisms that may be implicated in the response to altered gravity levels

Other tropisms, such as **thigmotropism**, also need to be taken into account while investigating graviresponse and response to altered gravity levels. The plant organ that is especially sensitive to touch is the root cap (Massa and Gilroy, 2003; Braam, 2005), which applies thigmotropic response as an obstacle avoidance tool during growth in the soil (Massa and Gilroy, 2003). The signaling in thigmotropism highly overlaps with gravitropism. Both tropisms involve Ca^{2+} signaling (Legué et al., 1997) and auxin redistribution (Lee et al., 2020). The interaction between thigmo- and gravitropisms (Migliaccio and Piconese, 2001) is thought to be associated with **waving** and **skewing** phenotypes in the root (reviewed in Oliva and Dunand, 2007). Waving consists in an oscillatory pattern of the root (Fig. 2a-b) and have been found in many *A. thaliana* ecotypes grown on 45° titled Petri dishes (plants above the media surface) and usually waved roots also presented skewing. Skewing is a root deviation from the direction of the gravity vector in one direction (Fig. 2c-d). When Petri dishes are titled 135° (plants below the media surface) skewing with reduced waving is presented (Schultz et al., 2017). Skewing has also been observed in plants grown during spaceflight (Califar et al., 2020) which suggests skewing can occur independently of gravitropism.

There are other tropisms that influence how plants grow in the space environment, such as **hydrotropism** (Kiss, 2007). Interaction between gravitropism and hydrotropism suggest that when hydrotropism is activated, gravitropism is repressed and *vice versa* (Morohashi et al., 2017). In addition, ROS, which promote gravitropism, negatively regulate hydrotropism (Krieger et al., 2016). This could suggest that, in microgravity, roots are more sensitive to water gradient than on Earth, as

observed in cucumber seedlings (Takahashi et al., 1999). In addition, the different behavior of water in the absence of gravity, and the manner it is delivered to the plants in different experimental hardwares could influence root growth. In fact, this different behavior of fluids, water in this case, in spaceflight could be the cause of hypoxia reported in numerous space experiments (Choi et al., 2019).

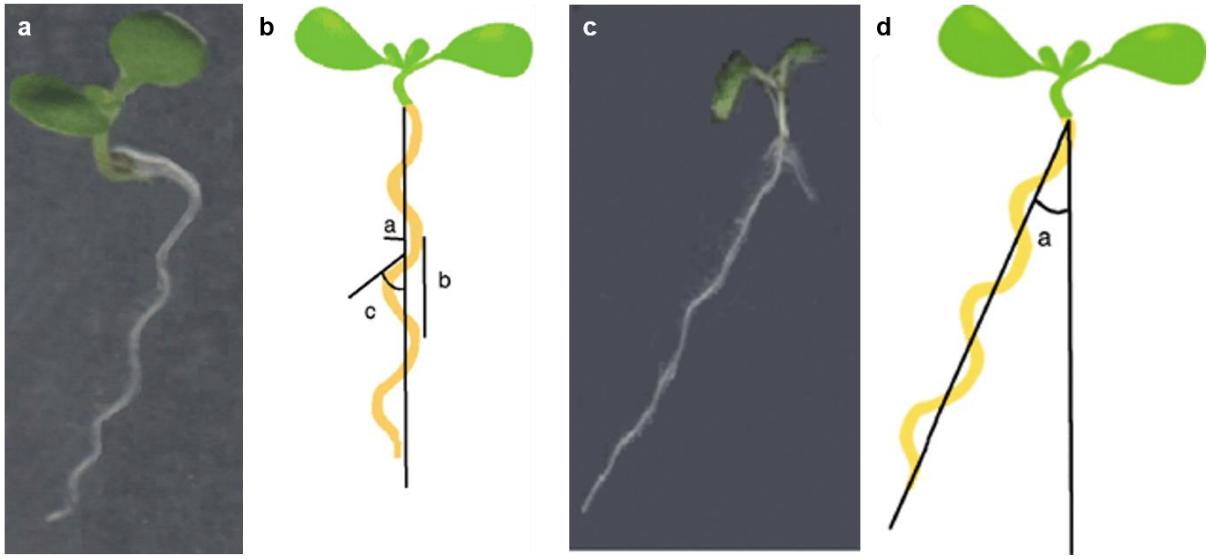

Figure 2. Waving and skewing phenotypes. Modified from Oliva and Dunand, (2007). a) Example of waving. b) Waving scheme with parameters: a, amplitude; b, wave frequency and c, wave tangent line (WTL). c) Example of skewing. d) Skewing scheme with parameter a: angle of deviation from the gravity vector.

4. Effects of microgravity on plants

a. Disrupted meristematic competence

Previous experiments in space have shown deleterious effects of spaceflight on plant development. In the ROOT experiment (Matía et al., 2005, 2010) 4-day-old etiolated *A. thaliana* seedlings, showed disrupted **meristematic competence**, with increased cell proliferation and decreased cell growth in the root meristem. Meristematic tissue is responsible for plant growth and development as the source of new cells. In these cells, cell growth and proliferation need to be closely coordinated for proper plant development. Meristematic cells divide when they gain a certain size and, in this way, proliferation and growth cycles assure correct meristematic activity and organ growth. When this coordination is interrupted, meristematic competence is disrupted (Mizukami, 2001). This effect of microgravity on meristematic competence was confirmed also in a simulated microgravity experiment on an RPM (Matía et al., 2010) and in diamagnetic levitation experiments (Manzano et al., 2013).

b. Cell cycle

Alterations on **cell cycle** progression are responsible for the increased cell proliferation observed in microgravity, which leads to the disruption of meristematic competence. This was confirmed by the use of MM2d *A. thaliana* cell culture (Menges and Murray, 2002) in simulated microgravity analyzed

by flow cytometry. The results indicated accelerated cell cycle progression in simulated microgravity compared to the 1 *g* control (Kamal et al., 2019a), which could be due to a reduction in G2 phase and a slight increment in G1 phase (Kamal et al., 2019b). The reason behind these alterations of cell cycle phases could be disruption in **G2/M checkpoint**. This checkpoint of the cell cycle allows division of cells which have obtained a certain size (reviewed in D'Ario and Sablowski, 2019), and an alteration of this control of cell cycle progression could lead to smaller cells entering in division, and, thus, a disrupted meristematic competence. Alteration of G2/M checkpoint in simulated microgravity is supported by a reduction in B1 cyclin expression compared to the 1 *g* control. CYCB1 plays a fundamental role in this control of cell cycle progression in the G2/M transition (Menges and Murray, 2002).

c. Nucleolus and ribosome biogenesis

Ribosome biogenesis was also reported to be affected in the ROOT experiment (Matía et al., 2005, 2010). Cell growth in meristematic cells is directly connected to protein production and, thus, ribosome production and nucleolar size (Guerrero et al., 1989). The relation between cell growth and nucleolar size is only applicable in meristematic cells, because they do not expand. On the contrary, in differentiating cells, cell expansion increases the size through accumulation of water in the vacuole (Baserga and Baserga, 2007; Sablowski and Dornelas, 2014). Therefore, the increase in size of differentiating cells is not related to protein synthesis and hence to ribosome biogenesis and the nucleolar activity.

Other studies in space environment have also described alterations in ribosome biogenesis (Ferl et al., 2014; Vandenbrink et al., 2019a; Angelos et al., 2021). **Nucleolin** is one the major nucleolar protein of proliferating tissues. It is involved in different steps of ribosome biogenesis, such as RNA Pol I transcription, processing of pre-rRNA, as well as assembly and nucleocytoplasmic transport of ribosomal proteins (Ginisty et al., 1999; Roger et al., 2003). In *A. thaliana* there are two nucleolin homologs, *At*NUC1 and *At*NUC2. *At*NUC1 is constitutively expressed but, when *At*NUC1 is repressed, NUC2 overexpression is induced (Pontvianne et al., 2007, 2010), probably due to the NUC1 repression of NUC2 expression (Durut et al., 2014). When NUC1 is depleted, plants display severe developmental constraints (Pontvianne et al., 2010), and even though *At*NUC2 is expressed in the *nuc1* mutant during environmental stress, it does not complement all the functions of NUC1. NUC2 depletion does not have clear phenotypic effect compared to wild type plants, only delayed flowering time (Durut et al., 2014).

Altered ribosome biogenesis in the space environment coincides with changes in the nucleolar ultrastructure (Matía et al., 2005, 2010). Nucleolar structure changes upon cellular conditions. It can be indicative of cellular type, activity or cell cycle phase. There are few components of the interphase nucleolus that can be distinguished in the electron micrographs: Fibrillar Centers (FCs), which can be homogeneous or heterogeneous; Dense Fibrillar Component (DFC) and Granular Component (GC) (Jordan, 1984; Risueño and Medina, 1986). Each component is made of different functional elements. Ribosomal genes are located in FCs and part of DFC. In addition, the transcription complex is assembled in FCs. Within DFC, different steps of pre-rRNA processing are carried out. The assembly of ribosomal proteins with mature rRNAs occurs in the GC, where they are exported to the cytoplasm for final ribosome assembly (González-Camacho and Medina, 2006). Thus, structural components of the

nucleolus change during the cell cycle. In the G1 phase of the cell cycle, nucleoli are moderately active, small, with DFC as the most abundant component. However, in G2, nucleoli are highly active, greatly enlarged, and contain multiple FCs and abundant GC (González-Camacho and Medina, 2006; Sáez-Vásquez and Medina, 2008). Alterations in the nucleolar ultrastructure by space environment were reported in the 'ROOT' space experiment (Matía et al., 2005, 2010). Nucleoli were smaller and less active, with reduced GC in microgravity in comparison to the 1 *g* controls.

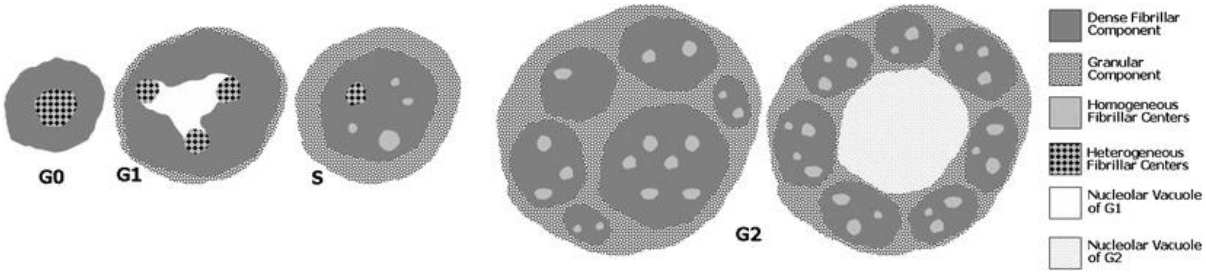

Figure 3. Nucleolar structure. From Gonzalez-Camacho and Medina 2006. Nucleolar models of the different steps in the cell cycle.

d. Transcriptomic changes due to microgravity and spaceflight

In recent years, many reports on transcriptomic analysis of *A. thaliana* seedlings in space environment have been published (Zupanska et al., 2013; Kwon et al., 2015; Basu et al., 2017; Johnson et al., 2017; Paul et al., 2017; Herranz et al., 2019; Vandenbrink et al., 2019; Choi et al., 2019; Kruse et al., 2020; Angelos et al., 2021; Villacampa et al., 2021a). In addition, some proteomic analysis were also included (Ferl et al., 2015; Basu et al., 2017; Kruse et al., 2020). These experiments were performed in various facilities, using different *A. thaliana* lines and light conditions which complicates direct comparisons between them. However, there are some common responses between different studies. One of the common responses to the space environment is **hypoxia** or altered oxidative state (Kwon et al., 2015; Basu et al., 2017; Johnson et al., 2017; Choi et al., 2019; Kruse et al., 2020; Angelos et al., 2021). In addition, **cell wall** metabolism is usually affected (Ferl et al., 2015; Johnson et al., 2017; Paul et al., 2017; Kruse et al., 2020). Other common alteration between transcriptomic studies is upregulation of Heat Shock Proteins (**HSPs**) or chaperons (Zupanska et al., 2013; Basu et al., 2017; Johnson et al., 2017; Choi et al., 2019; Angelos et al., 2021). **Cytoskeleton** alterations are also often found in spaceflight (Zupanska et al., 2013; Ferl et al., 2015; Kwon et al., 2015; Kruse et al., 2020). It has been suggested that cytoskeleton reorganization in spaceflight is connected to HSPs and oxidative stress alterations (Ban et al., 2013; Kruse et al., 2020).

Additional effects common to different studies include **plastid** genome overexpression (Kwon et al., 2015; Kruse et al., 2020; Angelos et al., 2021; Villacampa et al., 2021a), together with **photosynthesis** downregulation in microgravity (Vandenbrink et al., 2019a; Villacampa et al., 2021a).

5. Constraints of space research

Space research is very limited due to the low availability and high cost with the complicated logistics involved. This restricts the reproducibility of the results. In addition, it is often hard to compare results between different experiments due to different experimental conditions, and especially to the differences between the hardware used in the experiments. This is the reason why sometimes it is difficult to differentiate spaceflight effects from artefacts caused by hardware, as experiments performed in the same facilities often present more similarities (Barker et al., 2020). In the recent years, efforts have been made to compare all available results from different space experiments to identify the similarities between them, which could be considered real spaceflight effects. This initiative includes the **Genelab** database from NASA (Ray et al., 2019), **Space Omics** team from ESA (Madrigal et al., 2020), or the Test of Arabidopsis Space Transcriptome (**TOAST)** (Barker et al., 2020). The latter is an interactive tool that includes RNA-seq studies from Genelab and allows direct comparisons between the studies.

In addition, the assembly and exploitation of ISS has resulted in improved facilities for plant space research providing better physiological growth conditions. In this context, the European Modular Cultivation System (**EMCS**) (Brinckmann, 2005) represented a substantial advance compared to other commonly used hardware, with features such as the hydration of the seeds controlled from the Norwegian User Support and Operations Center (N-USOC), or atmospheric control (O_2, CO_2, humidity, ethylene removal and temperature). In addition, it provided an integrated centrifuge which allowed performing **partial gravity** research and 1 *g* control in space. Partial gravity research is very limited and SG experiment was the first to study partial gravity effects on higher plants in space (Kiss, 2014; Valbuena et al., 2018; Herranz et al., 2019; Villacampa et al., 2021a). Other results on partial gravity effect were performed using microgravity simulators with adapted settings, including diamagnetic levitation applied to plant cell cultures (Manzano et al., 2012), or RPM simulation on cell cultures (Kamal et al., 2018) and seedlings (Manzano et al., 2018). Taking all together, the EMCS provided an excellent incubator for biological research. However, it was decommissioned in 2018.

Nowadays, the more advanced hardware available on ISS include: VEGGIE (Massa et al., 2016, 2017) and the Advanced Plant Habitat (APH) (Monje et al., 2020). VEGGIE includes light-emitting diode (LED) lighting that can be programmed, a fan that recirculates the air and, in contrast to previous hardware, where plants were grown on Petri dishes or nitrocellulose membranes, the plants are grown on substrate. This hardware has been successfully used to grow adult plants in space (Khodadad et al., 2020). However, the most advanced hardware is the APH (Monje et al., 2020). This hardware includes atmospheric control, light intensity and spectral quality adjustments, in addition to O_2, CO_2, humidity, and temperature control. However, unfortunately, none of these advanced facilities is equipped with a centrifuge allowing partial gravity experiments.

6. The Seedling Growth and previous experiments

The SG series of space experiments was an ambitious project which included different ecotypes of *A. thaliana* seedlings, genotypes, light conditions and gravity levels. The background of the experiment was TROPI and ROOT space experiments.

The **ROOT** experiment (Matía et al., 2005) was directed by Dr. F. Javier Medina and it was carried out on the ISS as a part of the 'Cervantes' mission in 2003. As mentioned earlier, in this experiment 4 day-old etiolated *A. thaliana* seedlings were fixed for microscopic observation. The hardware used in this experiment allowed hydration and chemical fixation of the samples. However, it did not allow an active control of temperature or humidity throughout the experiment, relying on the general environmental control of these parameters in ISS. The results indicated a disrupted meristematic competence with increased proliferation and decreased cell growth compared to the 1 *g* control. This experiment was complemented with an analog experiment in simulated microgravity where similar results were obtained (Matía et al., 2005, 2010).

On the other hand, the **TROPI** experiment, directed by Dr. John Kiss was carried out on the ISS between 2006 (TROPI 1) and 2010 (TROPI 2) with the objective to study phototropism in the absence of gravity. This experiment applied the EMCS hardware (Brinckmann, 2005) (Fig. 4d) together with the TROPI hardware developed by NASA (Kiss et al., 2007) (Fig. 4a-c). It consisted of seed cassettes with white LED illumination, and red and blue LEDs for side photostimulation (Fig. 4b). This hardware included an anti-condensation system to facilitate imaging of the cassettes throughout the experiment and an ethylene removal system. The results of this experiment reported a novel positive phototropic response to red light of both hypocotyls and roots which was reduced with increasing levels of gravity (Millar et al., 2010; Kiss et al., 2012).

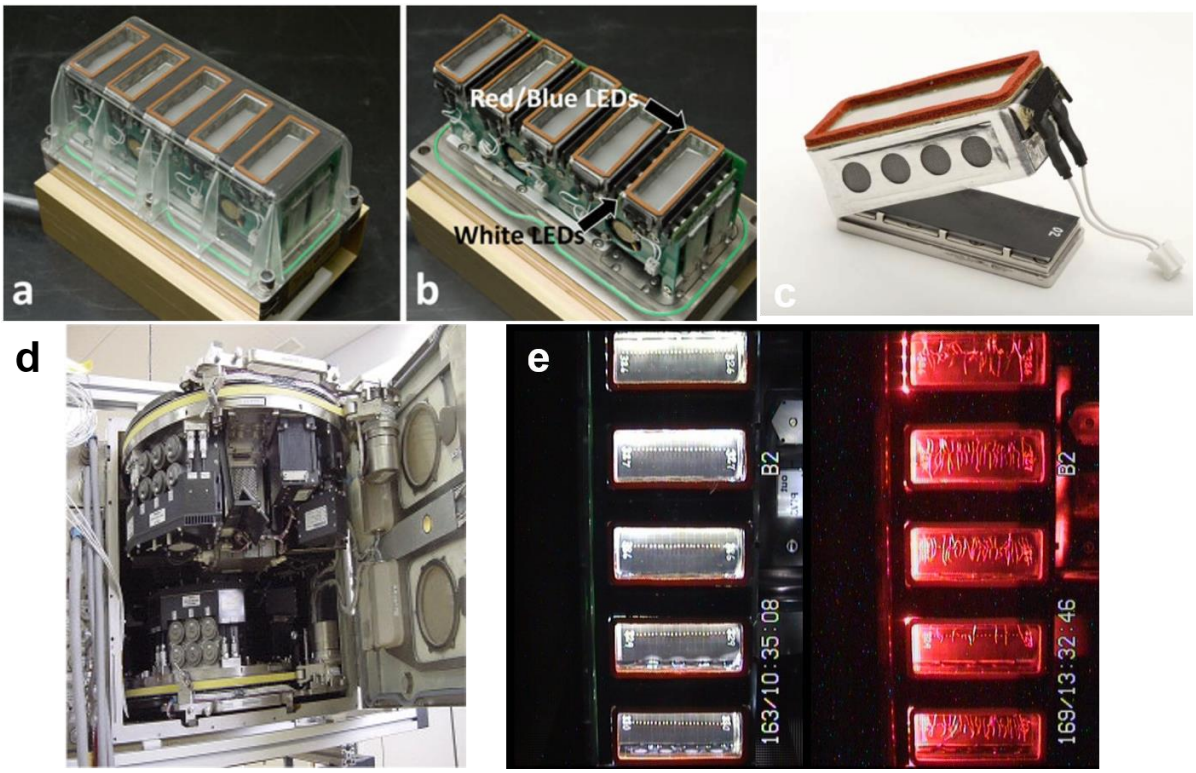

Figure 4. TROPI and EMCS hardware. a) Experimental Container (EC) with the 5 TROPI cassettes. b) EC with TROPI cassettes indication of light sources. c) TROPI cassette detail. d) European Module Cultivation System (EMCS). e) Cassettes images from the Seedling Growth (SG) experiment. Left, hydratation (beginning of the experiment). Right, seedlings at the end of the experiment, after 6 days of red light photostimulation. Adapted from Brinckmann, 2005 and Vandenbrink and Kiss, 2019.

SG series of space experiments were designed by Dr. F. Javier Medina and Dr. John Z. Kiss to investigate root phototropism and response to microgravity and partial gravity levels in *A. thaliana* seedlings, and the influence of light in modulating these plant responses. Hardware developed for the TROPI experiment (Kiss et al., 2007) was also used in the SG experiment in the EMCS cultivation system (Brinckmann, 2005) (Fig. 4). In SG1 and 2, phototropic responses to blue and red light photostimulation were studied in WT (Landsberg *erecta* ecotype; L*er*) as well as *phyA* and *phyB* mutants (Vandenbrink et al., 2016, 2019; Valbuena et al., 2018; Herranz et al., 2019). With this purpose, seedlings were grown under 1 *g* gravity level and constant white light for the first 4 days, followed by two days of microgravity and photostimulation. (Fig. 5a).

In the second part of SG2 and in SG3, the influence of spaceflight on ribosome biogenesis was studied in wild type seedlings (Columbia 0 ecotype; Col0) and *nuc1-2* and *nuc2-2* mutants (Manzano et al., 2020b), with red light photostimulation in part of the samples (Villacampa et al., 2021a). In this case, gravity was constant throughout the experiment (6 days) and the last two days seedlings were photostimulated with red light or kept in the dark (Fig. 5b).

In addition, a centrifuge integrated in the EMCS module (Brinckmann, 2005) onboard the ISS, enabled the study not only of the plant response to microgravity, but also to partial gravity levels.

Samples were frozen at the end of the experiments for molecular biology analysis. In SG3 also the FixBox hardware was applied, which was designed to allow the chemical fixation of the samples for confocal and electron microscopy observations (Manzano et al., 2020a).

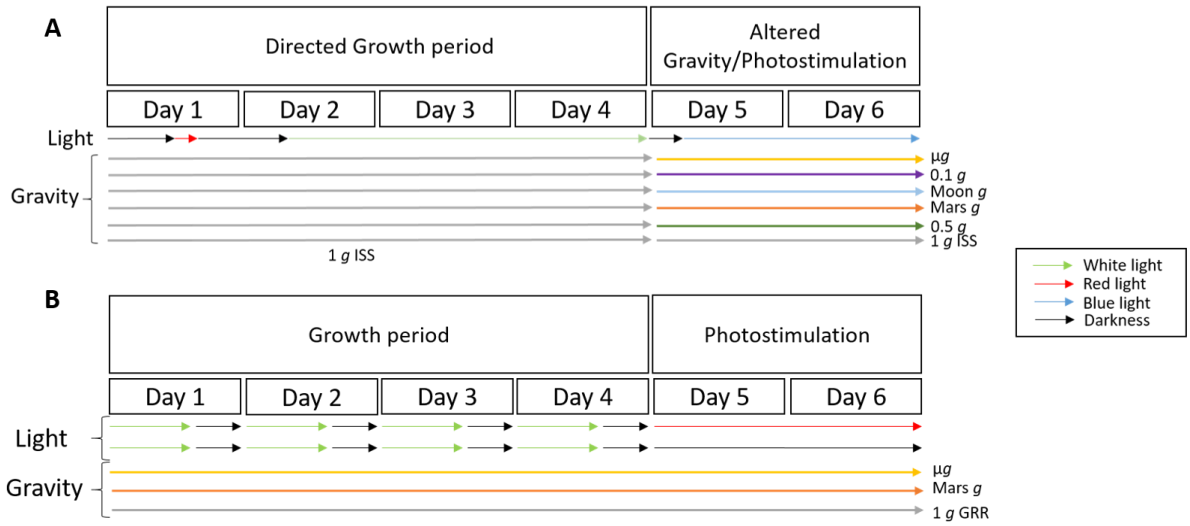

Figure 5. Seedling Growth experiments settings. Modified from Villacampa et al., 2021a. a) SG1-2 settings, with 4 days of 1*g* gravity and two days of altered gravity and photostimulation. b) SG2-3 settings, with constant gravity during the whole experiment and two days of photostimulation.

7. Simulated microgravity

Space research provides the best conditions to study the effect of real microgravity and partial gravity. Nevertheless, due to high cost and low availability of space experiments these opportunities are highly

limited. In effect, the use of microgravity or altered gravity simulators to study these conditions on Earth is necessary. The most common and simple device to simulate microgravity on Earth is the **2-D clinostat** (Fig. 6a, b). It was first used in the XIX century (Knight, 1806). This device rotates plants around one axis to avoid the sedimentation of the statoliths in the statocytes in effect, preventing gravity perception. Even though it has been applied in science for a long period of time, there is no consensus regarding proper speed and orientation settings. The correct application of the clinostat depends on the biological material, size of the experimental container and the time of microgravity simulation. Nevertheless, in the past in similar studies with young seedlings, slow (0.5 - 2 rpm) (Boucheron-Dubuisson et al., 2016; Deng et al., 2017) or fast (60 rpm) (Schüler et al., 2016; Wang et al., 2016; Polinski et al., 2017) clinorotation was used without a justification. Improper speed setting can impair the microgravity simulation. If the velocity is too low, the statoliths will be dragged on the border of the statocytes causing constant mechanostimulation, and if it is too high the centrifugal drift can be perceived by the statocytes in place of the gravity vector. The correct speed setting should minimize statoliths movements and their magnititude should not be detected by the statocytes.

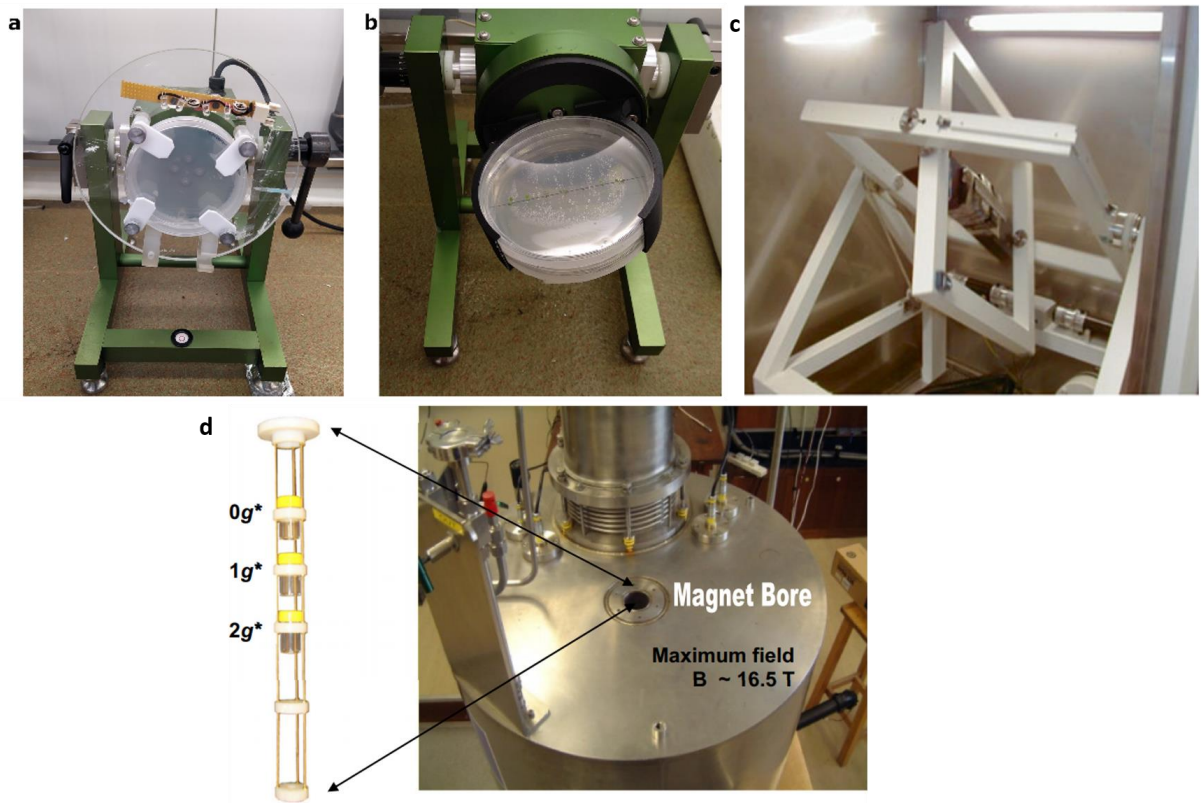

Figure 6. Microgravity simulators. Adapted from Villacampa et al., 2021b and Herranz et al., 2015. a) 2D-clinostat with vertical orientation. b) 2D-clinostat with horizontal orientation. Clinostat was part of the Zero Gravity Instrument Project (ZGIP) by the United Nations Office for Outer Space Affairs (UNOOSA) d) Random Positioning Machine (RPM). d) Diamagnetic levitation with the levels of gravity applied to the samples according to their position.

In addition, there are two possible modes of clinorotation depending on the sample orientation in respect to the rotation axis: vertical (Fig. 6a), with the seedling's long axis perpendicular to the clinorotation axis; or horizontal (Fig. 6b), with the seedling's long axis parallel to the rotation axis. The

two types of clinorotation were compared by Lorenzi and Perbal, (1990), Kuznetsov and Hasenstein, (1996) and John and Hasenstein, (2011), finding different outcomes for each of them. This variability in the clinorotation settings in various studies may introduce artefacts in the studies which do not reflect the plant's response to microgravity.

There are other devices which allow microgravity simulation on Earth (reviewed in Herranz et al., 2013). **3D-clinostats** and **RPMs** (Hoson et al., 1992, 1997; Kraft et al., 2000) rotate in two-axes, which reduces the variability of the orientation setting on the clinostat (Fig. 6c). The comparison between 2D-clinostat and RPM by Boucheron-Dubuisson et al., (2016) showed comparable results in *A. thaliana* seedlings. Moreover, the ROOT experiment results were reproduced on an RPM microgravity simulator (Matía et al., 2010). In addition, RPMs have been used to simulate partial *g*- levels (Manzano et al., 2018). **Diamagnetic levitation** is another simulated microgravity procedure (Manzano et al., 2013) (Fig. 6d). In this case, proper controls in order to distinguish between simulated microgravity response or response to the magnetic field are needed (Herranz et al., 2013; Manzano et al., 2013).

OBJECTIVES

OBJECTIVES

The main objective of this work is to investigate *A. thaliana* seedling´s response to microgravity (real and simulated) and partial gravity as stand-alone factors and combined with photostimulation with red or blue light.

To obtain this goal the following specific objectives were proposed:

- To identify the early response of *A. thaliana* seedlings to microgravity and partial gravity levels independent on the light condition. This objective is studied in Villacampa et al., 2021a. Specifically, anatomic changes upon exposure to microgravity and Mars gravity level are analyzed. Also, transcriptomic changes independent from light condition are analyzed for each gravity level.

- To analyze the response to microgravity and partial *g* in different light conditions. This objective is studied in Villacampa et al 2021a, Vandenbrink et al., 2019 and Herranz et al., 2019. In Villacampa et al., 2021a, we analyzed the effects of red light photostimulation on microgravity and Mars gravity level grown seedlings. In addition, the effects of real microgravity in blue light photostimulated seedlings is studied in Vandenbrink et al., 2019. This study is extended in Herranz et al., 2019 with the analysis of 5 levels of altered gravity levels in space.

- To analyze the response of the nucleolin mutants to red light and its possible implication in spaceflight response. This objective is fulfilled in Manzano et al., 2020, where we studied the response of *nuc1-2* and *nuc2-2* to red light photostimulation compared to the WT seedlings.

- To establish the proper use of the 2D-clinostat for microgravity simulation. In Villacampa et al., 2021b, we compared different clinostat settings which are commonly used, in order to analyze different outcomes and establish a common use of the clinostat for more reproducible and comparable results among different studies.

MATERIALS AND METHODS

MATERIALS AND METHODS

1. Plant Material

In the SG experiment (Herranz et al., 2019; Vandenbrink et al., 2019; Manzano et al., 2020b; Villacampa et al., 2021a), WT seeds, L*er* in SG1-2 and Col0 in SG2-3, were used. In addition, *nuc1-2* (Nottingham Arabidopsis Stock Centre (NASC) ID: SALK_002764 (Pontvianne et al., 2010)) and *nuc2-2* (NASC ID: GABI_178D01 (Durut et al., 2014)) seedlings were included in SG2-3 (Manzano et al., 2020b).

In the simulated microgravity study (Villacampa et al., 2021b), WT (Col0), DR5-β-glucuronidase (DR5-GUS) (Ulmasov et al., 1997, seeds kindly supplied by Dr. E. Carnero-Diaz, Sorbonne University, Paris, France) , DII-Venus (NASC ID: N799175, Brunoud et al., 2012) and PIN2-Green Fluorescence Protein (PIN2-GFP) seeds (Xu and Scheres, 2005; Abas et al., 2006) were used.

2. EMCS - Seedling Growth

For the space experiment Seedling Growth, the EMCS was used (Brinckmann, 2005). Seedlings were grown in the TROPI hardware cassettes as described in Vandenbrink and Kiss, 2019.

Seeds of WT, *nuc1-2*, and *nuc2-2* were surface sterilized in 70 % (v/v) Ethanol with 0.002 % (v/v) TX-100 for five minutes, followed by two washes with 100 % Ethanol. Then, seeds were air dried for at least 30 minutes.

Whatman filter paper (Whatman 17 CHR, Fisher Scientific #3017-915) was soaked in ½ MS medium pH 5.5 containing 5 % (v/v) macronutrients (Sigma #M0654), 5 % (v/v) micronutrients (Sigma #M0529), 0.01661 % (w/v) MES hydrate (Sigma #M2933) and 0.00381 % (w/v) MESK^+ (Sigma #M0895) and air dried for at least 2.5 h before the cassette assembly.

Seeds that presented regular shape, uniform color and texture were selected with a stereomicroscope to ensure high germination rates. They were attached to a gridded nitrocellulose membrane (VWR #28149-472) using 1 % (w/v) guar gum (Sigma #G-4129).

Lastly, cassettes were assembled as shown in Fig. 4c. Millipore filters (0.2 µm, Fisher Scientific #GSWP01300) were placed in the cassette base covering the ports. Then, the Whatman paper with the culture medium was set over the Millipore filter, and the nitrocellulose gridded membrane with the seeds was placed on the top. Afterwards the cassette was closed with the cover, and sealed with aluminum tape (Aluminum Foil Tape ¼ inch, 3M™ #S-18568).

a. Experimental conditions of SG

The experiment began with cassette hydration. A scheme of the experimental settings is shown in Fig. 5. Shortly, in SG1-2, seedlings were grown with 1 *g* gravity and continuous white light for the first 4 days, followed by two days of altered gravity conditions and red or blue light photostimulation. For the RNASeq analysis, only blue light stimulated seedlings were used. In SG 2-3, gravity levels were

constant throughout the experiment run (µ*g*, Mars g or 1 *g*). The first 4 days' seedlings were grown in a long day photoperiod regime (16/8 h) and the last two days they were photostimulated with red light or kept in the dark. Incubation temperature was 22 °C and the relative humidity was 80 %. The intensity of the white light was 30-40 µmol/m^2s, red light (λ-660 nm) 19 µmol/m^2s and blue light (λ-450 nm) 31 µmol/m^2s.

b. Fixation and sample storage

At the end of each run, the seedlings of SG1-2 were frozen at -80 °C in the Minus Eighty Degree Laboratory Freezer (MELFI) at the ISS. However, the samples of SG3 were either frozen, or fixed in the FixBox device (Manzano et al., 2020a) for confocal microscopy (5 % (v/v) formaldehyde (FA)) or electron microscopy (4.5 % (v/v) glutaraldehyde (GA) and 1.5 % (v/v) FA). The FixBoxes were kept at room temperature (RT) for three hours and then kept at 4 °C until return to Earth.

3. 2D-Clinostat

For the simulated microgravity experiments, we have used a 2-D clinostat (Fig. 6a and b). This clinostat is part of the Zero-Gravity Instrument Project (ZGIP), from the United Nations Office for Outer Space Affairs (UNOOSA) (Kojima et al., 2018).

The use of the 2-D clinostat with different settings have been studied in Villacampa et al., 2021b. We used two different clinorotation speeds, namely slow (1 rpm) and fast (60 rpm). In addition, we used two orientations of the sample in regard to the clinorotation axis: vertical, with the rotation axis perpendicular to the seedling's long axis (Fig. 6a); or horizontal, with the rotation axis parallel to the seedling's long axis (Fig. 6b).

For the simulated microgravity experiments, seedlings were surface sterilized in the same protocol as for the SG experiment. However, in this case seedlings were grown in Petri dishes containing ½ MS, 0.5 g/L 2-(N-morpholino)ethanesulfonic acid (MES) (M8250 Sigma–Aldrich, 1 % (w/v) sucrose and 0.8 % plant agar, pH adjusted to 5.6 with KOH. Seeds were stratified at 4 °C for 24 h before the start of the experiments.

The seedlings in the simulated microgravity experiments (Villacampa et al., 2021b) were grown with a long day photoperiod (16/8 h) positioned vertically for 5 days. Then, plates were covered with aluminum foil and placed in the clinostats for the different clinorotation conditions, kept in the vertical position for the 1 *g* control or rotated 90 ° for the directional growth control (90 °) to monitor the normal gravitropic response.

4. Morphometry

Root length and root morphology parameters were measured using ImageJ v1.53c. Vertical Growth Index (VGI), Horizontal Growth Index (HGI), Gravitropic Index (GI) (also named straightness (S)), and root angle (integral angular deviation) were measured as described in Grabov et al., 2005. Shortly, GI

is the ratio between direct distance from the beginning of the root until the root tip and root length (L); VGI is the ratio between the vertical distance of the root (Ly) and L and HGI is the ratio between the horizontal displacement of the root (Lx) and L. Root tip angle was measured as the direction of the root tip from time 0 (after 5 days of vertical growth) to 24 h after clinorotation, directional growth control (90 °) or 1 *g* control (Villacampa et al., 2021b).

5. Microscopy

a. Optical microscopy

ii. GUS Staining

DR5-GUS seedlings in Villacampa et al., 2021b were fixed in 90 % acetone at -20 °C for at least 1 day. Then, acetone was washed with 0.1 M sodium phosphate buffer pH 7.2, three times (10 minutes each). Next, seedlings were incubated overnight at 37 °C with the enzymatic reaction solution: 1 mM X-GlcA (X1405, Duchefa), 1 mM potassium ferricyanide (P4066, Sigma-Aldrich), 0.25 mM trihydrate ferricyanide (455989, Sigma-Aldrich) in 0.05 M sodium phosphate buffer pH 7.2. The following day, seedlings were washed three times in 0.05 M sodium phosphate buffer pH 7.2, mounted in 85 % glycerol and observed under a Leica DM2500 microscope. Staining intensity was quantified with ImageJ in the meristem area, with the image set to greyscale in the saturation channel (HSB Stack) (Villacampa et al., 2018, 2021b).

ii. DIC Microscopy

WT seedlings were fixed in 3 % FA, washed with Phosphate-buffered saline (PBS) and mounted onto slides with DABCO (D2522, Sigma-Aldrich). Samples were examined using Differential interference contrast (DIC) microscopy for statolith position determination in Villacampa et al., 2021b using Leica TCS SP5 microscope.

b. Confocal microscopy

Seedlings were fixed in 3 % FA for 1 h at RT (5 % and 3 h for the spaceflight samples) in PBS or Microtubule Stabilization Buffer (MTSB) (Pasternak et al., 2015) for PIN2-GFP seedlings (Villacampa et al., 2021b). Samples were washed three times with PBS. Seedlings were then digested with digestion solution (0.1 % pectinase (w/v) (17389, Sigma-Aldrich), 0.5 % (w/v) macerozyme (16419, Serva), 0.4 % (w/v) mannitol (105983, Merck), 10 % (v/v) glycerol and 0.02 % (v/v) Triton X-100 in PBS) at 37 °C for cell wall staining or digestion solution with cellulase (2 % (w/v) cellulase, 0.1 % (w/v) pectinase, 0.05% (w/v) macerozyme, 0.4% (w/v) mannitol, 10% glycerol (v/v) and 0.02% (v/v) TX-100 in PBS) for immunofluorescence. Samples were washed with PBS with 10 % glycerol and 0.02 % TX-100 three times. Seedlings were then transferred onto microscope slides and dehydrated with 90 % acetone at -20 °C.

i. Cell wall staining

Cell wall staining in wild type (Villacampa et al., 2021a), PIN2-GFP and DII-Venus (Villacampa et al., 2021b) seedlings was performed as follows: Seedlings were rehydrated with PBS containing 1 % NP-40 (I8896, Sigma-Aldrich) and 0.5 % Deoxycholic acid (DOC) (D2510, Sigma-Aldrich), and incubated with 2 % (v/v) SCRI Renaissance Stain 2200 (Musielak et al., 2015; Robert et al., 2015) (Renaissance Chemicals), 4 % (v/v) DMSO in PBS for 2 h at RT in darkness. Lastly, samples were washed twice with PBS before mounting onto the slides with DABCO. For confocal microscope observation, cell wall stain was excited with 405 nm with a UV laser with the confocal microscope Leica TCS SP5 with Acousto Optical Beam Splitter (AOBS).

ii. PIN2-GFP

In Villacampa et al., 2021b, after fixation with 3 % (v/v) FA in the MTSB buffer, PIN2-GFP seedlings were digested in the digestion solution without cellulose and the cell wall was stained. Samples were observed in the confocal microscope using 40X objective. The GFP signal was excited at 488 nm with the Argon laser.

iii. DII-Venus

In Villacampa et al., 2021b, DII-Venus seedlings were processed as PIN2-GFP, with the exception of the use of PBS in place of the MTSB buffer. The YFP signal was excited at 496 nm with the Argon laser.

iv. Fibrillarin immunofluorescence

In Villacampa et al., 2021a, WT (Col0) seedlings fixed in 5 % (v/v) FA in the SG experiment were posteriorly digested with the digestion solution with cellulase. After dehydration with acetone samples were stored at -20 °C. Before processing for confocal observation seedlings were rehydrated with 1 % NP-40 and 0.5 % DOC in PBS. Then, they were incubated with 20 mM glycine in PBS for 30 minutes at RT. Next, they were incubated with the blocking solution: 2 % (w/v) Bovine serum albumin (BSA) (Sigma #D6750) with 0,05 % (v/v) Tween (Sigma #P1379) in PBS. Samples were incubated overnight with the primary antibody α-fibrillarin (ab4566 [38F3], abcam) at 1:1000 dilution in blocking solution at 37 °C. Then, they were washed twice with 1 % NP-40 and 0.5 % DOC in PBS for 5 minutes, and incubated with the secondary antibody (A488 anti-ms IgM, A-21042, Molecular Probes), at 1:100 dilution in blocking solution for 3 h at 37 °C. Afterwards, samples were washed and nuclei were stained with 2-(4-amidinophenyl)-1H -indole-6-carboxamidine (DAPI) (Thermo #62248) for 5 min at RT. Lastly, samples were washed with PBS and seedlings were mounted with DABCO. Alexa 488 signal was excited at 488 nm with the Argon laser and DAPI nuclei stain at 405 nm with UV laser.

c. Electron microscopy

i. Epon

Seedlings in SG experiments were processed for electron microscopy observation as explained in Manzano et al., 2020a; Villacampa et al., 2021a. Shortly, seedlings were fixed at 4.5 % GA and 1.5 % FA in PBS for 3 h at RT (and space samples were kept at 4 °C until return to Earth). Then, samples were washed three times for 10 min in PBS and incubated in 1% (v/v) OsO_4 for 1 h at RT. Next, seedlings were washed twice with ddH_2O and dehydrated with increasing concentrations of ethanol: 25 % (v/v)

30 min RT, 50 % (v/v) 30 min RT, 70% (v/v) overnight at 4 °C. Next, dehydration continued with 80% ethanol for 30 min at RT, followed by 95 % and 100 % ethanol. Then, seedlings were infiltrated in Epon resin. The four components of the Epon resin (EMBED812 EMS #14900, Araldite GY 502 EMS #10900, DDSA EMS #13710 and DMP30 EMS #3013600), were mixed and stirred for 2 hours at RT. Resin infiltration was performed by immersing the seedlings in a mix of ethanol and resin in 2:1, 1:1 and 1:2 proportions, each for 1 h at RT. Lastly, samples were immersed in 100 % resin for 1 h and each root of the seedling transferred into a gelatine capsule. Each capsule was filled with Epon resin and closed. Resin polymerization was performed at 60 °C for 48 h.

ii. LR White

During the clinostat settings study (Villacampa et al., 2021b) seedlings were processed for electron microscopy observation as follows: seedlings were fixed in 2.5 % GA and 1.5 % FA in PBS and processed as previously described in González-Camacho and Medina, 2006. Post-fixation was performed as in the SG experiment with 1 % (v/v) OsO_4 for 1 h at RT. Seedlings were dehydrated with increasing concentrations of ethanol as described in the previous paragraph and samples were embedded in LR White resin (London Resin, Berkshire, UK). Resin was polymerized for 22 h at 60 °C.

6. RNASeq

a. RNA extraction and sequencing

RNA from whole seedlings was extracted from 8-10 seedlings pools from two cassettes (3 replicates) for the GLDS-313 and GLDS-314 datasets (SG2-3, (Manzano et al., 2020b; Villacampa et al., 2021a)). For the GLDS-251 (Herranz et al., 2019; Vandenbrink et al., 2019) RNA was extracted from whole cassette seedlings. RNA extraction in both cases was performed using MACHEREY-NAGEL extraction kit (#740949.250), which includes DNase treatment for 15 min. RNA quality was measured in the Bioanalyzer 2100 expert_Plant_RNA nano with Agilent RNA 6000 Nano Kit (Agilent Technologies#5067-1511). All samples had a RNA Integrity Number (RIN) > 7. GLDS-313 and 314 samples were processed as described in Manzano et al., 2020b; Villacampa et al., 2021a. They were sequenced on the Illumina HiSeq2500 sequencer at the Genomics Unit at the Centre for Genomic Regulation (CRG, Spain) with stranded RNA read type and 50bp read length. Sequencing libraries were generated with the Illumina TruSeq RNA Library Preparation Kit (Illumina, USA). Samples were individually indexed and combined at equimolar proportions into two pools, which were loaded onto two lanes of a flow cell. Sequencing was performed until 25 million reads per sample were reached (27,5±1 millions of sequences obtained). RNASeq transcriptome was analyzed with Galaxy (https://usegalaxy.org/) (Afgan et al., 2018). First, reads quality was examined with FASTQC. Fragments were trimmed with Trim Galore! (Krueger, 2015) with default settings. Reads were aligned with RNA STAR (Galaxy Version 2.7.2b) (Dobin et al., 2013), to *Arabidopsis* TAIR10 genome (https://www.arabidopsis.org). Then, gene counts were obtained with FeatureCounts (Galaxy Version 1.6.3) (Liao et al., 2014). Transcriptional datasets are available at NASA's Genelab database (Ray et al., 2019), with the accession numbers GLDS-313 (Manzano et al., 2020b) and GLDS-314 (Villacampa et al., 2021a).

Extracted RNA for the GLDS-251 dataset was stored at -80 °C and shipped on dry ice to the Murdoch Research Institute (Kannapolis, North Carolina, USA). RNA was sequenced as described in Vandenbrink et al., 2019. Shortly, 20 libraries were generated with the Illumina TruSeq RNA Library Preparation Kit. 125 bp paired end sequencing was performed on the Illumina HiSeq 2500. Reads were aligned with the HISAT2 pipeline (Kim et al., 2015) to the *Arabidopsis thaliana* TAIR10 genome. Trimmomatic (Bolger et al., 2014), was used to filter fragments with a Phred score below 33. Alignment was performed with HISAT2 (V2.1.0). Read assembly was done with StringTie (v1.3.4). This dataset is also available at the Genelab database with the accession number GLDS-251 (Herranz et al., 2019; Vandenbrink et al., 2019).

b. Differential Gene Expression Analysis

Table 1. RNA-seq datasets and comparisons of the Seedling Growth space experiment.

Genelab Dataset	Samples	Comparisons	Objective	Part of SG	General conditions
GLDS-251	µ*g*	µ*g*-1 *g* low *g*-1 *g* Moon g-1 *g* Mars g-1 *g* Reduced *g*-1 *g*	Effects if altered gravity levels compared to 1 *g* control	SG1-2	WT Ler ecotype, blue light photostimulation, altered gravity
	low *g* (0.09 ± 0.02 *g*)				
	Moon g (0.18 ± 0.04 *g*)				
	Mars g (0.36 ± 0.02 *g*)				
	Reduced *g* (0.57 ± 0.05 *g*)				
	1 *g* (ISS) (0.99 ± 0.06 *g*)				
GLDS-313	1 *g* GRR RL (WT)	WT RL-WT D *nuc1-2* RL-*nuc1-2* D *nuc2-2* RL-*nuc2-2* D	Effects of red light photostimulation on each genotype	Ground Control SG2-3	Ground Control, red light or dark, nucleolin mutants and WT
	1 *g* GRR D (WT)				
	nuc1-2 RL				
	nuc1-2 D	*nuc1-2* RL-WT RL *nuc2-2* RL-WT RL *nuc1-2* RL-*nuc2-2* RL *nuc1-2* D-WT D *nuc2-2* D-WT D *nuc1-2* D-*nuc2-2* D	Differences between genotypes in each light condition		
	nuc2-2 RL				
	nuc2-2 D				
GLDS-314	µg RL	µ*g* RL-1 *g* GRR RL Mars g RL-1 *g* GRR RL µ*g* D-1 *g* GRR D Mars g D-1 *g* GRR D	Effects of altered gravity levels compared to 1 *g* control	SG2-3	WT Col0 ecotype, red light or darkness, altered gravity
	µg D				
	Mars g RL				
	Mars g D	µ*g* RL-µ*g* D Mars g RL-Mars g D 1 *g* GRR RL-1 *g* GRR D	Effects of red light photostimulation on each gravity level		
	1 *g* GRR RL				
	1 *g* GRR D				

Deseq2 (v1.18.1; (Anders and Huber, 2010)) was used for differential expression analysis for all datasets. Comparisons between samples analyzed are detailed in Table 1. iDEP.91 (Ge et al., 2018) was used for Principal Component Analysis (PCA). For Gene Ontology (GO) analysis several tools were

used: ShinyGO (Ge et al., 2020), Metascape (Zhou et al., 2019) with custom analysis (adding molecular function and cellular component to the default settings), BinGO (Maere et al., 2005) with full list of GO terms (GO_full) and PANTHER (Mi et al., 2019) with the separate list of biological processes, molecular functions or cellular components. ShinyGO was also used to analyze the distribution of the Differentially Expressed Genes (DEGs) across the different chromosomes. For a general view of the similarities and differences of the DEGs, we used venn diagrams with jvenn (Bardou et al., 2014) and the Gene Expression Dynamics Inspector (GEDI v2.1) program analysis (Eichler et al., 2003). Gene lists of interest obtained with GEDI were extracted and analysed using Genemania in Cytoscape v3.6.1 (Montojo et al., 2010) with default settings. In addition, String v11.0 (Szklarczyk et al., 2019) was used for protein-protein interaction (PPI) analysis. Pathway analysis was performed with KEGG Mapper (Kanehisa and Sato, 2020). For the analysis of gene families enrichment in a specific comparison a Chi-squared test was used with GraphPad software v5.

RESULTS

RESULTS

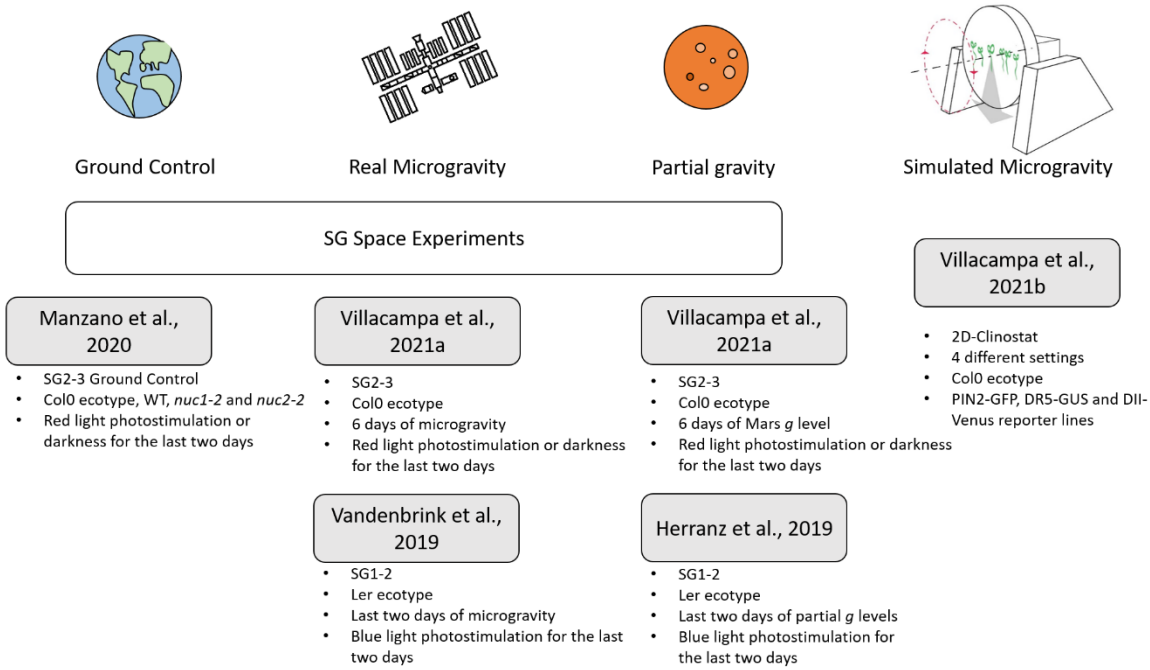

Figure 7. Results presented in different peer-reviewed journals. The results presented in this work, organized by publication and experimental condition. Four publications include results obtained in the Seedling Growth (SG) space experiments: Herranz et al., 2019; Vandenbrink et al., 2019; Manzano et al., 2020b; and Villacampa et al., 2021a. In Manzano et al., 2020b, we studied the effects of hardware and experimental conditions in ground control samples. Effects of microgravity on seedlings grown on the ISS was studied in Vandenbrink et al., 2019 and Villacampa et al., 2021. Partial gravity effects was analyzed in Herranz et al., 2019 and Villacampa et al., 2021a. Finally, in Villacampa et al., 2021b, we studied different modes of 2D-clinorotation to establish proper microgravity simulation conditions.

The experiments carried out to fulfill the objectives and the results obtained have been published in peer-reviewed journals as shown in Fig. 7:

1. Villacampa A, Ciska M, Manzano A, Vandenbrink JP, Kiss JZ, Herranz R, Medina FJ (2021a) From Spaceflight to Mars g -Levels: Adaptive response of A . thaliana seedlings in a reduced gravity environment is enhanced by red-light photostimulation. International Journal of Molecular Science, 22, 899
2. Vandenbrink JP, Herranz R, Poehlman WL, Alex Feltus F, Villacampa A, Ciska M, Javier Medina FJ, Kiss JZ (2019) RNA-seq analyses of Arabidopsis thaliana seedlings after exposure to blue-light phototropic stimuli in microgravity. American Journal of Botany, 106, 1466–1476.
3. Herranz R, Vandenbrink JP, Villacampa A, Manzano A, Poehlman WL, Feltus FA, Kiss JZ, Medina FJ (2019) RNAseq analysis of the response of Arabidopsis thaliana to fractional gravity under blue-light stimulation during spaceflight. Frontiers in Plant Science, 10, 1–11.
4. Manzano A, Villacampa A, Sáez-Vásquez J, Kiss JZ, Medina FJ, Herranz R (2020b) The importance of Earth reference controls in spaceflight –omics research: Characterization of nucleolin mutants from the Seedling Growth experiments. iScience, 2020, 101686.
5. Villacampa A, Sora L, Herranz R, Medina FJ, Ciska M (2021b) Analysis of graviresponse and

biological effects of vertical and horizontal clinorotation in arabidopsis thaliana root tip. Plants, 10, 1–20.

PhD candidate contributed to the RNA extraction, analysis of the RNA-seq gene expression results and manuscript preparation of articles 1, 2, 3 and 4.

In articles 1 and 4, she participated in the preparation of the experiment and processing of the samples. She processed the transcriptomic data and analyzed the differential expression analysis. She processed and analyzed the samples for confocal and electron microscopy and participated in the preparation of the manuscripts.

In article 5, she participated in experimental design, carried out the experiments and was involved in preparation and correction of the manuscript.

Three different RNA-seq datasets (Genelab Dataset, GLDS) are presented in this work: GLDS-251 (Vandenbrink et al., 2019 and Herranz et al., 2019), GLDS-313 (Manzano et al., 2020) and GLDS-314 (Villacampa et al., 2021a). A summary of RNA-seq datasets and comparisons is shown in Table 1.

1. From Spaceflight to Mars *g*-Levels: Adaptive Response of *A. Thaliana* Seedlings in a Reduced Gravity Environment Is Enhanced by Red-Light Photostimulation

Alicia Villacampa, Malgorzata Ciska, Aránzazu Manzano, Joshua P. Vandenbrink, John Z. Kiss, Raúl Herranz, F. Javier Medina

International Journal of Molecular Sciences 22(2), 899; doi: 10.3390/ijms22020899 (2021)

The effects of spaceflight and altered gravity level on plant development are important for space exploration in long-term spaceflight missions. The ISS provides the best environment for microgravity and partial gravity research. In this publication, we analyzed the effect of both real microgravity and Mars gravity levels in *A. thaliana* seedlings grown for 6-days on the ISS in the SG (2 and 3) space experiment (Fig. 5b). Partial gravity level was obtained thanks to a centrifuge integrated in the EMCS hardware on the ISS. Moreover, red light photostimulation was applied to seedlings at different gravity levels in order to investigate if this stimulus can overcome spaceflight effect on meristematic competence and ribosome biogenesis. At the end of the experiment, seedlings were either frozen for molecular analysis by RNA-seq (GLDS-314) or fixed using FixBox device (Manzano et al., 2020a) for microscopic analysis. We used confocal and electron microscopy, together with transcriptomic analysis to study the seedling's response to microgravity and Mars gravity levels. In addition, we studied the effects of red light photostimulation at different gravity levels.

We found red light increases meristem and nucleolar size as observed in the confocal microscopy images of the root meristem. In addition, the electron microscopic analysis of the meristematic nucleoli ultrastructure showed more active nucleoli in the red light photostimulated seedlings, as shown by higher GC content intermingled with DFCs and small FCs. In contrast, the seedlings kept in the dark, presented low GC content and heterogeneous FCs with condensed chromatin inside. In the RNA-seq analysis, we report downregulation of photosynthetic functions in red light photostimulated

seedlings in microgravity, as observed by the GO analysis of the DEGs. This downregulation of photosynthesis and light related GO categories was not present at Mars gravity level. In addition, an overexpression of plastid and mitochondrial genome expression was observed in microgravity in both light conditions, which is also present in other studies available in the Genelab database (Ray et al., 2019). However, Mars gravity level corrected these effects and promoted an adaptive response, with upregulation of Abscisic acid (ABA), ethylene and salicylic acid (SA) signaling pathways, and an enrichment of WRKY and ATAF1/2 CUC2 (cup-shaped cotyledon) (NAC) transcription factors (TFs) in the upregulated genes. This adaptive response was especially evident in the red light photostimulated seedlings.

In summary, a differential response to each gravity level was found. In microgravity seedlings promoted proliferation, as observed by increased meristem size and activation of auxin and cytokinin signaling pathways. Also, at Mars gravity level seedlings were able to activate an adaptive response to the new environment, enhanced by red light photostimulation.

2. RNA-seq analyses of *Arabidopsis thaliana* seedlings after exposure to blue-light phototropic stimuli in microgravity

Joshua P. Vandenbrink, Raúl Herranz, William L. Poehlman, F. Alex Feltus, Alicia Villacampa
Malgorzata Ciska, F. Javier Medina, John Z. Kiss

American Journal of Botany 106(11): 1466–1476. doi:10.1002/ajb2.1384 (2019)

Plants orient their growth according to different tropic signals. Gravity plays an essential role in determining plant growth direction on Earth. However, in space plants use tropic signals other than gravity to determine the direction of growth.

Here, we analyze the effects of real microgravity on gene expression in the blue light photostimulated *A. thaliana* seedlings, as a part of the SG1-2 space experiment on the ISS.

These seedlings were grown under continuous white light and 1 *g* for the first 4 days. The gravity level was obtained by the use of the centrifuge integrated in the EMCS hardware. During the last two days of the experiment the seedlings were grown exposed to microgravity (stopped centrifuge) or continued in 1 *g* (control) and were photostimulated with lateral blue light (Fig. 5a). Samples were frozen at the end of the experiment and they were posteriorly preserved in RNALater after the samples were recovered. Samples were stored at -80 °C until the RNA extraction for transcriptomic analysis (GLDS-251).

The transcriptomic analysis revealed several signaling routes altered by microgravity, specifically, photosynthesis and light associated pathways were downregulated, whereas ribosome and oxidative phosphorylation were upregulated. In more detail, transcripts encoding components of Photosystem I and II (PSI and PSII) were downregulated, highlighting the downregulation in light-harvesting chlorophyll a/b-binding (LHCB) transcripts. In addition, chlorophyll and porphyrin biosynthesis were also downregulated. These results show significantly altered gene expression by microgravity and help in the understanding of the plant's response to this environmental condition.

3. RNA-seq Analysis of the Response of *Arabidopsis thaliana* to Fractional Gravity Under Blue-Light Stimulation During Spaceflight

Raúl Herranz, Joshua P. Vandenbrink, Alicia Villacampa, Aránzazu Manzano, William L. Poehlman, Frank Alex Feltus, John Z. Kiss, Francisco Javier Medina

Frontiers in Plant Science 10:1529. doi: 10.3389/fpls.2019.01529 (2019)

For the cultivation of plants on satellites such as Moon or other planets, the effect of partial gravity levels on plants have to be studied. Nevertheless, this subject has not been studied in space until the SG experiments.

Here, we analyzed the response of blue light photostimulated *A. thaliana* seedlings to five different gravity levels; microgravity, low *g* (0.09 *g*), Moon gravity (0.18 *g*), Mars gravity (0.36 *g*) and reduced gravity (0.57 *g*) levels in the RNA samples obtained in SG1-2 space experiments (Fig. 5a). Partial gravity levels were obtained in the centrifuge integrated in the EMCS hardware on the ISS. The RNA-seq analysis that includes results reported in this publication, also included results presented in Vandenbrink et al., 2019 (GLDS-251).

The results of the transcriptomic analysis showed the relation between the increment of the number of DEG and the decrease in gravity level. Low gravity level (0.09 *g*), which is the condition that presented the highest number of DEGs in comparison to the 1 *g* control is an exception from the observed tendency. Microgravity and Moon gravity levels presented similar number of DEGs. Mars gravity level and reduced *g* presented the lowest number of DEGs in comparison to the 1 *g* control. Different genes and GO categories were affected by each gravity level. In microgravity, photosynthesis and light related GO were downregulated. However, low *g* produced a general stress response and Moon gravity level mainly affected cell wall and plasmatic membranes.

These results show different response of *A. thaliana* seedlings to partial gravity levels and are important for space exploration and for the development of bioregenerative life support systems.

4. The Importance of Earth Reference Controls in Spaceflight -Omics Research: Characterization of Nucleolin Mutants from the Seedling Growth Experiments

Aránzazu Manzano*, Alicia Villacampa*, Julio Sáez-Vásquez, John Z. Kiss, F. Javier Medina, Raúl Herranz

*These authors contributed equally

iScience 23(11) doi: 10.1016/j.isci.2020.101686 (2020)

Nucleolus and ribosome biogenesis has been found to be affected by spaceflight (Matía et al., 2010, Vandenbrink 2019, Ferl et al., 2014, Angelos et al., 2021). To further analyze how it is affected, we included two nucleolin mutants, *nuc1-2* and *nuc2-2*, into the SG2-3 space experiments.

As a first step of the analysis, we have compared the response of these mutant lines to the conditions of the space experiment in the ground control samples. The first 4 days, seedlings were grown under long-day photoperiod (16/8 h). The last two days, seedlings were photostimulated with red light or kept in the dark (Fig. 5b). Here, we analyzed the response to red light photostimulation or darkness of *nuc1-2* and *nuc2-2* seedlings compared to the WT (Col0) by RNA-seq (GLDS-313). We have compared gene expression in red light photostimulated seedlings with the ones that were kept in the dark, and also different genotypes within each light condition; in the dark and under red light photostimulation (Table 1).

The global response of the three genotypes showed a downregulation of genes involved in hypoxia and other abiotic stresses when photostimulated with red light in comparison with the seedlings that were kept in the dark for the last two days. This downregulation appears to be independent of nucleolin and nucleolin-related processes, since it was common to all three genotypes. However, the *nuc1-2* mutant and WT presented a downregulation of cold acclimation, response to karritin, hormone metabolism, and cell wall modification in red light versus darkness comparisons, which suggests NUC2 could be involved in these processes. In addition, when analyzing the differences between genotypes in the same light condition, *nuc1-2* showed the highest number of DEGs in comparison to WT. The differences of *nuc1-2* between both, *nuc2-2* and WT in the dark (3363 and 2121 DEG, respectively), were reduced to half in the red light photostimulated seedlings (1499 and 1069 DEG compared to WT or *nuc2-2*, respectively). This result shows red light partially neutralizes the negative effect of NUC1 mutation.

In addition, the results suggest NUC2 overexpression together with red light photostimulation could be beneficial for plant cultivation in space. The results from the *nuc1-2* and *nuc2-2* seedlings in the ground control will help to understand how these mutants respond to the space environment, different gravity levels and light conditions compared to the WT seedlings. Also, this study highlights the importance of ground control experiments for interpretation of the space experiments.

5. Analysis of graviresponse and biological effects of vertical and horizontal clinorotation in *Arabidopsis thaliana* root tip

Alicia Villacampa, Ludovico Sora, Raúl Herranz, Francisco Javier Medina, Malgorzata Ciska

Plants 10(4), 734; doi: 10.3390/plants10040734 (2021)

The limitations of space experiments produce a necessity of microgravity simulation on Earth to enable more research in the field. There are different ways to simulate microgravity. The simplest and most accessible is the 2D-clinostat. In order to establish the proper use of the clinostat in our experimental system, we compared commonly used settings.

We have compared vertical and horizontal clinorotation, and two velocities: slow (1 rpm) and fast (60 rpm) clinorotation. In order to analyze the response of 5 days-old *A. thaliana* seedlings to these clinostat settings, we measured root growth rate and direction, statolith position in the statocytes by DIC imaging of root columella cells, statocytes ultrastructure by electron microscopy, auxin PIN2 transporter levels and auxin distribution by confocal (PIN2-GFP and DII-Venus reporter lines) and

optical (DR5-GUS reporter) microscopy. We have analyzed seedling´s response to clinorotation after 1, 2 or 3 h to investigate the early response and after 24 h for a longer exposure.

The results show how fast clinorotation applied on *A. thaliana* seedlings induced directional growth. The root tip angle after 24 h of fast clinorotation depended on the seedling position on the Petri dish. We observed the root tips aimed towards the exterior of the Petri dish, with more pronounced angles in the seedlings placed further from the center of rotation. This root direction corresponded to the direction of centrifugal force which increases with the distance from the clinorotation axis. Also, statoliths sedimented on the bottom of statocytes in fast clinorotation as observed by DIC microscopy. These results show that microgravity simulation is limited in fast clinorotation to a very short distance from the center of rotation. In addition, different orientation of the samples in respect to the clinorotation axis produced different outcomes. We observed a stress response in horizontally clinorotated samples, which manifested in PIN2 internalization in the endodermis and structural damage in statocytes. As observed in electron micrographs of the statocytes the shape of mitochondria and lysosomes was affected and the lytic compartment was increased (higher number and size of vacuoles). Also, irregular cell walls were observed in horizontally clinorotated samples. This effects were not reported in real microgravity experiments. The stress response we observed, especially in the slow horizontal clinorotation, could be caused by a mechanostimulation due to the inclination of the Petri dish at different angles during the rotation cycles.

In conclusion, slow vertical clinorotation is the most suitable for microgravity simulation in our experimental system, with young seedlings grown on Petri dishes in a 2D-clinostat.

International Journal of
Molecular Sciences

MDPI

Article

From Spaceflight to Mars *g*-Levels: Adaptive Response of *A. Thaliana* Seedlings in a Reduced Gravity Environment Is Enhanced by Red-Light Photostimulation

Alicia Villacampa [1], Malgorzata Ciska [1], Aránzazu Manzano [1], Joshua P. Vandenbrink [2], John Z. Kiss [3], Raúl Herranz [1,*] and F. Javier Medina [1,*]

[1] Centro de Investigaciones Biológicas Margarita Salas (CSIC), Ramiro de Maeztu 9, 28040 Madrid, Spain; avillacampa@cib.csic.es (A.V.); mciska@cib.csic.es (M.C.); aranzazu@cib.csic.es (A.M.)
[2] School of Biological Sciences, Louisiana Tech University, Ruston, LA 71272, USA; jpvdb@latech.edu
[3] Department of Biology, University of North Carolina-Greensboro, Greensboro, NC 27402, USA; jzkiss@uncg.edu
* Correspondence: rherranz@cib.csic.es (R.H.); fjmedina@cib.csic.es (F.J.M.)

Abstract: The response of plants to the spaceflight environment and microgravity is still not well understood, although research has increased in this area. Even less is known about plants' response to partial or reduced gravity levels. In the absence of the directional cues provided by the gravity vector, the plant is especially perceptive to other cues such as light. Here, we investigate the response of *Arabidopsis thaliana* 6-day-old seedlings to microgravity and the Mars partial gravity level during spaceflight, as well as the effects of red-light photostimulation by determining meristematic cell growth and proliferation. These experiments involve microscopic techniques together with transcriptomic studies. We demonstrate that microgravity and partial gravity trigger differential responses. The microgravity environment activates hormonal routes responsible for proliferation/growth and upregulates plastid/mitochondrial-encoded transcripts, even in the dark. In contrast, the Mars gravity level inhibits these routes and activates responses to stress factors to restore cell growth parameters only when red photostimulation is provided. This response is accompanied by upregulation of numerous transcription factors such as the environmental acclimation-related WRKY-domain family. In the long term, these discoveries can be applied in the design of bioregenerative life support systems and space farming.

Keywords: microgravity; partial gravity; transcription factors; gene expression; root meristem

Citation: Villacampa, A.; Ciska, M.; Manzano, A.; Vandenbrink, J.P.; Kiss, J.Z.; Herranz, R.; Medina, F.J. From Spaceflight to Mars *g*-Levels: Adaptive Response of *A. Thaliana* Seedlings in a Reduced Gravity Environment Is Enhanced by Red-Light Photostimulation. *Int. J. Mol. Sci.* **2021**, *22*, 899. https://doi.org/10.3390/ijms22020899

Received: 15 December 2020
Accepted: 14 January 2021
Published: 18 January 2021

1. Introduction

The achievement of plant cultivation in space, also called "space farming," is an important step in the development of bioregenerative life support systems to enable long-term space exploration, since plants are fundamental elements for oxygen and nutrient supplies as well as waste recycling [1]. With this objective, it is important to study the response of plants to the space environment. Plants have been successfully grown in space on numerous occasions [2], even though major physiological changes, such as the alteration of cell proliferation rate and ribosome biogenesis, have been reported [3]. Most major physiological changes are regulated and tuned by phytohormones and transcription factors (TFs). These latter function as molecular switches activating or repressing the expression of genes or sets of genes in response to different stimuli, e.g., changes in the environmental conditions. Some changes in the phytohormone levels have been previously reported in experiments performed in real and simulated microgravity, such as a different distribution of cytokinin in real microgravity [4] and auxin accumulation in simulated microgravity [5]. However, more attention has been given to the changes in plant physiology (e.g., response to hypoxia, cell wall modifications, accelerated cell cycle) rather than to the hormone regulatory pathways and TFs.

Space exploration involves the exposure of plants to microgravity conditions, as they exist on spacecraft and stations orbiting the Earth, such as the International Space Station (ISS). Although microgravity effects have been extensively studied in living organisms, they are difficult to overcome since plants, like any other terrestrial organisms, have evolved in a constant gravity vector. Plants orient their growth according to the gravity vector (gravitropism), with positive root gravitropism and negative shoot gravitropism. Nevertheless, in microgravity, the cue for this tropism (i.e., the gravity vector) is not present.

Other tropisms are also involved in directing plant growth. For instance, using light as the tropistic cue, phototropism drives plant growth orientation with a negative root phototropism and positive shoot phototropism [6]. The interaction among gravitropism, phototropism and other tropisms, such as hydrotropism [7] and thigmotropism [8], produces the overall direction of plant growth [9], which is constantly adapted to the changing environmental conditions. These well-established positive and negative tropisms on Earth must be reevaluated in space since, in the absence of the gravity vector, new phototropic responses can be observed that were masked by gravitropism in the Earth. In fact, root positive phototropic response to red light [10] and blue light [11] have been reported in spaceflight studies. Different wavelengths of light are known to promote different responses on plant growth and development [12,13]. Thus, specific light conditions could be applied to overcome some of the deleterious effects on plant growth and development induced by microgravity. For example, red light is known to stimulate cell proliferation and promote ribosome biogenesis [14], both processes affected by spaceflight. In fact, red light has already been used in a similar experiment in simulated microgravity and was applied to *Arabidopsis thaliana* seedlings as a part of the Seedling Growth (SG) series (SG1 and SG2 experiments on the ISS) [15]. The results obtained were positive, in the sense of compensating at least a part of the alterations induced by microgravity.

Furthermore, the influence of partial or reduced gravity levels on the plant physiology should be investigated to enable human settlements on nearby planets [16]. In recent years, special attention has been given to Mars. Little is known so far on the plant response to partial gravity levels, which is important considering space agencies' plans to travel back to the Moon (Deep Space Gateway, DSG) in 2024 [17] and to Mars in the near future. With the purpose of studying how partial gravity levels can affect plant development, some studies have used analogs, such as random positioning machines (RPMs), to reproduce Moon or Mars gravity levels and study their effect on Earth [18]. Simultaneously, the European Modular Cultivation System (EMCS, [19]), which was installed in the ISS from 2008 to 2018, provided the ability to apply different *g*-forces in space by means of a built-in centrifuge. The SG experiment was executed in this hardware to test the contribution of red and blue light stimulation interaction with the reduced gravity stimuli [20]. Firstly, we used the EMCS to investigate transcriptomic changes in *A. thaliana* seedlings exposed to different *g*-levels for the last two days with blue light stimulation in the SG series (SG1 and SG2). We applied different gravity levels (microgravity, 0.1*g*; Moon; Mars; near earth *g*-level; 1*g*) to blue-light stimulated wild-type (WT) Landsberg ecotype *A. thaliana* seedlings and demonstrated a replacement of gravitropism by blue-light-based phototropism signaling at microgravity level [21], but a striking stress response was found at 0.1*g*. We also determined different components of the transcriptional response to the lack of gravity as the *g*-gradient is progressively reduced [22].

The use of transcriptomic techniques has provided vast data on gene expression in plants grown in space. *A. thaliana* is so far the most widely studied plant in space biology using omics techniques [21–31] and microscopic methods [4,32], although a few crop species have been recently incorporated to space studies [32–36]. Scarce material, high cost, and extensive logistics are highly limiting factors for space experiments, making the investigation of plant response to the space environment challenging, reinforcing the requirement of better controls and complementary research in ground simulation and reference facilities [37]. Moreover, there is a growing awareness in the space biology community to define and use the same criteria when describing the spaceflight experiment

metadata so the cross-comparisons between the spaceflight experiments can be performed more rigorously [38,39].

Here, we combined morphological and molecular approaches to describe the changes in 6-day-old *A. thaliana* seedlings (Col-0) grown in the SG experiments (SG2 and SG3) in three *g*-levels (microgravity, Mars gravity level and 1*g* ground reference run (GRR)) under red light photostimulation, and a control in darkness for the last two days of the experiment. In addition, we compared our results to other transcriptomic data obtained from *A. thaliana* seedlings grown during spaceflight and available in the GeneLab database ([40]; https://genelab.nasa.gov/) for further validation of our results. In the long term, our studies will pave the way to understand the molecular mechanisms to improve the cultivation conditions of plants on other planets.

2. Results

2.1. Anatomic Changes in Microgravity and Partial Gravity in Different Light Conditions

We analyzed the morphology of *A. thaliana* seedlings grown on the EMCS in the ISS. In our experimental conditions, the seeds germinated in altered gravity levels giving us a chance to observe how the plant deals with the new environment, meaning how they acclimate. The germination rate during the space experiment was similar to the one in the GRR (ISS samples 96.7%; GRR 93.93%) suggesting the plant activates these acclimation mechanisms already during germination.

We investigated the influence of different gravity levels and light conditions on meristem organization and size expressed in the length of the meristem (the distance from quiescent center to the first elongated cell in the epidermis) and in the number of meristematic cells in the epidermis (Figure 1A). The typical organization of the meristem with easily distinguished quiescent center and three layers of meristematic cells (epidermis, endodermis and cortex) was observed in all the conditions. These results suggest that altered gravity levels, and in general spaceflight conditions, do not disturb the well-conserved organization of the meristem in *A. thaliana*. The root cap columella also displayed its typical organization with the first meristematic layer followed by three to four layers of gravity-perceiving statocytes [41]. No difference in the number of layers of columella cells was observed among the conditions. In respect to the meristem length, in the seedlings grown in the dark, no significant changes were observed at any *g*-level. However, in the seedlings photostimulated with red light, a gradual increase in the meristem size was observed with the decrease of *g*-level (1*g* GRR < Mars < μ*g*), although the difference between Mars and μg was not significant (Figure 1B). In addition, the length of the meristem and the number of meristematic cells per meristematic layer were increased in the photostimulated seedlings in comparison to the seedlings grown at the same *g*-level in darkness, although the difference was only statistically significant at the Mars gravity level (Figure 1B). These observations were similar to those published in previous reports showing that red light stimulated proliferation [14,15].

Next, we estimated the nucleolar activity by measuring the area of immunofluorescent staining using an antibody against the nucleolar protein fibrillarin, in different *g*-levels and light conditions (Figure 1C,D). Fibrillarin is a well-known and abundant nucleolar protein involved in pre-rRNA processing regulation [42], and it can be used as a nucleolar marker. Under standard conditions of growth, the size of the nucleolus in the meristematic cells is directly related to its activity, determined by the production of the ribosomal units [43]. Therefore, the size and the structural features of the nucleolus are a reliable marker of the rate of ribosome biogenesis [44], which is determined by the demand in protein synthesis, meaning the higher the nucleolar size the higher protein production. A reduction in the size of the nucleolus was observed in meristems of the seedlings grown at Mars *g*-level without photostimulation. This reduction was significant in comparison to the nucleolus in red-light photostimulated seedlings at the same gravity level, and in comparison to the seedlings grown in 1*g* GRR and in microgravity without photostimulation. This indicates that the protein biosynthesis was also reduced in this condition. Red light seems to have a

positive effect on the nucleolar activity at the Mars *g*-level, since meristematic nucleoli in red photostimulated seedlings at this gravity level display similar size to the GRR seedlings. Surprisingly, nucleoli in seedlings grown in microgravity in both light conditions also had similar size as nucleoli in GRR seedlings (Figure 1D).

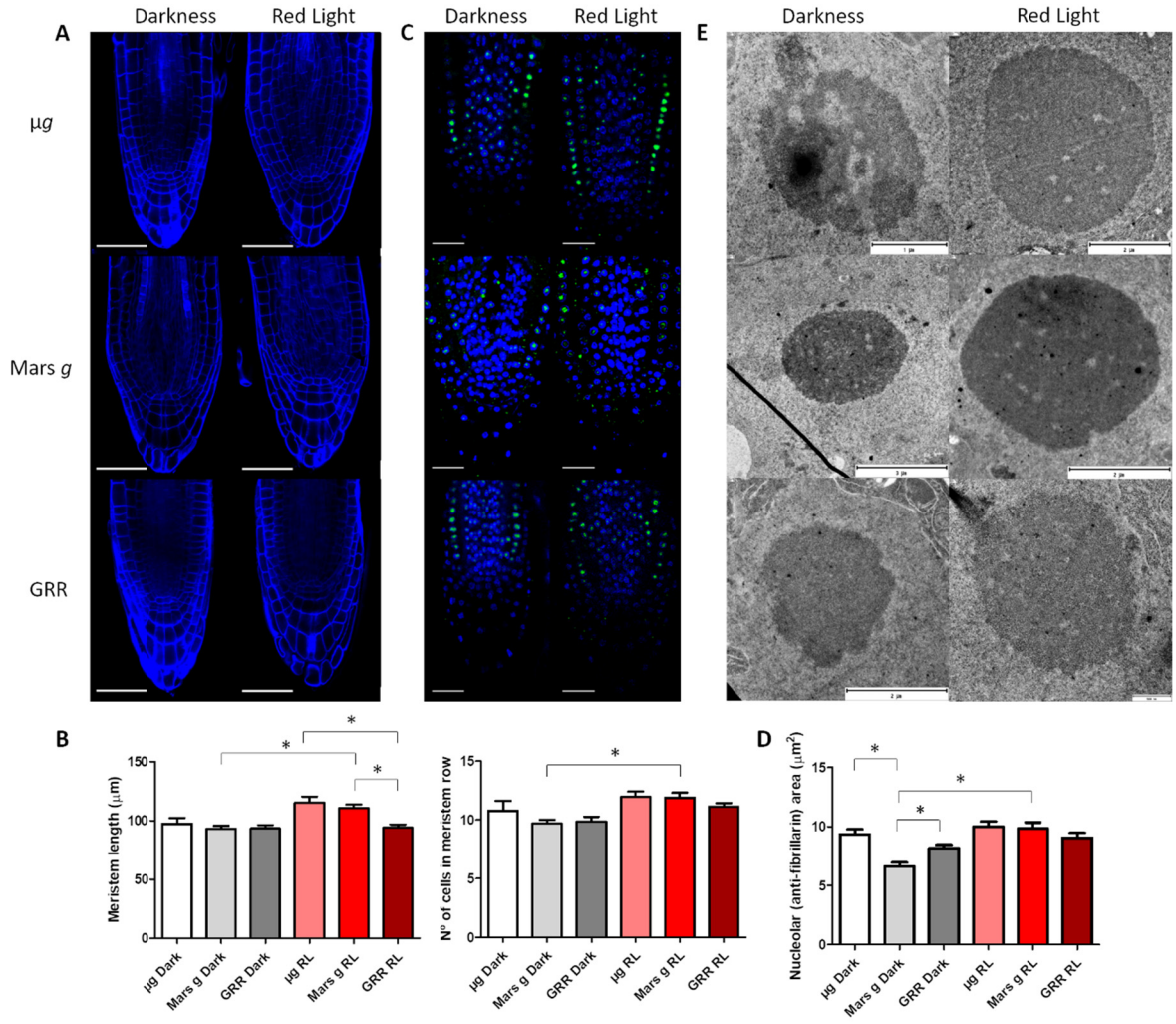

Figure 1. Meristem and nucleolus effects of microgravity and Mars gravity. (**A**) Confocal microscope images of cell-wall-stained root meristems of the different gravity and photostimulation conditions. Scale bar represents 50 µm. (**B**) Quantification of meristem length and number of cells per meristematic layer. Meristem length statistical analysis was made with ANOVA with Scheffe test post-hoc. Number of cells in the meristem row analysis was ANOVA with T3-Dunnett post-hoc (data not homoscedastic). In both cases the *p*-value for significance is 0.05. (**C**) Confocal images of immunostained root meristems; green: anti-fibrillarin, blue: DAPI. Scale bar represents 25 µm. (**D**) Nucleolar area (anti-fibrillarin immunostaining quantification) in μm^2. Statistical analysis was made using a non-parametric test with corrected *p*-value of 0.0033 (data without normal distribution. Bars represent mean + SED. * indicates significant statistical differences. (**E**) Electron microscope images of meristematic cell nucleoli. The difference in nucleolar size among different conditions is clearly observed. Furthermore, typical structural models corresponding to inactive nucleoli are seen in darkness conditions, especially in microgravity.

To investigate in more detail the changes that nucleolus undergoes in different light and gravity conditions, we analyzed nucleolar ultrastructure using TEM. In most conditions, nucleoli had a regular round shape and a typical structure, where three components could be distinguished: granular component (GC), dense fibrillar component (DFC) and fibrillar centers (FC) (Figure 1E). Despite the fact that we have not observed in microgravity conditions without photostimulation the reduction in nucleolar size that was observed

before in etiolated plants in the ROOT experiment [3], we could confirm in TEM images that nucleoli presented features typical for low-active nucleoli (low content of GC and heterogeneous FCs with condensed chromatin inside) [45]. However, in nucleoli of red-light photostimulated seedlings exposed to microgravity and partial gravity, features of active nucleoli, such as abundant GC intermingled with DFC and small FCs, were observed. No condensed intranucleolar chromatin was observed in these samples. This observation agrees with previous reports from our ROOT spaceflight experiment, where the combined effect of etiolation and microgravity caused a significant reduction in nucleolar activity [3]. Since, in the SG2 and SG3 experiments, the seedlings germinated and grew for four days with a photoperiod, the inhibitory effect of microgravity and darkness (last two days of culture) on nucleolar activity and nucleolar size could be diminished with respect to the experiments using etiolated seedlings.

2.2. Global Transcriptomics

Principal component analysis (PCA) of the replicates is shown in Figure 2A. The clustering of the replicates is consistent. There is a very clear separation among the three *g*-levels in the samples exposed to red-light photostimulation (µgrl, Marsrl and grrrl) but it is not well distinguished between the Marsd and grrd samples.

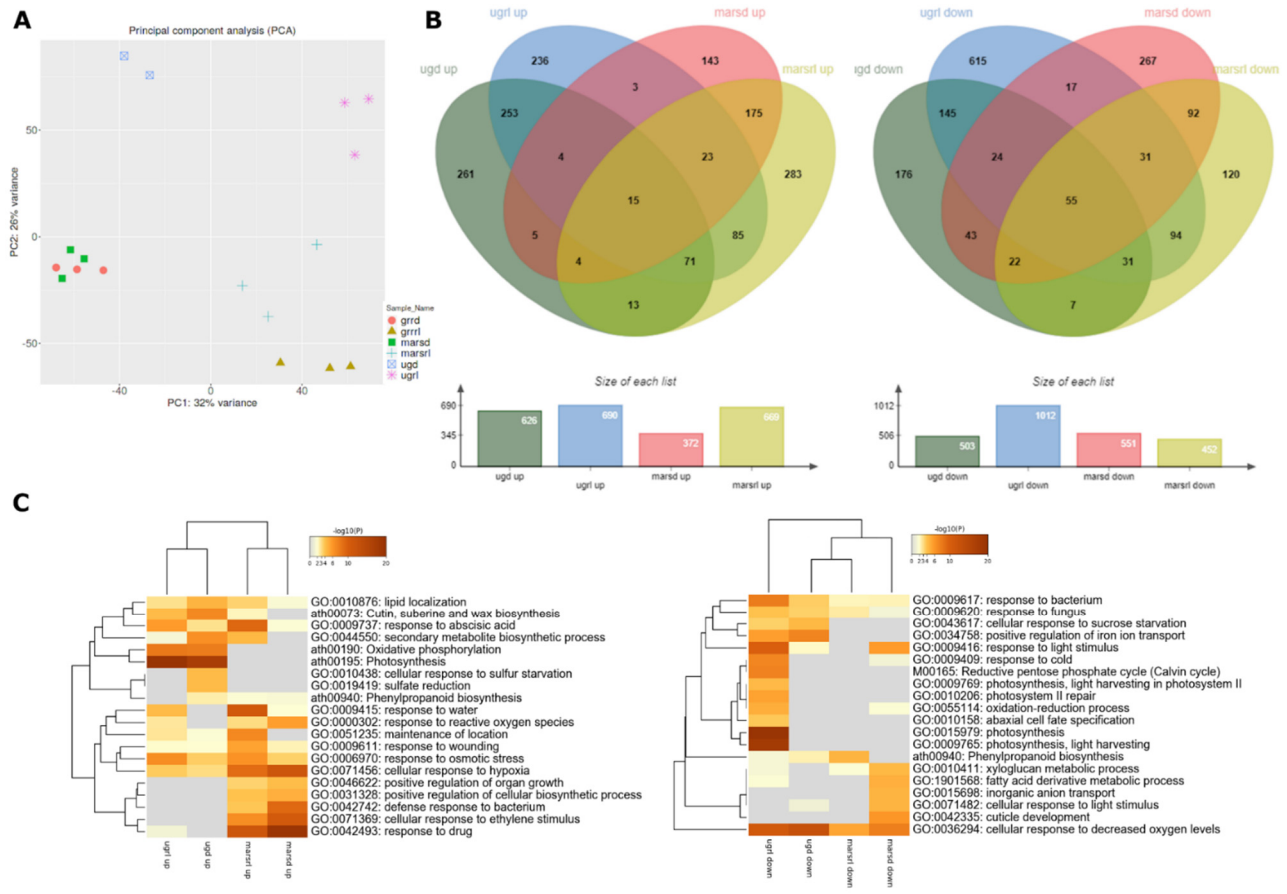

Figure 2. Global transcriptomic effects of microgravity and Mars gravity. (**A**) Principal component analysis (PCA) where all replicates included in RNASeq analysis are represented. (**B**) Venn diagrams with differentially expressed genes (DEGs) with q-value < 0.05 and $Log_2FC > 1.5$ (and < -1.5), separated in upregulated (**left**) and downregulated (**right**) genes. (**C**) Metascape Gene Ontology Heatmaps of top 20 enriched clusters for upregulated (**left**) and downregulated (**right**) DEGs.

To elaborate on this, we applied two different approaches to perform the comparisons in the transcriptomics data. First, to investigate the effect of different gravity levels on *A. thaliana* seedlings, we compared the transcriptomes of samples grown in microgravity or

Mars gravity level to the same light condition in 1-*g* GRR transcriptome as the reference; µgd-grrd, Marsd-grrd, µgrl-grrrl; Marsrl-grrrl. Next, to dissect the effect of red light at different *g*-levels, we compared the transcriptomes of seedlings grown in the same *g*-levels but in different light conditions; µgrl-µgd; Marsrl-Marsd, grrrl-grrd. In both cases, we used a q-value < 0.05 and a threshold fold change of $Log_2FC \pm 1.5$.

In the gravity level comparisons, more than 600 differentially expressed genes (DEGs) were upregulated in µgd, µgrl, and Marsrl, whereas in Marsd only half of this number (372) (Figure 2B). These results show that transcriptomes of the seedlings photostimulated by red light presented a similar number of upregulated DEGs at both gravity levels, but in seedlings grown in dark, twice as many DEGs were upregulated in microgravity than in Mars gravity. Approximately half of the upregulated DEGs are common for each gravity level independently of being exposed to darkness or photostimulation (253 and 175 in microgravity and Mars, respectively). Gene Ontology (GO) analysis of biological process categories of those sub-lists are shown in Figure S1. The low number of upregulated genes in the Marsd sample is in accordance with a small size of meristematic nucleoli in this condition, suggesting a reduced rate of protein biosynthesis, meaning that the transcriptome status is reflected at the proteome level. This effect could be a result of the upregulation of Ovate Family Protein 10 (OFP10), a transcription repressor [46] upregulated only in Marsd condition (Log_2FC 2; all Log_2FC values given in the text are statistically significant; q-value < 0.05).

Only 15 DEGs are upregulated in all four comparisons. Around 500 genes were downregulated in µgd, Marsd, and Marsrl, whereas in µgrl, there were twice as many (1012 genes). In this case, we observed twice the number of downregulated genes in the red-light photostimulated seedlings in microgravity in comparison to Mars *g*-level. This number is particularly high (615 DEGs) in µgrl only, and specifically enriched in photosynthesis function (Figure S1). A total of 55 DEGs are downregulated in the four conditions. There are also nearly a hundred up- and down-regulated genes in the red-light conditions (µgrl and Marsrl), which include abiotic stress responses in the upregulated DEG and metabolic biosynthetic pathways in the downregulated genes (Figure S1). In summary, seedlings grown at Mars *g*-level in darkness seem to be the least altered samples (in agreement with the PCA), while the ones grown in microgravity and photostimulated with red light show a high number of DEGs. Given the small variations observed in the plant anatomy, as reported in the preceding section, this dysregulation does not necessarily mean an adverse effect on the plant. Most likely, the changes in transcript levels also involve genes associated with the acclimation that the seedlings experience from the germination and during six-day exposure to altered gravity level. The red-light photostimulation comparison is discussed below.

In the Gene Ontology (GO) analysis, we used the total number of upregulated or downregulated DEGs to look for common and specific altered molecular functions in each condition. We observed that in the upregulated genes there was a clear clustering of common categories by *g*-levels rather than by light conditions (Figure 2C, left). Among the categories upregulated in all conditions, response to osmotic stress, wounding and cellular response to hypoxia could be identified. Photosynthesis categories are highly upregulated in microgravity, but not at Mars *g*-level. It is surprising that this category is equally upregulated in both light conditions, the red-light photostimulated sample and seedlings grown in darkness for the last two days. Another strongly upregulated category in microgravity was oxidative phosphorylation. On the other hand, categories specific for Mars conditions (both light treatments) include response to ethylene, drug, defense response and positive regulation of biosynthetic processes and organ growth.

Among the downregulated DEGs (Figure 2C, right), the common functions are related to hypoxia, while the rest of the downregulated functions seem to be specific for each *g*-level and light condition. In addition, in the µgrl sample, photosynthesis and light harvesting category was strongly downregulated. This result is in agreement with the previous results obtained in the SG1–2 experiments in the Ler ecotype, using blue-light

stimulated seedlings [21], confirming the role of light and phototropism as an alternative cue for plant development in the total absence of gravity. To determine if the same genes are being downregulated, we compared the two datasets and found 16 common genes. Even if the overlap of downregulated genes was not striking, there was an enrichment of photosynthesis function in those 16 genes specifically related to light harvesting in photosystem I and II, and five downregulated light-harvesting chlorophyll *a*/*b* binding (LHCB) proteins (Figure S2). These results suggest that the same function is affected by microgravity in both spaceflight experiments (i.e., one with red-light stimulation and the other with blue light).

Extended heatmaps with top 100 enriched clusters are shown in Figure S1. Common GO categories are either upregulated in both gravity conditions, such as the response to water, response to reactive oxygen species, response to osmotic stress, response to wounding and cellular response to hypoxia, or downregulated, such as cellular response to decreased oxygen levels. However, only a few or none of the dysregulated transcripts are common for both conditions in each category (Figure S3).

2.3. Dysregulation of Transcriptional Factors (TFs) and Hormonal Pathways in Microgravity and Partial Gravity

Many of the functional categories that are dysregulated in both microgravity and Mars gravity conditions such as osmotic and biotic stresses or response to hypoxia are regulated by both phytohormones and families of transcription factors [47–50]. Among the most over-represented TF families in the DEGs, we encountered the WRKY domain family, which forms one of the largest TF families in flowering plants, as well as other large families of TFs such as ethylene responsive factor (ERF), ATAF1/2 CUC2 (cup-shaped cotyledon) (NAC) and myeloblastosis (MYB). We tested by Chi-squared analyses whether a g iven TF family is overrepresented in each of the conditions and discovered that WRKY and NAC TFs are overrepresented in Mars *g*-level (both light conditions), and MYB TFs are overrepresented in Mars *g*-level (both light conditions) and in microgravity red-light photostimulated samples. In contrast, ERFs are overrepresented in all four conditions. Since WRKY TFs have an important role in plant acclimation and are "multifunctional switches," we focused on this family of TFs (reviewed in [47]). Data on WRKYs upregulated in the Mars conditions (both lights) are presented in Table 1. Although in microgravity WRKY were not overrepresented, one family member, *At*WRKY63, was significantly upregulated in both light conditions (µgd-grrd Log_2FC 2.56 and µgrl-grrrl Log_2FC 2.79).

We evaluated the influence of microgravity and Mars *g*-level on hormonal pathways using Kyoto Encyclopedia of Genes and Genomes (KEGG) pathway analyses. Few important hormonal pathways were significantly affected by microgravity and partial gravity, as seen in Figure 3 for the "plant hormone signal transduction pathway" (ath04075), including the expression level and significance for the four light/gravity conditions under study (µgd-grrd, µgrl-grrrl, Marsd-grrd, Marsrl-grrrl). Each signaling step includes the information of transcription levels of one or more genes involved in signal transduction (full list of genes is available at KEGG database under the ath04075 pathway identifier). According to KEGG Pathway analysis, the auxin pathway was activated at different steps in microgravity conditions (GRETCHEN HAGEN 3 (GH3) step in µgd and small auxin upregulated RNA (SAUR) in µgrl and repressed in Marsrl condition (GH3 step), suggesting cell enlargement and plant growth are promoted in microgravity but not at Mars *g*-level. *GH3* genes, downregulated in µgd (*DFL1*) and upregulated in Marsrl (*GH3.3* and *AT1G48660*) encode auxin-amido synthetases and promote the inactivation of indole acetic acid (IAA) [51]. Eleven SAUR genes which regulate auxin-mediated growth are upregulated in µgrl sample.

Table 1. Upregulated WRKY-domain transcription factors (TFs) in Mars gravity level. Statistically significant (q-value < 0.05) WRKY TF in marsd-grrd and marsrl-grrrl comparisons. Log_2FC for each TF in each comparison is shown. Reference list from this table is provided in the Supplementary Material.

Name	Group	Functions	Marsd-grrd	Marsrl-grrrl
*At*WRKY38	III	- negative roles in plant defense [1] - involved in SA signaling pathway [1] - JA-signaling repressor [2]	2.34	2.19
*At*WRKY40	II-a	- role in response to salinity/osmotic [3] - response to touch [4] - defense response	2.13	1.82
*At*WRKY45	I	- flooding stress [5] - phosphate ion transport [6]	1.19	0.81
*At*WRKY46	III	- regulates development, stress and hormonal response by facilitating growth of lateral roots in osmotic/salt stress through ABA signaling and auxin homeostasis [7] - role in the immune process; induced by *P. syringae* or SA [8] - cellular response to hypoxia [9]	3.73	3.61
*At*WRKY51	III	- mediates SA- and low oleic acid-dependent repression of JA signaling involved in plant defense [10]	1.85	2.14
*At*WRKY53	III	- positive effect on plant senescence [11] - role in the immune process - may play a role in SA signaling pathway [8] - negative regulation of senescence [12]	2.35	1.58
*At*WRKY54	III	- defense response - regulation of brassinosteroid, JA, SA and ethylene pathways (arabidopsis.org) - osmotic stress	2.82	2.00
*At*WRKY59	II-c	- regulation of transcription - induced by *P. syringae* or SA, [1]	4.34	3.02
*At*WRKY62	III	- negative role in plant defense.	2.77	2.48
*At*WRKY66	III	- regulation of transcription - (with AtWRKY44) development of the root hairs [13]	1.95	3.56
*At*WRKY75	II-c	- has a positive effect on leaf senescence [14] - participate in the regulation of phosphorus deficiency signaling [13]	1.78	1.61
*At*WRKY33	I_C	- binds to SIB1, JAZ1 and JAZ5 affecting JA-mediated defense signal pathway [15] - involved in abiotic stress response, in particular salt/osmotic stress (arabidopsis.org)	1.84	1.45
*At*WRKY70	III	- negative regulation of senescence [12] - role in the immune process may play a role in SA signaling pathway [8]	2.28	1.49

The cytokinin pathway was significantly activated ($Log_2FC > 1.5$) in microgravity through histidine phosphotransfer proteins (AHPs), which function as positive regulators of cytokinin signaling [52]. From the six members of this gene family expressed in *A. thaliana*, two were upregulated in microgravity: *AHP3* and *AHP4*. In Marsd conditions, this route was significantly inhibited at the CRE1 step (histidine kinase 2, *HK2*). The gibberellin pathway was significantly repressed at the TF step in microgravity (*PIF4, PIL6*).

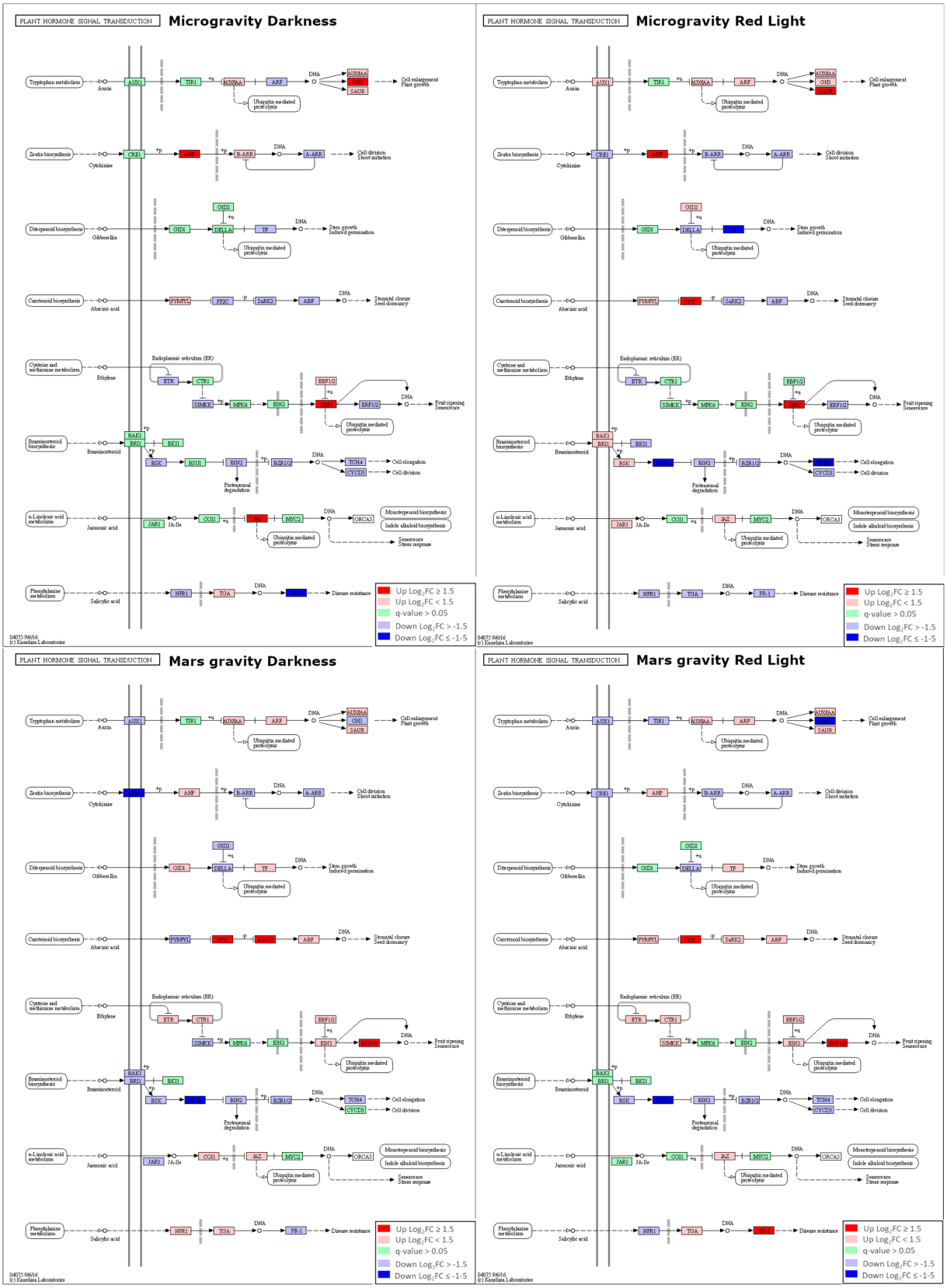

Figure 3. Hormone signaling changes in microgravity and Mars gravity. Plant hormone signal transduction (ath04075) Kyoto Encyclopedia of Genes and Genomes (KEGG) representation with color-coded changes in each experimental condition: microgravity darkness (µgd-grrd), microgravity red light (µgrl-grrrl), Mars gravity darkness (marsd-grrd) and Mars gravity red light (marsrl-grrrl).

At least one step of the abscisic acid (ABA) pathway is clearly activated in all conditions except for µgd (Figure 3). Among the upregulated genes that contribute to this activation are highly ABA-induced *PP2C* gene 2 (*HAI2*) and *HAI3* proteins and, in the case of the Marsrl samples, also SNF1-related protein kinase 2.9 (*SNRK2.9*) and *SNRK2.5.* The ethylene pathway was activated in all conditions; at EIN3 step in microgravity (*AT5G65100*) and ERF1/2 at Mars *g*-level (*ERF1, ERF2*), which is in agreement with the GO analysis and the overrepresentation of ERFs in the upregulated genes in all conditions.

The brassinosteroid pathway is significantly inhibited through BRI1 suppressor 1 (BSU1) protein in µgrl and Mars samples. In addition, *TOUCH 4 (TCH4*), which is involved in the response to mechanical stimulus, cold, hypoxia and regulates cell elongation (arabidopsis.org), is downregulated in all light and gravity conditions (although with threshold $Log_2FC > 1.5$ only in µgrl sample). Both microgravity and partial gravity influenced the transcription of jasmonate-ZIM domain (JAZ) proteins, which are transcriptional repressors in jasmonic acid (JA) signaling. *JAZ1* was upregulated in Mars gravity and *JAZ4* in microgravity. Additionally, *ABA-inducible BHLH-type transcription factor* (*AIB*) that interconnects JA-ABA pathways was also downregulated in microgravity conditions. The salicylic acid pathway was repressed in microgravity (*PR1-like*, *AT1G50060*) and activated in the Marsrl sample (*AT4G33720*) at the PR-1 step.

Similar analysis with light comparisons (µgrl-µgd, Marsrl-Marsd, grrrl-grrd) showed that red light activates the pathways regulating proliferation and growth: cytokinin pathway in microgravity and GRR samples and auxin pathway at Mars *g*-level (GH3 step) but does not alter significantly other hormonal pathways (Figure S4). These results suggest that the gravity level has more impact on hormonal pathways regulation than light conditions.

In summary, an activation of proliferation-promoting pathways (cytokinin and auxin) is evident in microgravity but not at Mars *g*-level. Further activation of the cytokinin pathway was observed with red-light photostimulation (µgrl-µgd comparison). At Mars *g*-level, red light reverses partial inhibition of auxin pathway (GH3 step) which is in agreement with its proliferation-activating effect. On the other hand, stress-related pathways, in particular ABA, ethylene and salicylic acid (SA) seem to be more activated at Mars *g*-level, which could suggest that in partial gravity, the plant perceives the stress signal and responds with activating acclimation mechanisms.

2.4. Plastid and Mitochondrial Genome Expression

We compared the distribution in the genome of DEGs in each condition using ShinyGO analyses [53] and found that in microgravity, the expression of genes encoded in the chloroplastic and mitochondrial genomes were over-represented. This enrichment in plastid and mitochondrial gene expression was specific to microgravity (Figure 4A) and not present in Mars *g*-level. Furthermore, we compared these results with the WT (Ler ecotype) blue-light dataset from the SG experiments (GLDS 251) containing transcriptomic data from seedlings exposed to the following partial gravity levels: microgravity, low gravity level (0.09 ± 0.02 g), Moon gravity (0.18 ± 0.04 g) and Mars gravity (0.36 ± 0.02 g) levels, and found a similar enrichment in chloroplastic and mitochondrial gene expression exclusively in microgravity, but not in any partial gravity including low gravity level (Figure 4B). This enrichment was detected in the upregulated DEGs, specifically 70 chloroplast-encoded genes were upregulated in microgravity dark and 83 in microgravity red-light conditions in our dataset (45 in the blue-light exposed samples from GLDS-251 dataset), and 10 mitochondrial genes were upregulated in microgravity dark and 30 in microgravity red light (5 in the blue dataset). The upregulated chloroplast-encoded transcripts involved multiple subunits of photosystem I and II and NAD(P)H dehydrogenase complex and electron transporters PETA (photosynthetic electron transfer A), PETB and PETD. The upregulated mitochondrion-encoded transcripts involved ribosomal proteins L16 and S3R, cytochrome oxidase 1 and 2 (COX1, COX2), NADH dehydrogenase subunits: 4, 5A and 5C and ATP-binding cassette I2 (ABCI2), a cytochrome C biogenesis protein.

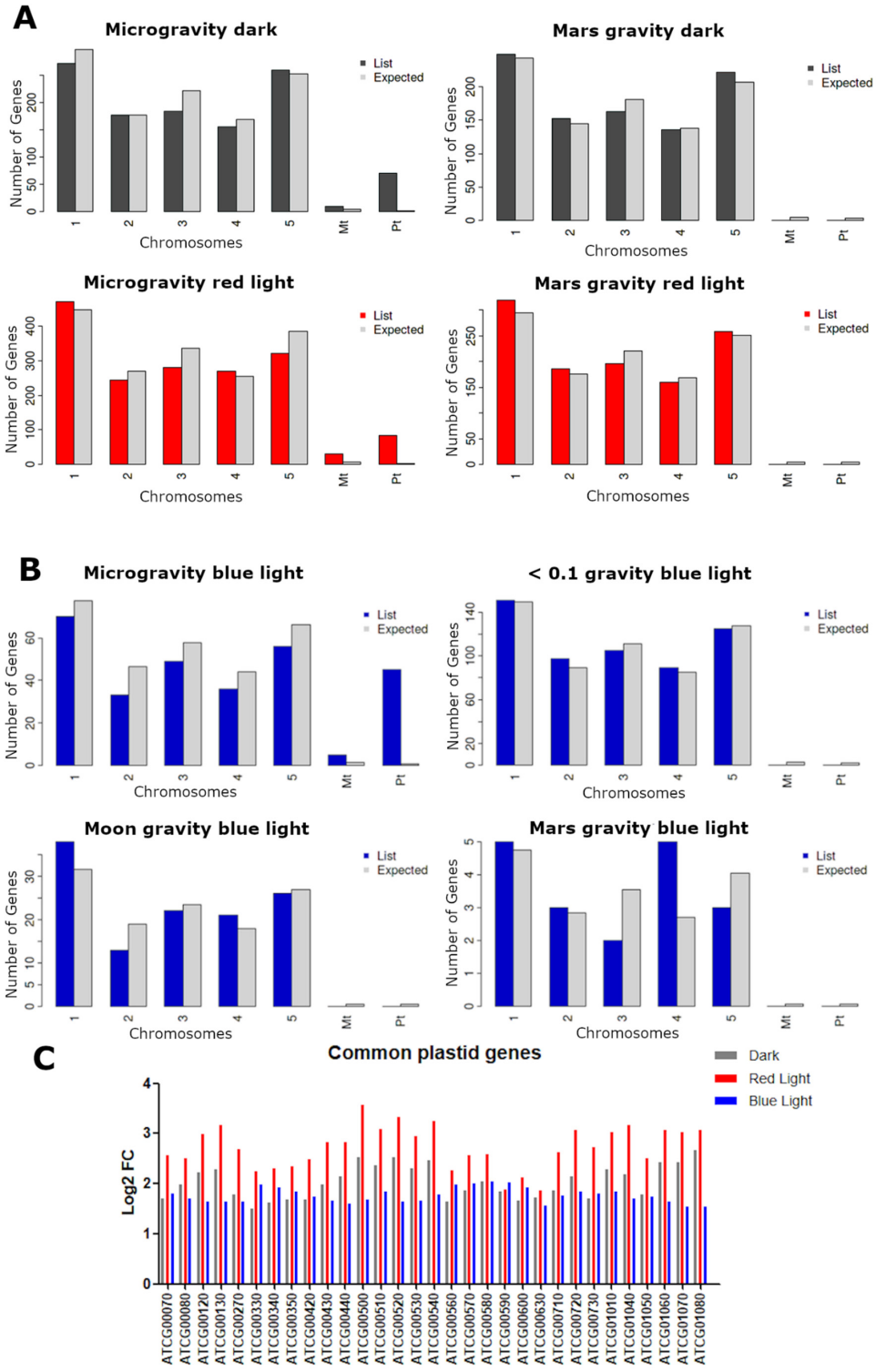

Figure 4. Plastid and mitochondrial genome expression in microgravity. (**A**) Distribution of DEGs across chromosomes in different comparisons: µgd-grrd, marsd-grrd, µgrl-grrrl and marsrl-grrrl. (**B**) Distribution of DEGs in GLDS-251 (NASA GeneLab Accession No.) blue-light stimulated seedlings in different gravity levels: microgravity, <0.1*g*, Moon gravity and Mars gravity. Bars (**A**,**B**) represent number of genes in query list (dark grey, red or blue) and expected number of genes (light grey). The distribution of the query genes is statistically significant (Chi-squared test) in microgravity dark (p-value: $1.1 \cdots 10^{-209}$), microgravity red light (p-value: $1.5 \cdots 10^{-207}$), mars red light (p-value: 0.014), microgravity blue light (p-value: 0). (**C**) Log_2FC of the common genes of the three microgravity comparisons: µgd-grrd (grey), µgrl-grrrl (red) and GLDS251 µ*g*-1*g* control with blue light stimulation (blue).

We also compared our results with datasets of two additional spaceflight experiments in which enrichment of organelle-encoded genes was reported in the transcriptomic data available in GeneLab (GLDS-38 and GLDS-44) [29,30]. These experiments were performed using the Biological Research in Canisters (BRIC) hardware without any lighting, so etiolated *A. thaliana* WT Col-0 seedlings grown in microgravity were used. Although not completely, there is a significant overlap in some of these genes in two or more experiment datasets (Table S3), even considering that it is not uncommon to see differences between spaceflight experiments [54]. The fact that this phenomenon is observed in experiments where different *A. thaliana* WT lines were used and different hardware and environmental conditions were applied, strongly suggests that it is one of the major microgravity effects. These results are consistent with studies of impaired mitochondrial function from drosophila [55] to humans [56].

This plastid and mitochondrial genome expressions were observed in the three different light conditions (blue light, red light, darkness). However, red light leads to generally higher upregulation levels and a greater number of genes were upregulated in our dataset of the red-light photostimulated seedlings compared to plants grown in darkness, or in the Ler dataset of blue-light photostimulated seedlings, as shown by the fold change of the common upregulated genes (Figure 4C). The level of change of all plastid and mitochondrial genes in the three light conditions is shown in Figure S5.

2.5. Dissecting the Contribution of the Red-Light Photostimulation to the Response to Each g-Level

To dissect the transcriptomic changes provoked by red-light photostimulation at each *g*-level, we performed an additional set of transcriptomic comparisons of the photostimulated seedlings versus the seedlings grown in darkness at 1*g*, Mars and microgravity levels (grrrl-grrd; Marsrl-Marsd; μgrl-μgd) (Figure 5). The first observation is the fact that the number of upregulated genes was much higher than the number of downregulated at all gravity levels. As expected, we have observed upregulation of genes related to photosynthesis, light harvesting, pigment biosynthesis and response to light stimulus in all gravity conditions including GRR. Other categories upregulated in all gravity conditions included transcripts involved in response to karrikin (which help stimulate seed germination and plant development), phenylpropanoid metabolic processes, secondary metabolic processes and, in microgravity (to a lesser degree in GRR), the reductive pentose phosphate cycle (Calvin cycle). Surprisingly among downregulated transcript categories, we found the ones related to red to far-red signaling pathway and the response to far red light, which indicates that feedback regulatory mechanisms were triggered to tune down the seedling response. Metascape analysis of upregulated transcript heatmap profiles clusters Mars comparison (Marsrl-Marsd) together with GRR comparison (grrrl-grrd), which suggests a more similar plant response in these conditions. In contrast, in downregulated transcript profiles, Mars comparison clusters together with microgravity comparison (μgrrl-μgd). These observations are also reflected in the higher number of upregulated genes common in Mars and GRR than the ones common in Mars and microgravity and a higher number of common genes downregulated between Mars and microgravity than those common for Mars and GRR, or microgravity and GRR (Figure 5). Taken together, these results could suggest that red-light photostimulation has a positive effect on seedlings in Mars gravity level, which is similar as in Earth conditions. Extended heatmaps are shown in Figure S6.

The processes that are the most affected in microgravity by red light include cell wall organization and biogenesis, cell cycle, microtubule-based processes, DNA replication initiation and trichoblast differentiation (Figure 5). This effect is less pronounced in the other gravity conditions, which suggests that red-light photostimulation has especially positive influence on seedlings in microgravity.

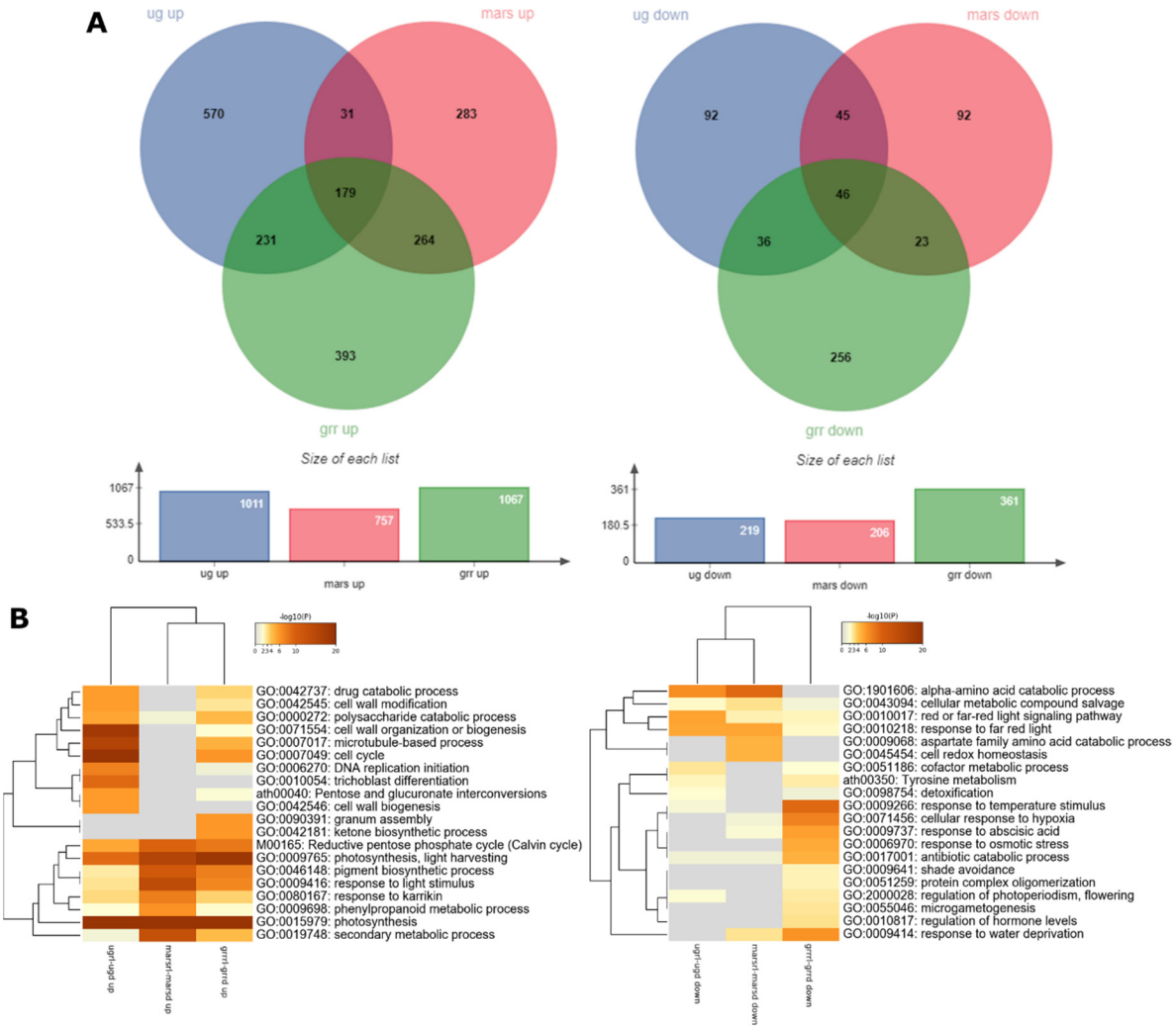

Figure 5. Red-Light induced changes in gene expression across gravity conditions. (**A**) Venn diagrams representing DEGs (with q-value < 0.05 and $Log_2FC > 1.5$ (or <-1.5). Left: upregulated genes. Right: downregulated genes. (**B**) Metascape Gene Ontology (GO) heatmaps of top 20 enriched clusters. Left: upregulated genes. Right: downregulated genes.

On the other hand, red light has an inhibitory effect on proteolysis in microgravity and Mars conditions, as seen by downregulation of the genes related to amino acid catabolic processes. This observation is in line with the positive effect of red light on biosynthesis and proliferation [14] and is reflected in the increased size of the nucleolus (and meristem) in the red-light photostimulated samples.

Among the most important transcripts in the cell cycle category upregulated in microgravity conditions were PROLIFERA (*PRL*; Log_2FC µgrl-µgd 2.16) and multiple cyclins: A2, A3, B1 (B1:1, :3, :4 (cyclin2)), B2(:1, :2, :3), D4 (:1; :2), P4(:1; :2, :3) as well as proliferation markers *AURORA1* and *AURORA2*. Upregulated genes encoding microtubule-related proteins included many subunits of the mitotic spindle, but also some important cytoskeleton-related proteins such as tubulin beta-1 chain (*TUB1*; Log_2FC µgrl-µgd 1.84) and SPIRAL1-LIKE4 (*SP1L4*; Log_2FC µgrl-µgd 1.69). *TUB1* encodes beta tubulin regulated by phytochrome A (phyA)-mediated far-red light high-irradiance and the phytochrome B (phyB)-mediated red-light high-irradiance responses [57]. SP1L4 regulates cortical microtubule organization essential for anisotropic cell growth [58].

In terms of cell wall enzymes and proteins, among the upregulated transcripts in microgravity light comparison were present numerous enzymes from the group of hydrolases (*Xyloglucan endotransglucosylase/hydrolase 12*, *XTH12*; *XTH13*; *XTH14*; *XTH20*; *XTH26*;

glycosyl hydrolase 9B13, GH9B13) and transferases (*galacturonosyltransferase 12, GAUT12*; *rhamnogalacturonan xylosyltransferase 1, RGXT1*; *glucuronoxylan methyltransferase 2, GXM2*) as well as *pectin methylesterase 46* (*PME46*), *pectin acetylesterase 10* (*PAE19*) and *polygalacturonase involved in expansion 1* (*PGX1*). In addition, numerous extensins (*LRX1*, *EXT2*, *EXT7*, *EXT8*, *EXT9*, *EXT10*, *EXT12*, *EXT13*, *EXT15*, *EXT16* and *EXT17*) and two fasciclin-like arabinogalactans (*FLA6*, *FLA7*) were present. These results suggest the cell wall undergoes profound modifications in this condition that might be related to increased cell growth and expansion [54,59].

3. Discussion

3.1. Red-Light Photostimulation has a Positive Effect on Cell Proliferation in Both Microgravity and Mars Gravity Conditions

Our morphometric studies indicate that features like meristem and nucleolus size are more robust in the red-light photostimulated seedlings. In the case of the nucleolus, although the difference in size between dark-grown and red-light photostimulated seedlings is not significant in microgravity, the features of nucleolar ultrastructure clearly indicate that red-light photostimulation increases nucleolar activity. Increased root meristem size (expressed as the length and the number of meristematic cells), nucleolar size and changes in nucleolar ultrastructure confirm positive effect of red light at Mars *g*-level, suggesting that the rates of both the meristematic cell proliferation and protein production were increased. On the other hand, the transcriptomic data from different light condition comparisons (grrrl-grrd; Marsrl- Marsd; µgrl-µgd) confirmed that in microgravity, cell cycle and proliferation related genes are upregulated and the hormonal routes promoting proliferation activated (Figure 5B and Figure S3).

Red and far-red light are perceived by photoreceptors termed phytochromes, which are expressed in different zones of the root (reviewed in [60]). PhyA and phyB, expressed mainly in the root tip, are involved in both red-light-induced positive root phototropism and gravitropism [61,62]. Red-light photostimulation of seedlings in GRR has a positive effect on the overall physiology in comparison to the seedlings kept in darkness for the last two days of cultivation [37]. In addition, red light is known to stimulate cell proliferation and ribosome biogenesis [14], which are observed in our results, particularly when the gravity vector cannot completely guide the plant development. In addition, red light also restored the meristematic competence balance, which was extensively described to be affected in early plant development in our previous ROOT experiment in the ISS in etiolated *A. thaliana* seedlings [3].

Thus, we conclude that red-light photostimulation could help plants to overcome some of the deleterious effects of the spaceflight environment. Similar effects were seen previously in our experiments with blue-light photostimulation [22].

3.2. Microgravity has a Deleterious Effect on Plant Physiology: Elevated Plastid and Mitochondrial Genome Expression is Observed in Microgravity, but Not in Partial Gravity

Dysregulation of the genes involved in photosynthesis was specific for microgravity condition. Photosynthesis-related genes were upregulated in both light conditions, which was related to the increased plastid genome expression (to be discussed further). On the other hand, in the µgrl sample, genes involved in photosynthesis were also downregulated. This is in agreement with the results of the previous SG experiment [21], although only 16 genes were common for both datasets obtained from different light conditions. Reduction in photosynthesis activity, and specifically in photosystem I complex, was observed in previous studies of *Brassica rapa* plants grown in space [63], and in *Oryza sativa* plants grown in simulated microgravity [64]. Furthermore, structural changes in chloroplasts, such as alterations of thylakoid membranes in seedlings grown in real [65] and simulated microgravity [66] were reported, as well as a reduction of chloroplast size in simulated microgravity [67]. Downregulation of LHDB proteins, which was observed in microgravity in red- (our dataset) and blue-light stimulated seedlings (GLDS-251) (Figure S2), is known

to affect stomatal closure in effect reducing photosynthetic activity. This downregulation also decreases plant tolerance to drought stress [68,69].

Dark-grown samples showed a general decrease in photosynthetic activity as demonstrated by the transcriptomic analysis of 1*g* GRR samples [37]. It is therefore not surprising that we have not observed this category in dysregulated genes in µgd-grrd comparison.

Additionally, few ERFs important for development of tolerance to a number of abiotic stressors were downregulated in microgravity: *Translucent Green* (*TG*), downregulated in microgravity and darkness, is involved in drought tolerance [70], *C-repeat/DRE binding factor 1* (*CBF1*) and *CBF2*, downregulated in microgravity in both light conditions, are involved in tolerance to freezing [71,72], *AtERF72*, also downregulated in both light conditions, is involved in the tolerance to peroxide (H_2O_2) and heat stress [73]. In summary, the downregulation of these ERFs in microgravity may have a negative effect on *A. thaliana* tolerance to adverse conditions.

Two organelles seem to be particularly affected in microgravity during space flight. Plastids contain 3000–4000 proteins and most of them are encoded in the nucleus [74]. Around 90 to 100 are encoded in the chloroplast genome [75]. The majority of these genes are upregulated in microgravity (70 in µgd and 83 µgrl). Mitochondria contain around 3000 proteins, from which 57 were identified in the mitochondrial genome [10,76]. In our dataset, we identified 10 of them in µgd, peaking to 30 out of 57 in µgrl and 10 in microgravity and darkness. Various factors influence plastid gene expression, such as light, temperature, plastid development or circadian clock [74]. Abscisic acid (ABA) represses transcription of chloroplast genes [77]. The ABA pathway was activated in the Mars samples, which could explain why this phenomenon is not observed in this condition. Upregulation of plastid-encoded genes was reported before in spaceflight experiments [29].

Mitochondria and chloroplasts are tightly involved in cellular metabolism and are thought to be initial sensors for cellular dysfunction caused by external stress. Research to date suggests that factors that participate in signaling between these organelles and the nucleus (anterograde communication: communication from nucleus to organelle; retrograde communication: from organelle to nucleus) also participate in the recognition of the stress level. The decision is whether to adjust the metabolism, or to execute programmed cell death (PCD) [78]. The key signaling molecules in mitochondrial dysfunction are ANAC017, ANAC013 and Alternative Oxidase 1a (AOX1a) [79]. *ANAC017* is only slightly downregulated in microgravity and *AOX1a* and *ANAC13* is only upregulated in Marsrl condition (around 1-fold). In addition, there is a set of mitochondrial proteins which are consistently upregulated in stress conditions when the dysfunction of mitochondria takes place [80–82], but only one of these is upregulated in the µgrl sample (*AT3G50930*) and three downregulated (µgd, µgrl: *AT1G20350*, *AT1G21400*; µgd: *AT4G15690*).

Based on our results, it would seem that there is a dysregulation of the chloroplast and mitochondrial genome expression, and this dysregulation is not perceived and corrected in the typical retrograde communication in response to organelle dysfunction. Moreover, this organelle dysfunction is not present in partial gravity level, probably because the retrograde communication is not disturbed. Supporting the last assumption is the fact that Sigma factor binding protein (SIB1), which binds sig1R factor (nuclear encoded factor that regulates the chloroplast genome expression) and has an important role in the retrograde communication, is downregulated in µgd, but upregulated in Mars conditions. *At*WRKY40 was shown to be a repressor of retrograde-mediated expression while *At*WRKY63 has an opposite activating effect [79]. The antagonistic functioning of WRKY40 and WRKY63 could also play a role in this dysregulation. At Mars *g*-level, *AtWRKY40* is upregulated, subduing the expression of stress-responsive genes (genes responding to mitochondrial and chloroplast dysfunction). On the other hand, upregulation of *AtWRKY63* could play a role in the dysfunction of both organelles. It has been reported that disturbed mitochondrial retrograde signaling leads to increased sensitivity of plants to stress conditions [83]. Mitochondrial retrograde signaling is involved in acclimation to flooding, and *At*WRKY40 is involved in promoting

this acclimation together with *At*WRKY45 [83], which is also upregulated at Mars *g*-level and downregulated in microgravity.

Mitochondria and WRKY40 also participate in response to touch and wounding. This response involves other signaling factors such as OM66 and mitochondrial dicarboxylate carriers DIC2, DIC1 [84,85]. The *OM66*, *AtWRKY40*, *DIC1* and *DIC2* are upregulated at the Mars *g*-level (both light conditions). It is possible that at the Mars *g*-level, the seedling is activating the response to touch in the search for the direction stimuli, whereas in microgravity this route is not activated (as *OM66*, *AtWRKY40, DIC1* and *DIC2* are not upregulated).

However, the mechanism involved in the perception of microgravity and the mechanism that causes the dysregulation of the organellar genome transcription remains unresolved. Nevertheless, our results show that by the combination of light with applying even low *g*-level, this stress response observed at the Mars *g*-level (and even more intense at the Moon *g*-level [18,22]) can be corrected.

3.3. Seedlings Grown at Mars g-Level Activate Stress Responses Involving WRKY TFs Possibly Leading to Acclimation

The acceleration similar to the Mars *g*-level in the EMCS centrifuge in orbit is enough to provide gravitropism cue to plants on the ISS as seen in Figure 6 and previously reported [15]. Consistently, the transcriptome changes observed at Mars *g*-level are very different from those found in *A. thaliana* exposed to microgravity, which is especially clear in the seedlings grown without photostimulation. DEGs involved in multiple stress responses, like hypoxia (decreased oxygen levels), drought, reactive oxygen species, osmotic and biotic stresses are altered in both gravity levels. These observations are in accordance with previous experiments in the microgravity and partial gravity conditions [22,25,54]. However, when we compare the number of common DEGs in microgravity and Mars conditions (Figure 2), we observe only 15 upregulated genes and 55 downregulated genes. In fact, even though common GO categories are upregulated and downregulated for both conditions, only a few or none of the specific DEGs are common for both gravity levels (Figure S2). Moreover, photosynthesis, which is highly affected by microgravity [21], does not seem to be disturbed at Mars *g*-level. It is evident that both conditions induce different responses in seedlings and, therefore, the strategies to grow plants, either during spaceflight or on a planet with reduced gravity, but enough in magnitude to trigger a full gravitropic response, should also be different.

GO categories common for all the samples are most likely related to the spaceflight conditions; however, the plant responds to these environmental factors differently in microgravity and Mars *g*-level, as suggested by the low number of common DEGs. The bioavailability of oxygen in the spaceflight environment is reduced and very dependent on the hardware used for the experiment in orbit, provoking the plant response to hypoxia [54,86]. This stress is closely related to waterlogging response (or water stress), also present in the upregulated group in the GO analysis; in fact, when a plant is submerged under water the availability of oxygen is reduced and response to hypoxia activated [87]. Morphological changes typical for plants in response to flooding, such as the appearance of adventitious roots in *A. thaliana* ("roots on the stem"; [87]), were observed in BRIC-16-Cyt experiment [88]. In addition, Stout et al. [89] demonstrated increased activity of fermentative enzymes in the roots of *B. rapa* grown in the space environment, which indicates root zone hypoxia. It is possible that the plant activates these known mechanisms to enhance oxygen intake. The response to the osmotic stress is also a category frequently dysregulated in space experiments [29]. The nature of this response is not well understood but it was suggested that plants could activate in microgravity the response to osmotic stress due to the absence of structural guide, compensating it with the stabilization of microtubules [29,90]. Nevertheless, the response to this stressor is also present in partial gravity where the seedling seems to perceive gravitational cues (Figure 6). Our results suggest that the hormonal and transcriptional routes involved in response to osmotic stress, such as the ABA pathway and ERF TFs upregulation, are activated. ERFs are characterized

by the presence of ERF DNA binding domain [91] and fulfill a wide range of functions in response to multiple stresses. Differential expression of ERFs was reported in adverse conditions such as waterlogging and hypoxia [92,93].

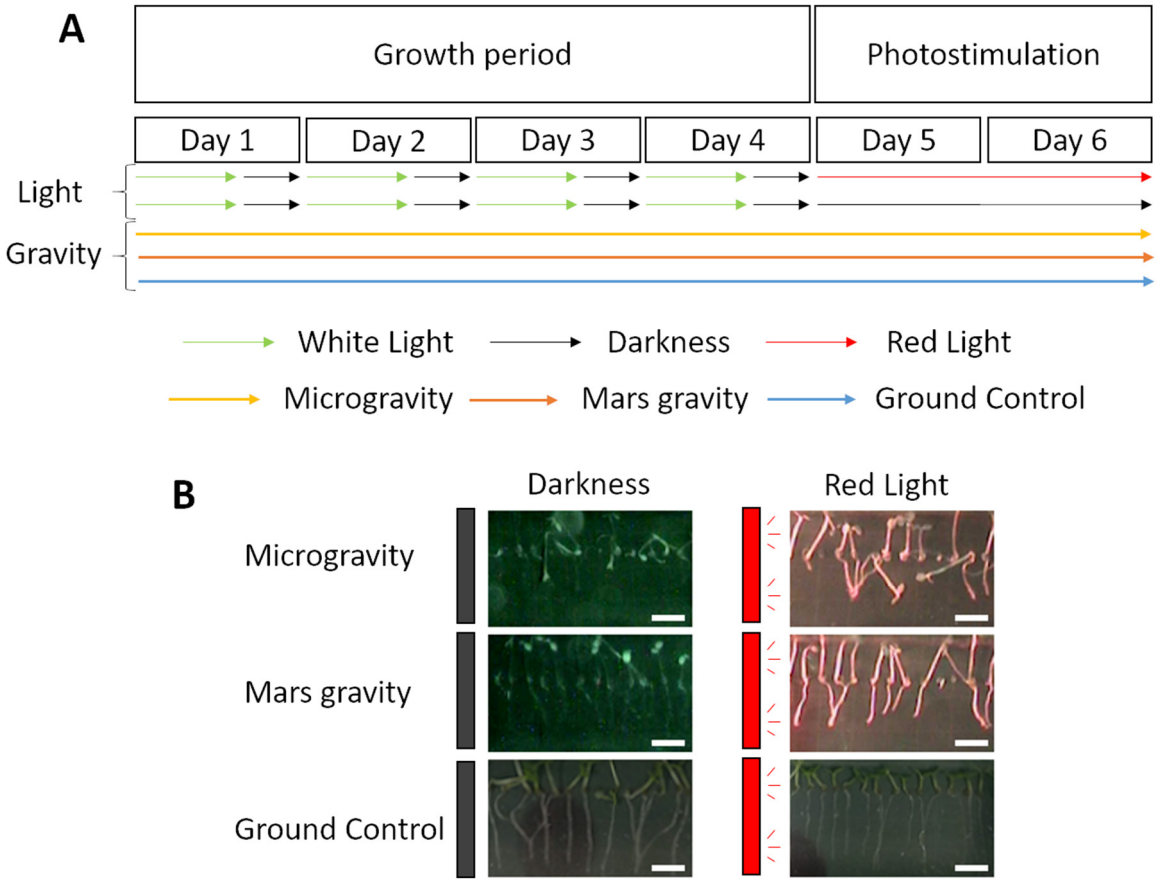

Figure 6. Experiment design. (**A**) Experimental timeline. Seedlings grown during six days in a long day photoperiod regime followed by two days of red-light photostimulation or darkness. (**B**) Images of seedlings at the end of the experiment. Grey and red rectangles at the left of the images represent light-emitting diode (LED) light position for photostimulation. Scale bar represents 3 mm.

At the Mars *g*-level, we observed a clear enrichment in WRKY TFs. They are involved in a wide variety of functions from abiotic and biotic stress response to developmental and multiple physiological processes on Earth [83,94–97]; reviewed in [47]. They also participate in hormonal response for example in JA/SA hormonal signaling. The WRKY family is defined by the presence of at least one WRKY DNA binding domain (DBD). They interact with W-box (with TTGACC/T motif) and clustered W-boxes located in the target genes that are activated or repressed under a specific condition. Most WRKY TFs are multifunctional meaning they play a role in a number of responses (see Table 1) thanks to multiple functional domains they contain (zinc-finger motifs, leucine zippers, kinase domain, (CaM)-binding domain etc.) [47,98,99]. For example, *AtWRKY75* which is upregulated at the Mars gravity level, plays a role in the immune process, response to osmotic stress, regulation of phosphorus deficiency signaling, development of the root hairs and has a positive effect on leaf senescence [100].

The multiple functional domains that each WRKY contains enable them to form complexes with numerous proteins and fulfil a wide range of functions [47]. This multi-functionality makes WRKY TFs a perfect target for genetic manipulation to create more resistant breeds that can be used in future space experiments. By modifying just one WRKY, a resistance to a set of abiotic and biotic stresses and developmental traits can be

achieved. Since TFs such as WRKY are key players in molecular breeding of crops due to their important role in the process of crop domestication [101,102], they have received a lot of attention in recent years. Genetic modification to obtain a specific positive trait was successfully used before, for example, to produce drought-resistant rice overexpressing *Os*WRKY30/70 [103,104]. Similar strategies could be applied also to develop cultivars for "space farming."

The upregulation of WRKY and other important TFs families, such as NACs, in Mars samples suggests that seedlings grown in partial gravity level activate multiple routes to cope with stress associated with space environment, and they can acclimate by modulating genome expression. On the other hand, among the genes upregulated in microgravity, a lower number of TFs can be found. In fact, as mentioned before, a number of ERFs which participate in development of tolerance to various adverse factors are downregulated in this condition.

Hormonal pathways promoting growth and proliferation are activated in microgravity and hormonal pathways promoting stress response are activated at Mars *g*-level

A summary of anatomical changes and changes in hormonal pathways is presented in Tables 2 and 3. Auxin and cytokinin pathways, two hormones regulating cell growth and proliferation, were disrupted differently in microgravity and Mars *g*-level. Our results suggest that both pathways were activated in the microgravity conditions, and few elements of these routes were repressed at Mars *g*-level. Dysregulation of auxin pathway in space-grown seedlings was reported in previous studies [23,29].

Table 2. Summary of anatomic changes in the root compared to the corresponding ground control. Arrow pointing up: increase. Arrow pointing down: decrease. Statistically significant changes are highlighted in red.

		Meristem Length	Meristem No. of Cells	Fibrillarin Area	Nucleolar Ultrastructure
Microgravity	Darkness	↑	↑	↑	↓
	Red Light	↑	↑	↑	↑
Mars gravity	Darkness	-	-	↓	↑
	Red Light	↑	↑	↑	↑

Table 3. Summary of phytohormone signaling changes in gene expression of each condition compared to the ground control. Arrow pointing up: upregulation. Arrow pointing down: downregulation. Red indicates stronger changes according to fold change (at least one step $Log_2FC > 1.5$).

		Auxin	CK	Brassino-steroids	ABA	Ethylene	JA	SA
Microgravity	Darkness	↑	↑	↓	↓	↑	↑	↓
	Red Light	↑	↑	↓	↑	↑	↑	↓
Mars gravity	Darkness	↓	↓	↓	↑	↑	↑	↑
	Red Light	↓	↓	↓	↑	↑	-	↑

The SA pathway was activated in red light at Mars *g* and inhibited in the microgravity darkness conditions, and the JA pathway was inhibited through JAZ proteins in all samples. Both SA and JA play major roles in the defense response to pathogens. The role of SA is to activate the resistance against biotrophic pathogens, whereas JA is involved in the activation of defense mechanisms [105]. Specifically, the principal function of JA is the promotion of the resistance to plant pathogens by production of defense compounds and, at the same time, it inhibits plant growth. Both, JA and SA, also participate in the response to abiotic stressors and development of tolerance. JA is involved in response to cold, drought, salinity and light (reviewed in [106]). SA was reported to be involved in

response to environmental stressors such as high and low temperature, drought, salinity and UV-B radiation (reviewed in [107]). SA-mediated mechanisms together with reactive oxygen species (ROS) and glutathione (GSH) regulate the transcription of different sets of defense genes in a spatio-temporal manner [108]. On the other hand, JA regulatory pathway act through the crosstalk with other phytohormone pathways including ABA, SA and ethylene [106] and is fine-tuned by numerous JA compounds and their different modes of action [109]. Hormones that promote plant growth, such as auxin, gibberellins and cytokinins, repress JA/SA mediated defense-response to prioritize the growth. On the other hand, activation of SA and JA routes can suppress these growth-promoting pathways to activate the defense [110].

JAZ proteins, which were upregulated in both gravity conditions, are transcriptional repressors in JA signaling [111], and by tuning down the response to JA, they enable the recovery of the organ growth [112]. They act on diverse TF families including bHLH, MYB or WRKY [113]. Furthermore, they interact with DELLA proteins to regulate JA and Gibberellin acid (GA) signaling [114], which leads to regulation of plant growth and plant defense response upon environmental conditions. JAZ1 was upregulated at Mars gravity and JAZ4 in microgravity. Apart from the leading role in plant resistance and defense, JAZ proteins are also implicated in the response to abiotic stresses. JAZ1 confers tolerance to alkaline stress [115] and JAZ4, which is not induced as other JAZ proteins by insects or wounding [116], was shown to be involved in control of leaf senescence [117], freezing tolerance [118], growth and development [113]. AIB, which interconnects JA-ABA pathways, was downregulated in microgravity conditions. AIB interacts with JAZ proteins to negatively regulate jasmonate responses. It is induced by ABA and participates in developing a drought tolerance [49]. The ABA pathway is strongly activated at Mars *g*-level. It is the most important regulator of the response to drought and osmotic stress in plants and a positive regulator of root hydrotropism [119]. ABA, together with MAP-kinase (MAPK) perception and signaling pathways, are involved in all abiotic stresses which cause the decrease of turgor pressure and water loss [48].

The ethylene pathway, together with ERFs, are involved in a wide range of stress responses. Although it has been suggested that the detection of an ethylene response in spaceflight experiments was an effect of the ethylene accumulated from the previous experiments, any ethylene accumulation during this experiment would have been erased from the hardware by a flushing procedure performed before the initiation of the experiment as well as by constant air flow by a connected gas removal module [20,21,120].

In summary, the dysregulation of different hormonal routes in our samples suggests that, in microgravity, the seedlings do not address the external stress and take the option of growing by activating growth and proliferation promoting auxin and cytokinin routes. On the other hand, in the Mars *g* samples, the growth-promoting routes are inhibited and ABA, ethylene and salicylic acid routes, known for their crucial role in response to osmotic, drought and biotic stresses, are activated.

4. Materials and Methods

4.1. Spaceflight Experiment and Procedures

The SG experiments were a series of spaceflight experiments aimed at investigating the response of young seedlings of *A. thaliana* to the joint stimuli of different levels of gravity and light. Here, we present results corresponding to part 2 and part 3 of the SG series (SG2 and SG3 experiments).

Experimental containers (ECs), each containing 5 culture chambers (cassettes) with 28 seeds attached to gridded nitrocellulose membrane with guar gum (as described in [37,121]) were used. SG2 was sent to the International Space Station (ISS) during the SpaceX CRS-4 (September 2014) and returned on CRS-5 (February 2015), and SG3 was sent to the ISS during the SpaceX CRS-11 campaign (June 2017) and returned a month later, on the same mission.

The experiment did not start until the ECs were loaded into the EMCS and the cassettes were hydrated [20]. Experimental conditions such as hydration, environmental humidity (>80%), gas exchange (O_2 levels kept at 10%; CO_2 at 0.45%) and temperature (22.5 °C ± 2 °C), were monitored and controlled remotely from the Norwegian User Support and Operation Centre (N-USOC, Trondheim, Norway). The GRR was performed at this site in the identical hardware using the same experimental conditions a few months later. During the experiment, seedlings were grown for four days in a long day photoperiod (16 h white light, 30–40 µmol/m^{2}s and 8 h darkness) at two nominal *g*-levels on board the ISS (microgravity and Mars gravity level nominally 0.3 *g* (0.34 ± 0.05 *g*), as provided by the EMCS centrifuge) and the Ground Reference Run 1*g* control. In the last two days of the timeline of the experiment, a change in the light conditions was introduced, half of the material was photostimulated with red light-emitting diodes (LEDs) on one lateral of the ECs, and the rest of the material was grown in darkness.

The timeline of the experiment is shown in Figure 6. The three gravity levels were constant for each EC throughout the duration of the experiment. Before the experiment began, flushing of the EMCS was performed to erase any possible traces of ethylene and other gases from previous experiments. When the six days of seedling growth were completed, the ISS astronauts then removed each EC from the EMCS and froze the samples at −80 °C in orbit (in the MELFI) or used the FixBox to fix the samples with aldehydes for morphological studies (as described in [37]). Germination rate was calculated as the percentage of germinated seeds.

4.2. Confocal Microscopy

The details of the spaceflight device (termed the FixBox) used for fixation of the samples in 5% (*w*/*v*) formaldehyde and the procedure are described in [122]. Briefly, seedlings were fixed in 5% (*w*/*v*) FA for 3 h at room temperature (RT) and then kept at 4 °C until return to Earth (µg and Mars *g*-level) or directly processed in the GRR. Fixative was rinsed three times in PBS and then seedlings were digested with digestion solution, containing: 2% (*w*/*v*) cellulase, 1% (*w*/*v*) pectinase, 0.05% (*w*/*v*) macerozyme, 0.4% (*w*/*v*) mannitol, 10% (*v*/*v*) glycerol and 0.2% (*v*/*v*) Triton x-100 in PBS for immunofluorescence with an anti-fibrillarin antibody (Abcam, Cambridge, UK, ab4566 [38F3]). For cell wall staining, the tissues were digested with enzymes not containing cellulose and with 0.5% macerozyme (*w*/*v*) and stained with SCRI 2200 a cellulose specific stain (Renaissance Chemicals, North Duffield, UK) [123,124]. Fibrillarin area and meristem size were measured with ImageJ v1.53c. Statistical analyses of the measurements were made using SPSS v25 software.

4.3. Electron Microscopy

The FixBox [122] was also used for fixation of the samples with 4.5% (*v*/*v*) glutaraldehyde (Sigma-Aldrich, St. Louis, MO, USA, #G5882) and 1.5% (*w*/*v*) formaldehyde (Electron Microscopy Sciences, Hatfield, PA, USA, #15710) in PBS for electron microscopy analysis. Following aldehyde fixation, samples were post-fixed in 1% (*w*/*v*) osmium tetroxide in PBS for 1 h and dehydrated in ethanol. Root tips were embedded in epoxy resin and then sectioned. Ultrathin sections were mounted on nickel grids coated with a 0.5% (*w*/*v*) Formvar film (Sigma-Aldrich, St. Louis, MO, USA, #09823) and stained with 5% (*w*/*v*) uranyl acetate (Electron Microscopy Sciences, Hatfield, PA, USA, #22400) and 0.3% (*w*/*v*) lead citrate (Electron Microscopy Sciences, Hatfield, PA, USA, #17800). Next, the samples were examined in a JEOL 1230 transmission electron microscope (TEM) at 80 kV.

4.4. RNA Extraction and Sequencing

Details of RNA extraction and sequencing are described in [37]. Briefly, the RNA extraction kit MACHEREY-NAGEL (Macherey-Nagel (MN), Düren, Germany, #740949) was used to extract RNA for pools of 8–10 seedlings. The RNA extraction kit includes DNAse treatment for 15 min. RNA quality was analyzed with the Bioanalyzer 2100 expert Plant RNA nano with Agilent RNA 6000 Nano Kit (Agilent Technologies, Santa Clara,

CA, USA, #5067-1511). Sequencing was performed on the Illumina HiSeq2500 sequencer (Center for Genomic Regulation, Barcelona, Spain) with stranded RNA read type and 50 bp read length. Seventeen total RNA samples were used to generate sequencing libraries using the Illumina TruSeq RNA Library Preparation Kit (Illumina, San Diego, CA, USA, #RS-122-2001). Samples were individually indexed. The samples then were combined at equimolar proportions into two pools. Each pool was loaded onto two lanes of a flow cell. Sequencing was performed until the 25 million reads per sample objective were reached (27.5 ± 1 millions of sequences obtained). Results from these studies have been deposited as the GLDS-314 and are available at NASA's GENELAB repository (DOI:10.26030/z5yf-jx91, https://genelab-data.ndc.nasa.gov/genelab/accession/GLDS-314, [40]).

4.5. Functional Analysis

Differential expression analysis was done using Deseq2 [125]. PCA was made using iDEP.91 [126]. Gene Ontology analysis of the DEGs was done using ShinyGO [53] with default settings and Metascape [127] with custom analysis adding molecular function and cellular component. ShinyGO was also used to analyze the distribution of query genes across the genome. Venn diagrams were made using jvenn [128]. String v11.0 was used for protein–protein interaction analysis [129]. Functional analysis of the dysregulated genes involved in phytohormone signaling pathway was performed using KEGG Pathway, the reference database for pathway mapping in KEGG MAPPER [130] available at Kyoto Encyclopedia of Genes and Genomes (KEGG). For the analysis of enrichment in a comparison of a specific gene family, a Chi-squared test was used using GraphPad software v5 (San Diego, CA, USA). The list of the identifiers and Log_2FC values of the genes dysregulated in microgravity (Table S1) and Mars *g*-level (Table S2) are given in the Supplementary Material.

5. Conclusions

We conclude that the response to reduced gravity does not show a gradual decrease in the intensity of the effects observed at microgravity, but clearly differentiated effects on plant growth and physiology are detected, as shown by anatomical and transcriptomic changes. In microgravity, *A. thaliana* accelerates cell proliferation and growth in the root meristem, even though some of the cellular processes, such as retrograde and anterograde communication, appear to be disturbed. This strategy could be activated by applying alternative directional cues, such as light (in particular, red light), and it could lead to adverse effects on the long-term plant development, considering the high energetic cost that it entails. On the other hand, at the Mars gravity level, the seedling perceives external stress and activates responses cooperating with the acclimation of the plant to the environmental conditions, such as upregulation of WRKY TFs. Red light increases cell proliferation at all gravity levels, as shown by microscopic and transcriptional analyses and it is particularly required to prime the adaptive stress response to the Mars *g*-level. In long-term applications, the combination of partial gravity level and red-light photostimulation could be used in space farming to avoid dysregulation of those pathways appearing affected in microgravity and to promote robust seedling growth.

Supplementary Materials: This article contains supplementary materials. Supplementary materials can be found at https://www.mdpi.com/1422-0067/22/2/899/s1. Figure S1. Extended Gene Ontology clusters affected by microgravity or Mars gravity, Figure S2. Common microgravity downregulated photosynthesis genes in GLDS-314 (µgrlgrrrl comparison, red photostimulated) and GLDS-251 (blue photostimulated), Figure S3. Venn diagrams of DEGs in common GO categories to the four comparisons, Figure S4. Hormone signal transduction changes in red light compared to darkness, Figure S5. Plastid and mitochondrial genome expression, Figure S6. Extended heatmaps of Gene Ontology analysis of the effect of red-light photostimulation across gravity levels, Table S1. List of the genes and the Log_2FC values of the dysregulated in microgravity, Table S2. List of the genes and the Log_2FC values of the dysregulated in Mars gravity, Table S3. Upregulated plastid and mitochondrial genes. List of references from Table 1.

Author Contributions: Conceptualization, R.H. and F.J.M.; methodology and investigation, A.V., M.C., A.M. and J.P.V.; writing—original draft, M.C., A.V. and R.H.; writing—review and editing, R.H., F.J.M. and J.Z.K.; supervision and funding acquisition, F.J.M., R.H. and J.Z.K. All authors have read and agreed to the published version of the manuscript.

Funding: This research was funded by the Agencia Estatal de Investigación of the Spanish Ministry of Science an Innovation, Grants #ESP2015-64323-R and #RTI2018-099309-B-I00 (co-funded by EU-ERDF) to F.J.M., by pre-doctoral fellowships to A.M. and A.V. from the Spanish National Program for Young Researchers Training (MINECO, Ref. #BES-2013-063933, #BES-2016-077976) and the Seedling Growth Project for ISS experimentation #LSRA2009-0932/ 1177, a shared project of ESA-ELIPS Program and NASA, to F.J.M. and J.Z.K. In addition, J.Z.K. is funded by Grants NNX12A065G and 80NSSC17K0546. This research is related to the Space Omics TT funded by the ESA contract 4000131202/20/NL/PG to R.H.

Data Availability Statement: The original sequencing data described in this study have been deposited at NASA's GENELAB repository as the GLDS-314 dataset (DOI: 10.26030/z5yf-jx91, https://genelab-data.ndc.nasa.gov/genelab/accession/GLDS-314, [40]).

Acknowledgments: We want to acknowledge the collaboration and support of many people who have contributed to the success of the experiments of the 'Seedling Growth' project, which are reported in this paper. This includes payload developers (Airbus), ESA and NASA managers, scientific collaborators (Eugenie Carnero-Diaz, Richard E. Edelmann, Julio Saez-Vasquez, Katherine D.L. Millar and Miguel Angel Valbuena) and the astronauts that performed the experiments on board the International Space Station, as well as the EMCS engineers and technicians (N-USOC) that performed the ground control operations.

Conflicts of Interest: The authors declare no conflict of interest. The funders had no role in the design of the study; in the collection, analyses, or interpretation of data; in the writing of the manuscript, or in the decision to publish the results.

Abbreviations

GRR	Ground Reference Run
EMCS	European Modular Cultivation System
ISS	International Space Station
SG	Seedling Growth experiment
DAPI	2-(4-amidinophenyl)-1H -indole-6-carboxamidine
GO	Gene Ontology
IAA	Indole acetic acid
JA	Jasmonic acid
SA	Salicylic acid
N-USOC	Norwegian User Support and Operation Center
PBS	Phosphate-Buffered Saline
RT	Room temperature
SED	Standard Error of the Difference
TEM	Transmission Electron Microscope
GC	Granular Component of the nucleolus
DFC	Dense Fibrillar Component of the nucleolus
FC	Fibrillar Centers of the nucleolus
µgd-grrd	comparison of transcriptome of seedlings grown in microgravity without photostimulation to the corresponding GRR
µgrl-grrrl	comparison of the transcriptome of seedlings photostimulated with red light for the last two days grown in microgravity to the corresponding GRR
Marsd-grrd	comparison of transcriptome of seedlings grown at Mars gravity level without photostimulation to the corresponding GRR

Marsrl-grrrl	comparison of the transcriptome of seedlings photostimulated with red light for the last two days grown at Mars gravity level to the corresponding GRR
µgrl-µgd, Marsrl-Marsd grrrl-grrd	transcriptomic data comparisons between two light conditions (red photostimulation and darkness) at each gravity level (µg, Mars *g*-level and 1*g* GRR)

References

1. Fu, Y.; Li, L.; Xie, B.; Dong, C.; Wang, M.; Jia, B.; Shao, L.; Dong, Y.; Deng, S.; Liu, H.; et al. How to establish a bioregenerative life support system for long-term crewed missions to the moon or mars. *Astrobiology* **2016**, *16*, 925–936. [CrossRef] [PubMed]
2. Vandenbrink, J.P.; Kiss, J.Z. Space, the final frontier: A critical review of recent experiments performed in microgravity. *Plant Sci.* **2016**, *243*, 115–119. [CrossRef] [PubMed]
3. Matía, I.; González-Camacho, F.; Herranz, R.; Kiss, J.Z.; Gasset, G.; van Loon, J.J.W.A.; Marco, R.; Medina, F.J. Plant cell proliferation and growth are altered by microgravity conditions in spaceflight. *J. Plant Physiol.* **2010**, *167*, 184–193. [CrossRef]
4. Ferl, R.J.; Paul, A.-L. The effect of spaceflight on the gravity-sensing auxin gradient of roots: GFP reporter gene microscopy on orbit. *NPJ Microgravity* **2016**, *2*, 15–23. [CrossRef]
5. Manzano, A.I.; Larkin, O.J.; Dijkstra, C.E.; Anthony, P.; Davey, M.R.; Eaves, L.; Hill, R.J.A.; Herranz, R.; Medina, F.J. Meristematic cell proliferation and ribosome biogenesis are decoupled in diamagnetically levitated *Arabidopsis* seedlings. *BMC Plant Biol.* **2013**, *13*, 124. [CrossRef]
6. Wyatt, S.E.; Kiss, J.Z. Plant tropisms: From Darwin to the International Space Station. *Am. J. Bot.* **2013**, *100*, 1–3. [CrossRef]
7. Kiss, J.Z. Where's the water? Hydrotropism in plants. *Proc. Natl. Acad. Sci. USA* **2007**, *104*, 4247–4248. [CrossRef]
8. Braam, J. In touch: Plant responses to mechanical stimuli. *New Phytol.* **2005**, *165*, 373–389. [CrossRef] [PubMed]
9. Muthert, L.W.F.; Izzo, L.G.; van Zanten, M.; Aronne, G. Root tropisms: Investigations on Earth and in space to unravel plant growth direction. *Front. Plant Sci.* **2020**, *10*, 1–22. [CrossRef] [PubMed]
10. Millar, K.D.L.; Kumar, P.; Correll, M.J.; Mullen, J.L.; Hangarter, R.P.; Edelmann, R.E.; Kiss, J.Z. A novel phototropic response to red light is revealed in microgravity. *New Phytol.* **2010**, *186*, 648–656. [CrossRef] [PubMed]
11. Vandenbrink, J.P.; Herranz, R.; Medina, F.J.; Edelmann, R.E.; Kiss, J.Z. A novel blue-light phototropic response is revealed in roots of *Arabidopsis thaliana* in microgravity. *Planta* **2016**, *244*, 1201–1215. [CrossRef] [PubMed]
12. Sullivan, J.A.; Deng, X.W. From seed to seed: The role of photoreceptors in *Arabidopsis* development. *Dev. Biol.* **2003**, *260*, 289–297. [CrossRef]
13. Yang, C. The effects of red, blue, and white light-emitting diodes on the growth, development, and edible quality of hydroponically grown lettuce (*Lactuca sativa* L. var. *capitata*). *Sci. Hortic.* **2013**, *150*, 86–91.
14. Reichler, S.A.; Balk, J.; Brown, M.E.; Woodruff, K.; Clark, G.B.; Roux, S.J. Light differentially regulates cell division and the mRNA abundance of pea nucleolin during de-etiolation. *Plant Physiol.* **2001**, *125*, 339–350. [CrossRef] [PubMed]
15. Valbuena, M.A.; Manzano, A.; Vandenbrink, J.P.; Pereda-Loth, V.; Carnero-Diaz, E.; Edelmann, R.E.; Kiss, J.Z.; Herranz, R.; Medina, F.J. The combined effects of real or simulated microgravity and red-light photoactivation on plant root meristematic cells. *Planta* **2018**, *248*, 691–704. [CrossRef]
16. Kiss, J.Z. Plant biology in reduced gravity on the Moon and Mars. *Plant Biol.* **2014**, *16*, 12–17. [CrossRef]
17. Crusan, J.; Bleacher, J.; Caram, J.; Craig, D.; Goodliff, K.; Herrmann, N.; Mahoney, E.; Smith, M. NASA's Gateway: An update on progress and plans for extending human presence to cislunar space. In Proceedings of the IEEE Conference on Aerospace, Big Sky, MT, USA, 2–9 March 2019.
18. Manzano, A.; Herranz, R.; den Toom, L.A.; te Slaa, S.; Borst, G.; Visser, M.; Medina, F.J.; van Loon, J.J.W.A. Novel, Moon and Mars, partial gravity simulation paradigms and their effects on the balance between cell growth and cell proliferation during early plant development. *NPJ Microgravity* **2018**, *4*, 1–11. [CrossRef]
19. Brinckmann, E. ESA hardware for plant research on the International Space Station. *Adv. Space Res.* **2005**, *36*, 1162–1166. [CrossRef]
20. Kiss, J.Z.; Aanes, G.; Schiefloe, M.; Coelho, L.H.F.; Millar, K.D.L.; Edelmann, R.E. Changes in operational procedures to improve spaceflight experiments in plant biology in the European Modular Cultivation System. *Adv. Space Res.* **2014**, *53*, 818–827. [CrossRef]
21. Vandenbrink, J.P.; Herranz, R.; Poehlman, W.L.; Feltus, F.A.; Villacampa, A.; Ciska, M.; Medina, F.J.; Kiss, J.Z. RNA-seq analyses of *Arabidopsis thaliana* seedlings after exposure to blue-light phototropic stimuli in microgravity. *Am. J. Bot.* **2019**, *106*, 1466–1476. [CrossRef]
22. Herranz, R.; Vandenbrink, J.P.; Villacampa, A.; Manzano, A.; Poehlman, W.L.; Feltus, F.A.; Kiss, J.Z.; Medina, F.J. RNAseq analysis of the response of *Arabidopsis thaliana* to fractional gravity under blue-light stimulation during spaceflight. *Front. Plant Sci.* **2019**, *10*, 1–11. [CrossRef] [PubMed]
23. Paul, A.-L.; Zupanska, A.K.; Schultz, E.R.; Ferl, R.J. Organ-specific remodeling of the *Arabidopsis* transcriptome in response to spaceflight. *BMC Plant Biol.* **2013**, *13*, 112. [CrossRef] [PubMed]
24. Basu, P.; Kruse, C.P.S.; Luesse, D.R.; Wyatt, S.E. Growth in spaceflight hardware results in alterations to the transcriptome and proteome. *Life Sci. Sp. Res.* **2017**, *15*, 88–96. [CrossRef] [PubMed]

25. Choi, W.-G.; Barker, R.J.; Kim, S.-H.; Swanson, S.J.; Gilroy, S. Variation in the transcriptome of different ecotypes of *Arabidopsis thaliana* reveals signatures of oxidative stress in plant responses to spaceflight. *Am. J. Bot.* **2019**, *106*, 123–136. [CrossRef] [PubMed]
26. Correll, M.J.; Pyle, T.P.; Millar, K.D.L.; Sun, Y.; Yao, J.; Edelmann, R.E.; Kiss, J.Z. Transcriptome analyses of *Arabidopsis thaliana* seedlings grown in space: Implications for gravity-responsive genes. *Planta* **2013**, *238*, 519–533. [CrossRef]
27. Fengler, S.; Spirer, I.; Neef, M.; Ecke, M.; Nieselt, K.; Hampp, R. A whole-genome microarray study of *Arabidopsis thaliana* semisolid callus cultures exposed to microgravity and nonmicrogravity related spaceflight conditions for 5 days on board of Shenzhou 8. *Biomed. Res. Int.* **2015**, *2015*. [CrossRef]
28. Hausmann, N.; Fengler, S.; Hennig, A.; Franz-Wachtel, M.; Hampp, R.; Neef, M. Cytosolic calcium, hydrogen peroxide and related gene expression and protein modulation in *Arabidopsis thaliana* cell cultures respond immediately to altered gravitation: Parabolic flight data. *Plant Biol.* **2014**, *16*, 120–128. [CrossRef]
29. Kruse, C.P.S.; Meyers, A.D.; Basu, P.; Hutchinson, S.; Luesse, D.R.; Wyatt, S.E. Spaceflight induces novel regulatory responses in *Arabidopsis* seedling as revealed by combined proteomic and transcriptomic analyses. *BMC Plant Biol.* **2020**, *20*, 1–16. [CrossRef]
30. Kwon, T.; Sparks, J.A.; Nakashima, J.; Allen, S.N.; Tang, Y.; Blancaflor, E.B. Transcriptional response of *Arabidopsis* seedlings during spaceflight reveals peroxidase and cell wall remodeling genes associated with root hair development. *Am. J. Bot.* **2015**, *102*, 21–35. [CrossRef]
31. Paul, A.L.; Popp, M.P.; Gurley, W.B.; Guy, C.; Norwood, K.L.; Ferl, R.J. *Arabidopsis* gene expression patterns are altered during spaceflight. *Adv. Space Res.* **2005**, *36*, 1175–1181. [CrossRef]
32. Yamazaki, C.; Fujii, N.; Miyazawa, Y.; Kamada, M.; Kasahara, H.; Osada, I.; Shimazu, T.; Fusejima, Y.; Higashibata, A.; Yamazaki, T.; et al. The gravity-induced re-localization of auxin efflux carrier CsPIN1 in cucumber seedlings: Spaceflight experiments for immunohistochemical microscopy. *NPJ Microgravity* **2016**, *2*, 1–7. [CrossRef] [PubMed]
33. Chandler, J.O.; Haas, F.B.; Khan, S.; Bowden, L.; Ignatz, M.; Enfissi, E.M.A.; Gawthorp, F.; Griffiths, A.; Fraser, P.D.; Rensing, S.A.; et al. Rocket science: The effect of spaceflight on germination physiology, ageing, and transcriptome of *Eruca sativa* seeds. *Life* **2020**, *10*, 49. [CrossRef] [PubMed]
34. Hoson, T.; Soga, K.; Wakabayashi, K.; Kamisaka, S.; Tanimoto, E. Growth and cell wall changes in rice roots during spaceflight. *Plant Soil* **2003**, *255*, 19–26. [CrossRef] [PubMed]
35. Jin, J.; Chen, H.; Cai, W. Transcriptome analysis of *Oryza sativa* calli under microgravity. *Microgravity Sci. Technol.* **2015**, *27*, 437–453. [CrossRef]
36. Sugimoto, M.; Oono, Y.; Gusev, O.; Matsumoto, T.; Yazawa, T.; Levinskikh, M.A.; Sychev, V.N.; Bingham, G.E.; Wheeler, R.; Hummerick, M. Genome-wide expression analysis of reactive oxygen species gene network in *Mizuna* plants grown in long-term spaceflight. *BMC Plant Biol.* **2014**, *14*, 1–11. [CrossRef]
37. Manzano, A.; Villacampa, A.; Sáez-Vásquez, J.; Kiss, J.Z.; Medina, F.J.; Herranz, R. The importance of Earth reference controls in spaceflight—Omics research: Characterization of nucleolin mutants from the seedling growth experiments. *iScience* **2020**, *23*, 101686. [CrossRef]
38. Rutter, L.; Barker, R.; Bezdan, D.; Cope, H.; Costes, S.V.; Degoricija, L.; Fisch, K.M.; Gabitto, M.I.; Gebre, S.; Giacomello, S.; et al. A new era for space life science: International standards for space omics processing. *Patterns* **2020**, *1*, 100148. [CrossRef]
39. Madrigal, P.; Gabel, A.; Villacampa, A.; Manzano, A.; Deane, C.S.; Bezdan, D.; Carnero-Diaz, E.; Medina, F.J.; Hardiman, G.; Grosse, I.; et al. Revamping space-omics in Europe. *Cell Syst.* **2020**, *11*, 555–556. [CrossRef]
40. Ray, S.; Gebre, S.; Fogle, H.; Berrios, D.C.; Tran, P.B.; Galazka, J.M.; Costes, S.V. GeneLab: Omics database for spaceflight experiments. *Bioinformatics* **2019**, *35*, 1753–1759. [CrossRef]
41. Kiss, J.Z. Mechanisms of the early phases of plant gravitropism. *CRC Crit. Rev. Plant Sci.* **2000**, *19*, 551–573. [CrossRef]
42. Barneche, F.; Steinmetz, F.; Echeverria, M. Fibrillarin genes encode both a conserved nucleolar protein and a novel snoRNA involved in rRNA methylation in *Arabidopsis thaliana*. *J. Biol. Chem.* **2000**. [CrossRef] [PubMed]
43. Guerrero, F.; De la Torre, C.; García-Herdugo, G. Control of nucleolar growth during interphase in higher plant meristem cells. *Protoplasma* **1989**, *152*, 96–100. [CrossRef]
44. Sáez-Vásquez, J.; Medina, F.J. The plant nucleolus. *Adv. Bot. Res.* **2008**, *47*, 1–46.
45. Manzano, A.I.; Herranz, R.; Manzano, A.; van Loon, J.J.W.A.; Medina, F.J. Early effects of altered gravity environments on plant cell growth and cell proliferation: Characterization of morphofunctional nucleolar types in an *Arabidopsis* cell culture system. *Front. Astron. Sp. Sci.* **2016**, *3*, 2. [CrossRef]
46. Wang, S.; Chang, Y.; Guo, J.; Zeng, Q.; Ellis, B.E.; Chen, J. *Arabidopsis* ovate family proteins, a novel transcriptional repressor family, control multiple aspects of plant growth and development. *PLoS ONE* **2011**, *6*, e23896. [CrossRef] [PubMed]
47. Phukan, U.J.; Jeena, G.S.; Shukla, R.K. WRKY transcription factors: Molecular regulation and stress responses in plants. *Front. Plant Sci.* **2016**, *7*, 1–14. [CrossRef]
48. Danquah, A.; de Zelicourt, A.; Colcombet, J.; Hirt, H. The role of ABA and MAPK signaling pathways in plant abiotic stress responses. *Biotechnol. Adv.* **2014**, *32*, 40–52. [CrossRef]
49. Li, H.; Sun, J.; Xu, Y.; Jiang, H.; Wu, X.; Li, C. The bHLH-type transcription factor AtAIB positively regulates ABA response in *Arabidopsis*. *Plant Mol. Biol.* **2007**, *65*, 655–665. [CrossRef]
50. Burke, R.; Schwarze, J.; Sherwood, O.L.; Jnaid, Y.; Mccabe, P.F.; Kacprzyk, J. Stressed to death: The role of transcription factors in plant programmed cell death induced by abiotic and biotic stimuli. *Front. Plant Sci.* **2020**, *11*, 1–12. [CrossRef]

51. Aoi, Y.; Tanaka, K.; Cook, S.D.; Hayashi, K.-I.; Kasahara, H. GH3 auxin-amido synthetases alter the ratio of indole-3-acetic acid and phenylacetic acid in *Arabidopsis*. *Plant Cell. Physiol.* **2020**, *61*, 596–605. [CrossRef]
52. Hutchison, C.E.; Li, J.; Argueso, C.; Gonzalez, M.; Lee, E.; Lewis, M.W.; Maxwell, B.B.; Perdue, T.D.; Schaller, G.E.; Alonso, J.M.; et al. The *Arabidopsis* histidine phosphotransfer proteins are redundant positive regulators of cytokinin signaling. *Plant Cell* **2006**, *18*, 3073–3087. [CrossRef] [PubMed]
53. Ge, S.X.; Jung, D.; Yao, R. ShinyGO: A graphical gene-set enrichment tool for animals and plants. *Bioinformatics* **2020**, *36*, 2628–2629. [CrossRef] [PubMed]
54. Johnson, C.M.; Subramanian, A.; Pattathil, S.; Correll, M.J.; Kiss, J.Z. Comparative transcriptomics indicate changes in cell wall organization and stress response in seedlings during spaceflight. *Am. J. Bot.* **2017**, *104*, 1219–1231. [CrossRef]
55. Herranz, R.; Benguría, A.; Laván, D.A.; López-Vidriero, I.; Gasset, G.; Medina, F.J.; van Loon, J.J.W.A.; Marco, R. Spaceflight-related suboptimal conditions can accentuate the altered gravity response of *Drosophila* transcriptome. *Mol. Ecol.* **2010**, *19*, 4255–4264. [CrossRef]
56. Silveira, W.A.; Fazelinia, H.; Rosenthal, S.B.; Mason, C.E.; Costes, S.V. Comprehensive multi-omics analysis reveals mitochondrial stress as a central biological hub for spaceflight impact. *Cell* **2020**, *183*, 1185–1201.e20. [CrossRef]
57. Leu, W.M.; Cao, X.L.; Wilson, T.J.; Snustad, D.P.; Chua, N.H. Phytochrome A and phytochrome B mediate the hypocotyl-specific downregulation of TUB1 by light in *Arabidopsis*. *Plant Cell* **1995**, *7*, 2187–2196. [PubMed]
58. Nakajima, K.; Kawamura, T.; Hashimoto, T. Role of the *SPIRAL*$_1$ gene family in anisotropic growth of *Arabidopsis thaliana*. *Plant Cell Physiol.* **2006**, *47*, 513–522. [CrossRef]
59. Wakabayashi, K.; Soga, K.; Hoson, T.; Kotake, T.; Yamazaki, T.; Ishioka, N.; Shimazu, T.; Kamada, M. Microgravity affects the level of matrix polysaccharide 1,3:1,4-β-glucans in cell walls of rice shoots by increasing the expression level of a gene involved in their breakdown. *Astrobiology* **2020**, *20*, 820–829. [CrossRef]
60. Mo, M.; Yokawa, K.; Wan, Y.; Baluška, F. How and why do root apices sense light under the soil surface? *Front. Plant Sci.* **2015**, *6*, 1–8. [CrossRef]
61. Kiss, J.Z.; Mullen, J.L.; Correll, M.J.; Hangarter, R.P. Phytochromes A and B mediate red-light-induced positive phototropism in roots. *Plant Physiol.* **2003**, *131*, 1411–1417. [CrossRef]
62. Correll, M.J.; Edelmann, R.E.; Hangarter, R.P.; Mullen, J.L.; Kiss, J.Z. Ground-based studies of tropisms in hardware developed for the European Modular Cultivation System (EMCS). *Adv. Space Res.* **2005**, *36*, 1203–1210. [CrossRef]
63. Jiao, S.; Hilaire, E.; Paulsen, A.Q.; Guikema, J.A. *Brassica rapa* plants adapted to microgravity with reduced photosystem I and its photochemical activity. *Physiol. Plant* **2004**, 281–290. [CrossRef]
64. Chen, B.; Zhang, A.; Lu, Q. Characterization of photosystem I in rice (*Oryza sativa* L.) seedlings upon exposure to random positioning machine. *Photosynth. Res.* **2013**, *116*, 93–105. [CrossRef] [PubMed]
65. Stutte, G.W.; Monje, O.; Hatfield, R.D.; Paul, A.L.; Ferl, R.J.; Simone, C.G. Microgravity effects on leaf morphology, cell structure, carbon metabolism and mRNA expression of dwarf wheat. *Planta* **2006**, *224*, 1038–1049. [CrossRef] [PubMed]
66. Mikhaylenko, N.F.; Sytnik, S.K.; Zolotareva, E.K. Effects of slow clinorotation on lipid contents and proton permeability of thylakoid membranes of pea chloroplasts. *Adv. Space Res.* **2001**, *27*, 1007–1010. [CrossRef]
67. Adamchuk, N.I. Ultrastructural and functional changes of photosynthetic apparatus of *Arabidopsis thaliana* (L.) Heynh induced by clinorotation. *Adv. Space Res.* **1998**, *177*, 1131–1134. [CrossRef]
68. Staneloni, R.J.; Rodriguez-Batiller, M.J.; Casal, J.J. Abscisic acid, high-light, and oxidative stress down-regulate a photosynthetic gene via a promoter motif not involved in phytochrome-mediated transcriptional regulation. *Mol. Plant* **2008**, *1*, 75–83. [CrossRef]
69. Xu, Y.; Liu, R.; Yan, L.; Liu, Z.; Jiang, S.; Shen, Y. Light-harvesting chlorophyll a/b-binding proteins are required for stomatal response to abscisic acid in *Arabidopsis*. *J. Exp. Bot.* **2012**, *63*, 1095–1106. [CrossRef] [PubMed]
70. Zhu, D.; Wu, Z.; Cao, G.; Li, J.; Wei, J.; Tsuge, T.; Hongya, G.; Takashi, A.; Li-Jia, Q. Translucent green, an ERF family transcription factor, controls water balance. *Mol. Plant* **2014**, *7*, 601–615. [CrossRef]
71. Gilmour, S.J.; Fowler, S.G.; Thomashow, M.F. *Arabidopsis* transcriptional activators CBF1, CBF2, and CBF3 have matching functional activities. *Plant Mol. Biol.* **2004**, *54*, 767–781. [CrossRef]
72. Jaglo-Ottosen, K.R.; Gilmour, S.J.; Zarka, D.G.; Schabenberger, O.; Thomashow, M.F. *Arabidopsis* CBF1 overexpression induces COR genes and enhances freezing tolerance. *Science* **1998**, *280*, 104–106. [CrossRef] [PubMed]
73. Ogawa, T.; Pan, L.; Kawai-Yamada, M.; Yu, L.H.; Yamamura, S.; Koyama, T.; Kitajima, S.; Ohme-Takagi, M.; Sato, F.; Uchimiya, H. Functional analysis of *Arabidopsis* ethylene-responsive element binding protein conferring resistance to Bax and abiotic stress-induced plant cell death. *Plant Physiol.* **2005**, *138*, 1436–1445. [CrossRef] [PubMed]
74. Leister, D.; Wang, L.; Kleine, T. Organellar gene expression and acclimation of plants to environmental stress. *Front. Plant Sci.* **2017**, *8*. [CrossRef] [PubMed]
75. Wicke, S.; Schneeweiss, G.M.; dePamphilis, C.W.; Müller, K.F.; Quandt, D. The evolution of the plastid chromosome in land plants: Gene content, gene order, gene function. *Plant Mol. Biol.* **2011**, *76*, 273–297. [CrossRef] [PubMed]
76. Unseld, M.; Marienfeld, J.R.; Brandt, P.; Brennicke, A. The mitochondrial genome of *Arabidopsis* thaliana contains 57 genes in 366,924 nucleotides. *Nat. Genet.* **1997**, *15*, 1–5. [CrossRef]
77. Yamburenko, M.V.; Zubo, Y.O.; Vanková, R.; Kusnetsov, V.V.; Kulaeva, O.N.; Börner, T. Abscisic acid represses the transcription of chloroplast genes. *J. Exp. Bot.* **2013**, *64*, 4491–4502. [CrossRef]

78. Vanlerberghe, G.C. Alternative oxidase: A mitochondrial respiratory pathway to maintain metabolic and signaling homeostasis during abiotic and biotic stress in plants. *Int. J. Mol. Sci.* **2013**, *14*, 6805–6847. [CrossRef]
79. Van Aken, O.; Zhang, B.; Law, S.; Narsai, R.; Whelan, J. AtWRKY40 and AtWRKY63 modulate the expression of stress-responsive nuclear genes encoding mitochondrial and chloroplast proteins. *Plant Physiol.* **2013**, *162*, 254–271. [CrossRef]
80. Van Aken, O.; Zhang, B.; Carrie, C.; Uggalla, V.; Paynter, E.; Giraud, E.; Whelan, J. Defining the mitochondrial stress response in *Arabidopsis thaliana*. *Mol. Plant* **2009**, *2*, 1310–1324. [CrossRef]
81. Schwarzländer, M.; König, A.C.; Sweetlove, L.J.; Finkemeier, I. The impact of impaired mitochondrial function on retrograde signalling: A meta-analysis of transcriptomic responses. *J. Exp. Bot.* **2012**, *63*, 1735–1750. [CrossRef]
82. Wang, Y.; Berkowitz, O.; Selinski, J.; Xu, Y.; Hartmann, A.; Whelan, J. Stress responsive mitochondrial proteins in *Arabidopsis thaliana*. *Free Radic. Biol. Med.* **2018**, *122*, 28–39. [CrossRef] [PubMed]
83. Meng, X.; Li, L.; Narsai, R.; De Clercq, I.; Whelan, J.; Berkowitz, O. Mitochondrial signalling is critical for acclimation and adaptation to flooding in *Arabidopsis thaliana*. *Plant J.* **2020**, *103*, 227–247. [CrossRef] [PubMed]
84. Van Aken, O.; De Clercq, I.; Ivanova, A.; Law, S.R.; van Breusegem, F.; Millar, A.H.; Whelan, L. Mitochondrial and chloroplast stress responses are modulated in distinct touch and chemical inhibition phases. *Plant Physiol.* **2016**, *171*, 2150–2165. [CrossRef] [PubMed]
85. Lee, D.; Polisensky, D.H.; Braam, J. Genome-wide identification of touch- and darkness-regulated *Arabidopsis* genes: A focus on calmodulin-like and XTH genes. *New Phytol.* **2005**, *165*, 429–444. [CrossRef] [PubMed]
86. Liao, J.; Liu, G.; Monje, O.; Stutte, G.W.; Porterfield, D.M. Induction of hypoxic root metabolism results from physical limitations in O_2 bioavailability in microgravity. *Adv. Space Res.* **2004**, *34*, 1579–1584. [CrossRef]
87. Pedersen, O.; Sauter, M.; Colmer, T.D.; Nakazono, M. Regulation of root adaptive anatomical andmorphological traits during low soil oxygen. *New Phytol.* **2020**. [CrossRef]
88. Millar, K.D.L.; Johnson, C.M.; Edelmann, R.E.; Kiss, J.Z. An endogenous growth pattern of roots is revealed in seedlings grown in microgravity. *Astrobiology* **2011**, *11*, 787–797. [CrossRef]
89. Stout, S.C.; Porterfield, D.M.; Briarty, L.G.; Kuang, A.; Musgrave, M.E. Evidence of root zone hypoxia in *Brassica rapa* L. grown in microgravity. *Int. J. Plant Sci.* **2001**, *162*, 249–255. [CrossRef]
90. Ban, Y.; Kobayashi, Y.; Hara, T.; Hamada, T.; Hashimoto, T.; Takeda, S.; Hattori, T. α-Tubulin is rapidly phosphorylated in response to hyperosmotic stress in rice and *Arabidopsis*. *Plant Cell Physiol.* **2013**, *54*, 848–858. [CrossRef]
91. Nakano, T.; Suzuki, K.; Fujimura, T.; Shinshi, H. Genome-wide analysis of the ERF gene family in *Arabidopsis* and rice. *Plant Physiol.* **2006**, *140*, 411–432. [CrossRef]
92. Rajhi, I.; Yamauchi, T.; Takahashi, H.; Nishiuchi, S.; Shiono, K. Identification of genes expressed in maize root cortical cells during lysigenous aerenchyma formation using laser microdissection and microarray analyses. *New Phytol.* **2011**, 351–368. [CrossRef] [PubMed]
93. Safavi-Rizi, V.; Herde, M.; Stöhr, C. RNA-Seq reveals novel genes and pathways associated with hypoxia duration and tolerance in tomato root. *Sci. Rep.* **2020**, *10*, 1–17.
94. Ding, Z.J.; Yan, J.Y.; Li, C.X.; Li, G.X.; Wu, Y.R.; Zheng, S.J. Transcription factor WRKY46 modulates the development of *Arabidopsis* lateral roots in osmotic/salt stress conditions via regulation of ABA signaling and auxin homeostasis. *Plant J.* **2015**, *84*, 56–69. [CrossRef] [PubMed]
95. Zhang, Y.; Yu, H.; Yang, X.; Li, Q.; Ling, J.; Wang, H.; Gu, X.; Huang, S.; Jiang, W. CsWRKY46, a WRKY transcription factor from cucumber, confers cold resistance in transgenic-plant by regulating a set of cold-stress responsive genes in an ABA-dependent manner. *Plant Physiol. Biochem.* **2016**, *108*, 478–487. [CrossRef] [PubMed]
96. Kim, K.C.; Lai, Z.; Fan, B.; Chen, Z. *Arabidopsis* WRKY38 and WRKY62 transcription factors interact with histone deacetylase 19 in basal defense. *Plant Cell* **2008**, *20*, 2357–2371. [CrossRef]
97. Finatto, T.; Viana, V.E.; Woyann, L.G.; Busanello, C.; da Maia, L.C.; de Oliveira, A.C. Can WRKY transcription factors help plants to overcome environmental challenges? *Genet. Mol. Biol.* **2018**, *41*, 533–544. [PubMed]
98. Chen, L.; Song, Y.; Li, S.; Zhang, L.; Zou, C.; Yu, D. The role of WRKY transcription factors in plant abiotic stresses. *Biochimica Biophysica Acta (BBA)-Gene Regul. Mech.* **2012**, *1819*, 120–128. [CrossRef]
99. Park, C.Y.; Lee, J.H.; Yoo, J.H.; Moon, B.C.; Choi, M.S.; Kang, Y.H.; Lee, S.M.; Kim, H.S.; Kang, K.Y.; Chung, W.S.; et al. WRKY group IId transcription factors interact with calmodulin. *FEBS Lett.* **2005**, *579*, 1545–1550. [CrossRef]
100. Li, Z.; Peng, J.; Wen, X.; Guo, H. Gene network analysis and functional studies of senescence-associated genes reveal novel regulators of *Arabidopsis* leaf senescence. *J. Integr. Plant Biol.* **2012**, *54*, 526–539. [CrossRef]
101. Century, K.; Reuber, T.L.; Ratcliffe, O.J. Regulating the regulators: The future prospects for transcription-factor-based agricultural biotechnology products. *Plant Physiol.* **2008**, *147*, 20–29. [CrossRef]
102. Doebley, J.F.; Gaut, B.S.; Smith, B.D. The molecular genetics of crop domestication. *Cell* **2006**, *127*, 1309–1321. [CrossRef] [PubMed]
103. Raineri, J.; Wang, S.; Peleg, Z.; Blumwald, E.; Chan, R.L. The rice transcription factor OsWRKY47 is a positive regulator of the response to water deficit stress. *Plant Mol. Biol.* **2015**, *88*, 401–413. [CrossRef] [PubMed]
104. Shen, H.; Liu, C.; Zhang, Y.; Meng, X.; Zhou, X.; Chu, C.; Wang, X. OsWRKY30 is activated by MAP kinases to confer drought tolerance in rice. *Plant Mol. Biol.* **2012**, *80*, 241–253. [CrossRef] [PubMed]
105. Caarls, L.; Pieterse, C.M.J.; Van Wees, S.C.M. How salicylic acid takes transcriptional control over jasmonic acid signaling. *Front. Plant Sci.* **2015**, *6*, 1–11. [CrossRef]

106. Wang, J.; Song, L.; Gong, X.; Xu, J.; Li, M. Functions of jasmonic acid in plant regulation and response to abiotic stress. *Int. J. Mol. Sci.* **2020**, *21*, 1446. [CrossRef]
107. Khan, M.I.R.; Fatma, M.; Per, T.S.; Anjum, N.A.; Khan, N.A. Salicylic acid-induced abiotic stress tolerance and underlying mechanisms in plants. *Front. Plant Sci.* **2015**, *6*, 1–17. [CrossRef]
108. Herrera-Vásquez, A.; Salinas, P.; Holuigue, L. Salicylic acid and reactive oxygen species interplay in the transcriptional control of defense genes expression. *Front. Plant Sci.* **2015**, *6*, 1–9. [CrossRef]
109. Wasternack, C.; Strnad, M. Jasmonate signaling in plant stress responses and development—Active and inactive compounds. *New Biotechnol.* **2016**, *33*, 604–613. [CrossRef]
110. Pieterse, C.M.J.; Van Der Does, D.; Zamioudis, C.; Leon-Reyes, A.; Van Wees, S.C.M. Hormonal modulation of plant immunity. *Annu. Rev. Cell Dev. Biol.* **2012**, *28*, 489–521. [CrossRef]
111. Kazan, K.; Manners, J.M. JAZ repressors and the orchestration of phytohormone crosstalk. *Trends Plant Sci.* **2012**, *17*, 22–31. [CrossRef]
112. Guo, Q.; Yoshida, Y.; Major, I.T.; Wang, K.; Sugimoto, K.; Kapali, G.; Havko, N.E.; Benning, C.; Howe, G.A. JAZ repressors of metabolic defense promote growth and reproductive fitness in *Arabidopsis*. *Proc. Natl. Acad. Sci. USA* **2018**, *115*, E10768–E10777. [CrossRef] [PubMed]
113. Oblessuc, P.R.; Obulareddy, N.; DeMott, L.; Matiolli, C.C.; Thompson, B.K.; Melotto, M. JAZ4 is involved in plant defense, growth, and development in *Arabidopsis*. *Plant J.* **2020**, *101*, 371–383. [CrossRef] [PubMed]
114. Qi, T.; Huang, H.; Wu, D.; Yan, J.; Qi, Y.; Song, S.; Xie, D. *Arabidopsis* DELLA and JAZ proteins bind the WD-Repeat/bHLH/MYB complex to modulate gibberellin and jasmonate signaling synergy. *Plant Cell* **2014**, *26*, 1118–1133. [CrossRef] [PubMed]
115. Zhu, D.; Li, R.; Liu, X.; Sun, M.; Wu, J.; Zhang, N.; Zhu, Y. The positive regulatory roles of the TIFY10 proteins in plant responses to alkaline stress. *PLoS ONE* **2014**, *9*, e111984. [CrossRef] [PubMed]
116. Hoo, S.C.; Koo, A.J.K.; Gao, X.; Jayanty, S.; Thines, B.; Jones, A.D.; Howe, G.A. Regulation and function of Arabidopsis JASMONATE ZIM-domain genes in response to wounding and herbivory. *Plant Physiol.* **2008**, *146*, 952–964.
117. Jiang, Y.; Liang, G.; Yang, S.; Yu, D. *Arabidopsis* WRKY57 functions as a node of convergence for jasmonic acid- and auxin-mediated signaling in jasmonic acid-induced leaf senescence. *Plant Cell* **2014**, *26*, 230–245. [CrossRef]
118. Hu, Y.; Jiang, L.; Wang, F.; Yu, D. Jasmonate regulates the INDUCER OF CBF expression-C-repeat binding factor/dre binding factor1 cascade and freezing tolerance in *Arabidopsis*. *Plant Cell* **2013**, *25*, 2907–2924. [CrossRef]
119. Takahashi, N.; Goto, N.; Okada, K.; Takahashi, H. Hydrotropism in abscisic acid, wavy, and gravitropic mutants of *Arabidopsis thaliana*. *Planta* **2002**, *216*, 203–211. [CrossRef]
120. Kiss, J.Z. Conducting plant experiments in space. In *Plant Gravitropism: Methods and Protocols*; Blancaflor, E.B., Ed.; Springer: New York, NY, USA, 2015; pp. 255–283.
121. Vandenbrink, J.P.; Kiss, J.Z. Preparation of a spaceflight experiment to study tropisms in Arabidopsis seedlings on the International Space Station. *Methods Mol. Biol.* **2019**, *1924*, 207–214.
122. Manzano, A.; Creus, E.; Tomás, A.; Valbuena, M.A.; Villacampa, A.; Ciska, M.; Edelmann, R.E.; Kiss, J.Z.; Medina, F.J.; Herranz, R. The fixbox: Hardware to provide on-orbit fixation capabilities to the EMCS on the ISS. *Microgravity Sci. Technol.* **2020**, *32*, 1105–1120. [CrossRef]
123. Musielak, T.J.; Schenkel, L.; Kolb, M.; Henschen, A.; Bayer, M. A simple and versatile cell wall staining protocol to study plant reproduction. *Plant Reprod.* **2015**, *28*, 161–169. [CrossRef] [PubMed]
124. Robert, H.S.; Grunewald, W.; Sauer, M.; Cannoot, B.; Soriano, M.; Swarup, R.; Weijers, D.; Bennett, M.; Boutilier, K.; Friml, J. Plant embryogenesis requires aux/lax-mediated auxin influx. *Development* **2015**, *142*, 702–711. [CrossRef] [PubMed]
125. Love, M.I.; Huber, W.; Anders, S. Moderated estimation of fold change and dispersion for RNA-seq data with DESeq2. *Genome Biol.* **2014**, *15*, 1–21. [CrossRef] [PubMed]
126. Ge, S.X.; Son, E.W.; Yao, R. iDEP: An integrated web application for differential expression and pathway analysis of RNA-Seq data. *BMC Bioinform.* **2018**, *19*, 1–24. [CrossRef]
127. Zhou, Y.; Zhou, B.; Pache, L.; Chang, M.; Khodabakhshi, A.H.; Tanaseichuk, O.; Benner, C.; Chanda, S.K. Metascape provides a biologist-oriented resource for the analysis of systems-level datasets. *Nat. Commun.* **2019**, *10*. [CrossRef]
128. Bardou, P.; Mariette, J.; Escudié, F.; Djemiel, C.; Klopp, C. Jvenn: An interactive Venn diagram viewer. *BMC Bioinform.* **2014**, *15*, 1–7. [CrossRef]
129. Szklarczyk, D.; Gable, A.L.; Lyon, D.; Junge, A.; Wyder, S.; Huerta-Cepas, J.; Simonovic, M.; Doncheva, N.T.; Morris, J.H.; Bork, P.; et al. STRING v11: Protein-protein association networks with increased coverage, supporting functional discovery in genome-wide experimental datasets. *Nucleic Acids Res.* **2019**, *47*, D607–D613. [CrossRef]
130. Kanehisa, M.; Sato, Y. KEGG mapper for inferring cellular functions from protein sequences. *Protein Sci.* **2020**, 28–35. [CrossRef]

RESEARCH ARTICLE

American Journal of Botany

Botanical Society of America
leading scientists and educators since 1893

RNA-seq analyses of *Arabidopsis thaliana* seedlings after exposure to blue-light phototropic stimuli in microgravity

Joshua P. Vandenbrink[1,2,5], Raul Herranz[3], William L. Poehlman[4], F. Alex Feltus[4], Alicia Villacampa[3], Malgorzata Ciska[3], F. Javier Medina[3], and John Z. Kiss[2]

Manuscript received 9 April 2019; revision accepted 17 September 2019.

[1] School of Biological Sciences, Louisiana Tech University, Ruston, LA 71272, USA

[2] Department of Biology, University of North Carolina at Greensboro, Greensboro, NC 27402, USA

[3] Centro de Investigaciones Biológicas (CSIC), Madrid E28040, Spain

[4] Department of Genetics and Biochemistry, Clemson University, Clemson, SC 29634, USA

[5] Author for correspondence (e-mail: jpvdb@latech.edu)

Citation: Vandenbrink, J. P., R. Herranz, W. L. Poehlman, F. A. Feltus, A. Villacampa, M. Ciska, F. J. Medina, and J. Z. Kiss. 2019. RNA-seq analyses of *Arabidopsis thaliana* seedlings after exposure to blue-light phototropic stimuli in microgravity. *American Journal of Botany* 106(11): 1466–1476.

doi:10.1002/ajb2.1384

PREMISE: Plants synthesize information from multiple environmental stimuli when determining their direction of growth. Gravity, being ubiquitous on Earth, plays a major role in determining the direction of growth and overall architecture of the plant. Here, we utilized the microgravity environment on board the International Space Station (ISS) to identify genes involved influencing growth and development of phototropically stimulated seedlings of *Arabidopsis thaliana*.

METHODS: Seedlings were grown on the ISS, and RNA was extracted from 7 samples (pools of 10–15 plants) grown in microgravity (μ*g*) or Earth gravity conditions (1-*g*). Transcriptomic analyses via RNA sequencing (RNA-seq) of differential gene expression was performed using the HISAT2-Stringtie-DESeq2 RNASeq pipeline. Differentially expressed genes were further characterized by using Pathway Analysis and enrichment for Gene Ontology classifications.

RESULTS: For 296 genes that were found significantly differentially expressed between plants in microgravity compared to 1-*g* controls, Pathway Analysis identified eight molecular pathways that were significantly affected by reduced gravity conditions. Specifically, light-associated pathways (e.g., photosynthesis-antenna proteins, photosynthesis, porphyrin, and chlorophyll metabolism) were significantly downregulated in microgravity.

CONCLUSIONS: Gene expression in *A. thaliana* seedlings grown in microgravity was significantly altered compared to that of the 1-*g* control. Understanding how plants grow in conditions of microgravity not only aids in our understanding of how plants grow and respond to the environment but will also help to efficiently grow plants during long-range space missions.

KEY WORDS European Modular Cultivation System; phototropism; spaceflight; transcriptomics; tropisms.

Due to their sessile nature, plants need to be able to integrate multiple external stimuli to direct their growth and development. These growth-mediated movements (or "tropisms") were first scientifically characterized by Darwin and Darwin (1880), who theorized the movement was modified circumnutation. Multiple external stimuli affect plant growth and development such as water availability (Kiss, 2007), mechanical forces (Braam, 2005), gravity (Chen et al., 1999; Kiss, 2000), and light (Briggs, 2014; Liscum et al., 2014; Vandenbrink et al., 2014a; Kutschera and Briggs, 2016), among others. Taken together, these tropisms play a large role in determining the overall architecture of the plant (Correll and Kiss, 2002). In addition, sensing and responding to these external cues are important for the plant to be able to adapt to changing environmental conditions.

Plants take multiple environmental stimuli into account when determining growth strategy. Typically, plants orient their roots toward the gravity vector (positive gravitropic response), whereas aerial organs orient away from the gravity vector (negative gravitropic response) and toward a blue/white light source (positive phototropic response; Chen et al., 1999; Kiss et al., 2003; Briggs, 2014; Kutschera and Briggs, 2016).

In addition, plants utilize blue-light cues to influence lateral root growth and other root architectural characteristics (Moni et al., 2015).

Light irradiation also affects root length (Laxmi et al., 2008; Silva-Navas et al., 2015). The effect of light on roots is significant, as light has been shown to penetrate several millimeters into the soil (Woolley and Stoller, 1978; Tester and Morris, 1987), with red and far-red light penetrating to greater depths than the remaining spectrum (Mandoli and Briggs, 1984). This light exposure has led roots to evolve blue-light receptors in the upper portion of the roots and red-light receptors more distal in the root due to the more penetrative quality of red light (Mo et al., 2015).

Plant gravitropism is divided into three stages: perception, transduction, and response. During the perception phase, starch-filled statoliths interact with cytoplasmic objects in the specialized gravity-sensing columella cells (Sack, 1991; Salisbury, 1993; Kiss, 2000; Vandenbrink et al., 2014b). Once the gravity signal is perceived, a differential auxin gradient is sent along opposing sides of the root to the root elongation zone (transduction stage), where differential plant growth occurs and leads to reorientation of the root in the direction of the gravity vector (reviewed by Vandenbrink et al., 2014b).

Growth of plants in conditions of real or simulated microgravity have allowed for the study of phototropic response in the absence of significant gravitational influences (Kiss, 2015). Recently, studies have aimed to characterize the link between the two tropistic responses. For instance, our previous study found that light perception by the roots had an effect on shoot gravitropic response in *Arabidopsis thaliana* (Hopkins and Kiss, 2012). In addition, phototropic curvature of roots in response to blue light illumination was shown to be intimately tied to the magnitude of the gravity vector (Vandenbrink et al., 2016).

Our recent spaceflight study also identified an association between the red-light phototropic response in roots and the magnitude of the gravity vector (Vandenbrink et al., 2016). In terms of cell growth and cell proliferation, it has been shown that when seedlings are grown in darkness, there is a lack of balance between these key plant development functions in microgravity (Matía et al., 2010). Further evidence for this observation was provided by analyzing a dark-grown, synchronized cell culture grown in simulated microgravity (Kamal et al., 2018). Recent spaceflight results show that red light can compensate for this effect (Valbuena et al., 2018), particularly increasing cell growth (measured by means of ribosome biosynthesis in the nucleolus) that was depleted without light stimulation.

In the present study, we used RNA expression profiling to begin characterizing the molecular mechanisms affected by conditions of microgravity in phototropically stimulated seedlings. Thus, in the present set of space experiments, we use transcriptomic techniques to characterize gene expression related to seedling growth in conditions of microgravity. Our most significant results demonstrate that light-associated pathways show significant downregulation in microgravity.

MATERIALS AND METHODS

Spaceflight experiment

Experiments with seeds of *Arabidopsis thaliana* ecotype Landsberg erecta (Ler) were flown to the International Space Station (ISS) via the SpaceX Dragon. Spaceflight experiments were conducted utilizing the European Modular Cultivation System (EMCS) in the Columbus Module of the ISS. The EMCS facility provides two centrifuges for the production of gravity vectors and atmospheric, temperature, and hydration monitoring and control (Brinckmann and Schiller, 2002; Brinckmann, 2005; Kiss et al., 2014). In addition, the EMCS contains a video camera for image acquisition as well as visual monitoring of the experiment. The seedling growth series of experiments was conducted in two parts to accommodate the experiment's large sample size. The first set of experiments (termed SG1) was uploaded on to the ISS via SpaceX CRS-2 (March 2013) followed by return via CRS-3 (May 2014), and the second set of seedlings (termed SG2) was carried to the ISS on SpaceX CRS-4 (September 2014) and returned on CRS-5 (February 2015).

Spaceflight procedures

Experimental containers (ECs) were sent to the ISS and loaded into the EMCS. Experimental conditions were controlled remotely from the Norwegian User Support and Operations Centre (N-USOC; Trondheim, Norway). Temperature within the ECs was held between 21.5° and 24.3°C, and relative humidity was held at 95%. The experiments were initiated via hydration of the seeds (Fig. 1). Plants were grown in microgravity and in a 1.0-*g* control. Seedlings were illuminated under white light (30–40 μmol m^{-2} s^{-1}) for 96 h, followed by 48 h of unidirectional photostimulation with blue light (1–40 μmol m^{-2} s^{-1}) perpendicular to the white light and gravity vector. Light sources were LEDs as previously described (Kiss et al., 2014). After the conclusion of the experiments, seedlings were frozen and stored at −80°C in the General Laboratory Active Cryogenic ISS Experiment Refrigerator (GLACIER) freezer of the ISS. Upon return of frozen seedlings to Earth, samples were transported on dry ice, and promptly preserved with RNA*later* (1.5 mL; ThermoFisher Scientific, Waltham, MA, USA) for subsequent RNA-seq analysis.

RNA sequencing and differential gene expression analysis

RNA was extracted individually for each EC, which consisted of 10–14 seedlings. Pooled RNA from an individual EC denotes one replicate. ECs that shared the same gravity conditions were pooled to allow ample RNA for RNA-seq analysis. A plant specific RNA extraction NucleoSpin kit (Macherey-Nagel, Bethlehem, PA, USA) including a DNase treatment was used to isolate whole plant mRNA. The quantity and quality of the extracted RNA was determined by a Nanodrop 2000 (Thermo Scientific). RNA remained frozen at −80°C until delivery. Extracted RNA was shipped on dry ice to the David H. Murdoch Research Institute in Kannapolis, NC, USA. During sequencing, pooled RNA samples were used to generate sequencing libraries using the Illumina TruSeq RNA Library Preparation Kit (Illumina, San Diego, CA, USA). Samples were individually indexed. The samples were pooled, and the following groups were established: microgravity (± 0.00 × *g*, 4 EC replicates) and 1-*g* control (0.99 ± 0.06 × *g*, 3 EC replicates). A 125-bp paired-end sequencing run was performed on the Illumina HiSeq2500. Quality reports for the pooled RNA are available in Appendices S1–S7.

Paired-end 125-bp reads were aligned with the Arabidopsis TAIR10 genome using the PBS-GEM workflow (https://github.com/wpoehlm/PBS-GEM) on the Clemson University Palmetto Cluster (Kim et al., 2015). Fragments with a Phred score below 33 were filtered using Trimmomatic (Bolger et al., 2014). The program HISAT2 (v2.1.0; Kim et al., 2015) was used to align sequencing reads to the reference genome using a minimum intron length of 60 and a maximum intron length of 2000. Annotated reference gene abundances were quantified using StringTie (v1.3.4; Pertea et al., 2015). Annotated reference genes were identified using the TAIR10 genome GFF3

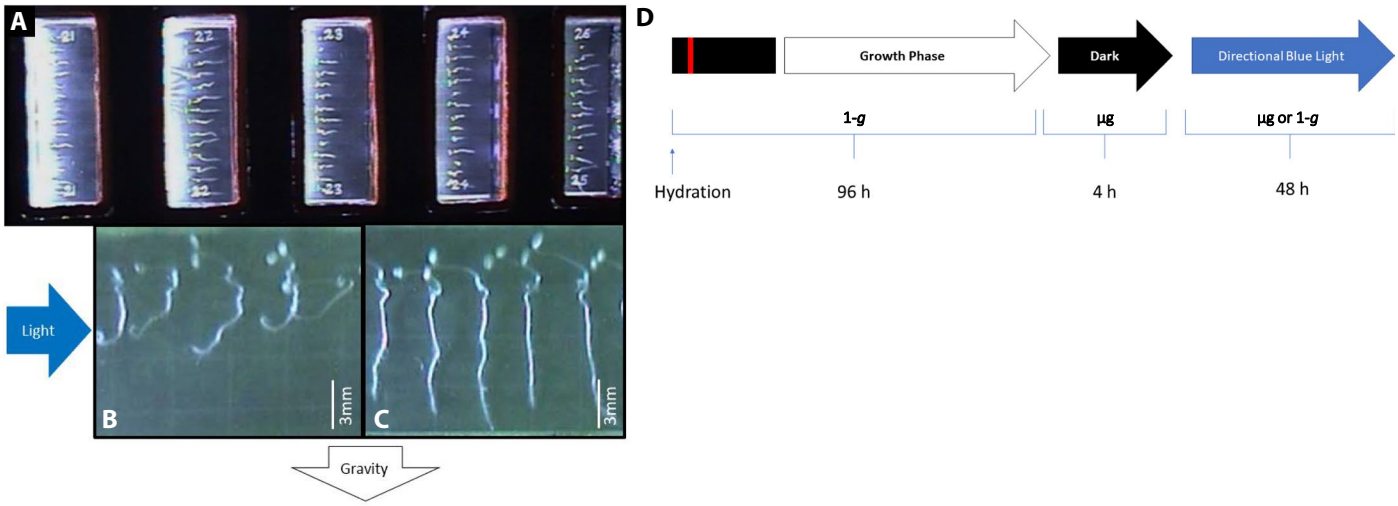

FIGURE 1. Images of seedlings of *Arabidopsis thaliana* growing on the International Space Station. (A) Five seedling cassettes positioned within the European Modular Cultivation System (EMCS). (B, C) Higher magnification view of seedlings grown in (B) conditions of microgravity and (C) 1-*g*. Blue light is introduced at 90° from the overhead white LEDs used during the growth phase. (D) Timeline of events for the seedling growth experiments. Seedlings are initially exposed to a 96-h, 1-*g* growth phase that begins with hydration of the seeds, followed by a short burst of red light to help initiate germination. Seedlings are initially grown at 1-*g* to ensure seedlings are properly oriented, then subjected to a 4-h microgravity dark period. Seedlings are then exposed to unidirectional blue light 90° from the initial white light present during the growth phase (either in µ*g* or 1-*g* control). Once the blue-light phase is complete, seedlings are frozen at −80°.

annotation file (https://www.arabidopsis.org/download_files/Genes/TAIR10_genome_release/TAIR10_gff3/TAIR10_GFF3_genes.gff).

Statistical analysis of differential gene expression was conducted with DESeq2 (v1.18.1; Anders and Huber, 2010). A multiple-test corrected *p*-value (*q*-value; Benjamini and Hochberg, 1995) of 0.05 was employed (Appendix S8). Principal component analysis (PCA) of the samples shows clustering of the microgravity and 1-*g* samples (Appendix S9). Genes identified as differentially expressed between the µ*g* and 1-*g* conditions were subsequently used for Generally Applicable Gene-set Enrichment (GAGE) for Pathway Analysis to identify genetic pathways enriched for differentially expressed genes (Luo et al., 2009). Last, gene ontology annotation of differentially expressed genes (µ*g* vs 1-*g*) was conducted utilizing Protein ANalysis THrough Evolutionary Relationships (PANTHER) Classification System version 13.1 (http://www.pantherdb.org; Thomas et al., 2003; Mi et al., 2013). The PANTHER statistical overrepresentation test was performed using the default settings. An outline of the RNA-seq and Pathway analysis is included (Appendix S10). The data were deposited into NASA's GeneLab (https://genelab.nasa.gov/; accession GLDS 251).

RESULTS

Identification of differentially expressed genes (DEGs)

We analyzed the transcriptome of *Arabidopsis thaliana* seedlings that were grown on the International Space Station (Fig. 1). Dry seeds were hydrated to initiate our spaceflight experiment as previously described (Vandenbrink and Kiss, 2019). Differential expression of genes between plants in µ*g* and Earth's gravity (1-*g*) was analyzed using DESeq2 (Anders and Huber, 2010) with genes from 1-*g* as the reference group. A *q*-value false discovery rate (Benjamini and Hochberg) of 0.05 was used to identify differentially expressed genes (DEGs). Comparison between genes from µ*g* and 1-*g* revealed 296 genes were significantly differentially expressed between microgravity and Earth's 1-*g* (Appendix S11).

Enrichment analysis of gene ontology caused by microgravity

After identification of DEGs, a Generally Applicable Gene-Set (GAGE)-Pathway Analysis was conducted between µ*g* and 1-*g* gravity conditions to determine whether any molecular pathways were significantly enriched with genes (identified as differentially expressed) to give a more holistic view of the effects of reduced gravity on plant molecular pathways (Luo et al., 2009). GAGE analysis revealed that eight pathways were significantly enriched (2 upregulated, 6 downregulated; FDR < 0.1) with genes identified as differentially expressed in the µ*g* vs 1-*g* group (Table 1). These pathways included photosynthesis (Fig. 2) and photosynthetic antenna proteins (Fig. 3) as being significantly downregulated. In addition, porphyrin and chlorophyll metabolism, starch and sucrose metabolism, carotenoid biosynthesis, and protein processing in the endoplasmic reticulum were all shown to be downregulated (Appendices S12–S15). Only two pathways, ribosome synthesis and oxidative phosphorylation were found to be upregulated (Appendices S16, S17).

In the Gene Ontology classifications of genes differentially expressed between µ*g* and 1-*g* using PANTHER (http://www.pantherdb.org; Thomas et al., 2003; Mi et al., 2013), the statistical overrepresentation test identified four molecular processes as overrepresented in the list of differentially expressed (DE) genes. In addition, analysis revealed six biological processes, five protein classes, and five cellular components showing statistical overrepresentation (Table 2). In regard to molecular function, catalytic activity accounted for 42% of genes differentially expressed, while binding and structural molecular activity accounted for 25% and 19%, respectively. Smaller contributing ontologies included receptor activity (2.0%), signal transducer activity (1.0%), and translation

TABLE 1. GAGE-Pathview overrepresentation test of genes identified as differentially expressed between μ*g* and 1-*g* gravity conditions.

Pathway	KEGG pathway identifier[a]	Gene set size	Geometric mean[b]	Stat mean[c]	*p*	FDR[d]
Unregulated PATHWAYS						
Ribosome	ath03010	307	2.34E-25	8.08	2.34E-15	2.62E-13
Oxidative phosphorylation	ath00190	120	1.73E-03	2.95	1.73E-03	9.80E-02
Downregulated pathways						
Photosynthesis – antenna proteins	ath00196	22	1.42E-05	–4.70	1.42E-05	1.61E-03
Photosynthesis	ath00195	45	2.08E-03	–2.98	2.08E-03	5.87E-02
Porphyrin and chlorophyll metabolism	ath00860	51	1.97E-03	–2.96	1.97E-03	5.87E-02
Protein processing in endoplasmic reticulum	ath04141	190	4.37E-03	–2.64	4.37E-03	8.23E-02
Starch and sucrose metabolism	ath00500	140	1.18E-03	–3.07	1.18E-03	5.87E-02
Carotenoid biosynthesis	ath00906	27	2.86E-03	–2.88	2.86E-03	6.46E-02

[a]Kyoto Encyclopedia of Genes and Genomes.
[b]Geometric mean of the individual *p*-values from multiple single array based gene set tests.
[c]Mean of the individual statistics from multiple single array based gene set tests.
[d]False discovery rate *q*-value adjustment of the global *p*-value using the Benjamini–Hochberg procedure.

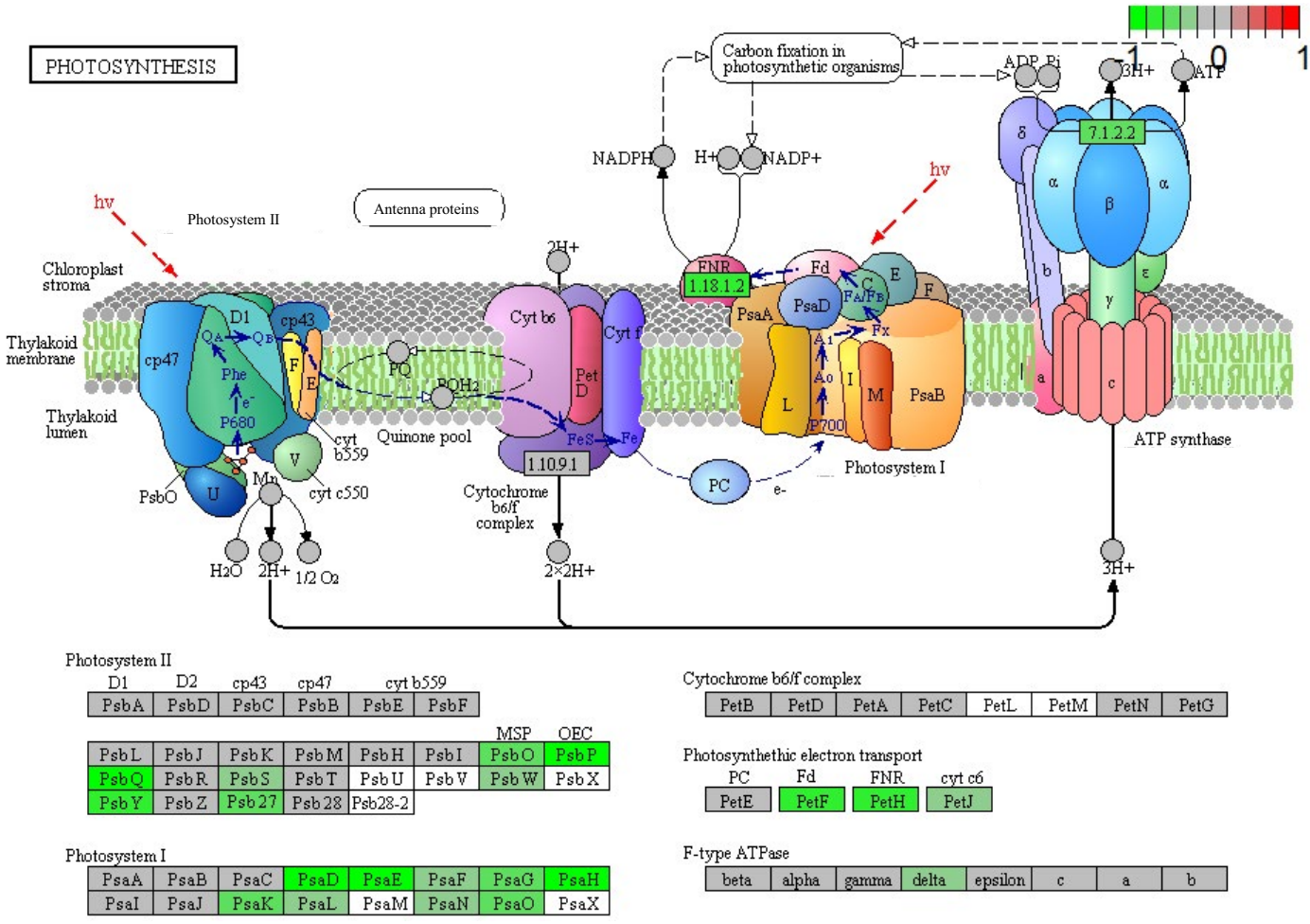

Photosystem II

D1	D2	cp43	cp47	cyt b559			
PsbA	PsbD	PsbC	PsbB	PsbE	PsbF		
						MSP	OEC
PsbL	PsbJ	PsbK	PsbM	PsbH	PsbI	PsbO	PsbP
PsbQ	PsbR	PsbS	PsbT	PsbU	PsbV	PsbW	PsbX
PsbY	PsbZ	Psb27	Psb28	Psb28-2			

Cytochrome b6/f complex

PetB	PetD	PetA	PetC	PetL	PetM	PetN	PetG

Photosynthethic electron transport

PC	Fd	FNR	cyt c6
PetE	PetF	PetH	PetJ

Photosystem I

PsaA	PsaB	PsaC	PsaD	PsaE	PsaF	PsaG	PsaH
PsaI	PsaJ	PsaK	PsaL	PsaM	PsaN	PsaO	PsaX

F-type ATPase

beta	alpha	gamma	delta	epsilon	c	a	b

FIGURE 2. Photosynthesis pathview of differentially expressed genes identified in conditions of microgravity when compared to 1-*g* control. Differentially expressed genes were identified using the HISAT2-Stringtie-DESeq analysis pathway ($p = 5.87E-02$). Genes highlighted with green indicate reduced expression when compared to 1-*g* control.

regulation activity (1.0%). Further division into categories of these ontologies is provided in Fig. 4.

The ontological breakdown of biological processes affected by microgravity was also conducted. Metabolic processes and cellular processes each accounted for 37.8% of gene classifications, accounting for the majority of genes identified as differentially expressed (Fig. 5), followed by response to stimulus (9.2%), cellular component organization of biogenesis (7.2%), localization (4.1%), biological replication

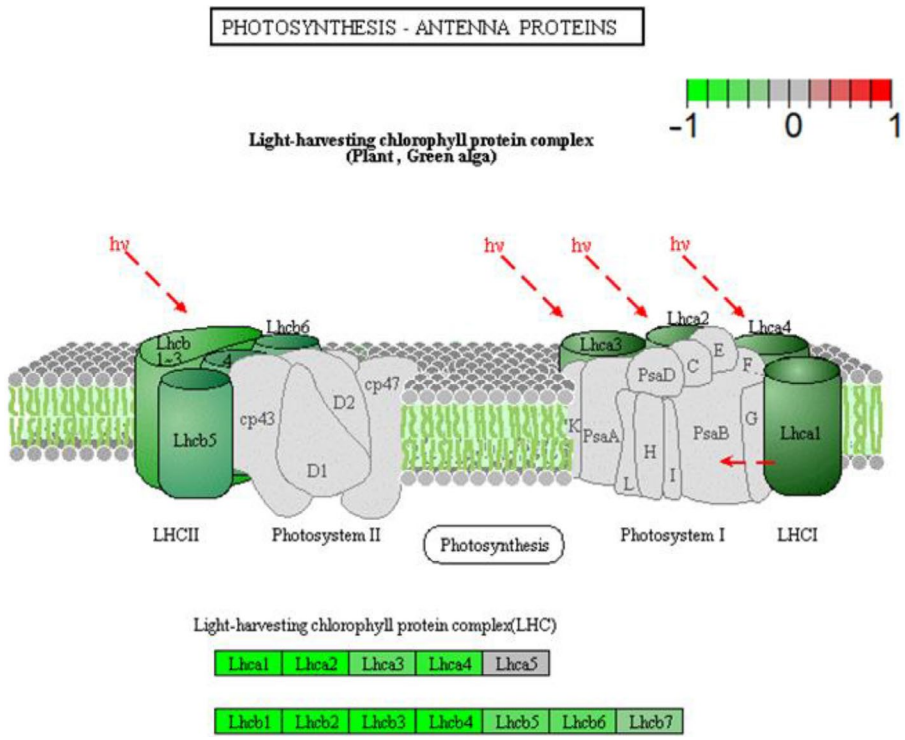

FIGURE 3. Photosynthesis – antenna proteins pathview of differentially expressed genes identified in conditions of microgravity when compared to 1-*g* control. Gene were identified using the HISAT2-Stringtie-DESeq analysis pathway (p = 1.61E-03). Genes highlighted with green indicate reduced expression when compared to 1-*g* control.

(2.0%), and single-multicellular organismal processes and death (1%). Further categorization of gene ontology classifications for cellular component and protein class are shown in Appendices S18 and S19.

DISCUSSION

Image analysis of seedlings grown during the seedling growth suite of experiments previously characterized a novel blue-light phototropic response in roots of *Arabidopsis thaliana* grown in conditions of microgravity (Vandenbrink et al., 2016). This relationship was shown to be linearly related to the magnitude of the gravity vector. To achieve a better understanding of how gravity affects these phototropically stimulated seedlings, we performed RNA-seq analyses to characterize changes in gene expression that may be associated with this novel phototropic response. Interestingly, GAGE-Pathview results indicated that genes constituting major pathways associated with light perception, photosynthesis, and biosynthesis of the photosynthetic complexes showed reduced expression in microgravity.

Photosynthesis and antenna proteins

The two pathways with the greatest statistical significance for downregulation in this study were involved with photosynthesis: antenna protein pathway and photosynthetic pathway (Figs. 2,3). Acclimation to changing light conditions is achieved through changes in expression to the antenna protein genes (Masuda and Fujita, 2008). Antenna proteins, which aid in plant acclimation to different light environments, had all but one light-harvesting chlorophyll protein complex (LHC) gene significantly downregulated (Appendix S12). In regard to the photosynthetic pathway, there was significant downregulation of genes associated with photosystems I and II (Fig. 3). This observation confirms a previous study that detailed an overall reduction in photosystem I (PSI) complexes, as well as a 30% reduction in photochemical activity on *Brassica rapa* plants grown aboard the space shuttle (Jiao et al., 2004). The reduction in photosystem I was accompanied by an overall reduction in biomass of the samples, correlating with a reduction in photosynthetic processes. In a simulated microgravity study, the observed reduction in photosystem I activity was supported by a study which grew *Oryza sativa* on a random positioning machine (RPM) and detailed a reduction in PSI activity, which was attributed to an overall reduction in the biosynthesis of PSI proteins (Chen et al., 2013).

In our present study, four genes associated with photosynthetic electron transport (petE: plastocyanin, petF: ferredoxin, petH: ferredoxin–NADP+ reductase, petJ: cytochrome c6) were significantly downregulated. This observation suggests that there is an interaction between gravity and the light harvesting machinery at a genetic level. This proposed interaction between gravity and light-related pathways may help explain the novel blue-light phototropic response in roots of *Arabidopsis* grown in microgravity (Vandenbrink et al., 2016).

Chlorophyll metabolism and chloroplast function

In addition to photosynthetic pathways, multiple pathways that are associated with light perception and photosynthesis were significantly downregulated. The porphyrin and chlorophyll metabolism pathway, which is responsible for the biosynthesis of chlorophyll pigment, also shows significant downregulation of genes (Appendix S12). Control of chlorophyll metabolism has been shown to be regulated by phytohormones, environmental signals, organ specificity, developmental stage, gene expression, proteolysis, among others (Masuda and Fujita, 2008). However, the relationship between gravity and chlorophyll biosynthesis is poorly understood.

When analyzing gene expression patterns, we found significant downregulation of genes responsible for heme biosynthesis (*HemA*, *HemL*, *HemB*, *HemC*, *HemD*, *HemE*, *HemF*, and *HemH*). These heme series of proteins are important for the biosynthesis of chlorophylls. In addition to the heme proteins, genes for multiple enzymes associated with the final processing of chlorophyll *a* and chlorophyll *b*, such as chlorophyll *b* reductase and chlorophyll synthase, were downregulated; Appendix S12). This observation suggests that reduction of gravity from 1-*g* to μ*g* potentially reduces the ability of the plant to synthesis mature chlorophyll. These latter results may have important implications for the use of plants in bioregenerative life support in space missions.

TABLE 2. PANTHER overrepresentation test of genes identified as differentially expressed (DE) between μ*g* and 1-*g* gravity conditions.

PANTHER Category	No. reference genes[a]	No. mapped genes[b]	Expected no. genes[c]	Fold enrichment[d]	+/–[e]	*p*-value[f]	FDR[g]
Biological process							
Generation of precursor metabolites and energy	263	21	2.89	7.27	+	6.61E-12	1.24E-09
Oxidative phosphorylation	58	10	0.64	15.7	+	3.28E-09	3.09E-07
Respiratory electron transport chain	153	13	1.68	7.74	+	3.70E-08	2.32E-06
Response to abiotic stimulus	175	13	1.92	6.76	+	1.60E-07	7.51E-06
Translation	308	14	3.38	4.14	+	1.32E-05	4.95E-04
Biosynthetic process	2090	41	22.95	1.79	+	4.26E-04	1.33E-02
Cation transport	67	5	0.74	6.8	+	1.13E-03	3.03E-02
Protein class							
Ribosomal protein	322	27	3.54	7.64	+	1.90E-15	3.35E-13
RNA binding protein	1115	33	12.24	2.7	+	4.03E-07	3.54E-05
Nucleic acid binding	1771	38	19.45	1.95	+	9.01E-05	3.96E-03
Ligand-gated ion channel	11	3	0.12	24.84	+	4.23E-04	1.49E-02
Winged helix/forkhead transcription factor	31	4	0.34	11.75	+	5.48E-04	1.61E-02
Anion channel	16	3	0.18	17.07	+	1.08E-03	2.38E-02
ATP synthase	47	4	0.52	7.75	+	2.28E-03	4.46E-02
Ion channel	57	3	0.63	4.79	+	2.76E-02	4.04E-01
Helix-turn-helix transcription factor	161	5	1.77	2.83	+	3.53E-02	4.78E-01
Cation transporter	140	4	1.54	2.6	+	7.24E-02	8.49E-01
Transporter	953	6	10.46	0.57	–	2.03E-01	1.70E+00
Receptor	74	1	0.81	1.23	+	5.60E-01	2.19E+00
Transcription factor	690	8	7.58	1.06	+	8.52E-01	2.42E+00
Cellular component							
Ribosome	325	23	3.57	6.44	+	6.44E-12	3.22E-10
Macromolecular complex	1919	52	21.07	2.47	+	2.46E-09	6.16E-08
Ribonucleoprotein complex	643	25	7.06	3.54	+	9.64E-08	1.61E-06
Mitochondrial inner membrane	128	11	1.41	7.83	+	3.77E-07	4.72E-06
Proton-transporting ATP synthase complex	25	5	0.27	18.21	+	1.67E-05	1.67E-04
Protein complex	1375	29	15.1	1.92	+	8.61E-04	7.17E-03
Cytoplasm	3618	60	39.73	1.51	+	1.12E-03	7.99E-03
Cytosol	776	18	8.52	2.11	+	4.35E-03	2.72E-02
Intracellular	5893	85	64.71	1.31	+	5.94E-03	3.30E-02
Membrane	2139	37	23.49	1.58	+	6.71E-03	3.36E-02
Cell part	6166	87	67.71	1.28	+	1.02E-02	4.25E-02
Thylakoid	46	2	0.51	3.96	+	9.58E-02	3.68E-01
Organelle	4563	59	50.11	1.18	+	1.86E-01	6.64E-01
Mitochondrion	417	3	4.58	0.66	–	6.35E-01	1.18E+00
Molecular function							
Structural constituent of ribosome	264	25	2.9	8.62	+	1.66E-15	2.60E-13
Structural molecule activity	530	28	5.82	4.81	+	2.28E-11	1.79E-09
Proton-transporting ATP synthase activity, rotational mechanism	25	5	0.27	18.21	+	1.67E-05	6.55E-04
Hydrogen ion transmembrane transporter activity	102	8	1.12	7.14	+	2.77E-05	8.71E-04
Ligand-gated ion channel activity	10	3	0.11	27.32	+	3.35E-04	8.76E-03
Anion channel activity	77	5	0.85	5.91	+	2.02E-03	4.52E-02
Ion channel activity	93	5	1.02	4.9	+	4.36E-03	8.57E-02
Transmembrane transporter activity	858	11	9.42	1.17	+	6.15E-01	1.97E+00
Transporter activity	996	11	10.94	1.01	+	8.78E-01	2.03E+00

[a]Number of genes in reference genome mapped to the annotation category.
[b]Number of identified DE genes mapped to annotation category.
[c]Number of DE genes predicted to be in annotation category.
[d]Fold enrichment of genes identified as DE (no. of DE genes/no. expected).
[e]Overrepresentation (+) or underrepresentation (–) when compared to expected.
[f]Determined by Fisher's exact test.
[g]False discovery rate determined by Benjamini-Hochberg procedure.

In addition to downregulation of genes associated with the production of chlorophyll, chloroplasts in plants grown in microgravity undergo significant changes, including more ovoid-shaped chloroplasts than plants grown in 1-*g*, and denser packing of thylakoid membranes of space-grown plants, with each of the membranes roughly 0.9 nm closer than those plants grown in 1-*g* (Stutte et al., 2006). In addition, a study of clinorotated *Arabidopsis* plants showed that the number of grana per chloroplast and overall size of the

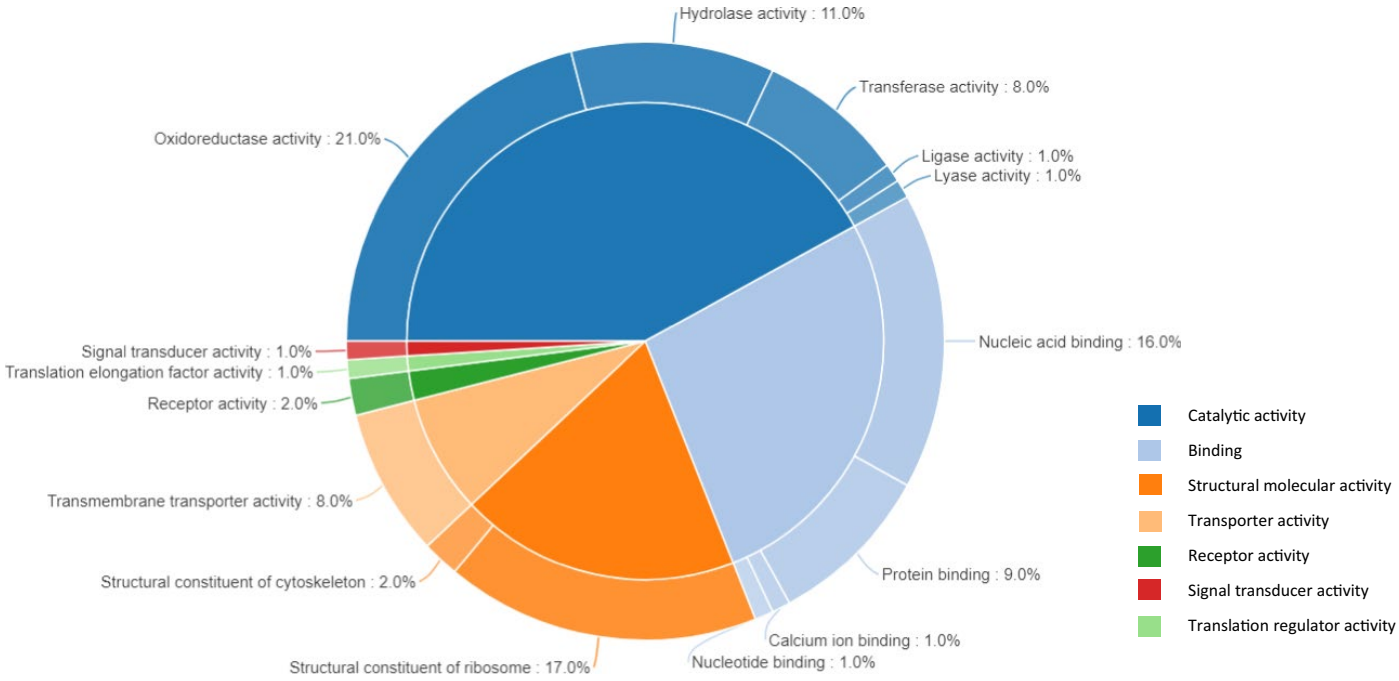

FIGURE 4. PANTHER molecular function of differentially expressed genes. Classification of the functions that proteins identified from differentially expressed genes perform on its direct molecular target (μ*g* vs. 1-*g*).

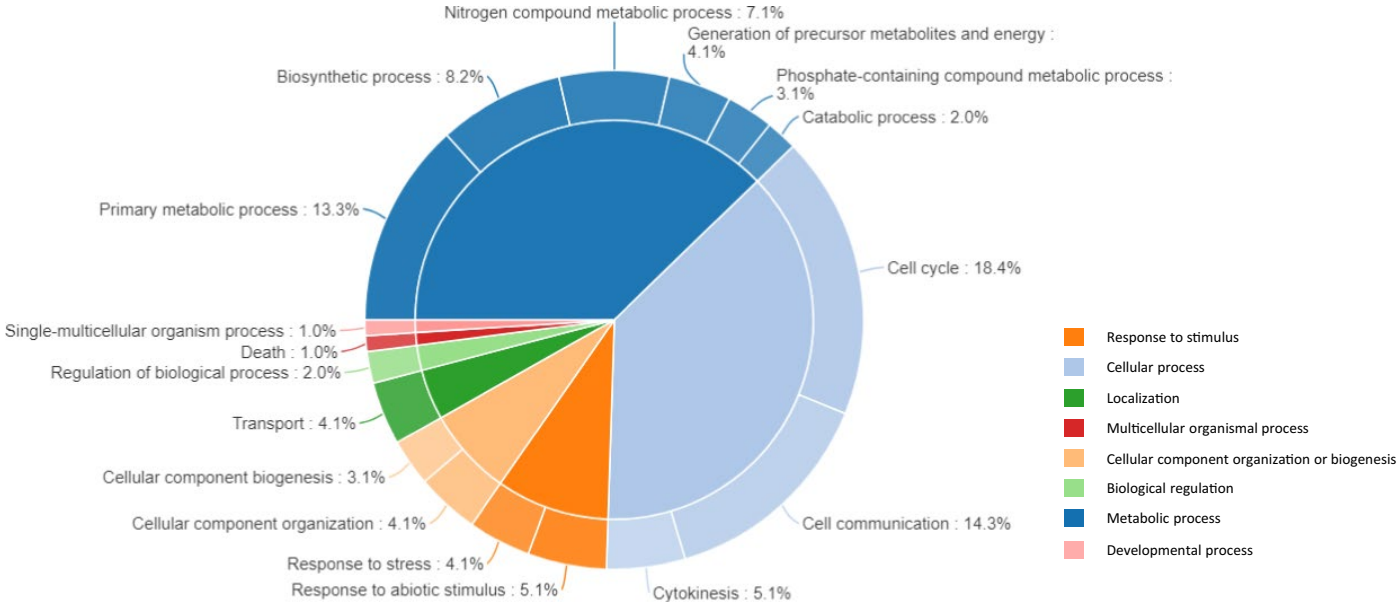

FIGURE 5. PANTHER biological process of differentially expressed genes. Classification of biological systems that identified differentially expressed genes belong to μ*g* vs. 1-*g*.

chloroplast were reduced (Adamchuk, 1998). An increase in proton permeability of the thylakoid membrane was also observed in seedlings grown on a 2-D clinostat (Mikhaylenko et al., 2001). Taken together, these observations suggest that the synthesis of chlorophyll and the formation of plant chloroplasts are significantly altered in conditions of microgravity.

Previous spaceflight research has considered the effects of microgravity environments on the biosynthesis of chlorophyll. Species of *Chlorella*, single-celled photosynthetic algae, showed alterations to their thylakoid membrane as well as a 35–50% decrease in chlorophyll content (Moleshko et al., 1991). Similarly, the chlorophyll content is reduced in wheat grown in microgravity for 19 days (Rumyantseva et al., 1990) and in pea plants grown in space (Laurinavichius et al., 1986). In addition to spaceflight studies, experiments utilizing simulated microgravity devices, such as clinostats and random positioning machines (RPMs), have also shown a decrease in chlorophyll content (Miyamoto et al., 2001). Also, Yamada et al. (1993) predicted that carbon metabolism was affected

by microgravity when starch granules in chloroplasts were found to be smaller in clinorotated plants.

Effects of experimental hardware on photosynthetic rates

There have been multiple studies of photosynthetic rates in plants exposed to microgravity, which have produced a wide range of results. Numerous reports (detailed above) have reported reductions in photosynthetic apparatuses, photosynthetic rates, chloroplast function and morphology, among others. However, in contrast, in other studies, no changes were found in chloroplast density (Stutte et al., 2006), chloroplast structure (Musgrave et al., 1998), or photosynthetic rate (Stutte et al., 2005), to name a few. When comparing results of these experiments, it is important to acknowledge the effects of the spaceflight hardware when interpreting the results. Multiple stresses and environmental stimuli are encountered when growing plants in microgravity (Kiss, 2015). These include (but are not limited to) lack of convection, reduced CO_2 levels, less than optimal temperature, elevated ethylene, spacecraft vibrations, increased radiation exposure, among others. Hardware exists to try to mitigate many of these environmental factors that are present on the International Space Station, but no perfect hardware exists for the growth of plants in space.

Stutte et al. (2006) grew plants in a facility (the Biomass Production System [BPS]) that aimed to limit the confounding hardware effects present in some spaceflight studies such as lack of convection, improper lighting, reduced CO_2 levels, temperature fluctuation, low humidity, and elevated ethylene. In the BPS, they found no apparent changes in photosynthetic rate and attributed previous findings of photosynthetic reduction in a microgravity environment to improper ventilation. However, here we used the European Modular Cultivation System, which contains an air scrubbing/filtration system designed to remove excess ethylene from the seedlings during the growth phase (Kiss et al., 2014; Kiss, 2015). Thus, even with proper ventilation of plants grown in space, expression of photosynthetic genes was reduced.

Interestingly, a few studies have shown an increase in chlorophyll content in space-grown pea plants (Abilov, 1986; Aliyev, 1987). This increase in chlorophyll content was also observed in clinorotated rice seedlings (Jagtap et al., 2011). However, these studies all observed this increased chlorophyll content in young seedlings. Jagtap et al. (2011) noted that chlorophyll content increases in clinorotated rice seedlings up to 5 days, then the trend reverses, and chlorophyll content starts to decrease. This observation suggests a temporal component to the effects of microgravity on chlorophyll production, with longer durations causing a decrease in chlorophyll biosynthesis.

Starch and sucrose metabolism

The relationship between starch and sucrose metabolism in microgravity has been explored in previous space flight and spaceflight analog studies. For example, soybean seedlings grown for 6 days under simulated microgravity conditions (clinorotation) were shown to have a decrease in starch concentration in cotyledons (Brown and Piastuch, 1994). In addition, in this study, the activity of ADP-glucose pyrophosphorylase was reduced. This observation corresponds with our own results, which show a downregulation of ADP-glucose pyrophosphorylase in the starch and sucrose metabolism pathway (Appendix S13). In addition, wheat leaves grown in conditions of altered gravity (clinorotation) were shown to have reduced sucrose and starch accumulation in leaves; however, ADP-glucose pyrophosphorylase activity did not decrease.

In contrast to the above reports, sweet potato stem cuttings flown in the Space Shuttle for 5 days showed substantially greater accumulation of soluble sugars, glucose, fructose, sucrose, and total starch. The space-flown sweet potatoes were exposed to ~50% higher concentrations of CO_2, which likely would account for the increase in sugar accumulation (Mortley et al., 2008). Similarly, soybean and potato plants grown for 5 days onboard the Space Shuttle observed compositional changes in starch granules; however, changes in starch content were attributed to ethylene effects (Kuznetsov et al., 2001). In addition, the reported ethylene effects were not observed in the sweet potato study (Mortley et al., 2008) nor in the present study, which both used methods of ethylene removal. Thus, reduction in starch and sucrose metabolism may be species or tissue specific, or alternatively, due to hardware effects.

Carotenoid biosynthesis

The carotenoid pathway also is associated with photosynthesis and light perception (Appendix S14). Carotenoids have been shown to be linked to chlorophyll production; carotenoid content increases in conjunction with chlorophyll biosynthesis (Howitt and Pogson, 2006). Xanthophylls are essential components of the plant photosynthetic apparatus (Lokstein et al., 2002) and important for the formation of stable pigment–protein complexes (Paulsen, 1995) and as ancillary light-harvesting pigments (Siefermann-Harms, 1987). In our present spaceflight experiment, the expression of xanthophyll biosynthetic genes was reduced. In addition, multiple genes associated with the lutein biosynthesis arm of the carotenoid pathway were downregulated. Lutein is the predominant carotenoid in photosynthetic tissue, playing a large role in the bulk antenna complex, or LHC II (Pogson et al., 1996). In addition, lutein optimizes antenna structure and organization to increase the efficiency of light harvesting (Lokstein et al., 2002).

Carotenoids, the second most-abundant group of pigments in nature, play an important protective role in light sensing. For instance, these photoreceptors act as photoprotective compounds that quench triplet chlorophyll and radical oxygen species derived from excess light absorption (Demmig-Adams et al., 1996). This nonphotochemical quenching also prevents damage to the thylakoid membrane, to which the chlorophyll and carotenoids are bound (Niyogi, 1999). In previous research on spaceflight-flown photosynthetic organisms, carotenoid content in organisms was reduced. For instance, a 50% reduction in carotenoid contents was found in the alga *Chlorella* (Moleshko et al., 1991) and a similar reduction in maize (Rumyantseva et al., 1990). These past studies further support our current findings of a reduction in gene expression associated with carotenoid biosynthesis in space-grown seedlings of *A. thaliana*.

Ribosome biogenesis and oxidative phosphorylation

In contrast with the downregulation of phototropism and related biosynthetic and metabolic pathways, we found two very clearly upregulated functions in microgravity-grown seedlings when compared to 1-*g* spaceflight samples: ribosome biosynthesis and oxidative phosphorylation (Appendices S16 and S17). In both true microgravity (Matía et al., 2010) and different simulated microgravity facilities using both seedlings and cell cultures (Manzano et al., 2013; Kamal et al., 2018), ribosome biogenesis was reduced.

Our recent spaceflight results showed that red light can compensate for this effect (Valbuena et al., 2018), particularly by increasing cell growth (measured by means of ribosome biosynthesis in the nucleolus) that was depleted without light stimulation. The results of our present space studies support that removing the gravitropic stimuli in combination with photostimulation can lead to higher levels of protein production and metabolism rates (oxidative phosphorylation).

CONCLUSIONS

The results of this study help to detail the influences of gravity on the development of phototropically stimulated seedlings. Analysis of the affected gene ontologies revealed that catalytic activity and binding activity were the most significantly affected molecular functions, while cellular processes and metabolic processes were the most significantly affected biological processes. Removal of the influence of gravity on blue-light-illuminated seedlings showed a reduction in gene expression in multiple pathways associated with photosynthesis, suggesting the gravity response influences development of seedlings exposed to directional blue light. In addition, pathways previously associated with light perception and response, such as carotenoid biosynthesis and starch metabolism, were also identified as downregulated, suggesting a possible interplay between plant growth in microgravity and plastid function. Taken together, these findings in concert suggest an intricate connection between gravity and growth of phototropically stimulated seedlings in *A. thaliana*.

ACKNOWLEDGMENTS

Funding was provided by grants NNX12A065G and 80NSSC17K0546 from NASA (PI = J. Z. Kiss). We thank the reviewers for insightful comments and review in preparation of this manuscript.

DATA AVAILABILITY

All sequences generated in this study are deposited in NASA GenLab (https://genelab.nasa.gov/) as data set GLDS 251.

SUPPORTING INFORMATION

Additional Supporting Information may be found online in the supporting information tab for this article.

APPENDIX S1. FASTQC results for pooled sample #111: microgravity (A) forward and (B) reverse paired-end reads.

APPENDIX S2. FASTQC results for pooled sample #114: microgravity (A) forward and (B) reverse paired-end reads.

APPENDIX S3. FASTQC results for pooled sample #116: microgravity (A) forward and (B) reverse paired-end reads.

APPENDIX S4. FASTQC results for pooled sample #120: microgravity (A) forward and (B) reverse paired-end reads.

APPENDIX S5. FASTQC results for pooled sample #175: 1-*g* (A) forward and (B) reverse paired-end reads.

APPENDIX S6. FASTQC results for pooled sample # 179: 1-*g* (A) forward and (B) reverse paired-end reads.

APPENDIX S7. FASTQC results for pooled sample # 235-239: 1-*g* (A) forward and (B) reverse paired-end reads.

APPENDIX S8. MA plot showing the log2 fold-change of normalized counts vs. the mean of normalized counts for microgravity samples (1-*g* control).

APPENDIX S9. Principal component analysis of microgravity (pink) and 1-*g* (blue) data sets generated from the seedling Growth series of spaceflight experiments.

APPENDIX S10. Diagram detailing the steps and software used for pathway analysis of differentially expressed genes. Seedlings were pooled based on gravity exposure (μ*g* or 1-*g*).

APPENDIX S11. Table of results for differential gene expression analysis with DESeq2.

APPENDIX S12. Porphyrin and chlorophyll metabolism pathview of differentially expressed genes identified from HISAT2-Stringtie-DESeq. p = 5.87E-02

APPENDIX S13. Starch and sucrose metabolism pathview of differentially expressed genes identified from HISAT2-Stringtie-DESeq. p = 5.87E-02

APPENDIX S14. Carotenoid biosynthesis pathview of differentially expressed genes identified from HISAT2-Stringtie-DESeq. p = 4.99E-09

APPENDIX S15. Protein processing in the endoplasmic reticulum pathview of differentially expressed genes identified from HISAT2-Stringtie-DESeq. p = 8.23E-02

APPENDIX S16. Ribosome pathview of differentially expressed genes identified from HISAT2-Stringtie-DESeq. p = 2.62E-13

APPENDIX S17. Oxidative phosphorylation pathview of differentially expressed genes identified from HISAT2-Stringtie-DESeq. p = 9.80E-02

APPENDIX S18. PANTHER cellular location of differentially expressed genes. Cellular localization of the protein products derived from genes identified as differentially expressed in conditions of microgravity.

APPENDIX S19. PANTHER protein class of differentially expressed genes. Ontological classification of protein products derived from genes identified as differentially expressed in conditions of microgravity.

LITERATURE CITED

Abilov, Z. 1986. The morphological and functional state of the photosynthetic system of plant cells grown for varying periods under space flight condition. *USSR Space Life Sciences Digest* 8: 15–18.

Adamchuk, N. 1998. Ultrastructural and functional changes of photosynthetic apparatus of *Arabidopsis thaliana* (L.) Hynh. induced by clinorotation. *Advances in Space Research* 21: 1131–1134.

Aliyev, A. 1987. The ultrastructure and physiological characteristics of the photosynthesis system of shoots of garden peas grown for 29 days on the "Salyut-7" space station. *USSR Space Life Sciences Digest* 10: 15–16.

Anders, S., and W. Huber. 2010. Differential expression analysis for sequence count data. *Genome Biology* 11: R106.

Benjamini, Y., and Y. Hochberg. 1995. Controlling the false discovery rate: a practical and powerful approach to multiple testing. *Journal of the Royal Statistical Society, B, Methodological* 57: 289–300.

Bolger, A. M., M. Lohse, and B. Usadel. 2014. Trimmomatic: a flexible trimmer for Illumina sequence data. *Bioinformatics* 15: 2114–2120.

Braam, J. 2005. In touch: plant responses to mechanical stimuli. *New Phytologist* 165: 373–389.

Briggs, W. R. 2014. Phototropism: some history, some puzzles, and a look ahead. *Plant Physiology* 164: 13–23.

Brinckmann, E. 2005. ESA hardware for plant research on the International Space Station. *Advances in Space Research* 36: 1162–1166.

Brinckmann, E., and P. Schiller. 2002. Experiments with small animals in BIOLAB and EMCS on the International Space Station. *Advances in Space Research* 30: 809–814.

Brown, C., and W. Piastuch. 1994. Starch metabolism in germinating soybean cotyledons is sensitive to clinorotation and centrifugation. *Plant, Cell & Environment* 17: 341–344.

Chen, R., E. Rosen, and P. H. Masson. 1999. Gravitropism in higher plants. *Plant Physiology* 120: 343–350.

Chen, B., A. Zhang, Q. Lu, T. Kuang, C. Lu, and X. Wen. 2013. Characterization of photosystem I in rice (*Oryza sativa* L.) seedlings upon exposure to random positioning machine. *Photosynthesis Research* 116: 93–105.

Correll, M. J., and J. Z. Kiss. 2002. Interactions between gravitropism and phototropism in plants. *Journal of Plant Growth Regulation* 21: 89–101.

Darwin, C., and F. Darwin. 1880. The power of movement in plants. Murray, London, UK.

Demmig-Adams, B., A. M. Gilmore, and W. Adams. 1996. Carotenoids 3: in vivo function of carotenoids in higher plants. *FASEB Journal* 10: 403–412.

Hopkins, J. A., and J. Z. Kiss. 2012. Phototropism and gravitropism in transgenic lines of *Arabidopsis* altered in the phytochrome pathway. *Physiologia Plantarum* 145: 461–473.

Howitt, C. A., and B. J. Pogson. 2006. Carotenoid accumulation and function in seeds and non-green tissues. *Plant, Cell & Environment* 29: 435–445.

Jagtap, S. S., R. B. Awhad, B. Santosh, and P. B. Vidyasagar. 2011. Effects of clinorotation on growth and chlorophyll content of rice seeds. *Microgravity Science and Technology* 23: 41–48.

Jiao, S., E. Hilaire, A. Q. Paulsen, and J. A. Guikema. 2004. *Brassica rapa* plants adapted to microgravity with reduced photosystem I and its photochemical activity. *Physiologia Plantarum* 122: 281–290.

Kamal, K. Y., R. Herranz, J. J. van Loon, and F. J. Medina. 2018. Cell cycle acceleration and changes in essential nuclear functions induced by simulated microgravity in a synchronized *Arabidopsis* cell culture. *Plant, Cell & Environment* 42: 480–494.

Kim, D., B. Langmead, and S. L. Salzberg. 2015. HISAT: a fast spliced aligner with low memory requirements. *Nature Methods* 12: 357–360.

Kiss, J. Z. 2000. Mechanisms of the early phases of plant gravitropism. *Critical Reviews in Plant Sciences* 19: 551–573.

Kiss, J. Z. 2007. Where's the water? Hydrotropism in plants. *Proceedings of the National Academy of Sciences, USA* 104: 4247–4248.

Kiss, J. Z. 2015. Conducting plant experiments in space. *Methods in Molecular Biology* 1309: 255–283.

Kiss, J. Z., J. L. Mullen, M. J. Correll, and R. P. Hangarter. 2003. Phytochromes A and B mediate red-light-induced positive phototropism in roots. *Plant Physiology* 131: 1411–1417.

Kiss, J. Z., G. Aanes, M. Schiefloe, L. H. Coelho, K. D. Millar, and R. E. Edelmann. 2014. Changes in operational procedures to improve spaceflight experiments in plant biology in the European Modular Cultivation System. *Advances in Space Research* 53: 818–827.

Kutschera, U., and W. R. Briggs. 2016. Phototropic solar tracking in sunflower plants: an integrative perspective. *Annals of Botany* 117: 1–8.

Kuznetsov, O., C. Brown, H. Levine, W. Piastuch, M. Sanwo-Lewandowski, and K. Hasenstein. 2001. Composition and physical properties of starch in microgravity-grown plants. *Advances in Space Research* 28: 651–658.

Laurinavichius, R., A. Yaroshyus, A. Marchyukaytis, D. Shvyaghdene, and A. Mashinskiy. 1986. Metabolism of pea plants grown under space flight conditions. *USSR Space Life Scence Digest* 4: 23–25.

Laxmi, A., J. Pan, M. Morsy, and R. Chen. 2008. Light plays an essential role in intracellular distribution of auxin efflux carrier PIN2 in *Arabidopsis thaliana*. *PLoS One* 3: e1510.

Liscum, E., S. K. Askinosie, D. L. Leuchtman, J. Morrow, K. T. Willenburg, and D. R. Coats. 2014. Phototropism: growing towards an understanding of plant movement. *Plant Cell* 26: 38–55.

Lokstein, H., L. Tian, J. E. Polle, and D. DellaPenna. 2002. Xanthophyll biosynthetic mutants of *Arabidopsis thaliana*: altered nonphotochemical quenching of chlorophyll fluorescence is due to changes in photosystem II antenna size and stability. *Biochimica et Biophysica Acta (BBA)-Bioenergetics* 1553: 309–319.

Luo, W., M. S. Friedman, K. Shedden, K. D. Hankenson, and P. J. Woolf. 2009. GAGE: generally applicable gene set enrichment for pathway analysis. *BMC Bioinformatics* 10: 161.

Mandoli, D. F., and W. R. Briggs. 1984. Fiber optics in plants. *Scientific American* 251: 90–98.

Manzano, A. I., O. J. Larkin, C. E. Dijkstra, P. Anthony, M. R. Davey, L. Eaves, R. J. Hill, et al. 2013. Meristematic cell proliferation and ribosome biogenesis are decoupled in diamagnetically levitated Arabidopsis seedlings. *BMC Plant Biology* 13: 124.

Masuda, T., and Y. Fujita. 2008. Regulation and evolution of chlorophyll metabolism. *Photochemical and Photobiological Sciences* 7: 1131–1149.

Matía, I., F. González-Camacho, R. Herranz, J. Z. Kiss, G. Gasset, J. J. van Loon, R. Marco, and F. J. Medina. 2010. Plant cell proliferation and growth are altered by microgravity conditions in spaceflight. *Journal of Plant Physiology* 167: 184–193.

Mi, H., Q. Dong, A. Muruganujan, P. Gaudet, S. Lewis, and P. D. Thomas. 2013. PANT HER version 7: improved phylogenetic trees, orthologs and collaboration with the Gene Ontology Consortium. *Nucleic Acids Research* 38: D204–D210. https://doi.org/10.1038/nprot.2013.092.

Mikhaylenko, N., S. Sytnik, and E. Zolotareva. 2001. Effects of slow clinorotation on lipid contents and proton permeability of thylakoid membranes of pea chloroplasts. *Advances in Space Research* 27: 1007–1010.

Miyamoto, K., T. Yuda, T. Shimazu, and J. Ueda. 2001. Leaf senescence under various gravity conditions: relevance to the dynamics of plant hormones. *Advances in Space Research* 27: 1017–1022.

Mo, M., K. Yokawa, Y. Wan, and F. Baluška. 2015. How and why do root apices sense light under the soil surface? *Frontiers in Plant Science* 6: 775.

Moleshko, G., A. Anton'Yan, V. Sycheyev, I. Solontsova, I. Shetlik, and Y. Doukha. 1991. The effects of space flight factors on the pigment system of one-celled algae. *USSR Space Life Science Digest* 31: 43–45.

Moni, A., A. Y. Lee, W. Briggs, and I. S. Han. 2015. The blue light receptor Phototropin 1 suppresses lateral root growth by controlling cell elongation. *Plant Biology* 17: 34–40.

Mortley, D. G., C. K. Bonsi, W. A. Hill, C. E. Morris, C. S. Williams, C. F. Davis, J. W. Williams, et al. 2008. Influence of microgravity environment on root growth, soluble sugars, and starch concentration of sweetpotato stem cuttings. *Journal of the American Society for Horticultural Science* 133: 327–332.

Musgrave, M. E., A. Kuang, C. S. Brown, and S. W. Matthews. 1998. Changes in *Arabidopsis* leaf ultrastructure, chlorophyll and carbohydrate content during spaceflight depend on ventilation. *Annals of Botany* 81: 503–512.

Niyogi, K. K. 1999. Photoprotection revisited: genetic and molecular approaches. *Annual Review of Plant Biology* 50: 333–359.

Paulsen, H. 1995. Chlorophyll *a*/*b*-binding proteins. *Photochemistry and Photobiology* 62: 367–382.

Pertea, M., G. M. Pertea, C. M. Antonescu, T.-C. Chang, J. T. Mendell, and S. L. Salzberg. 2015. StringTie enables improved reconstruction of a transcriptome from RNA-seq reads. *Nature Biotechnology* 33: 290–295.

Pogson, B., K. A. McDonald, M. Truong, G. Britton, and D. DellaPenna. 1996. Arabidopsis carotenoid mutants demonstrate that lutein is not essential for photosynthesis in higher plants. *Plant Cell* 8: 1627–1639.

Rumyantseva, V., M. Merzlyak, A. Mashinsky, and G. Nechitailo. 1990. The effect of space-flight factors on the pigment and lipid-composition of wheat plants. *Kosmicheskaia Biologiia i Aviakosmicheskaia Meditsina* 23: 53–55.

Sack, F. D. 1991. Plant gravity sensing. *International Review of Cytology* 127: 193–252.

Salisbury, F. B. 1993. Gravitropism: changing ideas. *Horticultural Reviews* 15: 233–278.

Siefermann-Harms, D. 1987. The light-harvesting and protective functions of carotenoids in photosynthetic membranes. *Physiologia Plantarum* 69: 561–568.

Silva-Navas, J., M. A. Moreno-Risueno, C. Manzano, M. Pallero-Baena, S. Navarro-Neila, B. Téllez-Robledo, J. M. Garcia-Mina, et al. 2015. D-Root: a system for cultivating plants with the roots in darkness or under different light conditions. *Plant Journal* 84: 244–255.

Stutte, G., O. Monje, G. D. Goins, and B. Tripathy. 2005. Microgravity effects on thylakoid, single leaf, and whole canopy photosynthesis of dwarf wheat. *Planta* 223: 46–56.

Stutte, G., O. Monje, R. Hatfield, A.-L. Paul, R. Ferl, and C. Simone. 2006. Microgravity effects on leaf morphology, cell structure, carbon metabolism and mRNA expression of dwarf wheat. *Planta* 224: 1038–1049.

Tester, M., and C. Morris. 1987. The penetration of light through soil. *Plant, Cell & Environment* 10: 281–286.

Thomas, P. D., A. Kejariwal, N. Guo, H. Mi, M. J. Campbell, A. Muruganujan, and B. Lazareva-Ulitsky. 2003. Applications for protein sequence-function evolution data: mRNA/protein expression analysis and coding SNP scoring tools. *Nucleic Acids Research* 34: W645–W650.

Valbuena, M. A., A. Manzano, J. P. Vandenbrink, V. Pereda-Loth, E. Carnero-Diaz, R. E. Edelmann, J. Z. Kiss, et al. 2018. The combined effects of real or simulated microgravity and red-light photoactivation on plant root meristematic cells. *Planta* 248: 691–704.

Vandenbrink, J. P., and J. Z. Kiss. 2019. Preparation of a spaceflight experiment to study tropisms in *Arabidopsis* seedlings on the International Space Station. *In* K. Yamamoto [ed.], Methods in Molecular Biology, vol. 1924, Phototropism, 207–214. Humana, NY, NY, USA.

Vandenbrink, J. P., E. A. Brown, S. L. Harmer, and B. K. Blackman. 2014a. Turning heads: The biology of solar tracking in sunflower. *Plant Science* 224: 20–26.

Vandenbrink, J. P., J. Z. Kiss, R. Herranz, and F. J. Medina. 2014b. Light and gravity signals synergize in modulating plant development. *Frontiers in Plant Science* 5: 563.

Vandenbrink, J. P., R. Herranz, F. J. Medina, R. E. Edelmann, and J. Z. Kiss. 2016. A novel blue-light phototropic response is revealed in roots of Arabidopsis thaliana in microgravity. *Planta* 44: 1201–1215.

Woolley, J. T., and E. W. Stoller. 1978. Light penetration and light-induced seed germination in soil. *Plant Physiology* 61: 597–600.

Yamada, M., Y. Takeuchi, H. Kasahara, S. Murakami, and M. Yamashita. 1993. Plant growth under clinostat-microgravity condition. *Biological Sciences in Space* 7: 116–119.

frontiers in Plant Science

ORIGINAL RESEARCH
published: 26 November 2019
doi: 10.3389/fpls.2019.01529

RNAseq Analysis of the Response of *Arabidopsis thaliana* to Fractional Gravity Under Blue-Light Stimulation During Spaceflight

Raúl Herranz[1], Joshua P. Vandenbrink[2,3], Alicia Villacampa[1], Aránzazu Manzano[1], William L. Poehlman[4], Frank Alex Feltus[4], John Z. Kiss[2] and Francisco Javier Medina[1]*

[1] Plant Microgravity Lab, Centro de Investigaciones Biológicas (CSIC), Madrid, Spain, [2] Department of Biology, University of North Carolina at Greensboro, Greensboro, NC, United States, [3] School of Biological Sciences, Louisiana Tech University, Ruston, LA, United States, [4] Department of Genetics and Biochemistry, Clemson University, Clemson, SC, United States

Introduction: Traveling to nearby extraterrestrial objects having a reduced gravity level (partial gravity) compared to Earth's gravity is becoming a realistic objective for space agencies. The use of plants as part of life support systems will require a better understanding of the interactions among plant growth responses including tropisms, under partial gravity conditions.

Materials and Methods: Here, we present results from our latest space experiments on the ISS, in which seeds of *Arabidopsis thaliana* were germinated, and seedlings grew for six days under different gravity levels, namely micro-*g*, several intermediate partial-*g* levels, and 1*g*, and were subjected to irradiation with blue light for the last 48 h. RNA was extracted from 20 samples for subsequent RNAseq analysis. Transcriptomic analysis was performed using the HISAT2-Stringtie-DESeq pipeline. Differentially expressed genes were further characterized for global responses using the GEDI tool, gene networks and for Gene Ontology (GO) enrichment.

Results: Differential gene expression analysis revealed only one differentially expressed gene (AT4G21560, VPS28-1 a vacuolar protein) across all gravity conditions using FDR correction ($q < 0.05$). However, the same 14 genes appeared differentially expressed when comparing either micro-*g,* low-*g* level (< 0.1*g*) or the Moon *g*-level with 1*g* control conditions. Apart from these 14-shared genes, the number of differentially expressed genes was similar in microgravity and the Moon *g*-level and increased in the intermediate *g*-level (< 0.1*g*), but it was then progressively reduced as the difference with the Earth gravity became smaller. The GO groups were differentially affected at each *g*-level: light and photosynthesis GO under microgravity, genes belonged to general stress, chemical and hormone responses under low-*g*, and a response related to cell wall and membrane structure and function under the Moon *g*-level.

Discussion: Transcriptional analyses of plants under blue light stimulation suggests that root blue-light phototropism may be enough to reduce the gravitational stress response caused by the lack of gravitropism in microgravity. Competition among tropisms induces an intense perturbation at the micro-*g* level, which shows an extensive stress response

OPEN ACCESS

Edited by:
Valérie Legué, Université Clermont Auvergne, France

Reviewed by:
Takayuki Hoson, Osaka City University, Japan
Franck Anicet Ditengou, University of Freiburg, Germany

****Correspondence:***
Raúl Herranz
r.herranz@csic.es

Specialty section:
This article was submitted to Plant Abiotic Stress, a section of the journal Frontiers in Plant Science

Received: *11 July 2019*
Accepted: *01 November 2019*
Published: *26 November 2019*

Citation:
Herranz R, Vandenbrink JP, Villacampa A, Manzano A, Poehlman WL, Feltus FA, Kiss JZ and Medina FJ (2019) RNAseq Analysis of the Response of Arabidopsis thaliana to Fractional Gravity Under Blue-Light Stimulation During Spaceflight. Front. Plant Sci. 10:1529. doi: 10.3389/fpls.2019.01529

that is progressively attenuated. Our results show a major effect on cell wall/membrane remodeling (detected at the interval from the Moon to Mars gravity), which can be potentially related to graviresistance mechanisms.

Keywords: Arabidopsis, fractional gravity, microgravity, stress response, RNA-Seq, spaceflight

INTRODUCTION

Long-term exploration of the Solar System will require that humans travel within a nearly close life-support systems, reducing to the minimum the amount of water, oxygen, and nutrients to be transported and optimizing the recycling of reusable waste. Such a system is being under development, for example, in the Melissa project from the European Space Agency (Godia et al., 2004), but it will require an edible plant to be successfully cultivated in the environmental conditions expected to be achieved during spaceflight and on arrival at nearby objects. Isolation chambers could avoid, at least partially, some of the suboptimal environmental conditions that can greatly compromise organism adaptation to spaceflight (Beckingham, 2010), including temperature, radiation, air, and soil composition constrains. However, providing artificial gravity will require large diameter centrifuge (Van Loon et al., 2008) or even expensive railroad-based platforms that could be subjected to other biological limitations.

Gravity influences the direction of plant growth and the pattern of development, from seedlings to adult plants (Volkmann and Baluska, 2006), and even gravitational effects on *in vitro* plant cell cultures have been reported (Babbick et al., 2007; Barjaktarovic et al., 2007). Light is the only tropistic response that plays a substantial role in determining overall plant architecture with a contribution similar to gravity. Typically, plants orient their roots towards the gravity vector (positive gravitropic response), and away from blue/white light exposure (negative phototropic response). Shoots show the opposite orientation, growing away from the gravity vector (negative gravitropic response) and towards a blue/white light source (positive phototropic response; Kutschera and Briggs, 2016; Briggs, 2014; Chen et al., 1999). Any tropistic response is divided into three stages; perception, transduction and response. During the perception phase, starch-filled statoliths interact with other cellular components in the specialized columella cells. Once the gravity signal is perceived, a differential auxin gradient develops along the root to the root elongation zone (transduction stage), where differential plant growth occurs and leads to reorientation of the root in the direction of the gravity vector (reviewed in Vandenbrink et al., 2014).

Phototropism and gravitropism have been well characterized, but little was known about the interaction among tropisms until recently. Experiments with plants in microgravity have allowed for the study of phototropism in the absence of the influence of gravity (Kiss, 2015). Our previous research showed that light perception by the roots can have an effect on shoot gravitropism in *Arabidopsis thaliana* (Hopkins and Kiss, 2012). In addition, phototropic curvature of roots in response to unilateral blue light was tied to the magnitude of the gravity vector (Vandenbrink et al., 2016). This latter study also identified an association between red-light-based phototropism in roots and the magnitude of the gravity vector. Other experiments involving assays of cell growth and cell proliferation have demonstrated that there is an imbalance between these key plant development functions in microgravity (Matía et al., 2010) in dark-grown plants. Recent spaceflight results also demonstrated that red light can compensate this effect (Valbuena et al., 2018), particularly increasing cell growth (i.e., as assayed by ribosome biosynthesis in the nucleolus) that was depleted without light stimulation.

Studies on the response of living organisms to altered gravity are greatly facilitated by the development of ground-based facilities for simulation of gravity alterations to perform basic science as well as to design and prepare for space experiments (Herranz et al., 2013). The biological system (cell proliferation and growth during early plant development) had previously been studied under real microgravity in the ISS (Driss-Ecole et al., 2008; Matía et al., 2010; Mazars et al., 2014). Similar effects to the ones observed during spaceflight (increased cell proliferation rates together with decreased cell growth parameters) also were observed in root meristem cells in simulated microgravity studies (Bouchern-Dubuisson et al., 2016; Valbuena et al., 2018) and in two partial-*g* paradigms. The imbalance of the cell proliferation and cell growth rates is also observable at the Moon´s gravity level, while less pronounced effects were observed at Mars *g* level (Kamal et al., 2018; Manzano et al., 2018).

In terms of spaceflight transcriptional experiments, a number of studies performed in orbit are available in public databases (Paul et al., 2012; Paul et al., 2013; Johnson et al., 2017; Zupanska et al., 2017). In these studies, some Gene Ontology categories as responses to biotic or abiotic stress, oxidative stress, cell wall reorganization and secondary metabolism remodeling commonly show the highest variation in gene expression. Transcriptional response in microgravity is different in each experiment, due to both the biological material (developmental stage or organ analyzed) and the technical/environmental constraints of each spaceflight experiment [late or early access to the sample during spaceflight, the hardware used, type of dissection/fixation/preservation see for example (Kruse et al., 2017)].

In a previous report, we focused on the effects of microgravity in the transcriptional profile of blue-light photostimulated seedlings (Vandenbrink et al., 2019). Here, we will describe the plant transcriptional response to several partial gravity levels in young blue-light photostimulated *A. thaliana* seedlings cultivated into the European Module Cultivation System (EMCS) centrifuge on board the International Space Station (ISS). The results from plants cultivated on the ISS

within the SEEDLING GROWTH experiment series illustrate the adaptation strategy of plants at the level of the whole transcriptome to cope with reduced gravity conditions.

MATERIALS AND METHODS

Seedling Growth Spaceflight Experiments

Seeds of *A. thaliana* ecotype *Landsberg erecta* (Ler) were flown to the ISS *via* the SpaceX Dragon. Spaceflight experiments were conducted utilizing the European Modular Cultivation System (EMCS) in the Columbus Module of the ISS. The EMCS facility provides two centrifuges for creation of simulated gravity vectors, as well as atmospheric, temperature and hydration monitoring and control (Brinckmann and Schiller, 2002; Brinckmann, 2005; Kiss et al., 2014). In addition, the EMCS contains a video camera for image acquisition as well as monitoring of growth. The Seedling Growth series of experiments was conducted in two parts. The first set of seedlings were uploaded on SpaceX CRS-2 (March 2013) followed by return *via* CRS-3 (May 2014), and the second set of seedlings were carried to the ISS on SpaceX CRS-4 (September 2014) and returned on CRS-5 (February 2015).

Spaceflight Procedures

Experimental containers were uploaded to the ISS and loaded into the EMCS as previously described (Kiss et al., 2014; Vandenbrink and Kiss, 2016; Vandenbrink et al., 2019). Experimental conditions were controlled remotely from the Norwegian User Support and Operations Centre (N-USOC; Trondheim, Norway). The experiment was initiated *via* hydration of the seeds. Plants were grown under 6 nominal gravity conditions produced by different rotational speeds on the EMCS centrifuge, microgravity (stopped EMCS centrifuge), 0.1, 0.3, 0.5, 0.8, and 1.0 *g*. The angular speed to generate each fractional gravity level was calculated for the cassette in the center of the Experimental Container. In the case of the 1.0 g cassettes, the value was calculated for the fifth cassette in order to prevent values higher than Earth nominal gravity. Seedlings were illuminated under white light (30–40 μmol m^{-2} s^{-1}) for 96 h, followed by 48 h of unidirectional photostimulation with blue light. Light sources were LEDs (Kiss et al., 2014). RNA-Seq analysis was only conducted on seedlings exposed to unidirectional blue light. After conclusion of the experiments, seedlings were frozen in dedicated holders by placing them at -80°C in the General Laboratory Active Cryogenic ISS Experiment Refrigerator (GLACIER) freezer of the ISS. Upon return of frozen seedlings to Earth, samples were transported on dry ice and immediately preserved with RNALater for subsequent RNA-Seq analysis.

RNA Extraction and Sequencing

RNA was extracted individually for each EC TROPI cassette for most of the samples (i.e. from 24 cassettes, 20 samples were obtained to collect approximately 10–15 seedlings per extraction). A plant specific RNA extraction NucleoSpin kit (MACHEREY-NAGEL, Catalog # 740949.250) including a DNase treatment was used to isolate whole plant mRNA. The quantity and quality of the extracted RNA was determined by Nanodrop 2000 (Thermo Scientific). Extracted RNA was keep frozen at −80 C until shipped on dry ice to the David H. Murdoch Research Institute in Kannapolis; North Carolina, USA. During sequencing, twenty total RNA samples were used to generate twenty sequencing libraries using the Illumina TruSeq RNA Library Preparation Kit (Illumina, USA). Samples were individually indexed. The samples then were combined at equimolar proportions into three pools with 6–7 samples per pool. Each pool was loaded onto a single lane of a flow cell. A 125bp paired end sequencing run was performed on the Illumina HiSeq2500.

Paired-end 125bp reads were aligned to the *Arabidopsis* TAIR10 genomes using the HISAT2 pipeline on the Clemson University Palmetto Cluster (Kim et al., 2015). Fragments with a Phred score below 33 were filtered using Trimmomatic (Trimmomatic, 2013). HISAT2 (*v2.1.0*) was used to align sequencing reads. Reads were assembled into transcripts using StringTie (*v1.3.4*). Annotation was conducted using TAIR10 FASTA sequence the TAIR10 genome GTF annotation file (https://www.arabidopsis.org). This transcriptional dataset has been submitted to the GENELAB database (https://genelab.nasa.gov) and it will be released with the reference GLDS-251.

Differential Gene Expression Analysis

Statistical analyses of differential gene expression was conducted utilizing DESeq2 (v1.18.1; Anders and Huber, 2010). A multiple-test corrected p-value (q-value; Benjamini and Hochberg, 1995) of 0.05 was employed. The 20 samples were organized to reduce the *g*-level interval within biological replicates so the following groups were established: microgravity (stopped EMCS centrifuge, 4 replicates), low gravity (0.09 ± 0.02*g*, 3 replicates), Moon gravity (0.18 ± 0.04*g*, 3 replicates), Mars gravity (0.36 ± 0.02*g*, 3 replicates), reduced Earth gravity (0.57 ± 0.05*g*, 4 replicates) and 1*g* control (0.99 ± 0.06*g*, 3 replicates). Venn Diagrams comparing the number of differentially expressed genes (DEG) across gravity levels were created using jvenn [http://jvenn.toulouse.inra.fr/app/index.html (Bardou et al., 2014)] with both q-value < 0.05 and p-value < 0.05. Afterwards, gene ontology (GO) analysis of specific groups of DEGs was performed using BinGO (Maere et al., 2005) with the full list of GO terms (GO_Full) or using PANTHER (Mi et al., 2019) with the molecular functions, biological process and cellular component GO lists. Subcellular localization of DEGs was analyzed using the abundance tool (MMAP) of the Subcellular Localization Database for Arabidopsis Proteins [SUBA4, (Hooper et al., 2017)].

For a global view of the whole genome transcriptional status along *g*-levels into the SG1 and SG2 experiment (comparisons versus 1*g*), global expression patterns were calculated using the Gene Expression Dynamics Inspector (GEDI v2.1) program analysis (Eichler et al., 2003). GEDI profile allows the visualization of the gene expression across the transcriptome generating a mosaic image or dot matrix, consisting of 5 x 9 pixels (average of 5–14 probe sets/tile) using a self-organizing map algorithm and standard setting of the software (Eichler et al., 2003). Analysis was done using the signal log2 ratio of the selected probe sets through using the 5,571 probes with any significant ($p < 0.05$) change in expression from more than 21,000 sequences

assignated to annotated genes. The same study was repeated adding the false discovery rate correction (FDR, q < 0.05, 861 genes). Each pixel represents a group or cluster of genes that share a similar transcriptional profile in any experimental condition. Each pixel has a color which reflects the average expression of the genes included in the cluster for each experimental condition compared to 1*g* control in each panel. The GEDI program SOM algorithm determines which genes should be assigned to each cluster, and then places similar clusters in a nearby area of the mosaic, creating an image and allowing global transcriptome analysis as a single entity for display in different gravitational conditions. For certain pixels of interest, the gene list extracted from the clusters was used to find functional links between genes using Genemania App embedded into the Cytoscape v3.6.1 (Shannon et al., 2003) software with default settings.

RESULTS

Identification of Differentially Expressed Genes (DEG)

We performed transcriptomic studies with young seedlings of *A. thaliana* that were grown on the ISS at different gravity levels depending on the rotational speed of the EMCS centrifuge (nominal *g* levels) and the distance of each cassette to the rotation center (**Figure 1**). Seeds were hydrated to initiate our spaceflight experiment as previously described (Kiss, 2015; Vandenbrink and Kiss, 2019) showing a positive blue-light phototropism in the microgravity samples that it is greatly reduced at 0.1*g*, and effectively negated at 0.3*g* and higher gravity levels (Vandenbrink et al., 2016). Root growth was also determined after blue-light stimulation. The results show longer roots in microgravity and 1*g* samples in comparison with 0.1*g* seedlings (Vandenbrink et al., 2016).

Differential expression analysis was conducted *via* DESeq2 (Anders and Huber, 2010) among all five reduced gravity conditions taking into account the calculated *g*-level experienced in each EC due to the geometry of the EMCS container (**Figure 1B**), using Earth's gravity (1*g*) as the reference group, extending previous results from the microgravity samples (Vandenbrink et al., 2019). Initially, a reduced stringency analysis was done to isolate all genes identified as differentially expressed with a p-value of $p < 0.05$. Comparison between μ*g* and 1*g* revealed 2067 differentially expressed genes, comparisons between low gravity (lower than 0.1*g)* and 1*g* peaked at 2552 genes, comparisons between Moon *g-level* and 1*g* reduced to 2088 genes, comparisons between Mars *g-level* and 1*g* revealed 978 genes, and lastly, comparisons between reduced Earth *g*-level (0.57*g)* and 1*g* identified only 411 differentially expressed genes (**Figure 2A**). In addition to an uncorrected p-value of $p < 0.05$, a stringent Benjamini and Hochberg (1995) FDR q-value <0.05 was used in the identification of differentially expressed genes (**Figure 2B**). Comparison between μ*g* and 1*g* revealed 296 differentially expressed genes, while fractional gravity comparisons between low gravity (lower than 0.1*g)* and 1*g* revealed 568 genes. Comparisons between Moon *g*-level and 1*g* revealed 123 genes and comparisons between Mars *g*-level and 1*g* revealed 19 genes. Lastly, comparisons between reduced Earth *g*-level (0.57*g)* and 1*g* identified only 2 differentially expressed genes. Only one DEG appeared in all reduced gravity conditions (AT4G21560, VPS28-1 a vacuolar protein sorting homolog gene), another in all but reduced Earth *g* level (AT5G45428). There were 12 common DEG in microgravity, low *g* and Moon *g* conditions, being most of them related with calcium signaling, redox status and stress response (**Supplementary Table 1**).

The ten most significant GO terms (BinGO full GO terms list) of the genes differentially expressed (obtained with the adjusted q-value in **Figure 2B**) specifically expressed in μ*g*, low-*g*, or Moon gravity only were identified (**Figures 2C–E**). Not only the number of significantly affected genes, but also the type of genes affected, were clearly different with the increasing partial *g* level. In microgravity, we observed an enrichment in GO terms related with light and photosynthesis. In low gravity, there was a quite global stress effect together with chemical and hormone responses. Finally, when plants are grown under the Moon gravity level, the more representative enrichment is related to cell wall and membrane structure and function related genes. In fact, the differential subcellular localization of the DEGs at the Moon *g* level shows a clear enrichment in plastid related genes and other cell wall/membrane systems, while the general stress response observed at the low *g* level is characterized by the very large unassigned Subcellular compartment group (**Supplementary Figure 1** and **Supplementary Table 2**).

Partial Gravity Differential Effect

Although the effects of partial-*g* on gene expression (at the levels of the Moon or Mars) appeared limited in the first analysis (**Figure 2**), we then evaluated how the expression recovers to normal values from microgravity to 1*g* condition by using a visual tool that creates a mosaic image for each *g*-level representing the gene expression level of similarly behaving DEG (in at least one of the conditions, n = 5571, $p < 0.05$ without FDR correction, **Figure 3** first row). Except in the case of the low *g* condition, it is clear that the areas in red (up-regulated gene clusters) and the areas in blue (down-regulated genes clusters) that appear in the microgravity panels became quantitative and qualitatively smaller with increasing *g*-level. In the case of the low *g* condition, different clusters and with greater expression changes appears, suggesting an overlapping of two different responses at <0.1*g* level. The same result is shown if we apply the FDR correction (n = 861, $p < 0.05$ and $q < 0.05$ FDR correction, **Figure 3** second row).

Additionally, we took advantage of the GEDI self-organizing maps to select the list of commonly upregulated genes due to reduced gravity from the clusters in the first row of the GEDI panels. When the list of obtained genes (**Supplementary Table 3**) is used as a query in GeneMANIA, a tool to create networks from gene database content, a putative pathway for gravity response is proposed. Several processes related to mitochondria, plastid, cell wall and cell membrane processes are clearly affected together with 4 proteins (out of 156 annotated in the genome) belonging to the F-box/RMI-like/FDB-like domain family (including members as *TIR-1* auxin signaling gene, cell wall remodeling and even cyclins, **Figure 4**).

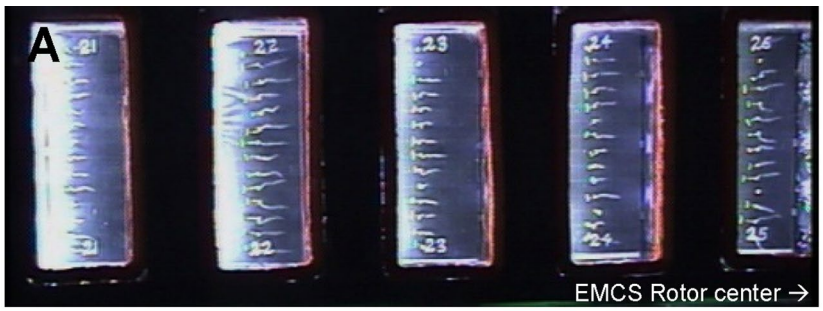

B

Distance from seedling cassette center to the EMCS center (mm)	270	238	206	174	142
Nominal 0.1*g*	**0.13**	**0.11**	0.10	0.08	**0.07**
Nominal 0.3*g*	**0.39**	**0.34**	0.30	0.25	**0.21**
Nominal 0.5*g*	**0.65**	**0.58**	0.50	0.42	**0.34**
Nominal 0.8*g*	**1.05**	**0.92**	0.80	0.68	**0.55**

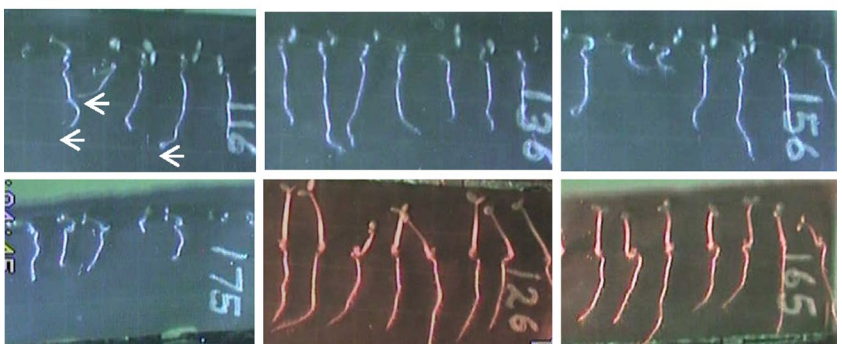

FIGURE 1 | Setup of SG1/SG2 experiment on board the International Space Station. **(A)** Image of an experimental container with 5 seedling cassettes inside the European Modular Cultivation System (EMCS) with the direction to the EMCS rotor center included. **(B)** Calculated *g*-level in each of the five culture chambers depending on the distance to the EMCS centrifuge rotor (note that only samples in the 3 positions in bold were included in this analysis, cassettes at 174 and 206 mm from EMCS center did not contain wildtype samples) and different EMCS rotational speed (nominal *g* value). Different background grey tones are used to indicate the samples that were used as replicates for low gravity (0.09 ± 0.02*g*, 3 replicates), Moon gravity (0.18 ± 0.04*g*, 3 replicates), Mars gravity (0.36 ± 0.02*g*, 3 replicates) and reduced Earth gravity (0.57 ± 0.05*g*, 4 replicates) and 1*g* control (0.99 ± 0.06*g*, 3 replicates) in addition to the microgravity samples (stopped centrifuge, 4 replicates). **(C)** Closer view of 6 day-old seedlings growing within a seed cassette at microgravity (CC116), low *g* (0.07*g*, CC136), Moon *g* (0.21*g*, CC156) or 1*g* control (1.05*g*, CC175) conditions with blue light stimulation (from the left). Hypocotyls show a clear positive phototropism at any *g*-level but roots only show this tropism at microgravity (arrows). For comparison, seed cassettes at low *g* (0.07*g*, CC126) and 1*g* control (1.05*g*, CC165) conditions exhibiting root positive phototropism to red light stimulation (from the left) are provided (see Vandenbrink et al., 2016 for a detailed phototropism discussion).

Finally, in an attempt to further dissect the differential response to partial gravity, we analyzed separately the up-regulated and down-regulated DEGs (**Figure 5** and **Supplementary Table 2**). We can observe a general pattern in which the number of DEG fades with increasing *g* level but with a remarkable exception. In the list of down-regulated DEGs without FDR correction there is an unusually high number of affected genes in both low *g* and Moon *g* level (not shown). These DEGs are more clearly confirmed only in low *g* after FDR correction, in which more than 50% of the non-corrected DEG remains significant after the FDR correction. These genes belong to stress related GO terms, particularly related with the accessibility to plant nutrients (**Figure 5**).

DISCUSSION

Blue Light Phototropism May Be Enough to Reduce the Gravitational Stress Response on Orbit

Image analysis of seedlings grown during the Seedling Growth suite of experiments previously characterized a novel

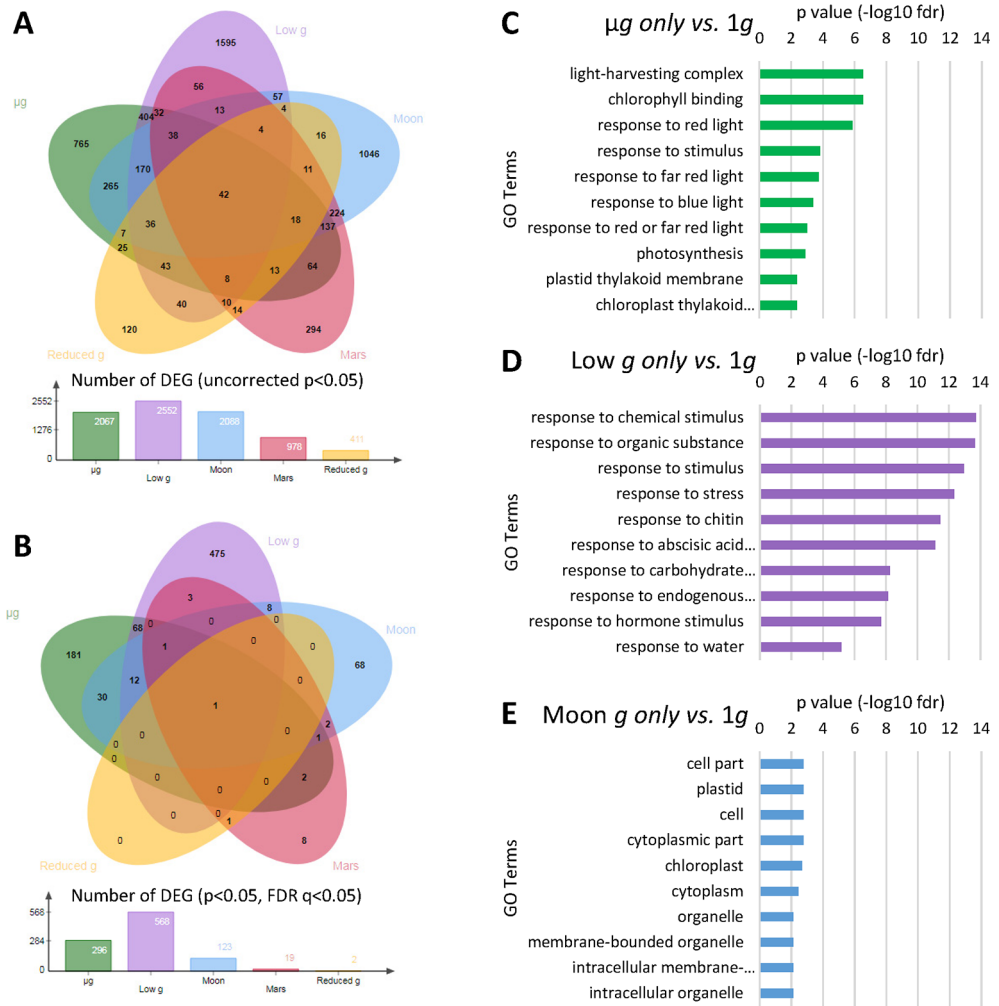

FIGURE 2 | Differentially expressed genes (DEGs) across the different gravity levels. **(A)** Venn diagram classifying DEGs using uncorrected p-value ($p < 0.05$). **(B)** Venn diagram classifying DEGs including an adjusted FDR q-value (p and $q < 0.05$). **(C)** Ten most significant gene ontology (BinGO GO Full Enrichment) categories from DEG in μg vs. 1*g* only (FDR $q < 0.05$). **(D)** Ten most significant gene ontology (BinGO GO Full Enrichment) categories from DEG in low gravity (circa 0.1*g*) vs. 1*g* only (FDR $q < 0.05$). **(E)** Ten most significant gene ontology (BinGO GO Full Enrichment) categories from DEG in Moon gravity vs. 1*g* only (FDR $q < 0.05$).

blue-light phototropic response in roots of *A. thaliana* grown in conditions of microgravity (Vandenbrink et al., 2016). This relationship was shown to be linearly related to the magnitude of the gravity vector for plants exposed to red light, but plants exposed to blue light showed rapid attenuation of the response in the presence of increasing gravity levels. To determine the differential response to reduced gravity and attempt to dissect the molecular mechanisms of gravisensing, we performed RNA-seq analysis to characterize changes in gene expression that may be associated with the novel blue phototropic response. Interestingly, the effect of blue-light illumination is clearly observable in the microgravity samples, with a clear enrichment in GO terms related with light perception, photosynthesis and biosynthesis of the photosynthetic complexes as previously reported (Vandenbrink et al., 2019), but it is barely appearing in the GO enrichment analyses that we performed on partial gravity samples, even bellow 0.1*g* (low *g* conditions). Surprisingly, the phototropic response to the blue light seems to be enough to cancel the effects of other genes of interest in gravitational research (as the ones observed at low *g* or Moon *g* level) to be not significantly affected in microgravity conditions. This result may be complementing previous reports from the same Seedling Growth spaceflight experiment but with plants exposed to red photostimulation. Fundamental plant functions, as cell proliferation and cell growth activity in root meristems, known to be affected by microgravity in the absence of light (Matía et al., 2010) are balanced just by providing a red photostimulation phase (Valbuena et al., 2018). In both red and blue photostimulation samples within the Seedling Growth experiment, roots are exhibiting a positive phototropism that can compensate the gravitropism stimuli role that it is required to preserve meristematic competence in orbit, as shown by the longer root growth in microgravity and 1*g* samples in comparison with 0.1*g* seedlings (Vandenbrink et al., 2016).

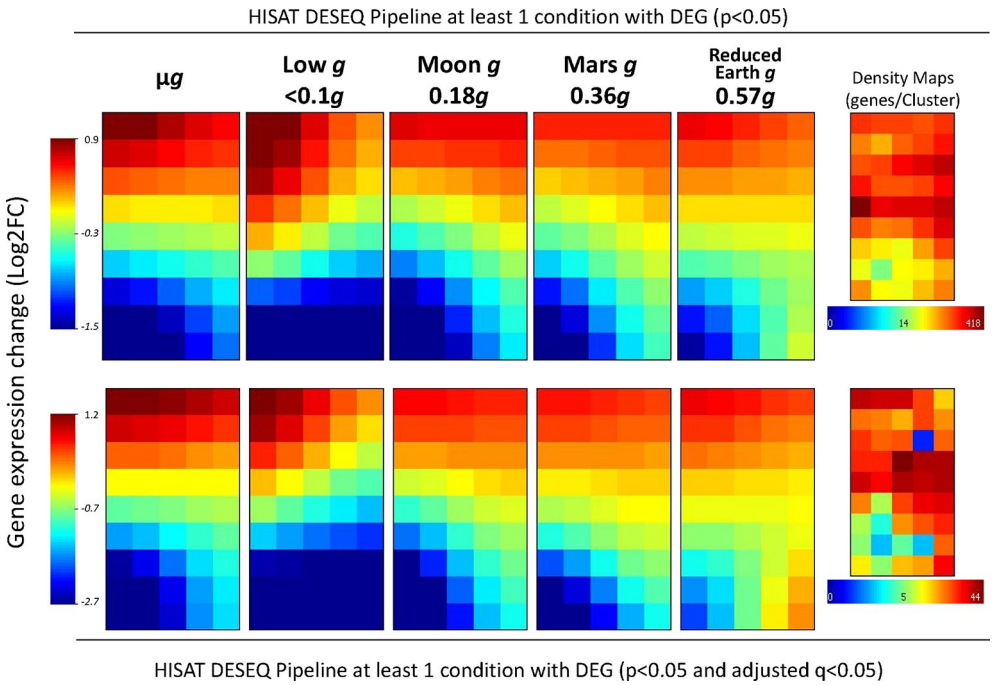

FIGURE 3 | Whole-genome transcriptional status variations along *g*-levels into the SG1/SG2 experiments (comparisons versus 1*g*). A 5x9 clustering analysis of the differentially expressed genes (in at least one of the partial *g* levels, using normal *p* values (first row, n = 5,571 genes) or adjusted *q*-values (second row, n = 861 genes) on the transcriptome have been done with the average of each gene expression level within a similarly expressed cluster across the samples. Values are shown according to the log2 ratio scales at the border of the figure (from highly overrepresented in red to highly down-represented in blue). The mean value of –0.3 or –0.7 indicates an overall repression in gene expression under microgravity. The gene density maps are shown in the middle of the figure for each analysis. Calculated *g*-levels have been obtained by considering replicates the more similar samples across the nominal μ*g*, 0.1*g*, 0.3*g*, 0.5*g*, 0.8*g* and 1*g* (precisely, μ*g* (4 replicates), 0.09 ± 0.02*g* (3 replicates), Moon level (0.18 ± 0.04*g*, 3 replicates), Mars-level (0.36 ± 0.02*g*, 3 replicates), 0.57 ± 0.05*g* (4 replicates) and control 1*g* (0.99 ± 0.06*g*, 3 replicates).

Low-*g* Effect: Competition Between Tropisms or Artifacts of Reduced-Gravity Simulation?

The large number of DEGs detected in the low-*g* conditions (<0.1*g*) is a striking result of this study. The type of transcriptional response observed in this group is similar to stress-related responses reported in other spaceflight or simulated microgravity datasets (Paul et al., 2012; Correll et al., 2013; Sugimoto et al., 2014; Ferl et al., 2015; Kwon et al., 2015; Johnson et al., 2017; Paul et al., 2017; Shi et al., 2017; Zupanska et al., 2017; Choi et al., 2019). In this case, there is a very clear component of "Response to General Stress" with a FDR q value $<10^{-10}$, without any other GO terms to be similarly affected. In contrast the responses at the microgravity level (FDR q value $<10^{-6}$), or at the Moon *g*-level (FDR q value $<10^{-2}$) are very subtle. We explain these results as being the consequence of the combination of two tropistic responses acting with very low intensity. It is very likely that the subtle blue phototropism and the weak gravitropism signal at approximately 0.09*g* are competing to take the leading role in providing the fundamental cue for driving seedling growth and plant development. The result is a stress for the plant (blue-LEDS are located laterally while the gravity vector is towards the bottom of the cassette), which needs to adapt its developmental plan to an environment without the usual tropistic cues. The transcriptional adaptation to provide a response to this evolutionary novel and challenging environment requires the modification of more than five hundred genes, while microgravity only requires half of this number.

An alternative explanation to the low-*g* effects that cannot be completely excluded could be put in connection with simulated microgravity experiments. Secondary effects of microgravity simulation facilities (shear or inertial forces) and even small variations in the environmental conditions of experimental and control samples may lead to gene expression variations in a similar set of genes as those observed in the low-*g* subgroup in this work. Similarly, it is important to take into account the existence of hardware effects when growing plants in real microgravity (Kiss, 2015), including lack of convection, reduced CO_2 levels, improper temperature, elevated ethylene, spacecraft vibrations, increased radiation exposure, among others.

However, the tropism conflict interpretation introduced early on this section seems to have a greater contribution than the artifacts of centrifugation in the low-*g* effects. A hardware side-effect explanation is less conceivable since the present study was conducted utilizing the European Modular Cultivation System, which contains an air scrubbing/filtration system designed for removing excess ethylene from the seedlings during the growth phase (Kiss et al., 2014; Kiss, 2015). Thus, even with proper ventilation, a reduction in gene expression of photosynthetic

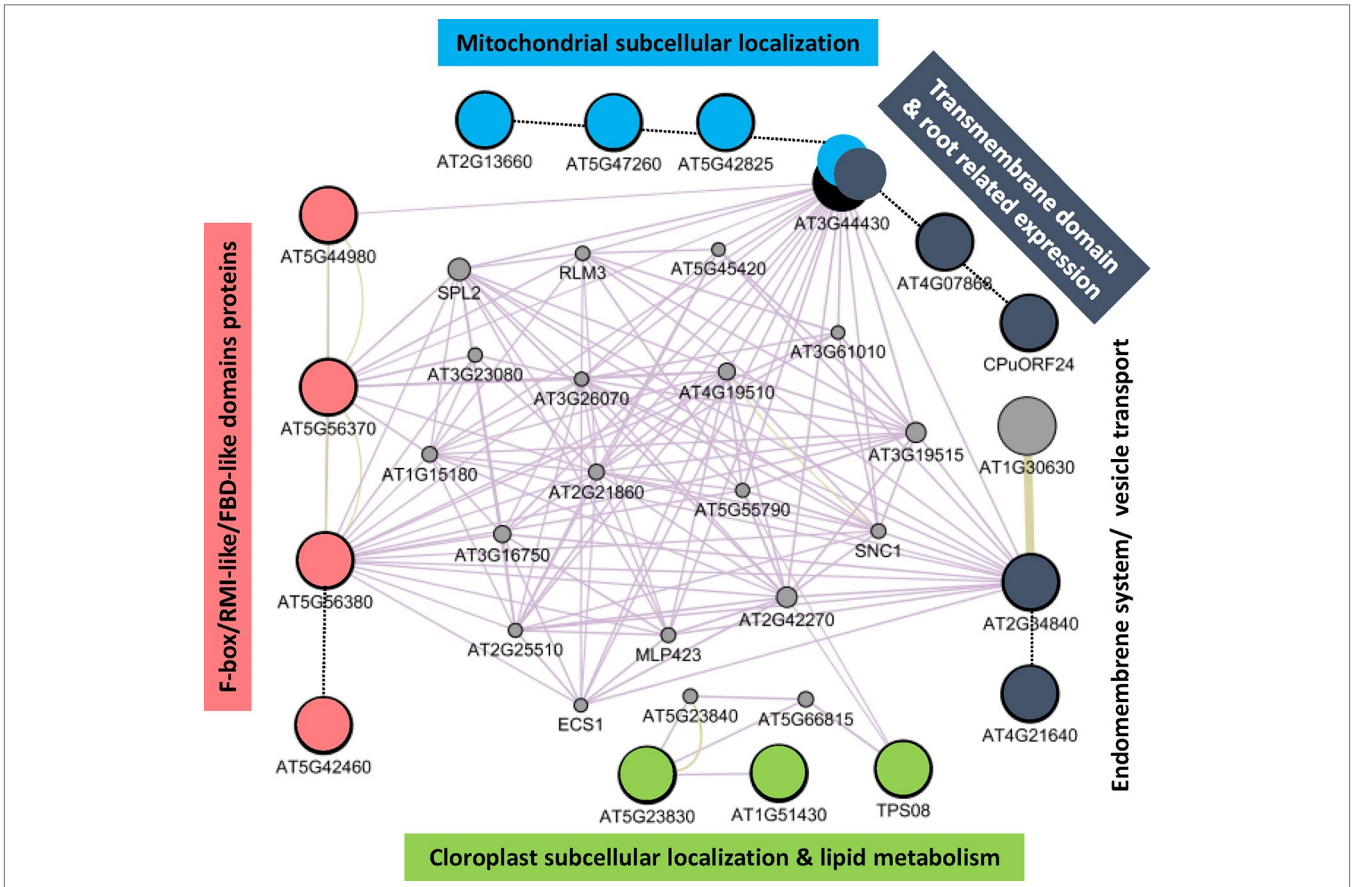

FIGURE 4 | Fifteen up-regulated genes in reduced gravity conditions can be connected in a gravity-response putative pathway. Large circles shown the genes detected in the first row clusters from the previous GEDI analysis (**Figure 3**) and small circles are candidates to be members of a shared pathway (as detected by Genemania App in Cytoscape v3.6.1). While most of the genes have unknown function, color have been used to highlight shared features among their GO properties. Solid lines shown related features as detected by Genemania app, dotted lines have been added by manual datamining comparisons. Note that four genes expressing F-box/RMI-like proteins (in red) out of 156 genes (related examples are auxin polar transport genes as TIR-1, cell wall remodeling and even cyclins) in the genome may be key in the definition of a microgravity specific pathway characterized by the highly interconnected nodes in this graph.

genes was observed in the microgravity samples (Vandenbrink et al., 2019). In the case of the samples exposed to centrifugation, the ventilation effect should be less important, but the centrifugation by itself could lead to additional stress in the samples. However, this centrifugation factor is also present in the 1*g* control sample, exposed to even higher angular speeds.

Spaceflight experimentation is required to verify that simulation strategies on Earth analogues are reliable and worthy. The continuous validation of the best simulation strategies will optimize and increase our chances of success in future spaceflight experiments (Herranz et al., 2013). Additional research in simulated low-*g* conditions on Earth or even in the Moon surface will help to extend and validate this research work.

Moon and Mars-*g* Effects and the Consequences for Manned Spaceflight Missions

Cultivating plants as part of life support systems in nearby objects of our planet will require us to expose the plants to the partial-*g* interval within the two values we examined here, namely, Moon *g*-level (0.18 ± 0.04*g*) and Mars gravity (0.36 ± 0.02*g*). Although some of the genes and GO terms observed affected at lower *g*-levels also appeared in these conditions, the existence of the gravitropic response, in combination with blue light illumination, seems to be enough to restore a nearly normal transcriptional state, particularly at the Mars *g*-level. These results are consistent with previous data coming from partial gravity simulation paradigms that validated that *Arabidopsis* developmental plan is still affected at the Moon *g*-level (even more intensely affected than in similar simulated microgravity samples) but that the "normal" developmental plan is almost completely restored at Mars *g*-levels (Kamal et al., 2018; Manzano et al., 2018).

The identity of some of the GO terms significantly affected at the Moon *g*-level suggest some structural stress at the level of the cell wall and membrane systems. This result is consistent with other results in spaceflight experiments (Kwon et al., 2015; Johnson et al., 2017; Zupanska et al., 2017). This effect is progressively weaker from Moon-*g* (almost similar to microgravity) to Mars-*g*, which shows a less intense response, but

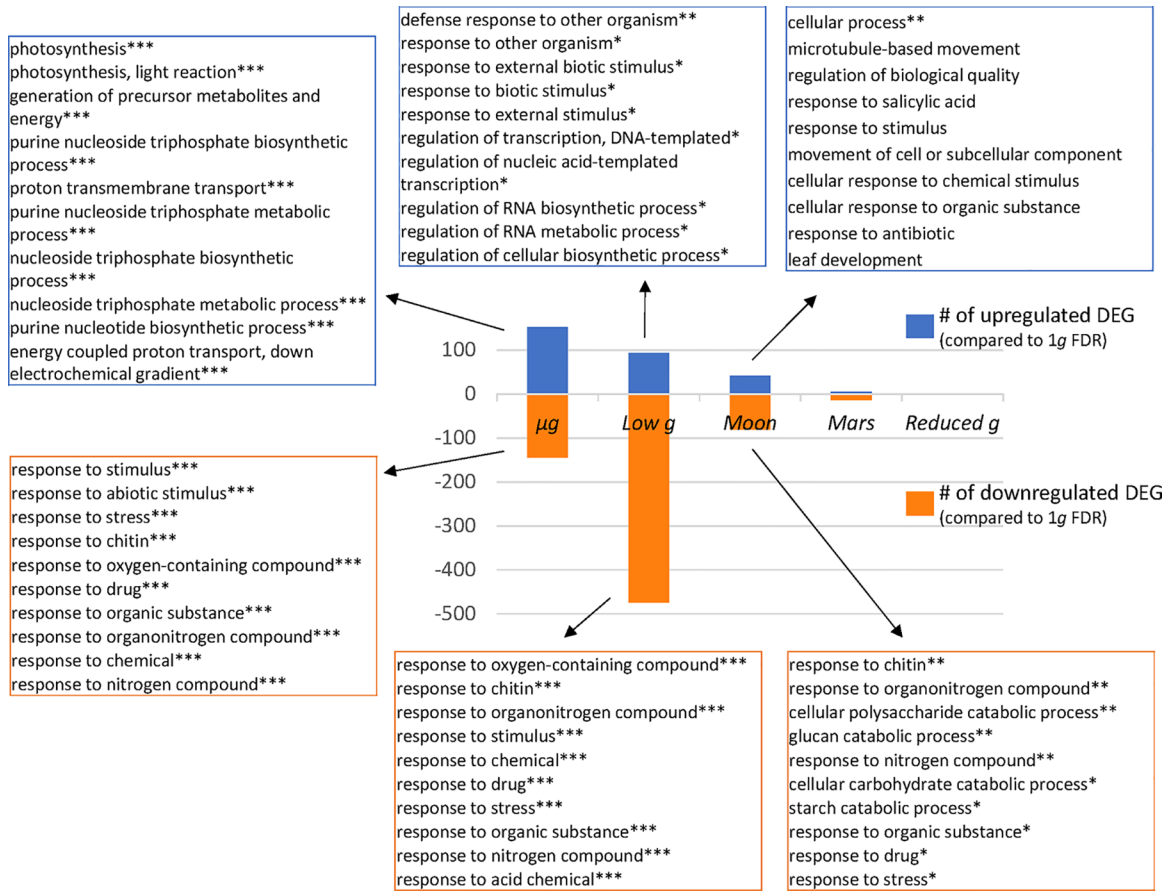

FIGURE 5 | Biological processes affected by reduced gravity (Panther Enrichment in biological process GO). Total number of up-regulated and down-regulated DEG ($p < 0.05$) are shown for the five reduced gravity conditions vs. 1*g* control. The ten most significant gene ontology (Panther biological process GO Enrichment) categories for the three upregulated and the three downregulated DEGs are shown for the microgravity, low gravity (circa 0.1*g*) and Moon gravity (0.18*g*) vs. 1*g* (*** FDR $q < 0.001$, **FDR $q < 0.01$, *FDR $q > 0.05$).

it is still visible at *g*-levels as high as 0.57*g*, when utilizing the less stringent analysis (**Figure 2A**). At these *g*-levels, gravitropism response may be acting and suppressing the recently described blue-light root phototropism, (already at the Moon *g*-level, see **Figure 1C**).

Therefore, we suggest that this transcriptional response could be related with the graviresistance signal that the cells without professional gravisensing organelles (as the statolith in the columella cells of the root) may use to detect *g*-force (Soga, 2013). Particularly at the Moon *g*-level, the very weak gravitropic signal may be still in conflict with a graviresistance tension in the cell wall and membrane systems (also weak), inducing and additional stress that is progressively removed when Mars *g*-level is reached. In that regard, we have found that some of the genes changing throughout the series of reduced gravity levels can be connected in a pathway in which certain genes may have a central position (**Figure 4**). The most connected nodes in the pathway would be the genes involved in the cross-talk between the cell-membrane-localized (AT3G44430 and AT2G34840) and the F-box/RMI-like/FDB-like domain proteins (AT5G56370 and AT5G56380) candidate genes. An important caveat to our results is that RNA was obtained from whole seedlings, despite our assumption that the root is the organ that can discriminate better the weak phototropism and gravitropism signals that are proposed here to be responsible of the transcriptional variations we have shown here.

CONCLUSIONS

The results of this study take advantage of the induction of subtle blue-light phototropism in roots in spaceflight to discern the transcriptional responses to different tropisms in orbit. Removal of the influence of gravity on blue-light-illuminated seedlings showed a reduction in gene expression in multiple pathways associated with photosynthesis, suggesting shared molecular pathways between the two tropistic responses, or a functional compensation among them.

It is important to emphasize that the effects shown at microgravity here are gradually removed by increasing *g*-load. While the phototropic effect is noted at the microgravity level, a general stress response is detected at <0.1*g*, probably due to

conflicting stimuli, just at the detection threshold of photo- and gravi-sensing mechanisms. Membrane-related gene ontologies became the more significant at the Moon *g*-level, and they become progressively weaker at higher *g*-levels, allowing us to discriminate the differential contribution of the classical statolith-based gravitropism from other responses based on cell tensegrity that may require a higher *g*-threshold to be fully active (Hoson et al., 2005; Hoson and Wakabayashi, 2015). Therefore, our results are starting to isolate, at the whole transcriptional level, the global effects that are produced by the gravitropism, phototropism and graviresistance mechanisms, working at different *g*-level thresholds. Future use of mutant lines will help us to confirm and extend these findings, which suggests an intricate connection between gravity and light perception in *A. thaliana*. In the long term, these results on the interaction among tropisms will be important for the use of plants in bioregenerative support systems needed for the human exploration of the Solar System.

DATA AVAILABILITY STATEMENT

The datasets generated for this study can be found in the GeneLab database https://genelab-data.ndc.nasa.gov/genelab/accession/GLDS-251/.

AUTHOR CONTRIBUTIONS

RH and JV designed this partial gravity experiment within the Seedling Growth and wrote the manuscript. JV, WP and FF performed the RNA seq including a preliminary processing of the data. RH, AV and AM performed GEDI and GO analysis. JK and FM designed and coordinated the whole Seedling Growth project series of experiments on board ISS and contributed writing the manuscript. All authors reviewed and agree with the manuscript content.

FUNDING

This work was supported by the Spanish "Plan Estatal de Investigación Científica y Técnica e Innovación" of the Ministry of Economy, Industry and Competitiveness (Grant numbers AYA2012–33982 and ESP2015–64323-R to FJM, cofounded by ERDF), by pre-doctoral fellowships to (AM) and (AV) from the Spanish National Program for Young Researchers Training (MINECO, Ref. BES-2013-063933, BES-2016-077976) and the Seedling Growth Project to the ISS LSRA2009-0932/1177 of ESA-ELIPS Program. Funding for the RNA-seq was provided by NASA Grants NNX12A065G and 80NSSC17K0546 to JZK. We acknowledge support of the publication fee by the CSIC Open Access Publication Support Initiative through its Unit of Information Resources for Research (URICI).

ACKNOWLEDGMENTS

We want to acknowledge the collaboration and support of the whole consortium of people who have contributed to the success of the experiments of the "Seedling Growth" project whose results are reported in this paper. This includes payload developers (Airbus) and EMCS managers (N-USOC), ESA and NASA managers, scientific collaborators (Drs. Eugenie Carnero-Diaz, Malgorzata Ciska, Richard Edelmann, Katherine Millar, Julio Saéz-Vásquez and Miguel Angel Valbuena) and the astronauts that performed the experiments on board the International Space Station.

SUPPLEMENTARY MATERIAL

The Supplementary Material for this article can be found online at: https://www.frontiersin.org/articles/10.3389/fpls.2019.01529/full#supplementary-material

REFERENCES

Anders, S., and Huber, W. (2010). Differential expression analysis for sequence count data. *Genome Biol.* 11, R106. doi: 10.1186/gb-2010-11-10-r106

Babbick, M., Dijkstra, C., Larkin, O. J., Anthony, P., Davey, M. R., Power, J. B., et al. (2007). Expression of transcription factors after short-term exposure of *Arabidopsis thaliana* cell cultures to hypergravity and simulated microgravity (2-D/3-D clinorotation, magnetic levitation). *Adv. Space Res.* 39, 1182–1189. doi: 10.1016/j.asr.2007.01.001

Bardou, P., Mariette, J., Escudie, F., Djemiel, C., and Klopp, C. (2014). jvenn: an interactive Venn diagram viewer. *BMC Bioinf.* 15, 293. doi: 10.1186/1471-2105-15-293

Barjaktarovic, Z., Nordheim, A., Lamkemeyer, T., Fladerer, C., Madlung, J., and Hampp, R. (2007). Time-course of changes in amounts of specific proteins upon exposure to hyper-g, 2-D clinorotation, and 3-D random positioning of *Arabidopsis* cell cultures. *J. Exp. Bot.* 58, 4357–4363. doi: 10.1093/jxb/erm302

Beckingham, K. M. (2010). Synergy between stresses: an interaction between spaceflight-associated conditions and the microgravity response. *Mol. Ecol.* 19, 4105–4107. doi: 10.1111/j.1365-294X.2010.04799.x

Benjamini, Y., and Hochberg, Y. (1995). Controlling the false discovery rate: a practical and powerful approach to multiple testing. *J. R. Stat. Soc B* 57, 289–300. doi: 10.1111/j.2517-6161.1995.tb02031.x

Bouchern-Dubuisson, E., Manzano, A. I., Le Disquet, I., Matia, I., Saez-Vasquez, J., Van Loon, J. J. W. A., et al. (2016). Functional alterations of root meristematic cells of *Arabidopsis thaliana* induced by a simulated microgravity environment. *J. Plant Physiol.* 207, 30–41. doi: 10.1016/j.jplph.2016.09.011

Briggs, W. R. (2014). Phototropism: some history, some puzzles, and a look ahead. *Plant Physiology* 164, 13–23.

Brinckmann, E., and Schiller, P. (2002). Experiments with small animals in BIOLAB and EMCS on the International Space Station. *Adv. Space Res.* 30, 809–814. doi: 10.1016/S0273-1177(02)00401-5

Brinckmann, E. (2005). ESA hardware for plant research on the International Space Station. *Adv. Space Res.* 36, 1162–1166. doi: 10.1016/j.asr.2005.02.019

Chen, R., Rosen, E., and Masson, P. H. (1999). Gravitropism in higher plants. *Plant Physiol.* 120, 343–350. doi: 10.1104/pp.120.2.343

Choi, W. G., Barker, R. J., Kim, S. H., Swanson, S. J., and Gilroy, S. (2019). Variation in the transcriptome of different ecotypes of *Arabidopsis thaliana* reveals signatures of oxidative stress in plant responses to spaceflight. *Am. J. Bot.* 106, 123–136. doi: 10.1002/ajb2.1223

Correll, M. J., Pyle, T. P., Millar, K. D., Sun, Y., Yao, J., Edelmann, R. E., et al. (2013). Transcriptome analyses of *Arabidopsis thaliana* seedlings grown in space: implications for gravity-responsive genes. *Planta* 238, 519–533. doi: 10.1007/s00425-013-1909-x

Driss-Ecole, D., Legue, V., Carnero-Diaz, E., and Perbal, G. (2008). Gravisensitivity and automorphogenesis of lentil seedling roots grown on

board the International Space Station. *Physiol. Plant* 134, 191–201. doi: 10.1111/j.1399-3054.2008.01121.x

Eichler, G. S., Huang, S., and Ingber, D. E. (2003). Gene Expression Dynamics Inspector (GEDI): for integrative analysis of expression profiles. *Bioinformatics* 19, 2321–2322. doi: 10.1093/bioinformatics/btg307

Ferl, R. J., Koh, J., Denison, F., and Paul, A. L. (2015). Spaceflight induces specific alterations in the proteomes of *Arabidopsis*. *Astrobiology* 15, 32–56. doi: 10.1089/ast.2014.1210

Godia, F., Albiol, J., Perez, J., Creus, N., Cabello, F., Montras, A., et al. (2004). The MELISSA pilot plant facility as as integration test-bed for advanced life support systems. *Adv. Space Res.* 34, 1483–1493. doi: 10.1016/j.asr.2003.08.038

Herranz, R., Anken, R., Boonstra, J., Braun, M., Christianen, P. C. M., Geest, M. D., et al. (2013). Ground-based facilities for simulation of microgravity, including terminology and organism-specific recommendations for their use. *Astrobiology* 13, 1–17. doi: 10.1089/ast.2012.0876

Hooper, C. M., Castleden, I. R., Tanz, S. K., Aryamanesh, N., and Millar, A. H. (2017). SUBA4: the interactive data analysis centre for *Arabidopsis* subcellular protein locations. *Nucleic Acids Res.* 45, D1064–D1074. doi: 10.1093/nar/gkw1041

Hopkins, J. A., and Kiss, J. Z. (2012). Phototropism and gravitropism in transgenic lines of *Arabidopsis* altered in the phytochrome pathway. *Physiol. Plant.* 145, 461–473. doi: 10.1111/j.1399-3054.2012.01607.x

Hoson, T., and Wakabayashi, K. (2015). Role of the plant cell wall in gravity resistance. *Phytochemistry* 112, 84–90. doi: 10.1016/j.phytochem.2014.08.022

Hoson, T., Saito, Y., Soga, K., and Wakabayashi, K. (2005). Signal perception, transduction, and response in gravity resistance. Another graviresponse in plants. *Adv. Space Res.* 36, 1196–1202. doi: 10.1016/j.asr.2005.04.095

Johnson, C. M., Subramanian, A., Pattathil, S., Correll, M. J., and Kiss, J. Z. (2017). Comparative transcriptomics indicate changes in cell wall organization and stress response in seedlings during spaceflight. *Am. J. Bot.* 104, 1219–1231. doi: 10.3732/ajb.1700079

Kamal, K. Y., Herranz, R., Van Loon, J. J. W. A., and Medina, F. J. (2018). Simulated microgravity, Mars gravity, and 2g hypergravity affect cell cycle regulation, ribosome biogenesis, and epigenetics in *Arabidopsis* cell cultures. *Plant Cell Environ.* 2019 (42), 480–494. doi: 10.1038/s41598-018-24942-7

Kim, D., Langmead, B., and Salzberg, S. L. (2015). HISAT: a fast spliced aligner with low memory requirements. *Nat. Methods* 12, 357–360. doi: 10.1038/nmeth.3317

Kiss, J. Z., Aanes, G., Schiefloe, M., Coelho, L. H., Millar, K. D., and Edelmann, R. E. (2014). Changes in operational procedures to improve spaceflight experiments in plant biology in the European Modular Cultivation System. *Adv. Space Res.* 53, 818–827. doi: 10.1016/j.asr.2013.12.024

Kiss, J. Z. (2015). Conducting plant experiments in space. *Methods In Mol. Biol.* 1309, 255–283. doi: 10.1007/978-1-4939-2697-8_19

Kruse, C. P. S., Basu, P., Luesse, D. R., and Wyatt, S. E. (2017). Transcriptome and proteome responses in RNAlater preserved tissue of *Arabidopsis thaliana*. *PloS One* 12, e0175943. doi: 10.1371/journal.pone.0175943

Kutschera, U., and W. R. Briggs. (2016). Phototropic solar tracking in sunflower plants: an integrative perspective. *Annals of Botany* 117, 1–8.

Kwon, T., Sparks, J. A., Nakashima, J., Allen, S. N., Tang, Y., and Blancaflor, E. B. (2015). Transcriptional response of Arabidopsis seedlings during spaceflight reveals peroxidase and cell wall remodeling genes associated with root hair development. *Am. J. Bot.* 102, 21–35. doi: 10.3732/ajb.1400458

Maere, S., Heymans, K., and Kuiper, M. (2005). BiNGO: a Cytoscape plugin to assess overrepresentation of gene ontology categories in biological networks. *Bioinformatics* 21, 3448–3449. doi: 10.1093/bioinformatics/bti551

Manzano, A., Herranz, R., den Toom, L. A., Slaa, S. T., Borst, G., Visser, M., et al. (2018). Novel, Moon and Mars, partial gravity simulation paradigms and their effects on the balance between cell growth and cell proliferation during early plant development. *NPJ Microgravity* 4, 9. doi: 10.1038/s41526-018-0041-4

Matía, I., Gonzalez-Camacho, F., Herranz, R., Kiss, J. Z., Gasset, G., Van Loon, J. J. W. A., et al. (2010). Plant cell proliferation and growth are altered by microgravity conditions in spaceflight. *J. Plant Physiol.* 167, 184–193. doi: 10.1016/j.jplph.2009.08.012

Mazars, C., Briere, C., Grat, S., Pichereaux, C., Rossignol, M., Pereda-Loth, V., et al. (2014). Microgravity induces changes in microsome-associated proteins of *Arabidopsis* seedlings grown on board the international space station. *PloS One* 9, e91814. doi: 10.1371/journal.pone.0091814

Mi, H., Muruganujan, A., Ebert, D., Huang, X., and Thomas, P. D. (2019). PANTHER version 14: more genomes, a new PANTHER GO-slim and improvements in enrichment analysis tools. *Nucleic Acids Res.* 47, D419–D426. doi: 10.1093/nar/gky1038

Paul, A. L., Zupanska, A. K., Ostrow, D. T., Zhang, Y., Sun, Y., Li, J. L., et al. (2012). Spaceflight transcriptomes: unique responses to a novel environment. *Astrobiology* 12, 40–56. doi: 10.1089/ast.2011.0696

Paul, A. L., Zupanska, A. K., Schultz, E. R., and Ferl, R. J. (2013). Organ-specific remodeling of the *Arabidopsis* transcriptome in response to spaceflight. *BMC Plant Biol.* 13, 112. doi: 10.1186/1471-2229-13-112

Paul, A. L., Sng, N. J., Zupanska, A. K., Krishnamurthy, A., Schultz, E. R., and Ferl, R. J. (2017). Genetic dissection of the *Arabidopsis* spaceflight transcriptome: Are some responses dispensable for the physiological adaptation of plants to spaceflight? *PloS One* 12, e0180186. doi: 10.1371/journal.pone.0180186

Shannon, P., Markiel, A., Ozier, O., Baliga, N. S., Wang, J. T., Ramage, D., et al. (2003). Cytoscape: a software environment for integrated models of biomolecular interaction networks. *Genome Res.* 13, 2498–2504. doi: 10.1101/gr.1239303

Shi, K., Gu, J., Guo, H., Zhao, L., Xie, Y., Xiong, H., et al. (2017). Transcriptome and proteomic analyses reveal multiple differences associated with chloroplast development in the spaceflight-induced wheat albino mutant mta. *PloS One* 12, e0177992. doi: 10.1371/journal.pone.0177992

Soga, K. (2013). Resistance of plants to gravitational force. *J. Plant Res.* 126, 589–596. doi: 10.1007/s10265-013-0572-4

Sugimoto, M., Oono, Y., Gusev, O., Matsumoto, T., Yazawa, T., Levinskikh, M. A., et al. (2014). Genome-wide expression analysis of reactive oxygen species gene network in Mizuna plants grown in long-term spaceflight. *BMC Plant Biol.* 14, 4. doi: 10.1186/1471-2229-14-4

Trimmomatic (2013). www.usadellab.org/cms/?page=trimmomatic [Online]. Available: http://www.usadellab.org/cms/index.php?page=trimmomatic [Accessed]

Valbuena, M. A., Manzano, A., Vandenbrink, J. P., Pereda-Loth, V., Carnero-Diaz, E., Edelmann, R. E., et al. (2018). The combined effects of real or simulated microgravity and red-light photoactivation on plant root meristematic cells. *Planta* 248, 691–704. doi: 10.1007/s00425-018-2930-x

Van Loon, J. J. W. A., Krause, J., Cunha, H., Goncalves, J., Almeida, H., and Schiller, P. (2008). The large diameter centrifuge, LDC, for life and physical sciences and technology, in: *Proc. of the 'Life in Space for Life on Earth Symposium', Angers, France*. Noordwijk, Netherlands: European Space Agency (ESA). (ESA SP-663, December 2008).

Vandenbrink, J. P., Brown, E. A., Harmer, S. L., and Blackman, B. K. (2014). Turning heads: the biology of solar tracking in sunflower. *Plant Science* 224, 20–26.

Vandenbrink, J. P., and Kiss, J. Z. (2016). Space, the final frontier: a critical review of recent experiments performed in microgravity. *Plant Sci.* 243, 115–119. doi: 10.1016/j.plantsci.2015.11.004

Vandenbrink, J. P., and Kiss, J. Z. (2019). Preparation of a apaceflight experiment to study tropisms in *Arabidopsis* seedlings on the International Space Station. *Methods Mol. Biol.* 1924, 207–214. doi: 10.1007/978-1-4939-9015-3_17

Vandenbrink, J. P., Herranz, R., Medina, F. J., Edelmann, R. E., and Kiss, J. Z. (2016). A novel blue-light phototropic response is revealed in roots of *Arabidopsis thaliana* in microgravity. *Planta* 244, 1201–1215. doi: 10.1007/s00425-016-2581-8

Vandenbrink, J. P., Herranz, R., Poehlman, W., Feltus, F. A., Villacampa, A., Ciska, M., et al. (2019). RNAseq analyses of *Arabidopsis thaliana* seedlings after exposure to blue-light phototropic stimuli in microgravity. *Am. J. Bot.* 106 (11), 1466–1476. In press. doi: 10.1002/ajb2.1384

Volkmann, D., and Baluska, F. (2006). Gravity: one of the driving forces for evolution. *Protoplasma* 229, 143–148. doi: 10.1007/s00709-006-0200-4

Zupanska, A. K., Schultz, E. R., Yao, J., Sng, N. J., Zhou, M., Callaham, J. B., et al. (2017). ARG1 functions in the physiological adaptation of undifferentiated plant cells to spaceflight. *Astrobiology* 17, 1077–1111. doi: 10.1089/ast.2016.1538

Conflict of Interest: The authors declare that the research was conducted in the absence of any commercial or financial relationships that could be construed as a potential conflict of interest.

iScience

CellPress
OPEN ACCESS

Article

The Importance of Earth Reference Controls in Spaceflight -Omics Research: Characterization of Nucleolin Mutants from the Seedling Growth Experiments

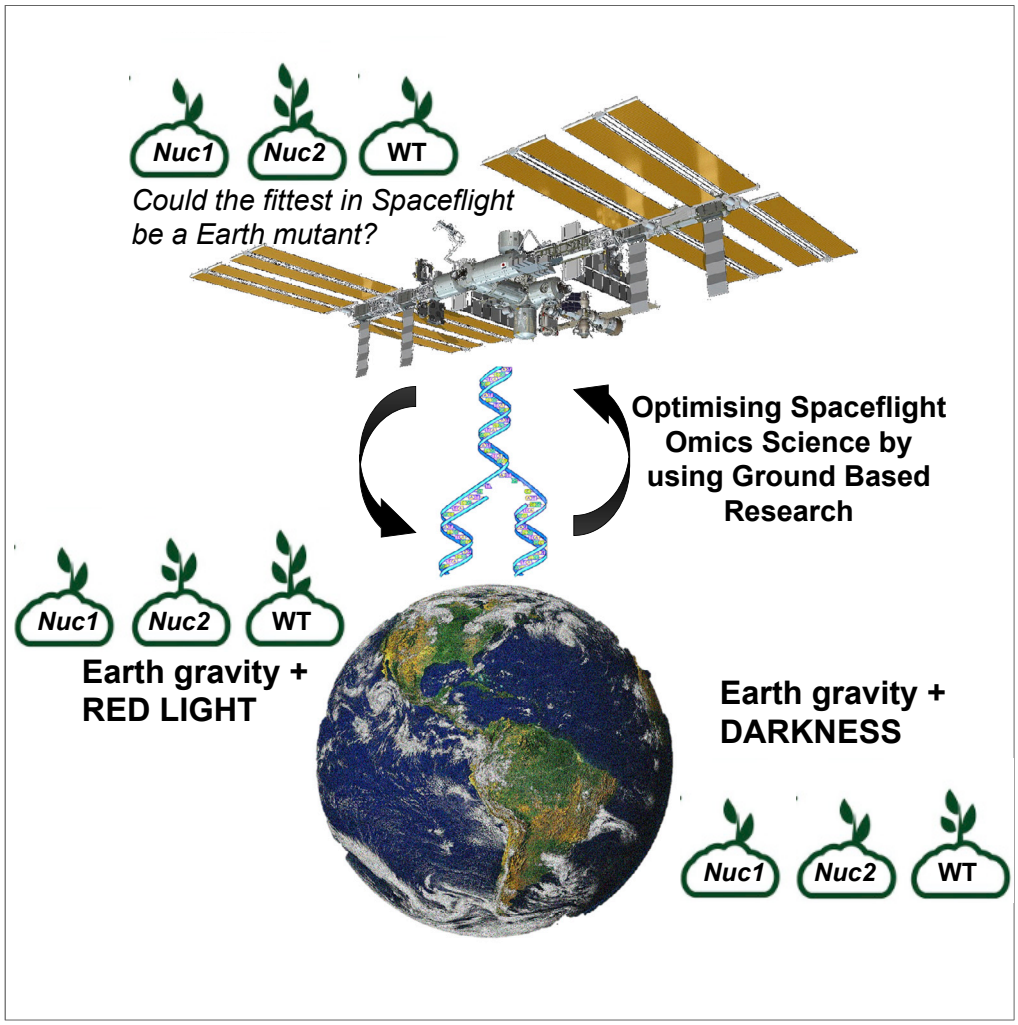

Aránzazu Manzano, Alicia Villacampa, Julio Sáez-Vásquez, John Z. Kiss, F. Javier Medina, Raúl Herranz

r.herranz@csic.es

HIGHLIGHTS

Ribosome synthesis is a target of spaceflight stressor effects on plant development

Nucleolin mutants promote a differential response to light/ darkness stress

Red light and NUC2 may counteract the spaceflight alterations in gene expression

Ground controls are important for the interpretation of spaceflight -omics experiments

Manzano et al., iScience *23*, 101686
November 20, 2020
https://doi.org/10.1016/j.isci.2020.101686

iScience

CellPress
OPEN ACCESS

Article

The Importance of Earth Reference Controls in Spaceflight -Omics Research: Characterization of Nucleolin Mutants from the Seedling Growth Experiments

Aránzazu Manzano,[1,5] Alicia Villacampa,[1,5] Julio Sáez-Vásquez,[2,3] John Z. Kiss,[4] F. Javier Medina,[1] and Raúl Herranz[1,6,*]

SUMMARY

Understanding plant adaptive responses to the space environment is a requisite for enabling space farming. Spaceflight produces deleterious effects on plant cells, particularly affecting ribosome biogenesis, a complex stress-sensitive process coordinated with cell division and differentiation, known to be activated by red light. Here, in a series of ground studies, we have used mutants from the two *Arabidopsis* nucleolin genes (*NUC1* and *NUC2*, nucleolar regulators of ribosome biogenesis) to better understand their role in adaptive response mechanisms to stress on Earth. Thus, we show that nucleolin stress-related gene *NUC2* can compensate for the environmental stress provided by darkness in *nuc1* plants, whereas *nuc2* plants are not able to provide a complete response to red light. These ground control findings, as part of the ESA/NASA Seedling Growth spaceflight experiments, will determine the basis for the identification of genetic backgrounds enabling an adaptive advantage for plants in future space experiments.

INTRODUCTION

Space exploration will soon include new human missions to the Moon as a first step in the human exploration of Mars. Recent studies in human (i.e., NASA Twin Study, Garrett-Bakelman et al., 2019) and mammalian systems (rodent missions, Beheshti et al., 2019; Ronca et al., 2019) are paving the way to understand the effects of the microgravity environment on human physiology, but human life in space will rely on the essential role of plants in bioregenerative life support systems (Zabel et al., 2016), not only as a source of water, food, and removal of CO_2 but also by providing a terrestrial-like environment for the psychological well-being of astronauts.

Due to their sessile condition, plants have to promote adaptive responses to cope with changes in environmental conditions. Light plays multiple roles in the mechanisms of these adaptive responses. On the one hand, light is the source of energy by means of photosynthesis and regulates indirectly cell proliferation and cell growth via the central regulator TOR kinase through the expression of S-phase genes, and also ribosome biogenesis (Caldana et al., 2013; Xiong et al., 2013; Sablowski and Carnier Dornelas, 2014). In addition, light is a major driver in the establishment of the patterns of plant growth and development, by means of phototropism and photomorphogenesis. In playing this role, light is associated with gravity as one of the major tropistic cues, such that gravitropism and phototropism (and the interaction between them) are essential modulators of plant development (Vandenbrink et al., 2014). At the cellular and molecular levels, plant development relies on the activity of cell growth and proliferation taking place in the meristems, which supply differentiated cells and are influenced by the tropistic cues (Perrot-Rechenmann, 2010).

Darkness is indeed a stress condition for plants. Several articles describe that in the dark, apical meristem proliferation is arrested in the G1 and G2 phases of the cell cycle (López-Juez et al., 2008; Mohammed et al., 2017), but in the root meristem, light induces the production of flavonols and other metabolites leading to

[1]Centro de Investigaciones Biológicas Margarita Salas (CSIC), Ramiro de Maeztu 9, 28040, Madrid, Spain

[2]CNRS, Laboratoire Génome et Développement des Plantes (LGDP), UMR 5096, 66860 Perpignan, France

[3]Univ. Perpignan Via Domitia, LGDP, UMR 5096, 66860 Perpignan, France

[4]Department of Biology, University of North Carolina-Greensboro, Greensboro, NC 27402, USA

[5]These authors contributed equally

[6]Lead Contact

*Correspondence: r.herranz@csic.es

https://doi.org/10.1016/j.isci.2020.101686

the reduction of cell proliferation (Silva-Navas et al., 2016). This reduction could be related to the sugar starvation that results from the inability to perform photosynthesis.

However, red light has a stimulating effect on ribosome biogenesis and cell proliferation. An increase in the mitotic index, in the expression of some regulators of these processes at both gene expression and protein levels, and in post-translational modifications of some protein factors has been described in plants irradiated with red light (Tong et al., 1997; Reichler et al., 2001).

The absence of gravity (weightlessness, or microgravity, as it exists in free-fall, or in spaceflight) is also, by itself, a stress condition for plants, and specifically for the functions of meristematic cells (Matía et al., 2010; Boucheron-Dubuisson et al., 2016). An experiment performed in the International Space Station (ISS) in which *Arabidopsis thaliana* seedlings grew for 4 days in darkness resulted in an increase in the rate of cell proliferation and a decrease in the cell growth rate, estimated by the activity of ribosome biogenesis in the nucleolus, compared with the 1*g* control (Matía et al., 2010). As the coordination of these two activities defines meristematic competence, the effect of the lack of tropistic stimuli, particularly of gravity signals, may result in serious alterations of the developmental pattern of the plant, as was also shown in simulated microgravity experiments (Boucheron-Dubuisson et al., 2016).

The Seedling Growth (SG) experiments, recently performed in the ISS, aimed at unraveling the link between phototropism and gravitropism, using the weightless environment of spaceflight (Vandenbrink et al., 2019; Herranz et al., 2019). In the first SG experiment, *A. thaliana* seedlings corresponding to wild-type (WT) ecotype *Landsberg erecta* (Ler) and two phytochrome mutants (*phyA* and *phyB*) known to be involved in phototropism (Kiss et al., 2003; Molas and Kiss, 2008) were grown in space for 6 days and photostimulated for the last 2 days, revealing differential blue and red light phototropism in space (Vandenbrink et al., 2016). The analysis of the expression of regulatory genes of cell cycle and ribosome biogenesis showed that red light irradiation produced a significant reversion of the uncoupling of cell proliferation and cell growth caused by microgravity in darkness (Matía et al., 2010) and, consequently, a compensation of the loss of meristematic competence (Valbuena et al., 2018).

In view of these results from our previous space experiments, we decided to focus on the cellular process of ribosome biogenesis for the successive spaceflight experiments of the SG project, with the purpose of testing the separate and synergistic effects of the light and gravity tropistic signals on specific molecular and cellular components of this process. Ribosome biogenesis, which takes place in the nucleolus, represents the most complex multi-step process that the cell must perform and is one of the most intricately regulated and controlled (Sáez-Vásquez and Medina, 2008; Pelletier et al., 2018). Therefore, its regulation must adapt to the environmental conditions in which the cell finds itself and coordinate with other cellular processes, such as cell division and differentiation. Several studies have described and used the nucleolus as a major stress sensor, using stress-induced changes in the organization and composition of this organelle (Mayer and Grummt, 2005; Boulon et al., 2010; Lewinska et al., 2010; Kalinina et al., 2018).

Briefly, ribosome biogenesis consists of the transcription of 45S rRNA genes (45S rDNA) containing the sequences of 18S, 5.8S, and 25S rRNAs, followed by the multi-step cleavage of 45S pre-rRNA to produce, in association with 5S rRNA and ribosomal proteins (RPs), the mature ribosomal subunits, which are then exported to the cytoplasm and assembled as mature ribosomes.

In addition to RPs, hundreds of non-ribosomal proteins (NRPs), or nucleolar proteins and small nucleolar RNAs are required for ribosome biogenesis, playing regulatory roles (Sáez-Vásquez and Delseny, 2019). Among NRPs, nucleolin is the most abundant protein of the nucleolus, where it plays a key role in the different steps involved in ribosome biogenesis, including RNA polymerase (Pol) I transcription, processing of pre-rRNA (Ginisty et al., 1999; Roger et al., 2003), and assembly and nucleocytoplasmic transport of ribosome particles (Bouvet et al., 1998). Moreover, nucleolin has been even implicated in other functions, with or without collateral relationship with ribosome biogenesis (Angelov et al., 2006; Ma et al., 2007; Mongelard and Bouvet, 2007; Stepiński, 2012).

Animal and yeast genomes encode a single nucleolin gene, whereas plants offer various examples of gene multiplicity. In *A. thaliana*, two genes encoding nucleolin proteins have been described: *NUC1* and *NUC2* (Pontvianne et al., 2007, 2010). The *NUC1* gene is highly and ubiquitously expressed in normal growth

conditions and NUC1 protein is required to inhibit *NUC2* gene expression at the transcriptional level and may also influence the accumulation of NUC2 protein. In contrast, *NUC2* is a functional protein-coding gene developmentally controlled in most plant tissues and organs (Durut et al., 2014). NUC1 and NUC2 proteins localize in the nucleolus.

Disruption of *NUC1* gene (*nuc1-2* mutant) leads to severe defects in plant growth and development. At the molecular level, this mutant produces *NUC2* expression, nucleolus disorganization, rDNA (NOR) heterochromatin decondensation, pre-rRNA accumulation, de-repression of specific rDNA variants, and demethylation of some sequences of rDNA (Pontvianne et al., 2010).

In contrast, disruption of *NUC2* gene (*nuc2-2* mutant) has much weaker effects. The *nuc2-2* mutant seedlings grow quite similarly to WT plants, but flowering occurs later. Knockout of the *NUC2* gene induces expression of some rDNA variants and hypermethylation of some sequences of pre-rRNA. In addition, NUC2 is required for the stability of rDNA variants' copy number (Durut et al., 2014).

In this article, in a series of ground studies to complement space experiments, we have exposed *A. thaliana* (ecotype Columbia) WT, *nuc1-2* and *nuc2-2* seedlings to two different illumination regimes at the beginning of the plant development (6 days from germination). In addition to highlighting the importance of Earth reference controls in spaceflight -omics experiments, our goal was to better understand the responses of nucleolin mutants to red light stimulation for further uses in space experiments under altered gravity conditions. The differential adaptive responses to the light are shown, suggesting that stress-related mutants may show a reduced response to environmental stress. In the long term, these results may lead to more efficient agriculture if an exaggerated response may reduce plant development under suboptimal environmental conditions.

RESULTS

Overall Transcriptional Profile Effects Confirm a Suitable Quality of Plant Material and Clustering of the Replicates

Two environmental conditions (light) are compared here, both of them as part of the SG Earth control reference experiment using the European Modular Cultivation System (EMCS). Seedlings were germinated in the same spaceflight hardware during 4 days with a day/night cycle of illumination, and then half of the samples were exposed to 2 days of darkness and the other group to 2 days of continuous red light (Figure 1A). After 6 days growth in the culture chamber (CC), the experiment was completed and the phenotypes of the three mutants were observed (Figure 1B, Supplemental Information, Figure S1). Seedling growth was homogeneous within each cassette, with clearly smaller seedlings in the case of the *nuc1-2* mutant. No clear phenotypical differences were observed in the root system physiology between darkness- and red light-stimulated samples (including the absence of red phototropism at 1*g* conditions). The phenotype was compared with a previous experiment with the same duration and genotypes but in petri dishes and with a 6-day photoperiod illumination profile (Manzano et al., 2020 submitted). Despite the effects of the TROPI cassette volume, the overall phenotype of the seedlings is also very similar in both studies.

The quality of the replicates and overall similarities among the illumination regimes and different plants used is shown by principal-component analysis (PCA, Figure 1C and Supplemental Information, Data S1). First, a clear difference between the transcriptional profile of the WT, *nuc1-2,* and *nuc2-2* plants exposed to darkness or red light photostimulation during the last 2 days of growth is shown by principal component 1 (PC1). Second, the differences between the genotypes can be observed in principal component 2 (PC2), where the *nuc1-2* genotype has the most disrupted nucleolus phenotype, in that the *nuc2-2* mutant is closer to the WT. The effect is clearer in the dark samples, because the red light stimulation produces more similarities among the three genotypes. Last, all the biological replicates included in the study cluster together according to the experimental condition, strengthening the statistical validity of the study. The use of three biological replicates (including up to 10 seedlings each) is enough considering the difficulties in increasing this number due to the availability of spaceflight research capabilities.

Global Effect of Red Light Photostimulation Differs in Each *Arabidopsis thaliana* Line

To understand the effect of the two lighting regimes (red light and darkness) on the transcriptional status, we compared seedlings with the differential illumination during the last 2 days of the plant growth period for each of the lines used (WT, *nuc1-2,* and *nuc2-2*).

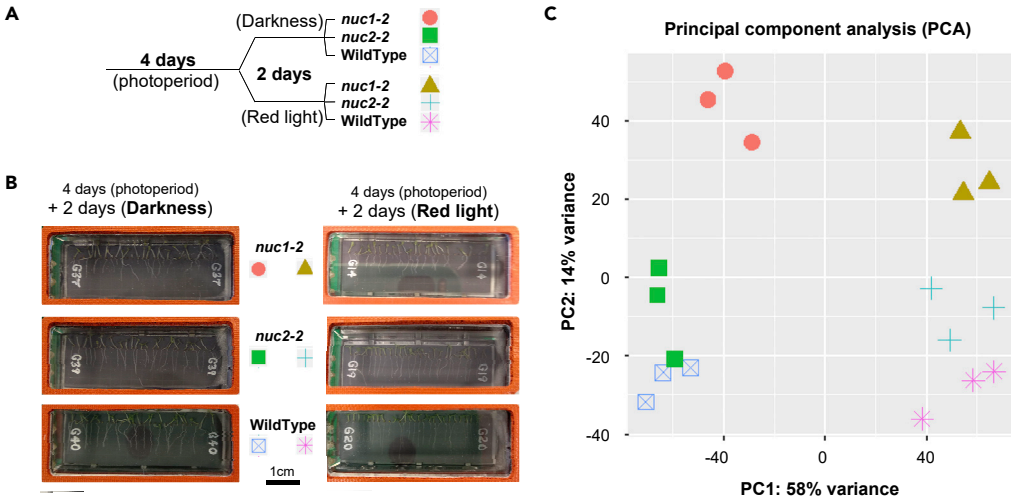

Figure 1. The Seedling Growth 2 Ground Reference Experiment

(A) Experimental design including the illumination profile for each sample including color code used as key.

(B) Images of 6-day-old seedlings (WildType, *nuc1-2,* and *nuc2-2,* under the two illumination options) inside the CC just before collection for freezing (additional photos are provided as Supplemental Information Figure S1). Scale bar, 1 cm (the gridded membrane has clearly defined grid lines spaced at 3.1 mm). The labels on the membrane represent the cassette # in the ground control.

(C) Principal-component analysis (PCA) of the 18 samples (three replicates per condition) using read counts data from FeatureCounts. This diagram gives an overview of the similarities and dissimilarities between samples and the experimental conditions' overall effects (see Data S1 for an RNA quality report on the red light samples). All replicates are consistently grouped according to their experimental conditions, and two clear PC1 (for illumination conditions during the last 2 days of growth: darkness and red light) and PC2 (for genetic background: WT, *nuc1-2,* and *nuc2-2*) are observed.

The number of differentially expressed genes (DEGs) in the WT is 1,428 genes, of which 1,067 have their expression activated and 361 have it repressed. In the *nuc1-2* mutant, the total number of DEGs is lower (1,001), mainly at the expense of the up-regulated genes (633 are over-expressed and 368 are repressed). The number of DEGs from the comparison (red light versus darkness) in the *nuc2-2* mutant is very similar as in the WT: a total of 1,017 up-regulated genes and 339 down-regulated genes, making a total of 1,365 DEGs (Figure 2).

Venn diagrams illustrate the group of DEGs that is affected in a single genotype or shared by others (Figure 2). Red light up-regulated genes affected only 298 genes in the WT, 134 genes in *nuc1-2* mutant, and 199 genes for *nuc2-2* mutant. On the other hand, the WT has 34 up-regulated genes in common with *nuc1-2* but a large collection of 353 genes in common with *nuc2-2* (note that the total number of up-regulated genes common for the three genotypes is 382), and only 83 genes for both nucleolin mutants (Figure 2B).

Among DEGs down-regulated by the red light compared with the dark, there is a similar number of unique DEGs for each of them; 139 genes for the WT, 142 genes for the *nuc1-2* mutant, and 104 genes for the *nuc2-2* mutant. In this case, the number of DEGs down-regulated in the three lines is 125 genes, without any of the pair comparisons reaching that level (the *nuc1-2* and *nuc2-2* mutants have 44 and 53 genes in common with WT, respectively, whereas the two nucleolin mutants share 57 down-regulated genes, Figure 2C).

In summary, the line with the least number of DEGs, when we compare plants illuminated with red light with those kept in darkness, is the *nuc1-2* mutant. As the down-regulation response seems similar in all genotypes, the global effect is mainly due to a higher number of up-regulated DEGs in both *nuc2-2* and WT genotypes. In fact, we can easily extrapolate from Figure 2B and compare the gene lists, including the common responses to red light (382 genes) and the list of up-regulated genes not detected in the *nuc1-2* phenotype (353 genes). The main difference between these lists is shown by the functional analysis "GO Enrichment" included in Figure 2. All genotypes show the obvious photosynthesis/light-harvesting response together with increased Calvin cycle activity, but the *nuc1-2* genotype is the only one lacking

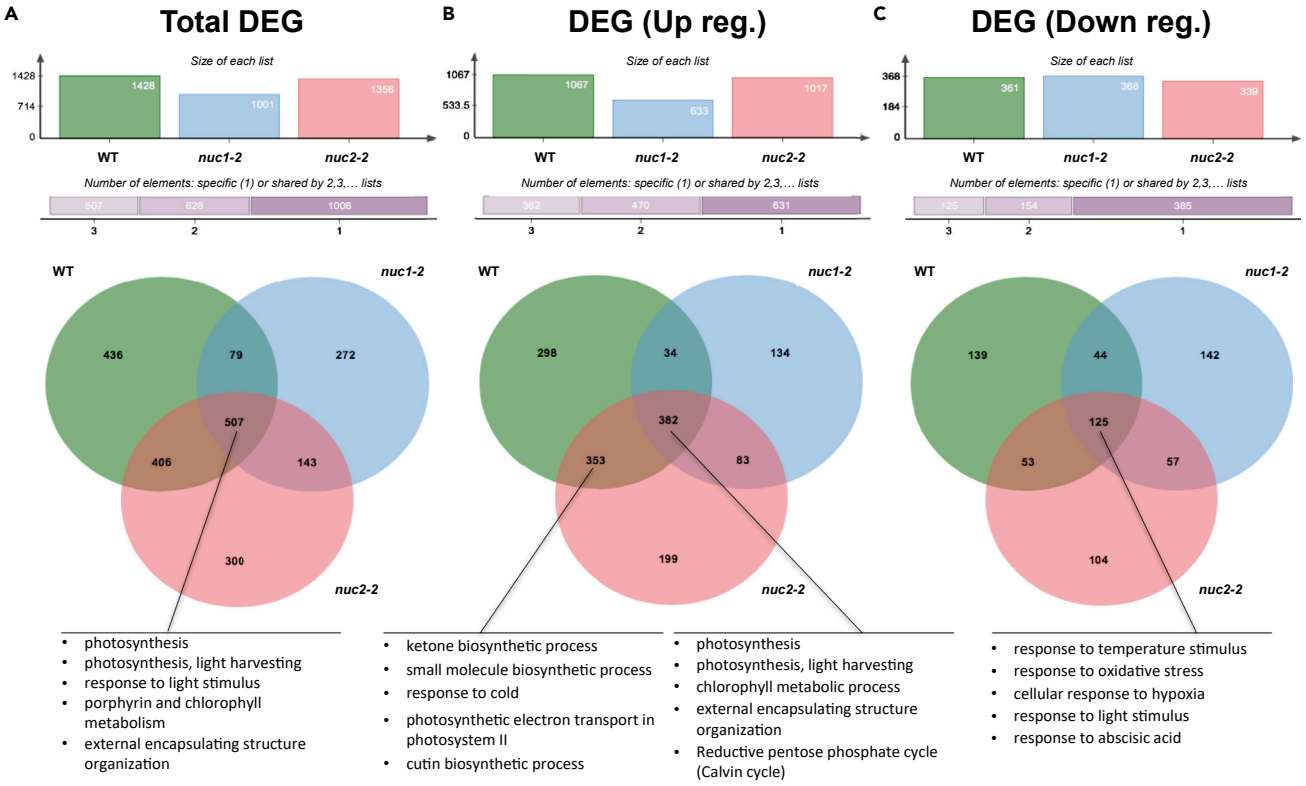

Figure 2. Differentially Expressed Genes (DEG p adj<0.05, Red Light Photostimulation versus Darkness) in WT and Nucleolin Mutants (*nuc1-2* and *nuc2-2*)

(A) Venn diagram comparing all DEGs and the five most significant gene ontology (GO Enrichment) categories in the common DEG in the three genotypes.

(B) Venn diagram comparing up-regulated DEGs and the five most significant gene ontology (GO Enrichment) categories in the common DEGs in the WT and *nuc2-2* genotypes and in the three genotypes, respectively.

(C) Venn diagram comparing down-regulated DEGs and the five most significant gene ontology (GO Enrichment) categories from common DEGs in the three genotypes.

an increased secondary metabolism, together with a response to stress elements (cold) observed in both WT and *nuc2-2*. These results suggest that the presence of the NUC1 protein is necessary for the known effect of red light in the stimulation of cell proliferation, but the NUC2 protein is not an important player in that response.

A complementary functional analysis has been done using the full lists of up- or down-regulated genes in each genotype, obtained by means of a Heatmap GO Enrichment. Up-regulated gene lists reveal that red light photostimulation versus darkness mainly leads to an unequivocal activation of genes involved in different phases of photosynthesis, together with processes that involve external encapsulation, secondary metabolism, and drug catabolism in all three *A. thaliana* lines examined (Supplemental Information, Figure S2A). Other significantly affected categories are the GO involving cell wall modification, pathogenesis, responses to insects, and defense mechanisms to bacteria. In addition to the mentioned GO groups, red light activates different biosynthetic processes (ketone, cutin, and small molecules) and the response to stimuli, such as cold and UV light, in the WT and *nuc2-2* mutant lines. Solely in the WT line, an enrichment in cell division-related genes (microtubule-based movement, cell cycle, meiotic cell cycle) is produced. In the case of down-regulated GO groups, red light photostimulation reduces expression of genes involved in the response to different stimuli (temperature, hypoxia, light, abscisic acid, oxidative stress) as well as the circadian rhythm of plants (Supplemental Information, Figure S2B). Additional down-regulated genes involved in the response to stress appear in WT and *nuc2-2* comparison (heat and osmotic stress), in the WT and *nuc1-2* comparison (cold acclimation, response to karrikin, hormone metabolism, and cell wall modification), or *nuc1-2* only (response to gibberellin). The two nucleolin mutant lines share a repression of the amino acid metabolism (alpha-amino acid catabolic process and leucine degradation).

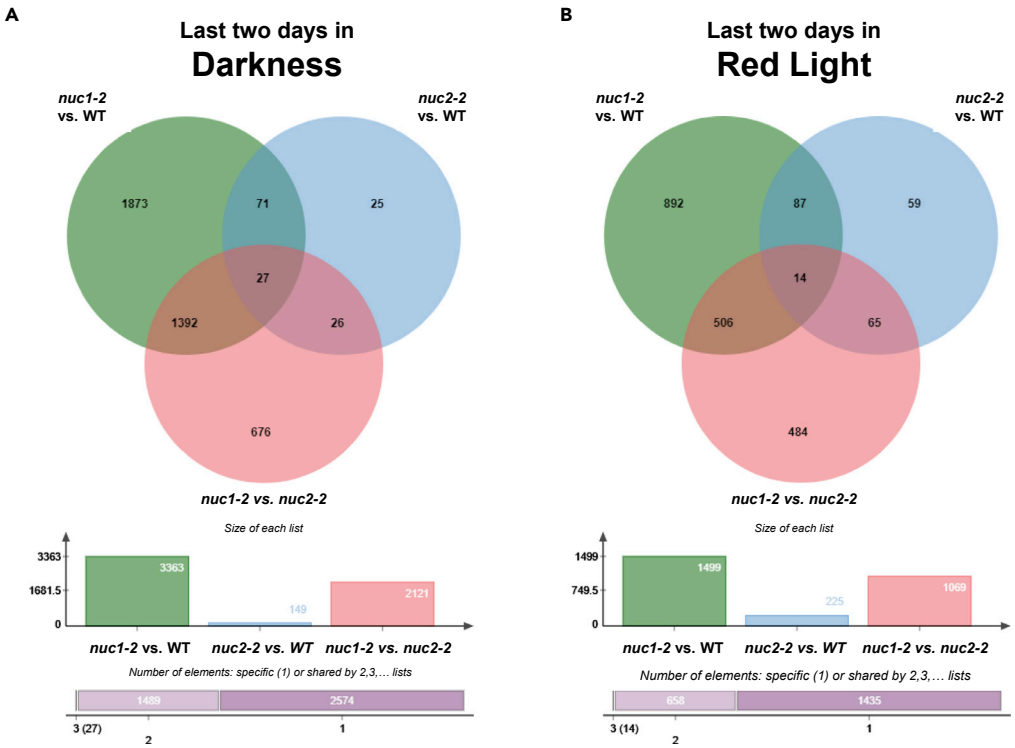

Figure 3. Differentially Expressed Genes (DEG p adj<0.05, in the Three Genotype Pair-Comparisons among WT, *nuc1-2*, and *nuc2-2*) within the Same Experimental Condition

(A) Venn diagram comparing all DEGs between plants exposed to darkness the last 2 days.

(B) Venn diagram comparing all DEGs between plants exposed to red light stimulation the last 2 days.

Dissecting Transcriptional Status for Each Genotype for Illumination Conditions at Normal Earth Gravity

To better understand the differences in the transcriptional status of each genotype that could be attributed to the illumination conditions designed to be used in the SG spaceflight experiment, we performed a series of comparisons between the different lines, namely, *nuc1-2* versus WT, *nuc2-2* versus WT, and *nuc1-2* versus *nuc2-2*, when they are either photostimulated with red light or kept in darkness for 48 h, after a growth period of 4 days under a 16 h/8 h white light photoperiod regime (regular growth condition).

The total number of DEGs when comparing the severe mutant *nuc1-2* with the WT is remarkable, with thousands of genes affected in the different illumination conditions. A similar result was obtained in the comparison of *nuc1-2* with *nuc2-2*. This number was much higher in the comparisons of the *nuc1-2* mutant with both the Col-0 and *nuc2-2* mutant in darkness: 3,363 genes and 2,121 genes, respectively. Under red light stimulation, the numbers dropped to half: 1,499 genes compared with the WT and 1,069 compared with *nuc2-2*, respectively. In contrast, the small number of DEGs between the WT and *nuc2-2* mild mutant (just 149 genes in darkness conditions) peaked to 225 when red light photostimulation was provided (Figure 3). The up- and down-regulated genes showed similar trends in this case (Supplemental Information, Figure S3).

The differential numbers in DEGs can be assigned to particular GO groups. Ontology analysis shows that both comparisons involving the *nuc1* mutant in the darkness produced an increase in the expression of genes mainly involved in cell division, such as cell cycle, meiotic cell cycle, microtubule cytoskeleton, nuclear chromosome segregation, cytokinesis, and cell cycle-G2/M transition (Supplemental Information, Figure S4A). Furthermore, in the *nuc1-2* versus WT and *nuc1-2* versus *nuc2-2* comparisons, categories of responses to different stimuli, namely, responses to auxin, red light, gravity, and UV and ionizing radiations, also appeared overrepresented. In the comparison *nuc1-2* versus *nuc2-2* in darkness, most functional categories (GO terms) appearing up-regulated in the *nuc1-2* mutant are related to the cell wall (cell wall

macromolecule catabolic process, pectin biosynthetic process), the cuticle (cuticle development and cutin, suberin, and wax biosyntheses), and the plasma membrane (anchored component of plasma membrane, very-long-chain fatty acid biosynthetic process, transmembrane receptor protein kinase activity).

The up-regulated processes when red light is applied are quite different (Supplemental Information, Figure S4B). In the *nuc1-2* versus WT and *nuc1-2* versus *nuc2-2* comparisons, DEGs appeared involved in cell wall (structural constituents of cell wall) and in development (positive regulation of growth, post-embryonic plant morphogenesis, cellular response to ethylene stimulus). In the *nuc1-2* versus *nuc2-2* comparison, many genes with a red-light-activated expression were involved in ribosome biogenesis (preribosome, maturation of SSU-rRNA, 90S preribosome, maturation of 5.8S RNA, ribosomal large subunit biogenesis).

The two nucleolin mutant lines relative to WT (*nuc1-2* versus WT and *nuc2-2* versus WT comparisons) in conditions of red light photoactivation have up-regulated genes involved in different response processes, such as the responses to hypoxia, drug, antibiotic, salicylic acid, and wounding. The number of response processes was increased in the *nuc2-2* versus WT comparison with the GO categories: responses to cold, bacterium, and abscisic acid.

The identification of common gene categories down-regulated in both darkness and red light conditions was more challenging (Supplemental Information, Figures S4C and S4D). In darkness, *nuc1-2* versus WT and *nuc1-2* versus *nuc2-2* comparisons were very similar and mainly related to developmental processes (regulation post-embryonic development, meristem development, regulation of seed development, plant organ senescence), mRNA quality (mRNA surveillance pathway), response to temperature (response to temperature stimulus, endopeptidase Clp complex, heat shock protein), and immune system (immune response, response to toxic substance, glutathione metabolism). In the comparisons indicated above, genes involved in long-day photoperiodism, flowering, rhythmic process, and response to light intensity were also less represented. In the same way, cellular responses to light stimulus category was over-represented in both nucleolin mutants with respect to WT and responses to light stimulus was a common GO category in all three comparisons. The gene categories repressed only in the *nuc1-2* versus *nuc2-2* comparison were involved in the spliceosome, protein demethylation, chromatin organization, mRNA binding, and histone acetyltransferase activity.

The gene categories with repressed expression under red light for any of the comparisons (*nuc1-2* versus *WT* and *nuc1-2* versus *nuc2-2*) were related to mRNA splicing (alternative mRNA splicing via spliceosome), light responses (response to light stimulus, photoperiodism flowering, circadian rhythm), photosynthesis (chlorophyll biosynthesis process, chloroplast envelope), and the immune system (immune system process, defense response to bacterium, regulation of salicylic acid metabolic process, Supplemental Information, Figure S4D).

Protein-Protein Interaction Networks Helps to Visualize the Differential Transcriptional State of *nuc1-2* Genotype in 1*g* Control References

Enrichment-PPI analysis (protein-protein interaction network) also showed that, in darkness, the mutant *nuc1-2* has up-regulated the expression of genes involved in the regulation of G2/M transition of the mitotic cell cycle, mitotic spindle assembly checkpoint, and auxin-activated signaling pathway, with respect to both the WT and the mutant *nuc2-2* (Figure 4). In the down-regulation side, *nuc1-2* mutant, when compared with WT, showed down-regulated genes involved in transcription regulator activity, sequence-specific DNA binding, defense response, and regulation of developmental process. In addition, the *nuc1-2* mutant has genes with repressed expression in darkness condition related to negative regulation of circadian rhythm, responses to light stimulus, and responses to jasmonic acid, when compared with WT and *nuc2-2* mutant (Figure 4). These results were in agreement with functional GO analysis (Supplemental Information, Figures S2 and S4).

DISCUSSION

Results from Spaceflight Experiments Can Have Several Limitations that Are Not Often Present in Other Biological -Omics Works

Major constraints of spaceflight experiments are the reduced amount of material and reproducibility, but other issues include the storage of samples before and after the experiment execution in space, causing staggered preparation and processing of the samples (Millar et al., 2010; Correll et al., 2013). In this

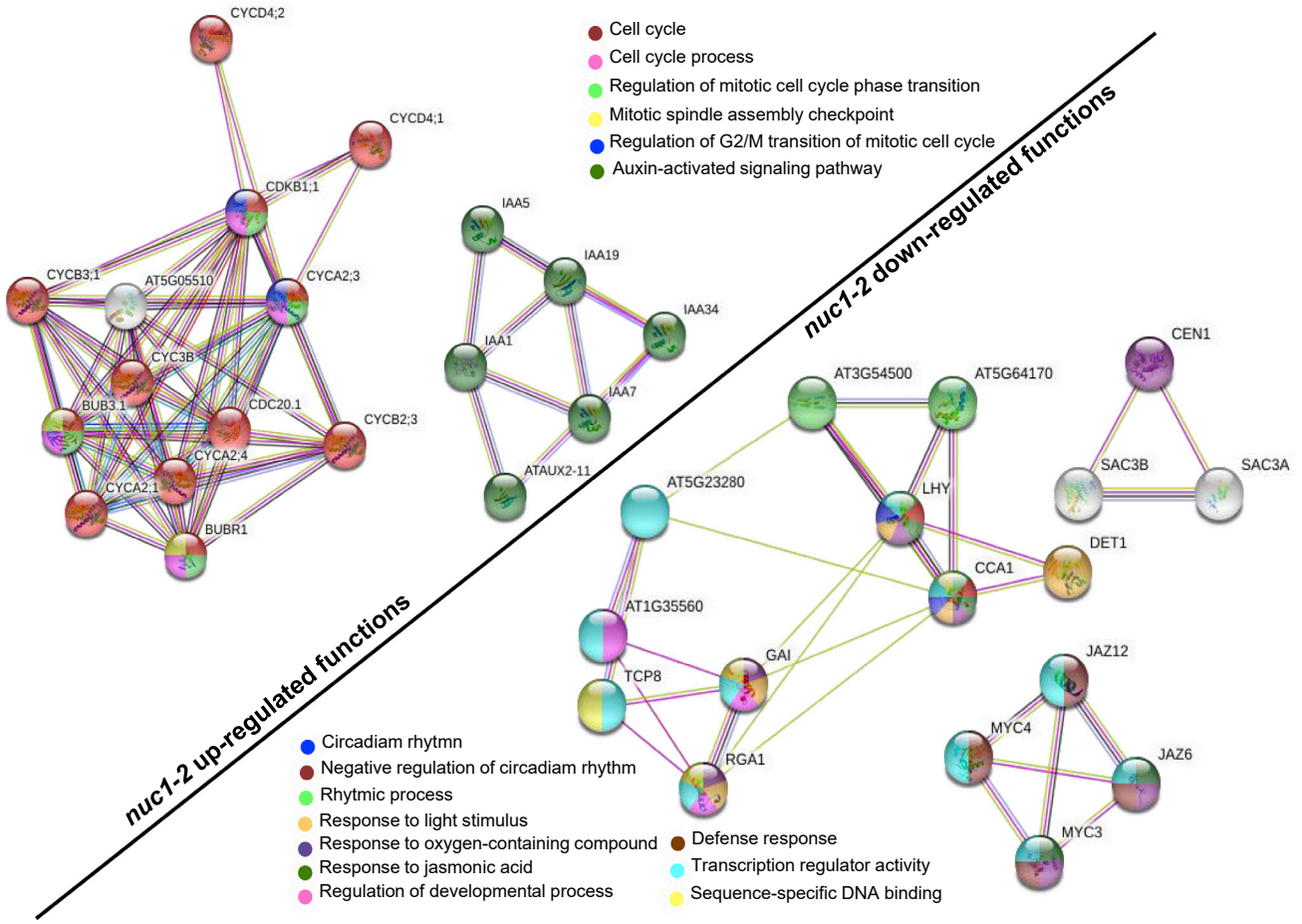

Figure 4. Protein-Protein Interaction Network of *Nuc1-2* Differential Response under Darkness Conditions

Enrichment network visualization for results from the over-represented gene lists in *Nuc1-2* versus the other genotypes. Gene in each node is represented by a chart indicating the functional category to which each one belongs (following the color legend). The networks show that processes such as cell cycle (left part or up-regulated genes), circadian rhythms, and stress responses (right part or down-regulated genes) are already affected in the 1×*g* control conditions as a reference for the Seedling Growth spaceflight experiments.

work, we have shown that, using the spaceflight hardware and procedures, we can perform a transcriptomic analysis with enough reliability to describe the differential transcriptional state of the nucleolin mutants under different light conditions. Three replicates could be considered low for current standards for animal -omics studies in Earth, but in our experiment each replica already represents the average of 10 plants. We show here that the replicates expected to be collected from the spaceflight experiment can be estimated to be sufficient for performing a sequencing study that allows clustering of the different genotypes and environmental conditions (Figure 1).

Due to logistical considerations, a specific constraint for plant space biology is the limited number of different mutants/genotypes that can be used in a spaceflight experiment in true microgravity. We have to be sure that the mutants of choice will provide valuable information. In that sense, the use of nucleolin mutants is a promising choice to provide insight into both the cell cycle and stress response mechanisms, apart from the ribosome biogenesis in which this protein is directly involved. These processes are known to be recurrently affected in space -omics experiments with plants (Choi et al., 2019; Ferl et al., 2015; Herranz et al., 2019; Johnson et al., 2017; Kruse et al., 2017; Paul et al., 2013, 2017). The analysis performed here allows us to know the specific functions assumed by the two nucleolin proteins of *A. thaliana* (NUC1 and NUC2) in different environmental conditions, such as red light photostimulation and darkness, affecting tropistic stimuli. This information can be considered as the 1*g* reference control required to obtain the best possible understanding of the changes produced by the spaceflight conditions on plant

development, and how the gravitational stress could be counteracted by changing phototropic stimuli. A longer-term goal is to use this knowledge for plant cultivation into bioregenerative life support systems.

The Transcriptomic Baseline for Nucleolin Mutants Is Different under Red Light Photostimulation and Darkness

Red light illumination mainly produces the activation of genes involved in photosynthesis, cell wall modification, drug catabolism, pathogenesis, and biotic stress response. Conversely, different abiotic stimuli responses (temperature, hypoxia, light, abscisic acid, oxidative stress) are down-regulated by the photostimulation treatment, as well as the circadian rhythm of plants. This transcriptional effect is similar in the three lines studied (Col-0 WT, *nuc1-2,* and *nuc2-2*), suggesting that it may be independent of the nucleolin protein functions. Therefore, the interpretation of transcriptional effects on plants' grown during spaceflight will be straightforward. In contrast, red light illumination produces a down-regulation of genes involved in the response to karritin, cold acclimation, and hormone metabolism in WT and *nuc1-2*, indicating that the NUC2 protein, and/or other proteins up-regulated in *nuc1-2* (Pontvianne et al., 2007), could participate in these functions. In addition, in the *nuc1-2* mutant, genes coding for response to gibberellin with the red light appear repressed. Gibberellin is a hormone involved in seed germination, bud and fruit formation, shoot longitudinal growth, and axial organ elongation (Hedden and Sponsel, 2015), which could support the relationship of defective plant growth and development with *NUC1* gene disruption.

Exposure to the dark during the last 2 days of cultivation of seedlings promotes gene categories mainly involved in processes of cell division and in the response to different stimuli (red light, UV, ionizing radiation, gravity, auxins). They are common in *nuc1-2* versus WT and *nuc1-2* versus *nuc2-2* comparisons and unique in *nuc1-2* versus WT comparison. These observations could indicate that, in a stress condition such as darkness, the NUC2 protein is capable of rescuing functions that the NUC1 protein performs under normal growth conditions. Indeed, a role of nucleolin in mitosis has been reported (de Carcer and Medina, 1999; Ma et al., 2007). Therefore, in the *nuc1* mutant, the NUC2 protein would be capable of performing functions necessary for plant survival, such as ribosome biogenesis regulation (Pontvianne et al., 2007), cell proliferation, and DNA repair. It is important to note that cell division GO was only significantly up represented in the WT when red light was provided (Figure 2B). In contrast, the gene categories down-regulated in darkness are mainly related to developmental processes, mRNA quality, response to temperature, and immune system. This may indicate that in the dark stress condition, the NUC2 protein is not capable of supplying the function of the NUC1 protein in these processes. These results, together with those previously described, indicate that the functional rescue of NUC1 by NUC2, when NUC1 is not expressed, would be only partial, which may be due to the structural difference between both proteins, including longer N-terminal acidic domain and less-conserved GAR domain I in the C terminal (Durut and Sáez-Vásquez, 2015).

Differential Role of Nucleolin Mutants' Transcriptomic Baseline May Offer New Insight in Spaceflight Experiments

Differential transcriptional response is observed when comparing the two nucleolin mutants. The categories of genes activated differentially in both mutants (*nuc1-2* versus *nuc2-2* comparison) are mainly involved in the cell wall and membrane systems. This finding is potentially interesting in space -omics to discriminate gravitropism from graviresistance mechanisms (Herranz and Medina, 2014) and could be related to the phenotype described in the *nuc1-2* mutant, in which a reduction in the cell number and a disorganization in every cell layer is observed in transversal sections of primary leaves (Pontvianne et al., 2007). Moreover, the gene categories repressed only in the above-mentioned comparison are involved in the spliceosome, protein demethylation, chromatin organization, mRNA binding, and histone acetyltransferase activity, which could be related to the described antagonist activity of these two proteins in pre-rRNA methylation and with their role in chromatin remodeling, RNA Pol I transcription, mRNA stability, and RNA/DNA metabolism (Pontvianne et al., 2010; Durut et al., 2014).

In the *nuc1-2* versus *nuc2-2* comparison under red light photostimulation, the ribosome biogenesis GO shows the most significant enrichment within the up-regulated genes (Supplemental Information, Figure S4B). This result indicates that the described activating effect of red light in this process depends more on the expression of NUC2 protein than on the NUC1 expression. Ultimately, the two nucleolin mutant lines, compared with WT, have genes up-regulated by red light involved in different response processes, such as the response to hypoxia, drug, antibiotic, salicylic acid, and wounding. These response

processes are extended in the *nuc2-2* versus WT comparison, including response to cold, bacteria, and abscisic acid. These results indicate that even though both nucleolar proteins, NUC1 and NUC2, are involved in response processes, the implication of NUC2 is higher as to the number of processes. Therefore, NUC2 has a greater response capacity to environmental signals, such as illumination with red light, thus being more sensitive.

A major challenge to be overcome in spaceflight -omics research is to differentiate and characterize which of the spaceflight environmental conditions (including not only microgravity and cosmic radiation but also the constraints imposed to the upload/download and storage processes in orbit, the gaseous atmosphere, among other factors) are responsible for each of the observed alterations in the transcriptome. According to our results, space -omics researchers need to pay special attention to the analysis of ground reference controls on Earth before conclusions can be made on the results obtained in spaceflight. In our particular example, the two nucleolin mutants are the perfect complement to the WT genotype to study how the NUC2 protein can replace the essential functions of NUC1 in orbit, and how light can modulate it, even rescuing WT transcriptional profiles in the *nuc1-2* mutant. The fact that *nuc2-2* mutant shows an increase in stress response GO when exposed to red light connects the red light stimulus with the modulation of the stress response. In parallel, the cell cycle and ribosome biogenesis functions required to be restored in microgravity are also light dependent in both the *nuc1-2* mutant (in Earth, as shown here) and the WT plants in orbit (Valbuena et al., 2018).

Limitations of the Study

Due to logistical constraints, this study lacks a continuously illuminated control set of samples performed simultaneously due to the absence of those samples in the spaceflight experiment as well as the reference experiment. The next step in this research is to analyze the samples from the space experiment in microgravity and the partial gravity conditions produced by the centrifuge in the EMCS on the ISS. We anticipate confirming that the duplicated nucleolin gene system works during spaceflight will lead us to discover novel mechanisms for plant adaptation to spaceflight conditions. Thus, this research will be eventually translated into better crops for life support systems in the human spaceflight ventures of the 21st century.

Resource Availability

Lead Contact

Further information and requests for materials should be directed to and will be fulfilled by the lead contact, Raúl Herranz (r.herranz@csic.es)

Materials Availability

Materials generated in this study are available from the lead contact with a completed materials transfer agreement.

Data and Code Availability

The GLDS-313 datasets generated during this study have been deposited and it is available at GENELAB repository (Ray et al., 2019). Original data have been deposited to (GENELAB: https://doi.org/10.26030/0g0m-dj21, https://genelab-data.ndc.nasa.gov/genelab/accession/GLDS-313)

METHODS

All methods can be found in the accompanying Transparent Methods supplemental file.

SUPPLEMENTAL INFORMATION

Supplemental Information can be found online at https://doi.org/10.1016/j.isci.2020.101686.

ACKNOWLEDGMENTS

We want to acknowledge the collaboration and support of many people who have contributed to the success of the experiments of the "Seedling Growth" project whose results are reported in this paper. This includes payload developers (Airbus), ESA and NASA managers, scientific collaborators (Drs. Eugenie Carnero-Diaz, Richard E. Edelmann, Joshua P. Vandenbrink, Malgorzata Ciska, Katherine D.L. Millar, and Miguel Angel Valbuena), and the astronauts who performed the experiments on board the International

Space Station as well as the EMCS managers (N-USOC) who performed the ground control operations. This work was supported by the Agencia Estatal de Investigación of the Spanish Ministry of Science and Innovation, Grants #ESP2015-64323-R and #RTI2018-099309-B-I00 (co-funded by EU-ERDF) to F.J.M., by predoctoral fellowships to A.M. and A.V. from the Spanish National Program for Young Researchers Training (MINECO, Ref. BES-2013-063933, BES-2016-077976), and the Seedling Growth Project to the ISS LSRA2009-0932/1177, a shared project of ESA-ELIPS Program and NASA. J.Z.K. is funded by Grants NNX12A065G and 80NSSC17K0546. These results are related to the Space Omics TT funded by the European Space Agency contract ESA 4000131202/20/NL/PG to R.H.

AUTHOR CONTRIBUTIONS

Conceptualization, R.H. and F.J.M.; Methodology and Investigation, A.V., A.M., and R.H.; Writing – Original Draft, A.M. and R.H.; Writing – Review & Editing, A.V., F.J.M., J.Z.K., and J.S.-V.; Supervision and Funding Acquisition, F.J.M., J.Z.K., and J.S.-V.

DECLARATION OF INTERESTS

The authors declare no competing interests.

Received: July 9, 2020
Revised: September 4, 2020
Accepted: October 10, 2020
Published: November 20, 2020

REFERENCES

Angelov, D., Bondarenko, V.A., Almagro, S., Menoni, H., Mongélard, F., Hans, F., Mietton, F., Studitsky, V.M., Hamiche, A., Dimitrov, S., and Bouvet, P. (2006). Nucleolin is a histone chaperone with FACT-like activity and assists remodeling of nucleosomes. EMBO J. *25*, 1669–1679.

Beheshti, A., Shirazi-Fard, Y., Choi, S., Berrios, D., Gebre, S.G., Galazka, J.M., and Costes, S.V. (2019). Exploring the effects of spaceflight on mouse physiology using the open access NASA genelab platform. J. Vis. Exp. *143*, 1–11.

Boucheron-Dubuisson, E., Manzano, A.I., Le Disquet, I., Matia, I., Saez-Vasquez, J., van Loon, J.J., Herranz, R., Carnero-Diaz, E., and Medina, F.J. (2016). Functional alterations of root meristematic cells of *Arabidopsis thaliana* induced by a simulated microgravity environment. J. Plant Physiol. *207*, 30–41.

Boulon, S., Westman, B.J., Hutten, S., Boisvert, F.M., and Lamond, A.I. (2010). The nucleolus under stress. Mol. Cell *40*, 216–227.

Bouvet, P., Diaz, J.J., Kindbeiter, K., Madjar, J.J., and Amalric, F. (1998). Nucleolin interacts with several ribosomal proteins through its RGG domain. J. Biol. Chem. *273*, 19025–19029.

de Carcer, G., and Medina, F.J. (1999). Simultaneous localization of transcription and early processing markers allows dissection of functional domains in the plant cell nucleolus. J. Struct. Biol. *128*, 139–151.

Caldana, C., Li, Y., Leisse, A., Zhang, Y., Bartholomaeus, L., Fernie, A.R., Willmitzer, L., and Giavalisco, P. (2013). Systemic analysis of inducible target of rapamycin mutants reveal a general metabolic switch controlling growth in *Arabidopsis thaliana*. Plant J. *73*, 897–909.

Choi, W.G., Barker, R.J., Kim, S.H., Swanson, S.J., and Gilroy, S. (2019). Variation in the transcriptome of different ecotypes of *Arabidopsis thaliana* reveals signatures of oxidative stress in plant responses to spaceflight. Am. J. Bot. *106*, 123–136.

Correll, M.J., Pyle, T.P., Millar, K.D., Sun, Y., Yao, J., Edelmann, R.E., and Kiss, J.Z. (2013). Transcriptome analyses of *Arabidopsis thaliana* seedlings grown in space: implications for gravity-responsive genes. Planta *238*, 519–533.

Durut, N., Abou-Ellail, M., Pontvianne, F., Das, S., Kojima, H., Ukai, S., de Bures, A., Comella, P., Nidelet, S., Rialle, S., et al. (2014). A duplicated NUCLEOLIN gene with antagonistic activity is required for chromatin organization of silent 45S rDNA in Arabidopsis. Plant Cell *26*, 1330–1344.

Durut, N., and Sáez-Vásquez, J. (2015). Nucleolin: dual roles in rDNA chromatin transcription. Gene *556*, 7–12.

Ferl, R.J., Koh, J., Denison, F., and Paul, A.L. (2015). Spaceflight induces specific alterations in the proteomes of Arabidopsis. Astrobiology *15*, 32–56.

Garrett-Bakelman, F.E., Darshi, M., Green, S.J., Gur, R.C., Lin, L., Macias, B.R., McKenna, M.J., Meydan, C., Mishra, T., Nasrini, J., et al. (2019). The NASA twins study: a multidimensional analysis of a year-long human spaceflight. Science *364*, https://doi.org/10.1126/science.aau8650.

Ginisty, H., Sicard, H., Roger, B., and Bouvet, P. (1999). Structure and functions of nucleolin. J. Cell Sci. *112*, 761–772.

Hedden, P., and Sponsel, V. (2015). A century of gibberellin research. J. Plant Growth Regul. *34*, 740–760.

Herranz, R., Vandenbrink, J.P., Villacampa, A., Manzano, A., Poehlman, W.L., Feltus, F.A., Kiss, J.Z., and Medina, F.J. (2019). RNAseq analysis of the response of *Arabidopsis thaliana* to fractional gravity under blue-light stimulation during spaceflight. Front. Plant Sci. *10*, 1–11.

Herranz, R., and Medina, F.J. (2014). Cell proliferation and plant development under novel altered gravity environments. Plant Biol. *16*, 23–30.

Johnson, C.M., Subramanian, A., Pattahil, S., Correll, M.J., and Kiss, J.Z. (2017). Comparative transcriptomics indicate changes in cell wall organization and stress response in seedlings during spaceflight. Am. J. Bot. *104*, 1219–1231.

Kalinina, N.O., Makarova, S., Makhotenko, A., Love, A.J., and Taliansky, M. (2018). The multiple functions of the nucleolus in plant development, disease and stress responses. Front. Plant Sci. *9*, 1–19.

Kiss, J.Z., Mullen, J.L., Correll, M.J., and Hangarter, R.P. (2003). Phytochromes A and B mediate red-light-induced positive phototropism in roots. Plant Physiol. *131*, 1411–1417.

Kruse, C.P.S., Basu, P., Luesse, D.R., and Wyatt, S.E. (2017). Transcriptome and proteome responses in RNAlater preserved tissue of *Arabidopsis thaliana*. PLoS One *12*, 1–10.

Lewinska, A., Wnuk, M., Grzelak, A., and Bartosz, G. (2010). Nucleolus as an oxidative stress sensor in the yeast *Saccharomyces cerevisiae*. Redox Rep. *15*, 87–96.

López-Juez, E., Dillon, E., Magyar, Z., Khan, S., Hazeldine, S., de Jager, S.M., Murray, J.A.H., Beemster, G.T.S., Bögre, L., and Shanahan, H. (2008). Distinct light-initiated gene expression and cell cycle programs in the shoot apex and cotyledons of Arabidopsis. Plant Cell *20*, 947–968.

Ma, N., Matsunaga, S., Takata, H., Ono-Maniwa, R., Uchiyama, S., and Fukui, K. (2007). Nucleolin functions in nucleolus formation and chromosome congression. J. Cell Sci. *120*, 2091–2105.

Manzano, A., Pereda-Loth, V., de Bures, A., Sáez-Vásquez, J., Herranz, R., and Medina, F.J. (2020). Interaction of light and gravity signals as a mechanism of counteracting alterations caused by simulated microgravity in proliferating plant cells. Under review. Am. J. Bot. https://doi.org/10.21203/rs.3.rs-29236/v1.

Matía, I., González-Camacho, F., Herranz, R., Kiss, J.K., Gasset, G., van Loon, J.J.W.A., Marco, R., and Medina, F.J. (2010). Plant cell proliferation and growth are altered by microgravity conditions in spaceflight. J. Plant Physiol. *167*, 184–193.

Mayer, C., and Grummt, I. (2005). Cellular stress and nucleolar function. Cell Cycle *4*, 1036–1038.

Millar, K.D., Kumar, P., Correll, M.J., Mullen, J.L., Hangarter, R.P., Edelmann, R.E., and Kiss, J.Z. (2010). A novel phototropic response to red light is revealed in microgravity. New Phytol. *186*, 648–656.

Mohammed, B., Bilooei, S.F., Dóczi, R., Grove, E., Railo, S., Palme, K., Ditengou, F.A., Bögre, L., and López-Juez, E. (2017). Converging energy and hormonal signalling control meristem activity, leaf initiation and growth. Plant Physiol. *176*, 1365–1381.

Molas, M.L., and Kiss, J.Z. (2008). PKS1 plays a role in red-light-based positive phototropism in roots. Plant Cell Environ. *31*, 842–849.

Mongelard, F., and Bouvet, P. (2007). Nucleolin: a multiFACeTed protein. Trends Cell Biol. *17*, 80–86.

Paul, A.L., Zupanska, A.K., Schultz, E.R., and Ferl, R.J. (2013). Organ-specific remodeling of the Arabidopsis transcriptome in response to spaceflight. BMC Plant Biol. *13*, 112.

Paul, A.L., Sng, N.J., Zupanska, A.K., Krishnamurthy, A., Schultz, E.R., and Ferl, R.J. (2017). Genetic dissection of the Arabidopsis spaceflight transcriptome: are some responses dispensable for the physiological adaptation of plants to spaceflight? PLoS One *12*, 1–24.

Pelletier, J., Thomas, G., and Volarević, S. (2018). Ribosome biogenesis in cancer: new players and therapeutic avenues. Nat. Rev. Cancer *18*, 51–63.

Perrot-Rechenmann, C. (2010). Cellular responses to auxin: division versus expansion. Cold Spring Harb. Perspect. Biol. *2*, 1–15.

Pontvianne, F., Matía, I., Douet, J., Tourmente, S., Medina, F.J., Echeverria, M., and Sáez-Vásquez, J. (2007). Characterization of AtNUC-L1 reveals a central role of nucleolin in nucleolus organization and silencing of AtNUC-L2 gene in Arabidopsis. Mol. Biol. Cell *18*, 369–379.

Pontvianne, F., Abou-Ellail, M., Douet, J., Comella, P., Matía, I., Chandrasekhara, C., DeBures, A., Blevins, T., Cooke, R., Medina, F.J., et al. (2010). Nucleolin is required for DNA methylation state and the expression of rRNA gene variants in *Arabidopsis thaliana*. PLoS Genet. *6*, 1–13.

Ray, S., Gebre, S., Fogle, H., Berrios, D.C., Tran, P.B., Galazka, J.M., and Coste, S.V. (2019). GeneLab: omics database for spaceflight experiments. Bioinformatics *35*, 1753–1759.

Reichler, S.A., Balk, J., Brown, M.E., Woodruff, K., Clark, G.B., and Roux, S.J. (2001). Light differentially regulates cell division and the mRNA abundance of pea nucleolin during de-etiolation. Plant Physiol. *125*, 339–350.

Roger, B., Moisand, A., Amalric, F., and Bouvet, P. (2003). Nucleolin provides a link between RNA polymerase I transcription and pre-ribosome assembly. Chromosoma *111*, 399–407.

Ronca, A.E., Moyer, E.L., Talyansky, Y., Lowe, M., Padmanabhan, S., Choi, S., Gong, C., Cadena, S.M., Stodieck, L., and Globus, R.K. (2019). Behavior of mice aboard the international space station. Sci. Rep. *9*, 1–14.

Sablowski, R., and Carnier Dornelas, M. (2014). Interplay between cell growth and cell cycle in plants. J. Exp. Bot. *65*, 2703–2714.

Sáez-Vásquez, J., and Delseny, M. (2019). Ribosome biogenesis in plants: from functional 45S ribosomal DNA organization to ribosome assembly factors. Plant Cell *31*, 1945–1967.

Sáez-Vásquez, J., and Medina, F.J. (2008). The plant nucleolus. Adv. Bot. Res. *47*, 1–46.

Silva-Navas, J., Moreno-Risueño, M.A., Manzano, C., Téllez-Robledo, B., Navarro-Neila, S., Carrasco, V., Pollmann, S., Gallego, F.J., and del Pozo, J.C. (2016). Flavonols mediate root phototropism and growth through regulation of proliferation-to-differentiation transition. Plant Cell *28*, 1372–1387.

Stepiński, D. (2012). Nucleolin level in plant root meristematic cells under chilling stress and recovery. Micron *43*, 870–875.

Tong, C.G., Reichler, S., Blumentahal, S., Balk, J., Hsieh, H.L., and Roux, S.J. (1997). Light regulation of the abundance of mRNA encoding a nucleolin-like protein localized in the nucleoli of pea nuclei. Plant Physiol. *114*, 643–652.

Valbuena, M.A., Manzano, A., Vandenbrink, J.P., Pereda-Loth, V., Carnero-Diaz, E., Edelmann, R.E., Kiss, J.Z., Herranz, R., and Medina, F.J. (2018). The combined effects of real or simulated microgravity and red-light photoactivation on plant root meristematic cells. Planta *248*, 691–704.

Vandenbrink, J.P., Kiss, J.Z., Herranz, R., and Medina, F.J. (2014). Light and gravity signals synergize in modulating plant development. Front. Plant Sci. *5*, 1–18.

Vandenbrink, J.P., Herranz, R., Medina, F.J., Edelmann, R.E., and Kiss, J.Z. (2016). A novel blue-light phototropic response is revealed in roots of *Arabidopsis thaliana* in microgravity. Planta *244*, 1201–1215.

Vandenbrink, J.P., Herranz, R., Poehlman, W., Feltus, F.A., Villacampa, A., Ciska, M., Medina, F.J., and Kiss, J.Z. (2019). RNA-seq analyses of *Arabidopsis thaliana* seedlings after exposure to blue-light phototropic stimuli in microgravity. Am. J. Bot. *106*, 1466–1476.

Xiong, Y., McCormack, M., Li, L., Hall, Q., Xiang, C., and Sheen, J. (2013). Glucose-TOR signalling reprograms the transcriptome and activates meristems. Nature *496*, 181–186.

Zabel, P., Bamsey, M., Schubert, D., and Tajmar, M. (2016). Review and analysis of over 40 years of space plant growth systems. Life Sci. Space Res. *10*, 1–16.

plants

MDPI

Article

Analysis of Graviresponse and Biological Effects of Vertical and Horizontal Clinorotation in *Arabidopsis thaliana* Root Tip

Alicia Villacampa [1], Ludovico Sora [1,2], Raúl Herranz [1], Francisco-Javier Medina [1] and Malgorzata Ciska [1,*]

[1] Centro de Investigaciones Biológicas Margarita Salas-CSIC, Ramiro de Maeztu 9, 28040 Madrid, Spain; avillacampa@cib.csic.es (A.V.); ludovico.sora@mail.polimi.it (L.S.); rherranz@cib.csic.es (R.H.); fjmedina@cib.csic.es (F.-J.M.)

[2] Department of Aerospace Science and Technology, Politecnico di Milano, Via La Masa 34, 20156 Milano, Italy

* Correspondence: mciska@cib.csic.es; Tel.: +34-91-837-3112 (ext. 4260); Fax: +34-91-536-0432

Abstract: Clinorotation was the first method designed to simulate microgravity on ground and it remains the most common and accessible simulation procedure. However, different experimental settings, namely angular velocity, sample orientation, and distance to the rotation center produce different responses in seedlings. Here, we compare *A. thaliana* root responses to the two most commonly used velocities, as examples of slow and fast clinorotation, and to vertical and horizontal clinorotation. We investigate their impact on the three stages of gravitropism: statolith sedimentation, asymmetrical auxin distribution, and differential elongation. We also investigate the statocyte ultrastructure by electron microscopy. Horizontal slow clinorotation induces changes in the statocyte ultrastructure related to a stress response and internalization of the PIN-FORMED 2 (PIN2) auxin transporter in the lower endodermis, probably due to enhanced mechano-stimulation. Additionally, fast clinorotation, as predicted, is only suitable within a very limited radius from the clinorotation center and triggers directional root growth according to the direction of the centrifugal force. Our study provides a full morphological picture of the stages of graviresponse in the root tip, and it is a valuable contribution to the field of microgravity simulation by clarifying the limitations of 2D-clinostats and proposing a proper use.

Keywords: microgravity simulation; gravitropism; gravity perception; plant; clinostat

Citation: Villacampa, A.; Sora, L.; Herranz, R.; Medina, F.-J.; Ciska, M. Analysis of Graviresponse and Biological Effects of Vertical and Horizontal Clinorotation in *Arabidopsis thaliana* Root Tip. *Plants* **2021**, *10*, 734. https://doi.org/10.3390/plants10040734

Academic Editor: Giovanna Aronne

Received: 10 March 2021
Accepted: 6 April 2021
Published: 9 April 2021

1. Introduction

The force of gravity is a permanent environmental factor that exerts fundamental influence on plant growth and development. In particular, the direction of the gravity vector determines the orientation of the plant growth in a process called gravitropism. The gravitropic response is commonly divided into three steps: gravity perception, transduction of the signal, and the growth response [1,2], although some authors split the perception phase into two steps, namely susception—the movement of the statoliths and their sedimentation, and perception—the transfer of the physical act into a physiological signal [3]. Gravity perception takes place in specialized cells called statocytes. These cells have starch-containing plastids, statoliths, which sediment in the direction of the gravity vector [4]. In the root, statocytes are located in the root cap, they are organized in tiers, and form a tissue called columella, whereas in the shoot, they are found in the endodermis [5]. Gravity perception in the root is preceded by the motion of statoliths in the root columella after plant reorientation to sediment according to the direction of the gravity vector. Columella of *A. thaliana* is a highly organized and dynamic structure. It consists of three to four layers of statocytes, sometimes called tiers or stories S1, S2, S3. Statocytes differentiate from the root cap meristem, formed by the columella root cap stem cells (CSC) which are located directly underneath the quiescent center (QC) and above the first layer of statocytes (S1) [6]. CSC activity ensures a constant regeneration of columella cells. The layers that follow (S1–S4)

assume first a role in gravity perception, and then they become secretory cells that are important for root tip protection [7–9]. The central cells of columella (central cells of the two layers that follow the meristem) are the most important for gravitropic response [10–12]. However, statoliths in S3 and S4 tiers, in which statocytes assume secretory functions, do not always sediment after turning the root [11]. It is not completely understood how gravity signal is transduced after statoliths sedimentation on the endoplasmic reticulum (ER) on the cell periphery. One of the most accepted hypothesis is that the physical contact of the statoliths and the cortical ER opens Ca^{2+} channels which creates a Ca^{2+} signal in the cytoplasm [12] that could lead to changes in auxin PIN-FORMED (PIN) transporters polarity [13]. The latest studies confirm that LAZY proteins also play a function in the early stages of gravitropic signal transduction [14–16]. It is well reported that auxin is involved in the final stages. According to the Cholodny–Went theory, the differential gradient of this phytohormone results in differential growth. The auxin gradient is formed by differential localization of auxin PIN transporters in response to gravity [17]. The involvement of PIN3, PIN7, and PIN2 in root gravitropic signaling was confirmed by numerous studies [18–20]. PIN3 and PIN7, located in the columella cells, change their distribution within minutes after the gravitropic stimuli, next PIN2 transports auxin through epidermis towards the root elongation zone [21,22]. The differential lateral distribution of auxin transport factors in response to a gravitropic stimulus, leads to auxin accumulation at the lower side of the root inhibiting cell expansion in the elongation zone and low auxin levels in the upper side of the root stimulate cell elongation [23]. In effect, non-uniform growth in the elongation zone enables the root to bend towards the new direction of the gravity vector.

Whereas many studies have been devoted to investigating the plant response to gravitropic stimuli, less is known about the mechanisms triggered by the plant in the absence of any gravity vector or when the magnitude of this vector is significantly lower than the Earth gravity, 1 g. This knowledge is necessary for any enterprise of space exploration, since the environment of outer space and of the nearby planets and satellites is characterized by a low or near-zero gravity force (microgravity). The experiments performed on the orbit in the International Space Station (ISS) provide the best conditions for real microgravity research, but are limited by the high cost and complex logistics. This has motivated scientists to look for more accessible ways to investigate the response of an organism to the low gravity levels. There are a number of hardware devices (also called Ground Based Facilities, GBF) that enable weightlessness simulation with the objective to prevent an organism from perceiving the gravity vector (reviewed in [24]). One of the first created simulators are clinostats that were originally designed to be used with plants [25] but later were also applied with different systems, as for example, in vitro cultures. In clinostats, weightlessness simulation is achieved by averaging the gravity vector during each cycle of rotation. It was designed to be used in plants due to the relatively long presentation time for the gravistimulus (the time that the stimulus must persist to trigger a gravitropic response) in comparison to animal models [26–28]. In *A. thaliana*, the presentation time is approximately 0.4–1 min [7,11,29]. In the perfect clinorotation settings the sedimentation fall of the statoliths is converted into quasi-circular paths by continuously rotating the whole plant and in effect the position of the statoliths remain virtually stationary within the cells [30]. It should be noted that, to perform an optimal simulation on a clinostat, the mechanism of graviperception of a given organism has to be taken into account. Despite the common use of clinostats and the vast research that was performed on these devices, no clear set of rules has been established as for the optimal clinostat settings. Angular velocity varies between studies from 1–2 rpm up to 60 rpm without a justification [31–35]. In addition, we can distinguish two types of clinorotation depending on the orientation of the sample in relation to the clinorotation axis: vertical clinorotation (VC), with the longitudinal growth axis of the plant perpendicular to the rotation axis, or horizontal clinorotation (HC), with the longitudinal seedling axis parallel to the rotation axis (see Figure 1) [36]. The possible impact of either of these two types of clinorotations was compared by [36–38], concluding that vertical and horizontal clinorotation result in different outcomes. Additionally, different effects of the centrifugal

force on plant growth in horizontal and vertical orientation were reported by [39], but there is not a consensus or evidence-based guideline in the best practice to use clinorotation in terms of speed, orientation of the Petri dishes containing samples and the maximum duration of the treatment.

Here, we explore *A. thaliana* responses to fast and slow horizontal and vertical clinorotation, by investigating the elements of each of the three gravitropism stages. We conclude that the seedling growth is modulated differently in fast and slow clinorotation as well as in vertical and horizontal. We have observed directional growth in fast clinorotation and differences in the statolith distribution in different clinorotation conditions. Finally, we observe increased stress response in columella cells and the meristem in horizontally clinorotated seedlings, that does not seem to be related to the gravitropic perception, but rather to enhanced mechano-stimulation. Our results confirm preliminary findings and a mathematical model described previously [40].

2. Results

2.1. Angular Velocity and Sample Orientation Influence Root Growth Direction and Rate

First, we analyzed root growth direction and rate after 24 h of fast or slow, horizontal or vertical clinorotation. In Figure 1, the sample orientation and acting forces in vertical or horizontal clinorotation are explained.

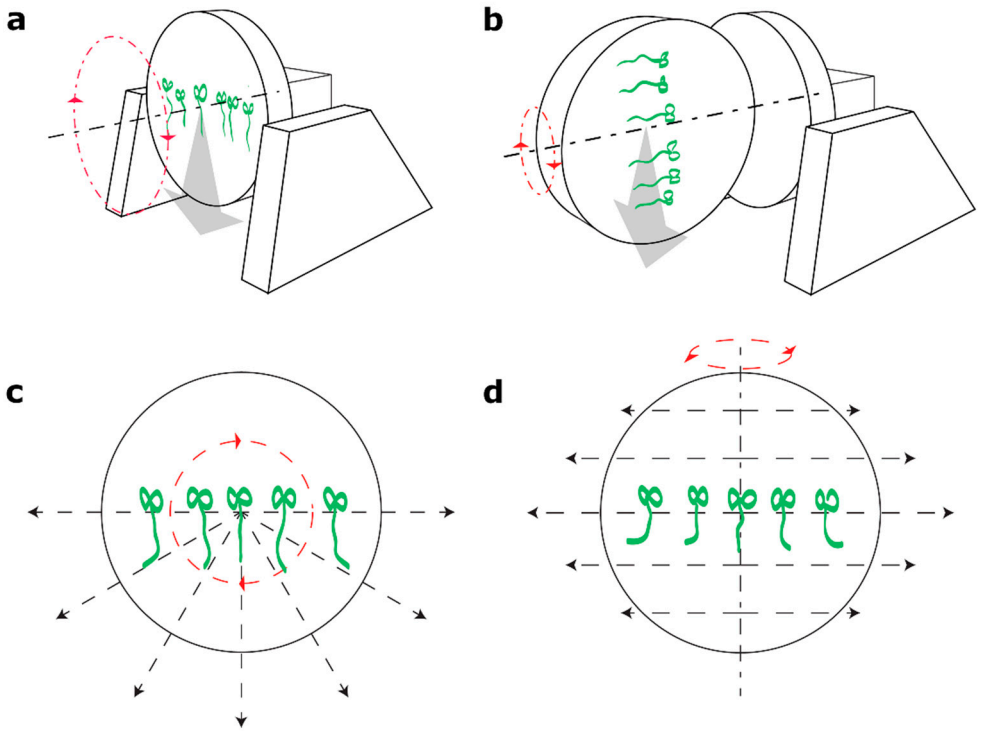

Figure 1. 2-D clinostat and sample orientation. Schematic representation of (**a**) Vertical clinorotation, (**b**) Horizontal clinorotation, (**c**) Theoretical forces and direction in vertical clinorotation, and (**d**) Theoretical forces and direction in horizontal clinorotation. Red dashed arrows—the direction of clinorotation; black dashed arrows—the direction of the centrifugal force; gray arrows —direction of the gravitational force.

Seedlings in the control group continued to grow vertically downwards with minor fluctuations. The directional growth control group after reorientation grew downwards according to the direction of the gravity vector (Figure 2a). In the slowly clinorotated samples roots turned slightly, but their direction did not reflect the direction of the centrifugal force vector suggesting it has a negligible magnitude at 1 rpm in our experimental settings. On the other hand, as shown in Figure 2a (and Figure S1), at 60 rpm, the centrifugal drift

had a significant impact on the direction of the root growth. As a result, a clear directional growth towards the outside of the Petri dish was observed in the seedlings that grew on the laterals at high angular velocity in both orientations (Figure 2a) due to high acceleration which increases with the distance from the clinorotation axis. The direction and the angle of the roots corresponded to the direction of the centrifugal force vector (black arrows in Figure 2a) and the angle of the root depended on the distance of the seedling from the clinorotation axis (Figure 2a). The plot correlation between the distance of the seedling to the center of rotation and the root tip angle is shown in Figure S1. It should be noted that the roots did not grow straight downwards in any of the conditions, meaning the root growth toward the gravity vector was inhibited by clinorotation. Nevertheless, in case of the fast clinorotation, centrifugal drift seemed to be perceived by the seedlings placed at a distance from the clinorotation axis (Figure S1).

The maximum centrifugal force for both configurations, vertical and horizontal, at slow clinorotation (1 rpm) across the entire Petri Dish (4.5 cm radius) was negligible (up to 5.04×10^{-5} g at the border of the Petri dish). In turn, the theoretical value of centrifugal acceleration in the fast clinorotation (60 rpm) is 0.18 g at 4.5 cm radius, which is above the graviperception threshold values reported before [41–43]. These calculations are in agreement with the growth pattern observed in the experiment.

We have observed that in the Horizontal Fast Clinorotation (HFC), the seedlings were often displaced after 24 h (see Figure 2a; the position of the seeds before the clinorotation is marked with short black lines along the line in the middle of the Petri dish). Sections of the seedlings detached from the substrate. It should be noted, that in the experimental setting when seedlings are grown on an agar surface on a Petri dish, in vertical clinorotation, the gravity vector acts along the surface and so does the centrifugal force (both acting in the same plane). On the other hand, in horizontal clinorotation, although the centrifugal force acts along the agar surface, the Petri dish changes constantly the angle with respect to the gravity vector, meaning that the gravity vector and the centrifugal force do not act in the same plane, except at the time when the Petri dish is positioned vertically (see Figure 1). This constant change causes the seedlings to partly detach from the agar. It is possible that in horizontal clinorotation the "change of phase" has an additional impact on the seedlings´ response. In this experimental setting, the gravity vector acts during half of the clinorotation cycle by "pushing" the seedling against the agar surface (agar side down) and during the other half of the cycle by "pulling" the seedling from the agar surface (top of the Petri dish down). As mentioned before, in vertical clinorotation this issue is not present, since both the gravity vector and the centrifugal force act along the agar surface.

To measure the influence of the speed and the orientation of the sample on the root growth rate we measured the length of the roots before the clinorotation (point 0 marked with arrows in the Figure 2a) and after 24 h (L, see Figure 2b). We have observed a significantly higher root growth rate in the HFC sample (Figure 2c).

We analyzed in more detail the root morphology using four values described before by [44], namely, integral averaged angular declination (α in Figure 2b) of the root tip, vertical growth index (VGI), horizontal growth index (HGI), and root straightness, later renamed as gravitropic index (GI) [20,45–48]. VGI is defined as the ratio between the straight line distance from the base of the root to the root tip and the root length. The closer VGI value is to 1, the straighter the root grows. On the other hand, HGI is the distance in the horizontal line between the base of the root and the root tip divided by the root length. The higher the deviation from the straight line, the higher is the value of the HGI (closer to 1). Here, we calculated horizontal and vertical growth indexes taking into account the distance from point 0 (start of the clinorotation) to the root tip after 24 h (Figure 2b).

The GI is the shortest distance from the base of the root to the root tip divided by the root length. Similar to the VGI, the closer the value is to one, the straighter is the root.

As expected, in the control the HGI was the lowest and VGI the highest and in the directional growth control the trend was opposite (Figure 2e,f). As indicated by HGI, VGI, and α values, roots of the seedlings exposed to vertical clinorotation deviated less from a

straight line than in case of horizontal clinorotation (Figure 2d–g). Although the differences between the values that correspond to the different clinorotation conditions were not significant, the trend was repeated in all parameters, including the plot of correlation between distance from the rotation axis and the angle of the root (Figure S1).

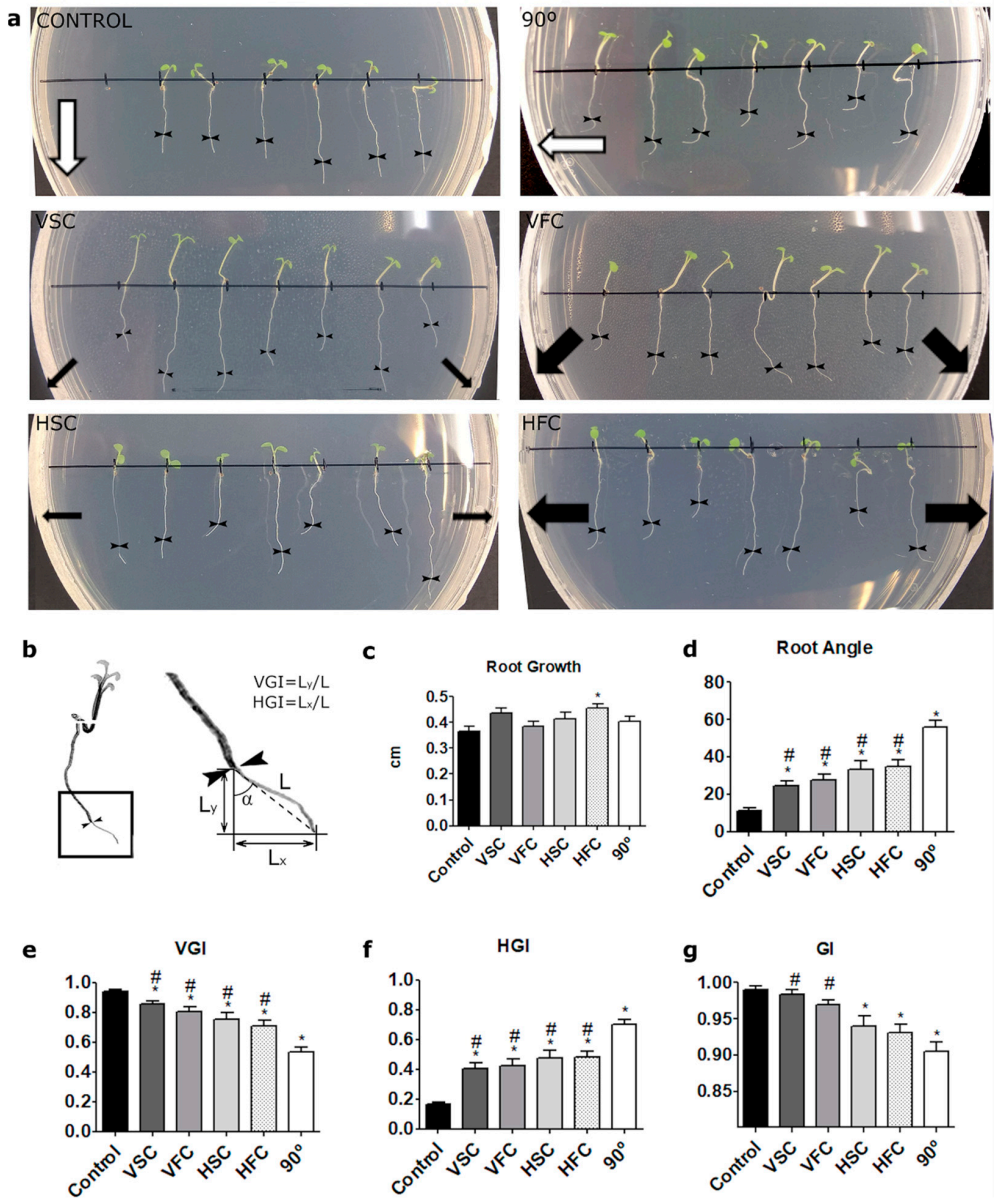

Figure 2. Root growth and direction upon clinorotation conditions. (**a**) Photographs of seedlings in the different experimental conditions (CONTROL, control; 90°, directional growth control; VSC, Vertical Slow Clinorotation; VFC, Vertical Fast Clinorotation; HSC, Horizontal Slow Clinorotation; HFC, Horizontal Fast Clinorotation). White arrows represent gravity direction and black arrows represent the direction and magnitude of centrifugal force (narrow arrow for low magnitude in slow clinorotation and wide arrow for high magnitude in fast clinorotation). (**b**) Schematic representation of root growth parameters quantified (**c**–**g**) Quantification of different root features: (**c**) the root growth, expressed as the length of the root from time point 0 (arrows) and after 24 h; (**d**) root angle, expressed as the absolute value of integral average angular declination; (**e**) VGI, Vertical Growth Index; (**f**) HGI, Horizontal Growth Index; (**g**) GI, Gravitropic index. * p-value < 0.05 compared to the control. # p-value < 0.05 compared to directional growth control, 90°.

2.2. Distribution of Statoliths in the Columella Is Influenced by Angular Velocity

We have investigated the distribution of statoliths in the columella in Differential Interference Contrast (DIC) images of formaldehyde (FA) fixed seedlings (Figure 3 and Figure S2).

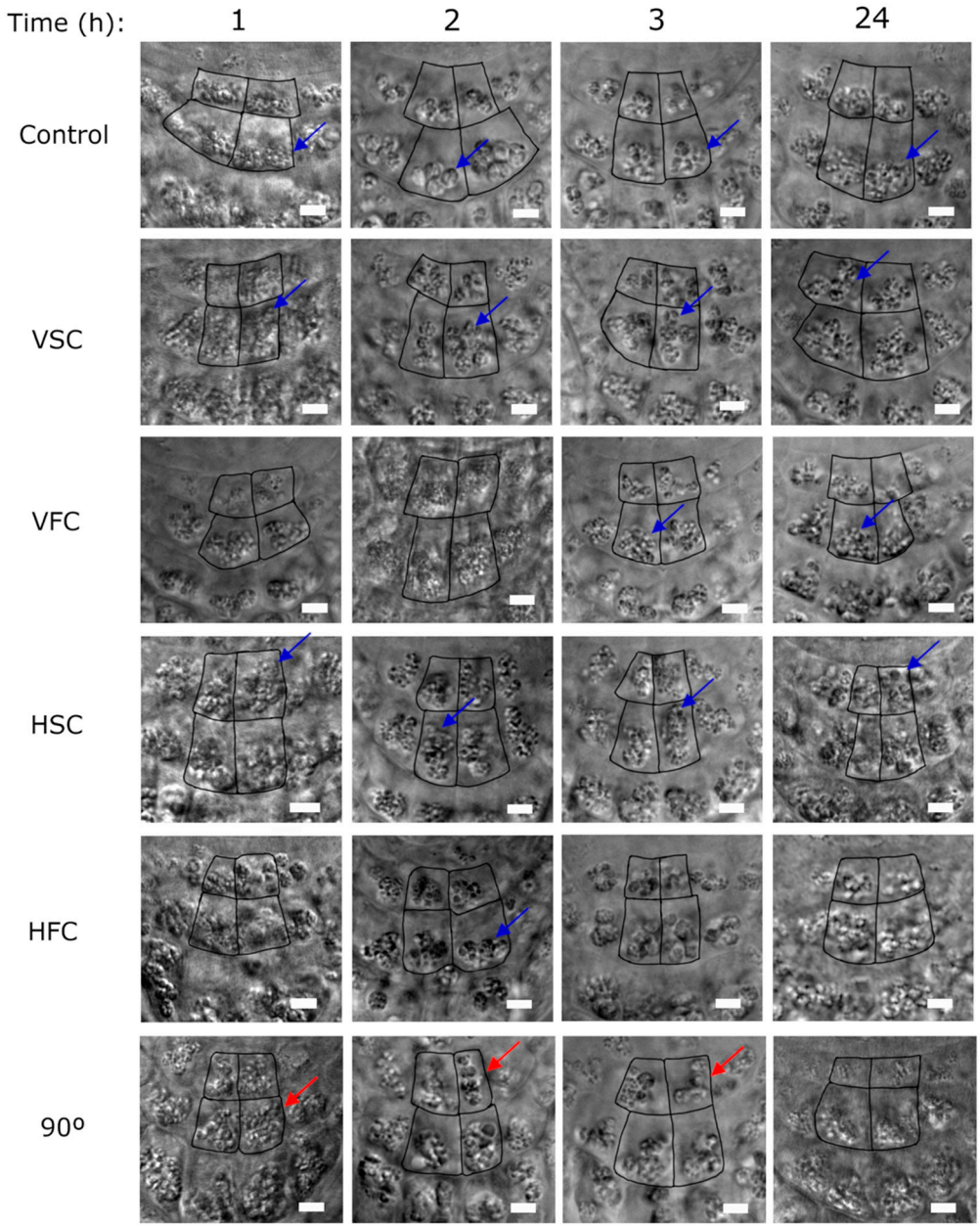

Figure 3. Statoliths position in Differential Interference Contrast (DIC) images. Detail of central S1 and S2 statocytes in the root columella at the different times (1, 2, 3, and 24 h) and conditions (Control; VSC, Vertical Slow Clinorotation; VFC, Vertical Fast Clinorotation; HSC, Horizontal Slow Clinorotation; HFC, Horizontal Fast Clinorotation; 90°, directional growth control). Blue arrows highlight statolith differential position among conditions. Red arrows indicate statoliths position changes due to the gravity vector in the directional growth control. Scale bar represents 5 μm2.

Taking into account the importance of each tier in the columella, we have focused on central statocytes (in S1 and S2 tiers) to compare the position of statoliths inside the statocytes in each condition. These are outlined in Figure 3.

Statoliths containing starch grains could be seen within statocytes in the DIC images. Although other organelles and internal cellular structures, such as the nucleus or ER, could not be distinguished, the contour of the statocytes could be observed. In the central statocytes of columella in the control roots, groups of statoliths could be seen located close to the bottom of the cell (Figure 3, blue arrows in the control sample). In the directional growth control, statoliths were clustered, close to one lateral cell wall of the statocyte, at 1, 2, and 3 hours after the turn (Figure 3, red arrows). After 24 h, the statoliths were located in the lower part of the statocytes when the root has already changed its orientation and grew downwards, according to the gravity vector. In the slow clinorotated samples, Vertical Slow Clinorotation (VSC) and Horizontal Slow Clinorotation (HSC), groups of statoliths were observed more dispersed throughout the statocytes in comparison to the controls and samples exposed to Fast Clinorotation (FC) for 3 and 24 h (blue arrows in Figure 3 in VSC and HSC samples). In the fast clinorotated samples, statoliths formed groups located in the lower part of the cell (blue arrows in Figure 3 in Vertical Fast Clinorotation (VFC) and HFC samples). This pattern was more evident in the VFC than in HFC, in which some statoliths could be seen in the center or even in the upper part of the cell (Figure 3). Although the fixation of the samples was performed immediately after clinostat was stopped (stationary mode), the differences observed between the conditions confirm that the minimal time of this procedure did not significantly influence the position of the statoliths.

2.3. Statocytes' Ultrastructure Is Affected by Horizontal Clinorotation and Displays Features of Stress Response

We investigated in more detail the cell ultrastructure of central statocytes in S1 and S2 tiers, in different conditions, by electron microscopy. Statocytes show a polar distribution, meaning that the nucleus is located in the upper part and the statoliths in the lower part of the cell. We have observed this typical layout in all the conditions (Figure 4a). The round nucleus, enclosed in a double nuclear membrane, did not present any abnormalities in any condition. Near the nucleus, numerous mitochondria and lysosomes were located. Mitochondria presented elongated (oblong) shape with compact cristae in cross sections, although round mitochondria with more loosely organized cristae were also observed in HSC (Figure 4b). In controls and in vertically clinorotated samples, the outline of lysosomes showed round shape, whereas in HSC sample their shape was more oblong (Figure S3). In fast clinorotated samples the size, and in HFC the number of lysosomes was reduced. A complex ER system could be observed in all the conditions in the lower part of the cell and also in a simpler form on the laterals and close to the nucleus. Multiple Golgi bodies were present distributed around the cell, which confirmed high secretory activity. Statoliths containing multiple starch grains and sometimes fibrous bundles [49] could be observed in the central and lower part of the cell and in the sample turned 90°, also in the upper part in proximity to the nucleus. Statoliths were of regular round or oblong shapes, although in the directional growth control (90°) and HFC, irregular shapes were observed (Figure 4a). Occasional vacuoles were observed in the controls and vertically clinorotated samples. In horizontally clinorotated samples, the vacuoles were bigger and numerous in the HSC sample. Cell walls in all conditions could be easily distinguished between plasma membranes of adjoining cells and middle lamella was sometimes visible (Figure 4c). The walls were mostly thin, although thicker regions could be also seen (Figure 4a). Plasmodesmata connecting cells from different tiers (up/down) could be often seen, suggesting close communication between these cells. Vesicles (endosomes) were often observed between the cell membrane and the cell wall. In controls and vertically clinorotated samples, the cell walls delimited mostly straight rectangular cells; nevertheless, in horizontally clinorotated samples, the anticlinal and bottom cell walls had often irregular wavy shape, especially pronounced in the HSC sample (Figure 4a,c; Figure S4) which could suggest they underwent prolonged mechanical stress.

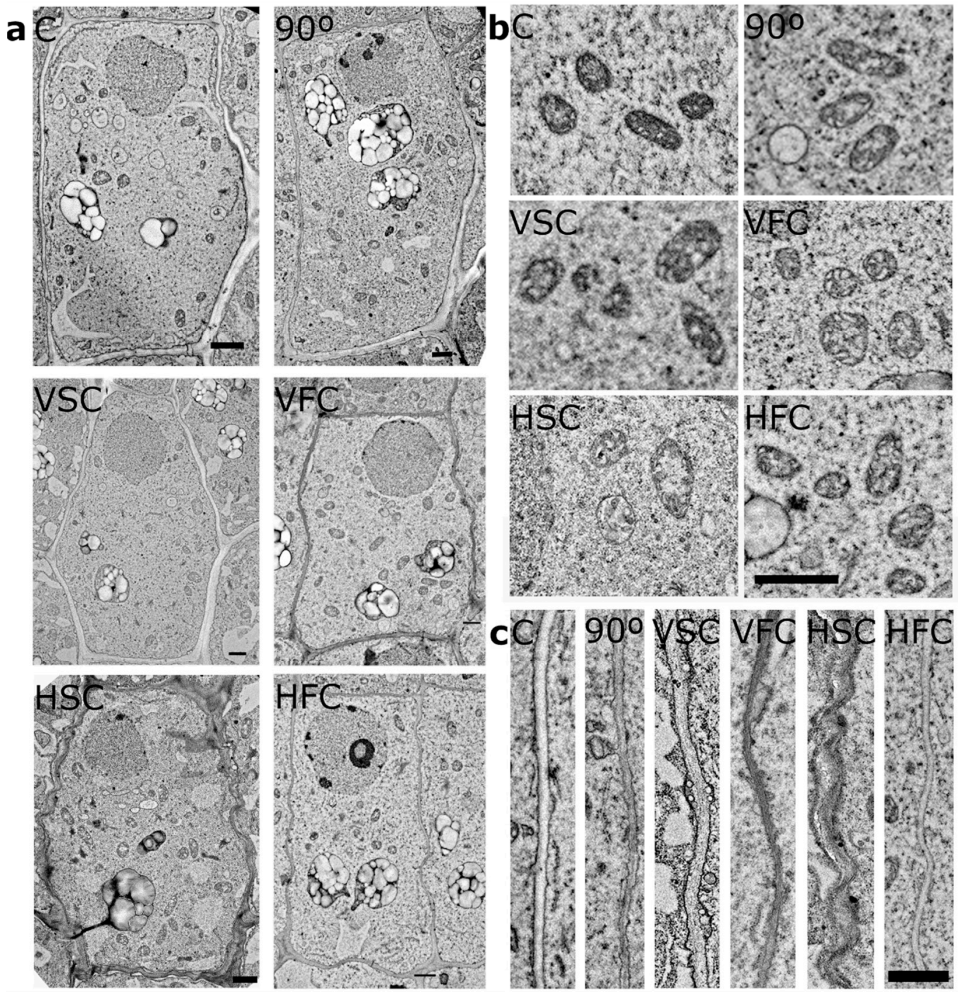

Figure 4. Statocytes ultrastructure. (**a**) Electron microscopy images of representative statocytes of S2 central columella tier in the different experimental conditions: Control (C), directional growth control (90°), Vertical Slow Clinorotation (VSC), Vertical Fast Clinorotation (VFC), Horizontal Slow Clinorotation (HSC), and Horizontal Fast Clinorotation (HFC). (**b**) Detail of mitochondria structure. (**c**) Detail of lateral cell wall structure. Scale bar represents 1 μm.

2.4. The Distribution of PIN2, an Auxin Transporter, Is Affected in the Horizontal but Not Vertical Clinorotation

Auxin is one of the most important phytohormones, and it plays an essential role in regulating root growth. In the meristem, auxin promotes proliferation (mitosis), whereas in the elongation zone, it inhibits cell expansion [50,51]. It is transported from the shoot to the root meristem through the central part of the root and an auxin maximum is formed around the quiescent center. From there, auxin is transported, first by PIN3 and PIN7, and then by PIN2 proteins, up to the elongation zone through epidermal cells by basipetal transport, sometimes called the reflux loop [17,22,52]. This transport is responsible for asymmetrical changes in auxin gradient that modulate cell expansion in the elongation zone, enabling the root to bend in response to reorientation. We have investigated changes in auxin transport in the PIN2-Green Fluorescence Protein (PIN2-GFP) reporter line (Figure 5), as well as auxin levels and distribution, using DR5-β-glucuronidase (DR5-GUS) and DII-Venus reporter lines exposed to different clinorotation conditions (Figure 6 and Figure S5, respectively).

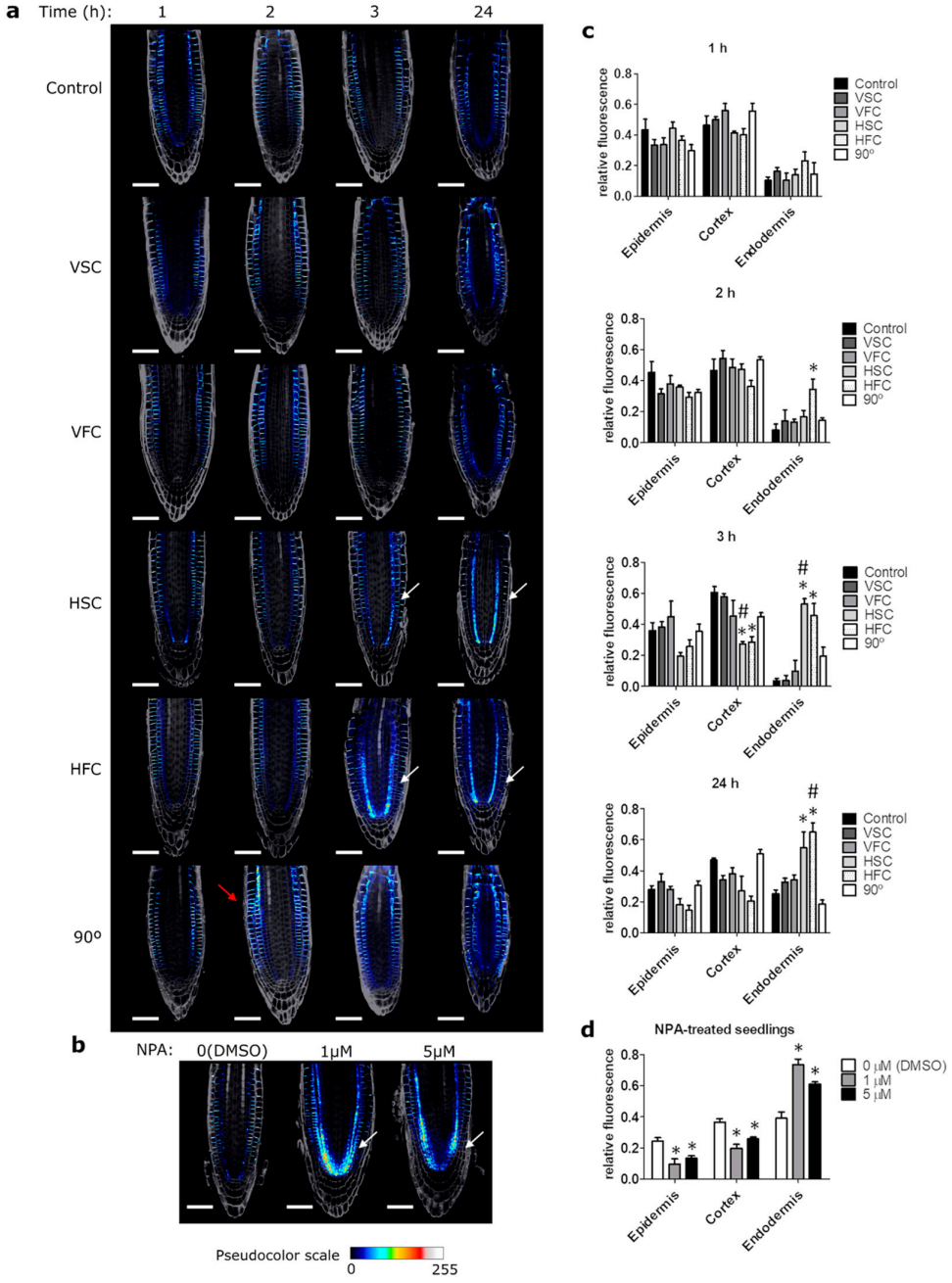

Figure 5. PIN-FORMED2 (PIN2) distribution and levels in the root meristem. (**a**) Confocal microscope images of PIN2-Green Fluorescence Protein (GFP) reporter line. Pseudocolor reflecting the intensity of the GFP signal was applied with the Lookup Table Royal Tool in the ImageJ software; Grey: cell wall staining with Renaissance SR2200. Experimental conditions: Control; VSC, Vertical Slow Clinorotation; VFC, Vertical Fast Clinorotation; HSC, Horizontal Slow Clinorotation; HFC, Horizontal Fast Clinorotation; 90°, directional growth control. At times 1, 2, 3, and 24 h of exposure to these conditions. White arrows highlight endodermis accumulation. Red arrow: PIN2 redistribution to new gravity vector. Scale bar represents 50 µm (**b**) PIN2-GFP seedlings grew for 5 days with 0 (DMSO), 1 or 5 µM naphthylphthalamic acid (NPA). Scale bar represents 50 µm. (**c**) Relative fluorescence GFP intensity in the different meristem cell layers at the different times and experimental conditions. (**d**) GFP relative intensity at each meristem layer in seedlings grown for 5 days with 0 (Dimethyl Sulfoxide, DMSO), 1 or 5 µM NPA. * p-value < 0.05 compared to control at the same time and layer (or 0 µm DMSO in the NPA-treated seedlings), # p-value < 0.05 compared to the same time and clinorotation speed but different orientation.

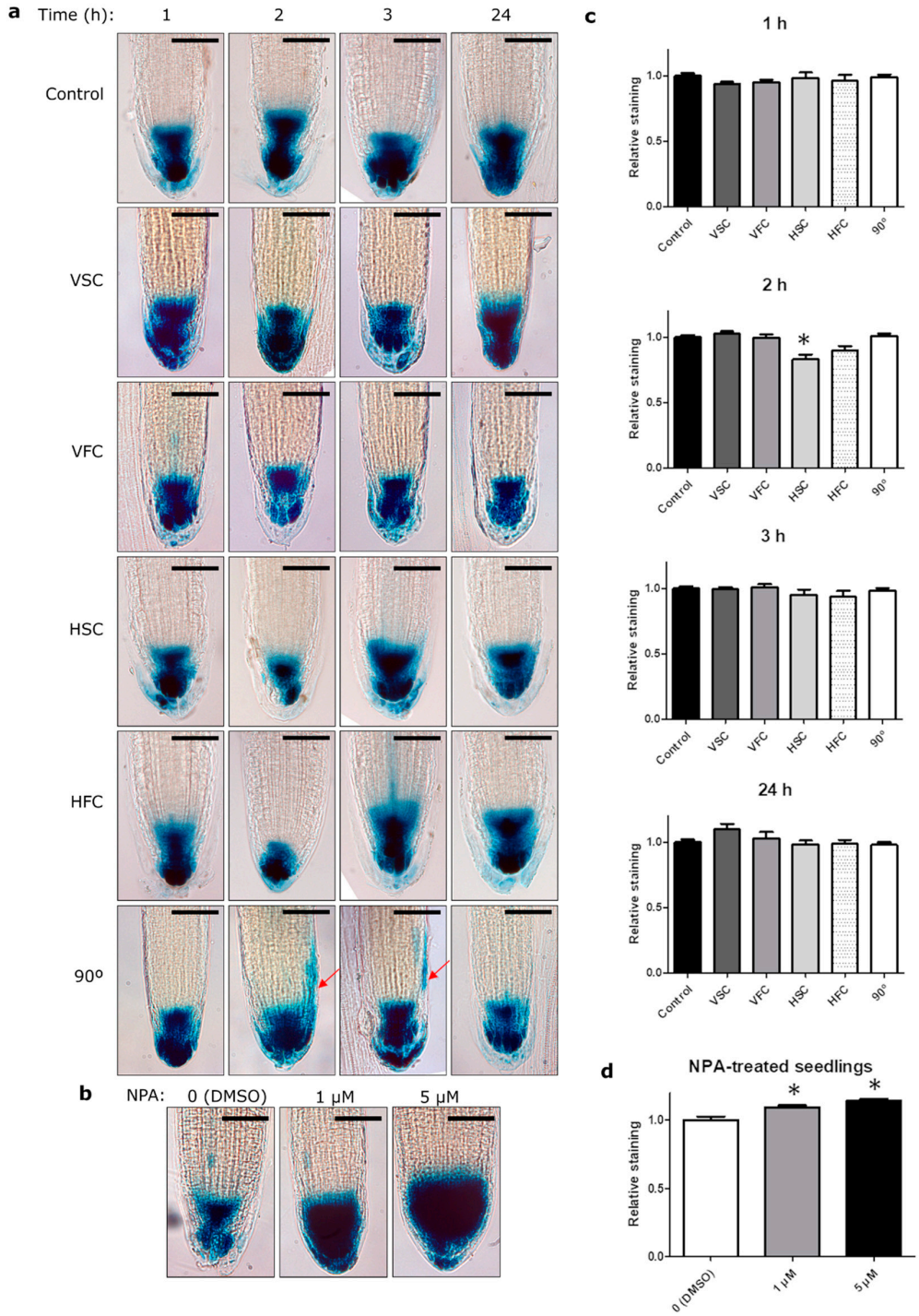

Figure 6. Auxin distribution among clinorotation conditions. (**a**) Optical microscope images of DR5-β-glucuronidase (DR5-GUS) reporter line seedlings exposed to the different experimental conditions: Control; VSC, Vertical Slow Clinorotation; VFC, Vertical Fast Clinorotation; HSC, Horizontal Slow Clinorotation; HFC, Horizontal Fast Clinorotation; 90°, directional growth control; after 1, 2, 3, or 24 h of exposure. Red arrows indicate auxin redistribution. Scale bar represents 50 µm (**b**) DR5-GUS seedlings grew for 5 days with 0 (DMSO), 1 or 5 µM NPA. Scale bar represents 50 µm. (**c**) DR5 relative staining quantification at the different times (1, 2, 3, and 24 h) and conditions. (**d**) NPA-treated seedlings DR5-GUS relative staining quantification. Bars represent mean + SEM. * *p*-value < 0.05.

In the directional growth control (90°) we observed asymmetric changes in PIN2-GFP distribution, characteristic for gravitropic response, with accumulation on the lower side.

This distribution was especially conspicuous 2 h after the reorientation (Figure 5a, red arrow), whereas in the control sample the distribution was symmetric at all times. In the clinorotated samples the asymmetric distribution was not observed, although in the horizontal clinorotation we have observed PIN2 internalization in the lower endodermis, that was confirmed by fluorescent signal quantification in the different meristematic layers: epidermis, cortex, and endodermis (Figure 5a,c). To investigate if this distribution is related to auxin transport inhibition, we have grown PIN2-GFP seedlings on medium complemented with naphthylphthalamic acid (NPA), an auxin transport inhibitor that inhibits gravitropic response [23], at different concentrations (Figure 5b). Indeed, the PIN2 accumulation in the lower endodermis was observed in NPA treated seedlings, suggesting that the observed distribution is a result of auxin transport inhibition (Figure 5b,d). The samples horizontally clinorotated for 24 h showed PIN2 intracellular accumulation, similar to that in the sample treated with 1 µM NPA (Figure 5). The typical polar distribution of PIN2 in the meristematic epidermis and cortex was not affected in NPA-treated plants, in agreement with previous reports [53].

Next, we investigated auxin distribution and levels during clinorotation in DR5 and DII-Venus reporter lines (Figure 6 and Figure S5). DR5 is a synthetic auxin response element that is highly responsive to auxin level changes. We have used a fusion of DR5 and a minimal 35S Cauliflower mosaic virus (CaMV) promoter with GUS reporter gene in DR5-GUS reporter line [54]. DR5 (TGTCTC) binds to auxin response factors and responds rapidly to active auxin concentration between 10^{-8} and 10^{-5} M and remains at high levels up to 10^{-4} M [55]. This makes it a suitable tool for tracking the accumulation of auxin in combination with the GUS reporter gene.

DII-Venus is a more modern auxin sensor, which combines VENUS fast maturing form of yellow fluorescent protein and Aux/ Indole-3-acetic acid (IAA) auxin-interaction domain (domain II; DII) expressed under a constitutive promoter [56]. It enables tracking of Aux/IAA-dependent degradation of VENUS fluorescent protein. This provides a tool to monitor dynamic changes of auxin levels that does not depend on a complex auxin response pathway, as is the case of DR5. DII-Venus is constitutively expressed in nuclei and it is degraded upon contact with auxin, resulting in loss of fluorescent signal and directly reflecting auxin levels in the cell [56].

The typical auxin distribution in the root meristem with an auxin maximum around the region of quiescent center and diminishing levels towards the elongation zone, was observed in all conditions. In the directional growth control (90°) we have observed asymmetric auxin distribution at the meristem laterals after 1–3 h after the reorientation (Figure 6, red arrows). No obvious changes in the auxin distribution pattern was observed in any of the clinorotation conditions.

We have also grown DII-Venus and DR5-GUS seedlings on a medium supplemented with NPA at different concentrations, to investigate whether the distribution of PIN2-GFP corresponding to auxin transport inhibition is reflected in auxin accumulation in these reporter lines in any of the different clinorotation conditions. The seedlings treated with NPA showed gradual accumulation of GUS signal in the central and lateral parts of the root tip in DR5-GUS line and gradual decrease in DII-Venus signal that depended on NPA concentration (Figure 6b, d, and Figure S5b). Nevertheless, a similar pattern was not observed in any of the clinorotated samples (Figure 6a and Figure S5a).

We quantified DR5 relative staining to investigate the changes in auxin levels in different conditions. The only statistically significant difference was a minor reduction in auxin levels after 2 h of HSC in comparison to control (Figure 6c). On the other hand, a clear increase in GUS signal was observed in NPA-treated seedlings.

3. Discussion

The clinostat is an important tool for investigating the graviresponse of plants and, in particular, the impact of microgravity, thus being a useful complement to space experiments. It was designed to be applied in plants for their slow gravitropic response [26–28] but

nowadays is also used in experiments with animals and in vitro cell cultures [57–62]. Since the first use of clinostat in plant studies [25,27,28] gravitropism was extensively studied and today is much better understood. The response of the plant to reorientation is a dynamic sequence of processes that leads to a non-uniform growth in the elongation zone in approximately 3 h, according to the direction of the gravity vector [23,63]. The three phases of gravitropism can be distinguished: gravity perception in the columella, signal transduction that results in auxin distribution gradient, and non-uniform elongation that leads to the root bending. Each phase takes a certain time, but the gravity perception, which is the key step to take into account for an optimal microgravity simulation, takes approximately 6 minutes (370 s after reorientation) [12].

Although clinostats are widely used, little bibliography is available on comparison of fast and slow [64], or vertical and horizontal clinorotation [36–38,65]. In this respect, it is worth mentioning that we have previously developed a mathematical model which enabled calculation of the clinostat setting for an optimal microgravity simulation. Given the size of the experimental container, optimal angular velocity can be calculated as a function of the time of clinorotation, and vice versa [40].

The present study confirms that all clinorotation conditions are enough to avoid the root growth according to gravity vector. Nevertheless, in fast clinorotation, centrifugal force led to conspicuous directional growth, as will be discussed further. In the slow clinorotated samples, non-directional, random root growth was observed, similar to the growth observed in plants grown in real microgravity conditions [66,67]. A study in the International Space Station showed that the orientation of roots in microgravity was not random, but was the result of automorphogenesis and autotropism, successively. First, the embryonic root curved strongly away from cotyledons, and then it grew straight [42]. As shown in the DIC images of root columella, under slow clinorotation, statoliths appeared dispersed in statocytes similar to what was observed in plants grown in real microgravity [36,68–72].

Clear directional growth was triggered at high angular velocities by centrifugal force in the seedlings placed furthest away from the clinorotation axis. The value of this force is proportional to the distance from the clinorotation axis, meaning that the plants positioned further from the center of the Petri dish perceived the centrifugal force and responded to it. Thus, fast clinorotation would only be appropriate in a very limited radius from the center of rotation, or for short times of microgravity simulation. Previously, researchers applied the criterion of centrifugal force limit to determine the usable space for effective microgravity simulation during clinorotation [31,38,73,74]. These limits ranged between 0.00009 g – 0.2 g and were determined by investigating the minimal centrifugal force that caused directional growth in oats clinorotated horizontally (0.0001 g) [41], in lentils in a centrifuge in the GRAVI-1 space experiment (0.000014 g) [42], or the partial- g effect on rhizoids of *Chara globularis* in parabolic flights (0.05 g) [43]. In our experimental setting, at 1 rpm, the centrifugal force is below most of the reported perception thresholds (at the edge of the Petri dish; 4.5 cm from the clinorotation center, 0.00005 g) which was confirmed by our morphological study. On the other hand, at 60 rpm the centrifugal force (at the edge of the Petri Dish; 4.5 cm from the clinorotation center, 0.18 g) exceeds the graviperception thresholds at a short distance from the clinorotation axis and triggers directional growth, as shown in the morphological study.

Taking into account that the directional growth was not observed in slow clinorotation our morphological study suggests that slow clinorotation is more suitable for microgravity simulation in *A. thaliana* seedlings. This is in agreement with previous reports indicating that angular velocity values between 0.33 and 2 rpm result in effective clinorotation (microgravity simulation) [30,38,75], and with our preliminary results [40].

We can distinguish vertical or horizontal clinorotation depending on the orientation of the sample in relation to rotation axis [36]. Previous studies have shown that the type of the clinorotation (vertical or horizontal) influences the plant response in a different way. John and Hasenstein [38], have demonstrated that horizontal clinorotation (1–5 rpm) is less effective in nullifying gravitropic signals than vertical clinorotation. Seedlings

were turned 90° before clinorotation for up to 15 min and then clinorotated vertically or horizontally. Seedlings that were horizontally clinorotated showed more pronounced directional growth than the vertically clinorotated ones. Lorenzi and Perbal [36], compared cell ultrastructure and concluded that VSC has similar effect on the position of the nucleus as real microgravity.

Moreover, a number of studies pointed out that horizontal clinorotation is associated with higher stress response [49,65,69,73], although this aspect was later extrapolated as a general effect of clinorotation. This observation is in agreement with our results, as we observed altered ultrastructure of statocytes (Figure 4) and PIN2 intracellular accumulation (Figure 5) in horizontally clinorotated samples. The ultrastructural changes we report, especially pronounced in HSC, such as increased vacuolar compartment, changes in outline shape and ultrastructure of mitochondria, and irregular cell wall shape, were postulated to be linked to the response to abiotic stress in *A. thaliana* and *Pisum sativum* [76,77]. Additionally, seedlings of *P. sativum* exposed for 3 days to horizontal clinorotation showed increased levels of stress indicators, such as heat shock proteins HSP70 and HSP90 [65]. Increased lipid breakdown was observed in rapeseed (*Brassica napus*) seedlings after HSC (1 rpm) for 5 days. Columella degradation, as well as ultrastructural alterations, in agreement with our result of irregular cell wall shape and increased lytic compartment, were reported for horizontally clinorotated *Lepidium sativum* seedlings for 20 h [73]. In addition, in two-axis clinostat experiments, where the sample is clinorotated in both horizontal and vertical orientations, columella degradation, as well as increased lytic compartment and irregular cell wall shape, were observed in white clover (*Trifolium repens*) clinorotated for 72 h [49,69]. These alterations were not observed in real microgravity [49,69], which suggests that they could be an artifact of the simulation and not due a microgravity effect. This stress response was not observed in vertical clinorotation in our study.

PIN2 is expressed in root epidermis and cortex under normal conditions, a pattern that was observed in control and vertically clinorotated seedlings. Samples exposed to horizontal clinorotation for prolonged periods of time (3 h and more) additionally presented intracellular localization in the endodermis. PIN2 localization in the endodermis was previously described in seedlings with disrupted symplastic signaling to and from the endodermis [78] and in mutants deficient in Calcium-Dependent Protein Kinase-Related Kinase 5 (CRK5) protein, a plasma membrane-associated kinase which phosphorylates the hydrophilic loop of PIN2 [79]. Nevertheless, the endodermal localization of PIN2 in both cases was associated with diminished levels of PIN2 in epidermis and endodermis, which was observed in NPA-treated seedlings, but not in horizontally clinorotated samples. Intracellular localization of PIN2-GFP in lytic vacuoles in the epidermis was previously described in seedlings treated with concanamycin A (an inhibitor of vacuolar proton ATPases which reduces protein degradation) and after incubation in the dark for 6 h [80]. Nevertheless, we only observed the intracellular PIN2 localization in the endodermis. Endodermis-deficient *sgr* (*shoot gravitropism*) mutants were deficient in shoot gravitropism but presented normal root gravitropism, suggesting that this layer is not crucial for root gravitropism [5,81]. The mechanism and function of the intracellular PIN2 localization in the endodermis under prolonged horizontal clinorotation are not clear but might be related to the intensification of mechanical stimuli.

Although reports of increased stress response to horizontal clinorotation are substantial, it is not well understood what is the nature of the stress. A suggestive and feasible possibility is that this stress would be related to the thigmotropic reaction. In vertical clinorotation, the gravity vector and centrifugal force act on the same plane, along the agar surface; therefore, thigmotropic stimuli are constant. On the other hand, in horizontal clinorotation, the position of the Petri dish with respect to the gravity vector changes constantly, meaning that the Petri dish is tilted at different angles (from 1° to 360°) during the clinorotation cycle. In fact, it is well established that seedlings grown on a tilted agar surface present altered growth patterns; waving, coiling, and skewing [82–84]. A plausible explanation for this phenomenon is that, since the root is not able to penetrate agar sur-

face, it is perceived as an obstacle and activates the obstacle avoidance mechanism [85]. This mechanism is regulated by the columella [85,86]. While thigmotropic reaction is activated, gravitropism is attenuated [85]. Although the mechanism of obstacle avoidance is not well understood, it was recently reported that auxin and Ca^{2+} are involved in this process [86,87], factors that are also key players in gravitropism. Obstacle avoidance is fulfilled by two acts of root bending, with the first bend appearing just 20 minutes after the contact with an obstacle [87]. This suggests that thigmotropic growth response is faster than the gravitropic response, in which asymmetrical growth appears approximately 3 h after reorientation [23,63]. It is possible that, during the HSC, the repetitive cycles when the Petri dish is tilted (agar down—more friction, top of the Petri dish down—no friction) could be enough for the root to detect agar surface as an obstacle and trigger the thigmotropic response. In effect, this response would be triggered in each clinorotation cycle and could lead to the accumulation of mechanical stimuli and stress response. This hypothesis is supported by the fact that in HFC, where the clinorotation cycles are shorter, severe ultrastructural changes in statocytes were not observed, which could suggest that the duration of the mechanical stimuli was under the limit of the thigmotropic perception.

Revisiting the case of the Random Position Machine (RPM), this device is particularly interesting as a combination of HFC and VFC, usually involving fast angular speed and sudden changes in direction caused by the operation in real random mode [88]. Actually, centrifugal forces and the experimental design requirement of aligning seedling growth with the rotating axis become irrelevant in this simulator, due to forces averaging in the three dimensions. However, it would be conceivable that the overall stress response in the statocytes could be even higher than the one reported here. Our comparisons of RPM experiments with real microgravity and low g levels (< 0.1 g) produced by centrifugation in orbit [89,90] suggest that the seedlings may respond in the RPM, not only to microgravity alterations, but also to a certain misbalance in the different tropism signals (gravity, light, touch, water, etc.) that is also observed in partial gravity conditions recreated in orbit. Otherwise, clinostat and RPM produced comparable results with *A. thaliana* seedlings in a parallel study on the effects of simulated microgravity on root meristematic cells [32].

To sum up, different clinostat settings can produce different forces in combination with the gravity force. One of the drawbacks of clinostats and other ground based facilities used for microgravity simulation is the fact that most studies only deal with the gravitropic response, when other tropisms, such as thigmotropism, may apply and should be taken into account. Considering that the mechanisms regulating these responses are still not well-understood any simulator may introduce artefacts. Further investigation of the plant physiological response to different simulation conditions and its comparison to the response to real microgravity will help us to discern the effect of microgravity from other aspects of the mechanical simulators and help us to improve the simulation quality.

4. Materials and Methods

4.1. Material, Growth Conditions, and Quantification

The 2D-clinostat was granted to our laboratory by the Zero-Gravity Instrument Project (ZGIP, United Nations Office for Outer Space Affairs (UNOOSA)). An adaptor, designed and constructed ad hoc with a 3D-printer, was used for horizontal clinorotation (Figure S6). The two orientations in the use of the clinostat are shown in Figure 1. Horizontal clinorotation with the seedlings parallel to the rotation axis (as shown Figure 1b) was previously applied in multiple studies [31,32,34,35,91].

Seeds were surface sterilized with 70% ethanol with 0.01% Triton X-100 followed by 95% ethanol for 3 minutes and air-dried. In total, 7 seeds were positioned in the middle of the 9 cm Petri dish. Seedlings were grown on Murashige and Skoog (MS) medium (M0221, Duchefa) with 0.5 g/L 2-(*N*-morpholino)ethanesulfonic acid (MES) (M8250 Sigma–Aldrich), 1% sucrose (107651, Merck), and 0.8% plant agar (P1001, Duchefa) for 5 days at 23 °C under long day regime (16 h/8 h) vertically for 5 days to obtain straight root growth according to the gravity vector. After 5 days, seedlings were clinorotated for 24 h on a clinostat

horizontally (H) or vertically (V) at two speeds; at 1 rpm (slow clinorotation, SC) and at 60 rpm (FC). Parallel to the experiment we performed two controls, one kept in the vertical position (1 g control) and another one turned 90 degrees and kept in vertical position (directional growth control). Samples were grown in darkness under the four conditions. A total of three runs were performed for horizontal and vertical clinorotation (position of the plants in respect to the rotation axis is presented in Figure 1) for each experiment. In total around 21 seedlings of each sample were analyzed in each experimental procedure. Pictures were taken before and after 1, 2, 3, 24 h of exposure to each condition. Root length and growth during 24 h of clinorotation and in controls (Figure 2a) were measured with ImageJ software. Vertical and horizontal growth indexes and the integral averaged angular declination (α) were calculated from time 0 as described in [44] (Figure 2b). GI was determined from the base of the root to the tip as in [44].

For NPA treatment, seedlings were grown on medium complemented with 0 (0.01% (v/v) Dimethyl sulfoxide (DMSO)), 1 or 5 μM NPA in DMSO for 5 days.

4.2. Optical and Electron Microscopy

For microscopical analysis, samples were fixed immediately after the clinorotation, taking care of minimizing the time elapsed between the arrest of the clinostat and the interaction of the fixative with samples. First, the fixative was directly added to the Petri dish just after the release from the clinostat, for an immediate arrest of the vital activity. Then, seedlings were transferred to centrifuge tubes filled with fixative solution. For GUS staining, DR5-GUS seedlings [54] (seeds kindly supplied by Dr. E. Carnero-Diaz, Sorbonne University, Paris, France) were fixed in 90% acetone at −20 °C for 12 days. Seedlings were washed 3 times with 0.1 M sodium phosphate buffer pH 7.2 and GUS signal was revealed by enzymatic reaction with 1 mM X-GlcA (X1405, Duchefa), 1 mM potassium ferricyanide (P4066, Sigma–Aldrich), 0.25 mM trihydrate ferricyanide (455989, Sigma–Aldrich) in 0.05 M sodium phosphate buffer pH 7.2, at 37 °C overnight. Samples were washed 3 times in 0.05 M sodium phosphate buffer pH 7.2, mounted in 85% glycerol and observed under a Leica DM2500 microscope. Staining intensity was quantified with ImageJ in the meristem area in grey scale in the saturation channel (HSB Stack) [40].

For electron microscopy the *A. thaliana* seedlings were fixed in 2.5% glutaraldehyde (GA) and 1.5% formaldehyde (FA) and processed as previously described in [92]. Samples were embedded in LR White resin (London Resin, Berkshire, UK).

4.3. Confocal Microscopy

For confocal microscopy, Wild Type (WT) (Col0) and DII-Venus [56] (Nottingham Arabidopsis Stock Centre (NASC) ID: N799175) seedlings were fixed in 3% formaldehyde in Phosphate-buffered saline (PBS), as described in paragraph 4.2., for 1 h at room temperature (RT). Next samples were washed three times in PBS and digested for 1 h in 0.1% pectinase (17389, Sigma–Aldrich, St. Louis, MO, USA), 0.5% macerozyme (16419, Serva, Heidelberg, Germany), 0.4% mannitol (105983, Merck), 10% glycerol, and 0.02% Triton X-100 in PBS at 37 °C. Next, seedlings were washed 3 times with 10 % glycerol and 0.02 % Triton X-100 in PBS. PIN2-GFP seedlings [22,93] were processed as above but substituting PBS for Microtubule Stabilizing Buffer (MTSB) [94]. Seedlings were mounted onto poly-L-lysine coated multi-well microscope slides and dehydrated with a drop of 90% acetone in each well. For cell wall staining, samples were first permeabilized with 1% NP-40 (I8896, Sigma–Aldrich, St. Louis, MO, USA) and 0.5% Deoxycholic acid (DOC) (D2510, Sigma-Aldrich, St. Louis, MO, USA) in PBS and then stained for 2 h with 2% SCRI Renaissance Stain 2200 [95,96] (Renaissance Chemicals, North Duffield, UK) with 4% DMSO (81802, Sigma–Aldrich, St. Louis, MO, USA) protected from light. Finally, samples were washed twice with PBS and mounted in 1,4-Diazabicyclo[2.2.2]octane (DABCO) (D2522, Sigma–Aldrich).

Images were obtained with a confocal microscope Leica TCS SP5 with Acousto Optical Beam Splitter (AOBS) using 63 X or 40 X oil immersion optics. Yellow Fluorescence Protein (YFP) (DII-Venus) and GFP (PIN2-GFP) were excited at 496 nm and SRCI Renaissance

Stain 2200 at 405 nm with Argon and UV lasers, respectively. Pseudocolor reflecting the intensity of the GFP and YFP signal was applied with the Lookup Table Royal Tool in the ImageJ software. Relative fluorescence intensity in the different meristem layers was quantified using ImageJ, selecting the area with the SCRI Renaissance Stain 2200 channel and quantifying the intensity in grey scale in the GFP channel. Differential Interference Contrast (DIC) images of columella were taken using Leica TCS SP5 microscope to observe the localization of the statoliths within statocytes.

4.4. Statistics

In order to analyze statistical differences, SPSS software was used. Data from 3 independent experiments (7 seedlings for each condition in each experiment, in total 21 seedlings per condition) were analyzed. Normality was tested with Kolmogorov–Smirnov test, and homocedasticity with Levene test. Statistical differences were tested with ANOVA (root growth), ANOVA with Welch correction (HGI and PIN2-GFP fluorescence in meristematic layers) or U-test Mann–Whitney Wilcoxon (VGI, GI, root angle, and DR5-GUS staining) upon normality and homocedasticity test results.

5. Conclusions

Our results confirm that the plant responds differently to vertical and horizontal clinorotation and that the latter is related to the stress response, which is especially evidenced in horizontal slow clinorotation. This stress response is not present in vertical clinorotation. In fast clinorotation directional growth is triggered by centrifugal force which is proportional to the distance from the clinorotation axis. Taking into account that the stress response is not observed in the slow vertical clinorotation and that the growth pattern and the statolith distribution in this condition are similar to the ones observed in real microgravity experiments, we conclude that VSC is the least susceptible to artefacts related to microgravity simulation.

Supplementary Materials: The following are available online at https://www.mdpi.com/article/10.3390/plants10040734/s1, Figure S1: Relation between the distance from the rotation center and the angle of the root, Figure S2: DIC images of columella, Figure S3: Detail of lysosomes in statocytes, Figure S4: Columella structure. Figure S5: Auxin distribution with DII-Venus reporter seedlings, Figure S6: Clinostat used in this study.

Author Contributions: Conceptualization, M.C. and F.-J.M.; Methodology, A.V., M.C., and R.H.; Validation, A.V., L.S., and M.C.; Formal Analysis, A.V. and L.S.; Investigation M.C. and F.-J.M., Data Curation, A.V.; Writing – Original Draft Preparation, M.C. and A.V.; Writing – Review and Editing, M.C., F.-J.M., A.V., L.S., and R.H.; Visualization, A.V. and M.C.; Supervision, M.C. and F.-J.M.; Project Administration, F.-J.M.; Funding Acquisition, F.-J.M. and R.H. All authors have read and agreed to the published version of the manuscript.

Funding: This research was funded by Agencia Estatal de Investigación of the Spanish Ministry of Science and Innovation, Grants #ESP2015-64323-R and #RTI2018-099309-B-I00 (co-funded by EU-ERDF), awarded to FJM. The clinostat was obtained by a Grant of the United Nations Zero-Gravity Instrument Project (ZGIP), second and third cycle calls 2014/2018 (UNOOSA), awarded to RH and FJM. AV is a recipient of a contract of the Spanish National Program for Young Researchers Training (BES-2016-077976).

Institutional Review Board Statement: Not applicable.

Informed Consent Statement: Not applicable.

Acknowledgments: The work was possible thanks to the funds provided by Agencia Estatal de Investigación of the Spanish Ministry of Science and Innovation, Grants #ESP2015-64323-R and #RTI2018-099309-B-I00 (co-funded by EU-ERDF), awarded to FJM. The clinostat was obtained by a Grant of the United Nations Zero-Gravity Instrument Project (ZGIP), second and third cycle calls 2014/2018 (UNOOSA), awarded to RH and FJM. AV is a recipient of a contract of the Spanish National Program for Young Researchers Training (BES-2016-077976). We wish to acknowledge Julio Martin Santos (3DOHMS), who designed and printed the adaptor for horizontal clinorotation,

Enrique García Isidoro for assistance with Figure 1 and physical concepts and Fernando Escolar Antúnez for assistance in processing of resin-embedded samples for electron microscopy.

Conflicts of Interest: The authors declare no conflict of interest

References

1. Sato, E.M.; Hijazi, H.; Bennett, M.J.; Vissenberg, K.; Swarup, R. New insights into root gravitropic signalling. *J. Exp. Bot.* **2015**, *66*, 2155–2165. [CrossRef]
2. Swarup, R.; Bennett, M.J. Root gravitropism. *Annu. Plant. Rev. Online* **2018**, 157–174.
3. Morita, M.T. Directional gravity sensing in gravitropism. *Annu. Rev. Plant. Biol.* **2010**, *61*, 705–720. [CrossRef] [PubMed]
4. Sack, F.D.; Suyemoto, M.M.; Leopold, A.C. Amyloplast sedimentation and organelle saltation in living corn columella cells. *Am. J. Bot.* **1986**, *73*, 1692–1698. [CrossRef] [PubMed]
5. Fukaki, H.; Wysocka-Diller, J.; Kato, T.; Fujisawa, H.; Benfey, P.N.; Tasaka, M. Genetic evidence that the endodermis is essential for shoot gravitropism in *Arabidopsis thaliana*. *Plant J.* **1998**, *14*, 425–430. [CrossRef] [PubMed]
6. Hong, J.H.; Chu, H.; Zhang, C.; Ghosh, D.; Gong, X.; Xu, J. A quantitative analysis of stem cell homeostasis in the *Arabidopsis* columella root cap. *Front. Plant. Sci.* **2015**, *6*, 206. [CrossRef] [PubMed]
7. Kiss, J.Z.; Hertel, R.; Sack, F.D. Amyloplasts are necessary for full gravitropic sensitivity in roots of *Arabidopsis thaliana*. *Planta* **1989**, *177*, 198–206. [CrossRef]
8. Sack, F.D. Plant gravity sensing. *Int. Rev. Cytol.* **1991**, *127*, 193–252.
9. Baum, S.F.; Rost, T.L. Root apical oragnization in *Arabidopsis thaliana*. *Protoplasma* **1996**, *192*, 178–188. [CrossRef]
10. Olsen, G.M.; Mirza, J.I.; Maher, E.P.; Iversen, T.-H. Ultrastructure and movements of cell organelles in the root cap of agravitropic mutants and normal seedlings of *Arabidopsis thaliana*. *Physiol. Plant.* **1984**, *60*, 523–531. [CrossRef]
11. Blancaflor, E.B.; Fasano, J.M.; Gilroy, S. Mapping the functional roles of cap cells in the response of arabidopsis primary roots to gravity. *Plant Physiol.* **1998**, *116*, 213–222. [CrossRef] [PubMed]
12. Leitz, G.; Kang, B.H.; Schoenwaelder, M.E.A. Statolith sedimentation kinetics and force transduction to the cortical endoplasmic reticulum in gravity-sensing *Arabidopsis* columella cells. *Plant. Cell* **2009**, *21*, 843–860. [CrossRef]
13. Zhang, J.; Vanneste, S.; Brewer, P.B.; Michniewicz, M.; Grones, P.; Kleine-Vehn, J.; Löfke, C.; Teichmann, T.; Bielach, A.; Cannoot, B.; et al. Inositol trisphosphate-induced Ca^{2+} signaling modulates auxin transport and pin polarity. *Dev. Cell* **2011**, *20*, 855–866. [CrossRef]
14. Yoshihara, T.; Spalding, E.P. LAZY genes mediate the effects of gravity on auxin gradients and plant architecture. *Plant. Physiol.* **2017**, *175*, 959–969. [CrossRef] [PubMed]
15. Nakamura, M.; Nishimura, T.; Morita, M.T. Bridging the gap between amyloplasts and directional auxin transport in plant gravitropism. *Curr. Opin. Plant. Biol.* **2019**, *52*, 54–60. [CrossRef] [PubMed]
16. Furutani, M.; Hirano, Y.; Nishimura, T.; Nakamura, M.; Taniguchi, M.; Suzuki, K.; Oshida, R.; Kondo, C.; Sun, S.; Kato, K.; et al. Polar recruitment of RLD by LAZY1-like protein during gravity signaling in root branch angle control. *Nat. Commun.* **2020**, *11*, 76. [CrossRef] [PubMed]
17. Wisniewska, J.; Xu, J.; Seifartová, D.; Brewer, P.B.; Růžička, K.; Blilou, L. Polar PIN localization directs auxin flow in plants. *Science* **2006**, *312*, 883. [CrossRef]
18. Müller, A.; Guan, C.; Gälweiler, L.; Tänzler, P.; Huijser, P.; Marchant, A.; Parry, G.; Bennett, M.; Wisman, E.; Palme, K. AtPIN2 defines a locus of *Arabidopsis* for root gravitropism control. *EMBO J.* **1998**, *17*, 6903–6911. [CrossRef]
19. Friml, J.; Wiśniewska, J.; Benková, E.; Mendgen, K.; Palme, K. Lateral relocation of auxin efflux regulator PIN3 mediates tropism in *Arabidopsis*. *Nature* **2002**, *415*, 806–809. [CrossRef] [PubMed]
20. Kleine-Vehn, J.; Ding, Z.; Jones, A.R.; Tasaka, M.; Morita, M.T.; Friml, J. Gravity-induced PIN transcytosis for polarization of auxin fluxes in gravity-sensing root cells. *Proc. Natl. Acad. Sci. USA* **2010**, *107*, 22344–22349. [CrossRef]
21. Luschnig, C.; Gaxiola, R.A.; Grisafi, P.; Fink, G.R. EIR1, a root-specific protein involved in auxin transport, is required for gravitropism in *Arabidopsis thaliana*. *Genes Dev.* **1998**, *12*, 2175–2187. [CrossRef]
22. Abas, L.; Benjamins, R.; Malenica, N.; Paciorek, T.T.; Wiřniewska, J.; Moulinier-Anzola, J.C.; Sieberer, T.; Friml, J.; Luschnig, C. Intracellular trafficking and proteolysis of the *Arabidopsis* auxin-efflux facilitator PIN2 are involved in root gravitropism. *Nat. Cell Biol.* **2006**, *8*, 249–256. [CrossRef]
23. Rashotte, A.M.; Brady, S.R.; Reed, R.C.; Ante, S.J.; Muday, G.K. Basipetal auxin transport is required for gravitropism in roots of *Arabidopsis*. *Plant Physiol.* **2000**, *122*, 481–490. [CrossRef]
24. Herranz, R.; Anken, R.; Boonstra, J.; Braun, M.; Christianen, P.C.M.; De Geest, M.; Hauslage, J.; Hilbig, R.; Hill, R.J.A.; Lebert, M.; et al. Ground-based facilities for simulation of microgravity: Organism-specific recommendations for their use, and recommended terminology. *Astrobiology* **2013**, *13*, 1–17. [CrossRef] [PubMed]
25. Knight, T.A. On the direction of the radicle and germen during the vegetation of seeds. *Philos. Trans. R. Soc. Lond.* **1806**, *96*, 99–108.
26. Hawker, L.E. A quantitative study of the geotropism of seedlings with special reference to the nature and development of their statolith apparatus. *Ann. Bot.* **1932**, *os-46*, 121–157. [CrossRef]
27. von Sachs, J. Über Ausschliessung der geotropischen und heliotropischen Krümmungen wärend des Wachsthums. *Würzburg Arb* **1879**, *2*, 209–225.
28. Ciesielski, T. Untersuchungen über die Abwärtskrümmung der Wurzel. *Beitraege Zur Biol Der Pflanz* **1872**, *1*, 1–31.

29. Moseyko, N.; Zhu, T.; Chang, H.S.; Wang, X.; Feldman, L.J. Transcription profiling of the early gravitropic response in *Arabidopsis* using high-density oligonucleotide probe microarrays. *Plant Physiol.* **2002**, *130*, 720–728. [CrossRef]
30. Dedolph, R.R.; Dipert, M.H. The physical basis of gravity stimulus nullification by clinostat rotation. *Plant Physiol.* **1971**, *47*, 756–764. [CrossRef] [PubMed]
31. Wang, H.; Li, X.; Krause, L.; Görög, M.; Schüler, O.; Hauslage, J.; Hemmersbach, R.; Kircher, S.; Lasok, H.; Haser, T.; et al. 2-D Clinostat for simulated microgravity experiments with *Arabidopsis* seedlings. *Microgravity Sci. Technol.* **2016**, *28*, 59–66. [CrossRef]
32. Boucheron-Dubuisson, E.; Manzano, A.I.; Le Disquet, I.; Matia, I.; Saez-Vasquez, J.; van Loon, J.J.W.A.; Herranz, R.; Carnero-Diaz, E.; Medina, F.J. Functional alterations of root meristematic cells of *Arabidopsis thaliana* induced by a simulated microgravity environment. *J. Plant Physiol.* **2016**, *207*, 30–41. [CrossRef]
33. Deng, C.; Wang, T.; Wu, J.; Xu, W.; Li, H.; Liu, M.; Wu, L.; Lu, J.; Bian, B. Effect of modeled microgravity on radiation-induced adaptive response of root growth in *Arabidopsis thaliana*. *Mutat Res.* **2017**, *796*, 20–28. [CrossRef] [PubMed]
34. Polinski, E.; Schueler, O.; Krause, L.; Wimmer, M.A.; Hemmersbach, R.; Goldbach, H.E. 2-D clinorotation alters the uptake of some nutrients in *Arabidopsis thaliana*. *J. Plant Physiol.* **2017**, *212*, 54–57. [CrossRef] [PubMed]
35. Schüler, O.; Krause, L.; Görög, M.; Hauslage, J.; Kesseler, L.; Böhmer, M.; Hemmersbach, R. ARADISH—Development of a standardized plant growth chamber for experiments in gravitational biology using ground based facilities. *Microgravity Sci. Technol.* **2016**, *28*, 297–305. [CrossRef]
36. Lorenzi, G.; Perbal, G. Root growth and statocyte polarity in lentil seedling roots grown in microgravity or on a slowly rotating clinostat. *Physiol. Plant.* **1990**, *78*, 532–537. [CrossRef]
37. Kuznetsov, O.A.; Hasenstein, K.H. Intracellular magnetophoresis of Amyloplasts and induction of root curvature. *Planta* **1996**, *198*, 87–94. [CrossRef]
38. John, S.P.; Hasenstein, K.H. Effects of mechanostimulation on gravitropism and signal persistence in flax roots. *Plant Signal. Behav* **2011**, *6*, 1365–1370. [CrossRef]
39. Dümmer, M.; Forreiter, C.; Galland, P. Gravitropism in *Arabidopsis thaliana*: Root-specific action of the EHB gene and violation of the resultant law. *J. Plant Physiol.* **2015**, *189*, 24–33. [CrossRef]
40. Villacampa, A.; Sora, L.; Medina, J.F.; Ciska, M. Optimal clinorotation settings for microgravity simulation in A. thaliana seedlings. In Proceedings of the 69th International Astronautical Congress (IAC), Bremen, Germany, 1–5 October 2018.
41. Shen-Miller, J.; Hinchman, R.; Gordon, S.A. Thresholds for georesponse to acceleration in gravity-compensated avena seedlings. *Plant Physiol.* **1968**, *43*, 338–344. [CrossRef]
42. Driss-Ecole, D.; Legué, V.; Carnero-Diaz, E.; Perbal, G. Gravisensitivity and automorphogenesis of lentil seedling roots grown on board the International Space Station. *Physiol. Plant.* **2008**, *134*, 191–201. [CrossRef]
43. Limbach, C.; Hauslage, J.; Schäfer, C.; Braun, M. How to activate a plant gravireceptor. Early mechanisms of gravity sensing studied in characean rhizoids during parabolic flights. *Plant Physiol.* **2005**, *139*, 1030–1040. [CrossRef] [PubMed]
44. Grabov, A.; Ashley, M.K.; Rigas, S.; Hatzopoulos, P.; Dolan, L.; Vicente-Agullo, F. Morphometric analysis of root shape. *New Phytol.* **2005**, *165*, 641–651. [CrossRef]
45. Doyle, S.M.; Rigal, A.; Grones, P.; Karady, M.; Barange, D.K.; Majda, M.; Pařízková, B.; Karampelias, M.; Zwiewka, M.; Pěnčík, A.; et al. A role for the auxin precursor anthranilic acid in root gravitropism via regulation of PIN-FORMED protein polarity and relocalisation in *Arabidopsis*. *New Phytol.* **2019**, *223*, 1420–1432. [CrossRef]
46. Feraru, E.; Feraru, M.I.; Kleine-Vehn, J.; Martinière, A.; Mouille, G.; Vanneste, S.; Vernhettes, S.; Runions, J.; Friml, J. PIN polarity maintenance by the cell wall in *Arabidopsis*. *Curr. Biol.* **2011**, *21*, 338–343. [CrossRef] [PubMed]
47. Xuan, W.; Audenaert, D.; Parizot, B.; Möller, B.K.; Njo, M.F.; De Rybel, B.; Van Isterdael, G.; Mähönen, A.P.; Vanneste, S.; Beeckman, T. Root cap-derived auxin pre-patterns the longitudinal axis of the *Arabidopsis* root. *Curr. Biol.* **2015**, *25*, 1381–1388. [CrossRef]
48. Zemová, R.; Zwiewka, M.; Bielach, A.; Robert, H.S.; Friml, J. A forward genetic screen for new regulators of auxin-mediated degradation of auxin transport proteins in *Arabidopsis thaliana*. *J. Plant Growth Regul.* **2016**, *35*, 465–476. [CrossRef]
49. Smith, J.D.; Todd, P.; Andrew Staehelin, L. Modulation of statolith mass and grouping in white clover (*Trifolium repens*) grown in 1-g, microgravity and on the clinostat. *Plant J.* **1997**, *12*, 1361–1373. [CrossRef]
50. Ding, Z.; Friml, J. Auxin regulates distal stem cell differentiation in *Arabidopsis* roots. *Proc. Natl. Acad. Sci. USA* **2010**, *107*, 12046. [CrossRef] [PubMed]
51. Barbez, E.; Dünser, K.; Gaidora, A.; Lendl, T.; Busch, W. Auxin steers root cell expansion via apoplastic pH regulation in *Arabidopsis thaliana*. *Proc. Natl. Acad. Sci. USA* **2017**, *114*, E4884–E4893. [CrossRef] [PubMed]
52. Swarup, R.; Kramer, E.M.; Perry, P.; Knox, K.; Leyser, H.M.O.; Haseloff, J.; Beemster, G.T.S.; Bhalerao, R.; Bennett, M.J. Root gravitropism requires lateral root cap and epidermal cells for transport and response to a mobile auxin signal. *Nat. Cell Biol.* **2005**, *7*, 1057–1065. [CrossRef] [PubMed]
53. Rahman, A.; Bannigan, A.; Sulaman, W.; Priit, P.; Blancaflor, E.B.; Baskin, T.I. Auxin, actin and growth of the *Arabidopsis thaliana* primary root. *Plant J.* **2007**, *50*, 514–528. [CrossRef] [PubMed]
54. Ulmasov, T.; Murfett, J.; Hagen, G.; Guilfoyle, T.J. Aux/IAA proteins repress expression of reporter genes containing natural and highly active synthetic auxin response elements. *Plant Cell* **1997**, *9*, 1963–1971. [PubMed]
55. Sabatini, S.; Beis, D.; Wolkenfelt, H.; Murfett, J.; Guilfoyle, T.; Malamy, J.; Benfey, P.; Leyser, O.; Bechtold, N.; Weisbeek, P.; et al. An auxin-dependent distal organizer of pattern and polarity in the Arabidopsis root. *Cell* **1999**, *99*, 463–472. [CrossRef]

56. Brunoud, G.; Wells, D.M.; Oliva, M.; Larrieu, A.; Mirabet, V.; Burrow, A.H.; Beeckman, T.; Kepinski, S.; Traas, J.; Bennett, M.J.; et al. A novel sensor to map auxin response and distribution at high spatio-temporal resolution. *Nature* **2012**, *482*, 103–106. [CrossRef] [PubMed]
57. Herranz, R.; Benguría, A.; Laván, D.A.; López-Vidriero, I.; Gasset, G.; Medina, J.F.; van Loon, J.J.W.A.; Marco, R. Spaceflight-related suboptimal conditions can accentuate the altered gravity response of *Drosophila* transcriptome. *Mol. Ecol.* **2010**, *19*, 4255–4264. [CrossRef]
58. Brungs, S.; Hauslage, J.; Hilbig, R.; Hemmersbach, R.; Anken, R. Effects of simulated weightlessness on fish otolith growth: Clinostat versus Rotating-Wall Vessel. *Adv. Sp. Res.* **2011**, *48*, 792–798. [CrossRef]
59. Thiel, C.S.; Paulsen, K.; Bradacs, G.; Lust, K.; Tauber, S.; Dumrese, C.; Hilliger, A.; Schoppmann, K.; Biskup, J.; Gölz, N.; et al. Rapid alterations of cell cycle control proteins in human T lymphocytes in microgravity. *Cell Commun. Signal.* **2012**, *10*, 1. [CrossRef]
60. Eiermann, P.; Kopp, S.; Hauslage, J.; Hemmersbach, R.; Gerzer, R.; Ivanova, K. Adaptation of a 2-D clinostat for simulated microgravity experiments with adherent cells. *Microgravity Sci. Technol.* **2013**, *25*, 153–159. [CrossRef]
61. Fischer, J.; Schoppmann, K.; Knie, M.; Laforsch, C. Responses of microcrustaceans to simulated microgravity (2D-clinorotation)—Preliminary assessments for the development of Bioregenerative Life Support Systems (BLSS). *Microgravity Sci Technol* **2016**, *28*, 337–344. [CrossRef]
62. Unruh, E.; Brungs, S.; Langer, S.; Bornemann, G.; Frett, T.; Hansen, P.D. Comprehensive study of the influence of altered gravity on the oxidative burst of mussel (*Mytilus edulis*) hemocytes. *Microgravity Sci. Technol.* **2016**, *28*, 275–285. [CrossRef]
63. Zhang, Y.; Xiao, G.; Wang, X.; Zhang, X.; Friml, J. Evolution of fast root gravitropism in seed plants. *Nat. Commun.* **2019**, *10*, 4–13. [CrossRef]
64. Hilaire, E.; Paulsen, A.Q.; Brown, C.S.; Guikema, J.A. Effects of clinorotation and microgravity on sweet clover columella cells treated with cytochalasin D. *Physiol. Plant.* **1995**, *95*, 267–273. [CrossRef] [PubMed]
65. Kozeko, L.; Kordyum, E. The stress protein level under clinorotation in context of the seedling developmental program and the stress response. *Microgravity Sci. Technol.* **2006**, *18*, 254–256. [CrossRef]
66. Matía, I.; González-Camacho, F.; Herranz, R.; Kiss, J.Z.; Gasset, G.; van Loon, J.J.W.A.; Marco, R.; Medina, F.J. Plant cell proliferation and growth are altered by microgravity conditions in spaceflight. *J. Plant Physiol.* **2010**, *167*, 184–193. [CrossRef]
67. Paul, A.L.; Sng, N.J.; Zupanska, A.K.; Krishnamurthy, A.; Schultz, E.R.; Ferl, R.J. Genetic dissection of the *Arabidopsis* spaceflight transcriptome: Are some responses dispensable for the physiological adaptation of plants to spaceflight? *PLoS ONE* **2017**, *12*, e0180186. [CrossRef] [PubMed]
68. Perbal, G.; Driss-Ecole, D. Polarity of statocytes in lentil seedling roots grown in space (Spacelab D1 Mission). *Physiol. Plant.* **1989**, *75*, 518–524. [CrossRef]
69. Smith, J.D.; Staehelin, L.A.; Todd, P. Early root cap development and graviresponse in white clover (*Trifolium repens*) grown in space and on a two-axis clinostat. *J. Plant Physiol.* **1999**, *155*, 543–550. [CrossRef]
70. Volkmann, D.; Baluska, F.; Lichtscheidl, I.; Driss-Ecole, D.; Perbal, G. Statoliths motions in gravity-perceiving plant cells: Does actomyosin counteract gravity? *FASEB J.* **1999**, *13*, S143–S147. [CrossRef]
71. Kraft, T.F.B.; Van Loon, J.J.W.A.; Kiss, J.Z. Plastid position in *Arabidopsis* columella cells is similar in microgravity and on a random-positioning machine. *Planta* **2000**, *211*, 415–422. [CrossRef]
72. Perbal, G.; Lefranc, A.; Jeune, B.; Driss-Ecole, D. Mechanotransduction in root gravity sensing cells. *Physiol. Plant.* **2004**, *120*, 303–311. [CrossRef] [PubMed]
73. Hensel, W.; Sievers, A. Effects of prolonged omnilateral gravistimulation on the ultrastructure of statocytes and on the graviresponse of roots. *Planta* **1980**, *150*, 338–346. [CrossRef] [PubMed]
74. Aarrouf, J.; Darbelley, N.; Demandre, C.; Razafindramboa, N.; Perbal, G. Effect of horizontal clinorotation on the root system development and on lipid breakdown in rapeseed (*Brassica napus*) seedlings. *Plant Cell Physiol.* **1999**, *40*, 396–405. [CrossRef] [PubMed]
75. Lyon, C.J. Choice of rotation rate for the horizontal clinostat. *Plant Physiol.* **1970**, *46*, 355–358. [CrossRef]
76. Eleftheriou, E.P.; Adamakis, I.D.S.; Panteris, E.; Fatsiou, M. Chromium-induced ultrastructural changes and oxidative stress in roots of *Arabidopsis thaliana*. *Int. J. Mol. Sci.* **2015**, *16*, 15852–15871. [CrossRef]
77. Adamakis, I.D.S.; Eleftheriou, E.P. Structural evidence of programmed cell death induction by tungsten in root tip cells of *Pisum sativum*. *Plants* **2019**, *8*, 62. [CrossRef]
78. Wu, S.; Lexy, R.O.; Xu, M.; Sang, Y.; Chen, X.; Yu, Q.; Gallagher, K.L. Symplastic signaling instructs cell division, cell expansion, and cell polarity in the ground tissue of *Arabidopsis thaliana* roots. *Proc. Natl. Acad. Sci. USA* **2016**, *113*, 11621–11626. [CrossRef]
79. Rigó, G.; Ayaydin, F.; Tietz, O.; Zsigmond, L.; Salchert, K.; Darula, Z.; Medzihradszky, K.F.; Szabados, L.; Palme, K.; Koncz, C.; et al. Inactivation of plasma membrane—Localized CDPK-RELATED KINASE5 decelerates PIN2 exocytosis and root gravitropic response in *Arabidopsis*. *Plant Cell* **2013**, *25*, 1592–1608. [CrossRef]
80. Kleine-Vehn, J.; Leitner, J.; Zwiewka, M.; Sauer, M.; Abas, L.; Luschnig, C. Differential degradation of PIN2 auxin efflux carrier by retromer-dependent vacuolar targeting. *Proc. Natl. Acad. Sci. USA* **2008**, *105*, 17812–17817. [CrossRef]
81. Fukaki, H.; Fujisawa, H.; Tasaka, M. SGR1, SGR2, and SGR3: Novel genetic loci involved in shoot gravitropism in *Arabidopsis thaliana*. *Plant Physiol.* **1996**, *110*, 945–955. [CrossRef] [PubMed]
82. Okada, K.; Shimura, Y. Reversible root tip rotation in arabidopsis seedlings induced by obstacle-touching stimulus. *Science* **1990**, *250*, 274–276. [CrossRef]

83. Simmons, C.; Migliaccio, F.; Masson, P.; Caspar, T.; Söll, D. A novel root gravitropism mutant of *Arabidopsis thaliana* exhibiting altered auxin physiology. *Physiol. Plant.* **1995**, *93*, 790–798. [CrossRef]
84. Thompson, M.V.; Holbrook, N.M. Root-gel interactions and the root waving behavior of *Arabidopsis*. *Plant Physiol.* **2004**, *135*, 1822–1837. [CrossRef]
85. Massa, G.D.; Gilroy, S. Touch modulates gravity sensing to regulate the growth of primary roots of *Arabidopsis thaliana*. *Plant. J.* **2003**, *33*, 435–445. [CrossRef] [PubMed]
86. Legué, V.; Biancaflor, E.; Wymer, C.; Perbal, G.; Fantin, D.; Gilroy, S. Cytoplasmic free Ca^{2+} in arabidopsis roots changes in response to touch but not gravity. *Plant Physiol.* **1997**, *114*, 789–800. [CrossRef] [PubMed]
87. Lee, H.J.; Kim, H.S.; Park, J.M.; Cho, H.S.; Jeon, J.H. PIN-mediated polar auxin transport facilitates root-obstacle avoidance. *New Phytol.* **2020**, *225*, 1285–1296. [CrossRef]
88. van Loon, J.J.W.A. Some history and use of the random positioning machine, RPM, in gravity related research. *Adv. Sp. Res.* **2007**, *39*, 1161–1165. [CrossRef]
89. Herranz, R.; Vandenbrink, J.P.; Villacampa, A.; Manzano, A.; Poehlman, W.L.; Feltus, F.A.; Kiss, J.Z.; Medina, F.J. RNAseq analysis of the response of *Arabidopsis thaliana* to fractional gravity under blue-light stimulation during spaceflight. *Front. Plant. Sci.* **2019**, *10*, 1529. [CrossRef] [PubMed]
90. Manzano, A.; Herranz, R.; Den Toom, L.A.; Te Slaa, S.; Borst, G.; Visser, M.; Medina, F.J.; van Loon, J.J.W.A. Novel, Moon and Mars, partial gravity simulation paradigms and their effects on the balance between cell growth and cell proliferation during early plant development. *NPJ Microgravity* **2018**, *4*, 9. [CrossRef]
91. Hilaire, E.; Peterson, B.V.; Guikema, J.A.; Brown, C.S. Clinorotation affects morphology and ethylene production in soybean seedlings. *Plant. Cell Physiol.* **1996**, *37*, 929–934. [CrossRef]
92. González-Camacho, F.; Medina, F.J. The nucleolar structure and the activity of NopA100, a nucleolin-like protein, during the cell cycle in proliferating plant cells. *Histochem. Cell Biol.* **2006**, *125*, 139–153. [CrossRef]
93. Xu, J.; Scheres, B. Dissection of *Arabidopsis* ADP-RIBOSYLATION FACTOR 1 Function in Epidermal Cell Polarity. *Plant Cell.* **2005**, *17*, 525–536. [CrossRef] [PubMed]
94. Pasternak, T.; Tietz, O.; Rapp, K.; Begheldo, M.; Nitschke, R.; Ruperti, B.; Palme, K. Protocol: An improved and universal procedure for whole-mount immunolocalization in plants. *Plant Methods* **2015**, *11*, 50. [CrossRef] [PubMed]
95. Musielak, T.J.; Schenkel, L.; Kolb, M.; Henschen, A.; Bayer, M. A simple and versatile cell wall staining protocol to study plant reproduction. *Plant Reprod.* **2015**, *28*, 161–169. [CrossRef]
96. Robert, H.S.; Grunewald, W.; Sauer, M.; Cannoot, B.; Soriano, M.; Swarup, R.; Weijers, D.; Bennett, M.; Boutilier, K.; Friml, J. Plant embryogenesis requires aux/lax-mediated auxin influx. *Development* **2015**, *142*, 702–711. [CrossRef] [PubMed]

DISCUSSION

DISCUSSION

1. Similarities between spaceflight global transcriptome studies

Real microgravity experiments are very limited. Nevertheless, platforms such as Genelab (Ray et al., 2019) allow comparisons between different experiments to find similar patterns and to establish common processes affected by spaceflight. This helps to overcome the variability between experiments caused by different hardware, duration of the experiment or biological material, and to find the common spaceflight effects. The issue of this result variability is especially clear in the example of Johnson et al., (2017) where samples grown in the same hardware (BRIC) and using similar biological materials (*A. thaliana* seedlings from different ecotypes and cell cultures) are compared. They found very little overlap in the DEG among three different studies in similar conditions.

However, there are often some similar GO categories found in different space experiments, such as elevated hypoxic response (Kwon et al., 2015; Basu et al., 2017; Johnson et al., 2017; Choi et al., 2019; Kruse et al., 2020), increased HSP expression (Zupanska et al., 2013; Basu et al., 2017; Johnson et al., 2017; Choi et al., 2019) or cell wall metabolism (Ferl et al., 2015; Johnson et al., 2017; Paul et al., 2017; Kruse et al., 2020). In our case, cell wall related alterations were found in GLDS-251 at Moon gravity level (Herranz et al., 2019). In addition, alterations of the oxidative state and hypoxic responses were also found enriched at microgravity and Mars gravity level in GLDS-314 (Villacampa et al., 2021a). Analysis in TOAST, a database which allows direct comparisons between the studies available at Genelab, confirmed some of the common effects described in different studies and highlighted affected mitochondrial function as one of the effects usually found in plant space biology (Barker et al., 2020). Therefore, the comparisons between different studies, facilitates the validation of the results.

In the SG experiments which generated two RNA-seq datasets for microgravity so far (GLDS-251 and GLDS-314) clear similarities between the experiments were established, which strongly suggest these processes are affected by this condition and highlights the good reproducibility of the SG space experiment results. This was possible thanks to the EMCS hardware advanced level, with temperature, O2, CO2 and humidity control and an ethylene removal system (Brinckmann, 2005). In addition, we have compared our results from the SG experiment with other available studies in the Genelab dataset confirming observed tendencies, which further reinforces the results and discards hardware specific effects.

Nevertheless, the knowledge on partial gravity is very limited so far. Our laboratory is a pioneer in this field as we investigated it in the SG experiments (Valbuena et al., 2018; Herranz et al., 2019; Villacampa et al., 2021a) and using different microgravity simulators with adapted settings (Manzano et al., 2012, 2018; Kamal et al., 2018), but, until now, no other studies are available in which our results can be compared.

2. Microgravity has a vast impact on the transcriptome and meristematic activity in *A. thaliana* seedlings in SG experiment

Although the two datasets of SG series with altered gravity levels (GLDS-251 and GLDS-314) present differences in applied conditions; L*er* and Col0 *A. thaliana* ecotypes, different light and gravity conditions throughout the experiment, there are two clear tendencies in microgravity condition for

both datasets: photosynthesis downregulation in red and blue light stimulated seedlings, and plastid and mitochondrial genome overexpression in all light conditions.

a. Downregulation of photosynthesis

As described in Vandenbrink et al., (2019) and Villacampa et al., (2021), photosynthesis was downregulated in microgravity in the seedlings photostimulated with blue or red light, respectively. In both cases the GO analysis showed downregulation in PSI and PSII, photosynthetic electron transport chain and chlorophyll metabolism. However, only 16 genes were commonly downregulated in the two datasets. These downregulated genes included transcripts encoding LHDB proteins (Fig. 8). This downregulation could affect stomatal closure and decrease photosynthetic activity. In addition, downregulation of these proteins has been linked to decreased tolerance to drought stress (Staneloni et al., 2008; Xu et al., 2012). Affected photosynthesis functions during spaceflight have been reported before. Reduction in PSI activity was found in *Brassica rapa* (Jiao et al., 2004), and in *Oryza sativa* (Chen et al., 2013) grown in space. In addition, structural alterations of chloroplast, affecting thylakoid membranes, were found in wheat seedlings grown in space (Stutte et al., 2006) and in pea plants grown under simulated microgravity (Mikhaylenko et al., 2001). Moreover, lower number of chloroplasts that also exhibited reduced size were found in *A. thaliana* (L.) Heynh exposed to clinorotation (Adamchuk, 1998). Reduction in chlorophyll content was also found in wheat (Rumyantseva et al., 1990) and pea seedlings in real microgravity (Laurinavichius et al., 1986) and in *Solanum lycopersicum* L. in simulated microgravity (Colla et al., 2007).

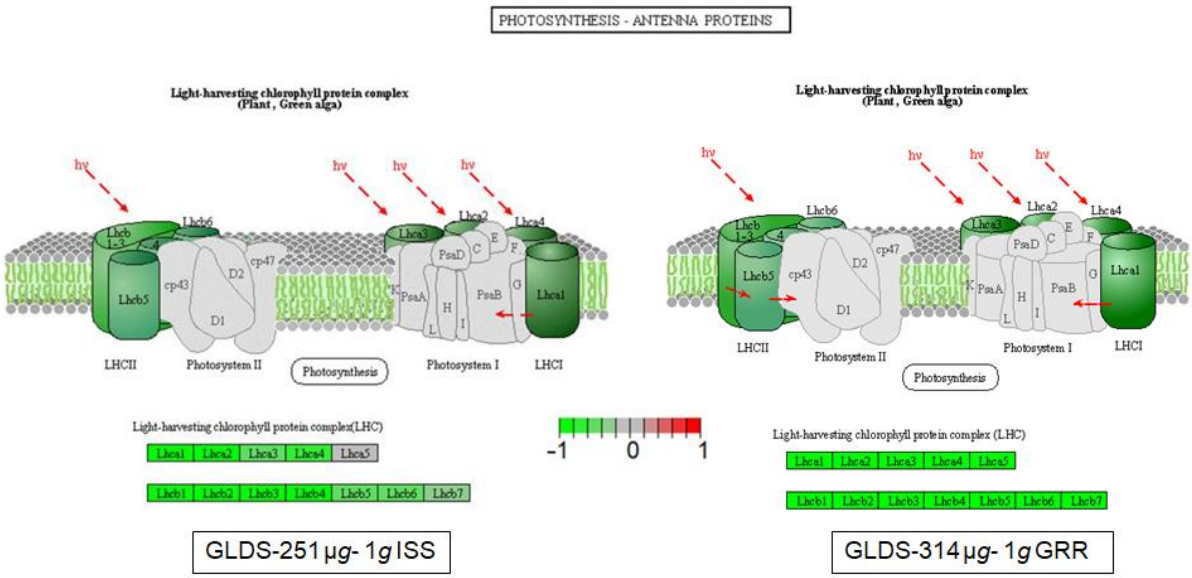

Figure 8. Common response to microgravity in GLDS-251 and GLDS-314 datasets. Modified from Vandenbrink et al., 2019. Left, GLDS-251 µ*g* compared to 1 *g* control (ISS). Right, GLDS-314 µ*g* with red light photostimulation compared to 1 *g* control (ground control). Kyoto Encyclopedia of Genes and Genomes (KEGG) pathway identifier ath00196, photosynthesis - antenna proteins.

b. Plastid and mitochondrial genome overexpression

High plastid and mitochondrial genome expression was found in microgravity in all three light conditions. This overexpression was also reported in other studies submitted to the Genelab database

(GLDS-38, GLDS-44 and GLDS-321) (Kwon et al., 2015; Kruse et al., 2020; Angelos et al., 2021). Although they were performed in different experimental hardware (BRIC) and with etiolated seedlings, the tendency was clear. In addition, affected mitochondrial function in spaceflight experiments has been reported not only in plants (Barker et al., 2020), but also in other organisms, such as *Drosophila* sp. or humans (Herranz et al., 2010; Silveira et al., 2020). The presence of this phenomenon in different studies further confirms it is a microgravity specific effect.

The majority of the chloroplast genes which are encoded in the *A. thaliana* plastid genome (around 90) (Wicke et al., 2011) are upregulated in microgravity (70 in µ*g*d, 83 µ*g*rl and 45 in µ*g* and blue light). In addition, out of the 57 mitochondrial proteins encoded in this organelle genome in *A. thaliana* (Unseld et al., 1997), we identified 10 upregulated in µ*g*d, 30 in µ*g*rl and 5 in µ*g* and blue light. There are different factors that influence plastid gene expression, such as light, temperature, plastid development or circadian clock (Leister et al., 2017). In addition, ABA represses plastid genome expression (Yamburenko et al., 2013), which is in agreement with its upregulation at Mars gravity level, where was no enrichment in plastid or mitochondrial genome expression compared to the ground control. Both organelles are sensors for cellular dysfunction caused by external stress. In fact, some of the factors involved in nucleus-organelle signaling are involved directly in response to stress (Vanlerberghe, 2013). This mechanism adjusts cell metabolism in order to adapt it to the new environment or triggers the programmed cell death (PCD) (Vanlerberghe, 2013). The general organelle genome expression in all samples exposed to microgravity suggests there is a dysregulation in the nucleus-organelle communication. There are two types of nucleus-organelle communication, anterograde, nucleus to organelle signaling, or retrograde, organelle to nucleus signaling. The dysregulation could take place in either of them, anterograde, if the nucleus response does not reach the organelles, or retrograde, if the nucleus does not perceive the upregulation of plastid and mitochondrial genome expression. Sigma factor binding protein (SIB1), which binds sigma-1 receptor (sig1R), plays a role in retrograde communication and it is downregulated in microgravity and upregulated in Mars gravity level. In addition, WRKY40, which is upregulated at Mars gravity level, is a repressor of retrograde-mediated organelle genome expression and WRKY63, which is upregulated in microgravity, is its activator (Van Aken et al., 2013). These dysregulations support the hypothesis of retrograde communication defects. The disturbed mitochondrial retrograde signaling is known to increase sensitivity to stress conditions (Meng et al., 2020). Also, retrograde signaling is involved in acclimation to flooding (Meng et al., 2020). WRKY40 and WKRY45 are part of this acclimation (Meng et al., 2020), and both are upregulated at Mars gravity. Mitochondria and WRKY40 are also involved in response to touch and wounding (Lee et al., 2005; van Aken et al., 2016). The factors involved in these responses, Outer Mitochondrial membrane protein of 66 kDa (OM66), Dicarboxylate Carrier 1 and 2 (DIC1 and DIC2), are upregulated at Mars *g* level, which suggests an activation of these routes in this condition and a lack of the response in microgravity. None of the light conditions, darkness or photostimulation with red light for the last two days, or photostimulation with blue light, are able to restore normal organelle genome expression in microgravity. However, it is corrected by applying even a low *g* level, as observed in the GLDS-251 dataset.

The relation between the downregulation of photosynthetic functions and the overexpression of the plastid genome needs to be considered. Kruse et al., 2020 proposed the plastid genome overexpression could be an attempt of the seedlings to enhance light signaling to compensate for the lack of gravity in dark grown seedlings. However, we have found this overexpression at different light

conditions and it is more pronounced in red light photostimulated seedlings than in the seedlings that were kept in the dark, which shows this effect is not exclusive of etiolated seedlings. However, the downregulation of photosynthesis functions in the seedlings with red or blue light photostimulation could be in fact a result of alterations in nuclear-organelle communication which would cause a general dysfunction of this organelle.

c. Meristematic competence

Other effects of microgravity, as shown in the GLDS-314 dataset, included an increase in cell proliferation, as shown by an increased meristem size and the number of cells in the meristem row. Also, an increase in nucleolar size in microgravity suggested increased protein production and cell growth. These increments were especially evident in plants exposed to red light photostimulation. In previous space experiments, a decoupling between cell proliferation and growth was reported (Matía et al., 2005, 2010), with an increased cell proliferation and decreased cell growth. Similar results were also obtained in simulated microgravity on an RPM (Matía et al., 2010; Manzano et al., 2018). We did not observe meristematic competence decoupling in the SG2-3 experimental conditions. In this case, both cell proliferation, as represented by meristem size and number of cells in the meristem row, and cell growth, reflected as the nucleolus area, were incremented in microgravity. In addition, ribosome biogenesis pathway was upregulated in the GLDS-251 dataset. This difference between the results in the ROOT and the SG experiments could be due to different light conditions in both experiments. In the ROOT experiment (Matía et al., 2005) and the cited simulated microgravity experiments where decoupling of proliferation and cell growth was observed (Matía et al., 2010; Manzano et al., 2018), etiolated seedlings were used, meaning they were grown in the darkness for the duration of the experiment. On the other hand, in the SG experiment, seedlings were grown under continuous white light condition for the first 4 days in SG1-2 and photoperiod for the first 4 days in SG2-3 (Fig. 5). Nevertheless, decreased nucleolar activity was found in the seedlings kept in the dark for the last two days in the SG3, which is in agreement with the observation for etiolated seedlings in the ROOT experiment.

In addition, the transcriptomic analysis of phytohormone signaling in SG3 samples, indicated an activation of proliferation promoting pathways in microgravity, such as cytokinin and auxin. Cytokinin alterations in spaceflight were reported before (Ferl and Paul, 2016), as well as auxin accumulation in simulated microgravity with diamagnetic levitation (Manzano et al., 2013).

3. Partial gravity influences the transcriptome and meristematic activity in *A. thaliana* seedlings in a different way than microgravity in Seedling Growth space experiment

Partial gravity research is even more scarce than microgravity studies. Only the results of the SG experiment and the recent germination of cotton seed on the Moon surface provide data on the plant's response to partial gravity levels so far (Herranz et al., 2019; Villacampa et al., 2021; Xie et al., 2021 (preprint)). Moreover, simulation experiments have also been performed (Manzano et al., 2012, 2018; Kamal et al., 2018). The response to different gravity levels other than microgravity is important for plant cultivation on other planets (Karoliussen et al., 2013; Medina, 2021). The use of EMCS (Brinckmann, 2005), now decommissioned, allowed us to apply different levels of *g*-force in space.

With the analysis of the two datasets, GLDS-251 and GLDS-314, we can corroborate how *A. thaliana* seedlings respond to different gravity levels. In GLDS-251, we observed that a very low gravity force (0.09 *g*) activates a more pronounced stress response in the seedlings than the microgravity itself. This could be a consequence of two tropic stimuli acting at a low magnitude in different directions, with the blue light signal perpendicular to the gravity signal. The stress is attenuated at Moon gravity level (0.18 *g*), in which the response is more related to plasma membrane organelles. On the other hand, at Mars gravity level (0.36 *g*) and reduced gravity level (0.57 *g*) there are no significant differences compared to the 1 *g* control. These results are in agreement with results in altered gravity simulators, where Moon gravity level caused similar alterations to microgravity, but samples exposed to Mars gravity level were more similar to the static control (Manzano et al., 2018).

On the other hand, in the GLDS-314 we did observe significant alterations in gene expression at Mars gravity level. The differences between the two datasets are many: ecotype, different light conditions, exposure to altered gravity for 6 (GLDS-314) or 2 days (GLDS-251), 1 *g* control in space (GLDS-251) or ground control (GLDS-314). All these aspects can explain why there are more alterations at Mars gravity level in the GLDS-314 than in the GLDS-251 dataset (Herranz et al., 2019). In the GLDS-314 dataset, Mars gravity level caused a more adaptive response than microgravity, which is in agreement with the GLDS-251 results, where Mars gravity level had showed less stress responses than microgravity, low *g* or Moon gravity level. In the images of the seedlings in the cassettes in Villacampa et al., (2021a), we observed that Mars gravity level was enough to direct seedlings growth downward, similar to the direction in 1 *g* control. In addition, transcriptomic phytohormone pathway analysis showed activation of the routes related to abiotic stress response, such as ABA and ethylene signaling pathways. These routes are involved in the response to osmotic stress, which is a common dysregulated category in space experiments (Kruse et al., 2020). The reason behind the activation of osmotic stress response in spaceflight is not completely understood, but it has been suggested it could be due to an attempt of the seedlings to compensate for the lack of structural guide with the stabilization of microtubules (Ban et al., 2013; Kruse et al., 2020).

In addition, the upregulation of WRKY TFs in both light conditions at Mars gravity level shows that adaptive mechanisms were activated. WRKYs are one of the biggest TF families in flowering plants and many of their members have been reported to be involved in both abiotic and biotic stress responses, Jasmonic acid (JA) and SA signaling (Schluttenhofer et al., 2014; Zhang et al., 2017), as well as acclimation processes (reviewed in Phukan et al., 2016). Most WRKYs are multifunctional TFs, containing different domains. This makes them good targets for engineering more resistant crops. In fact, overexpression of OsWRKY30/70 produced drought resistant rice (Shen et al., 2012), which could be implemented for space farming. There was also an enrichment of NAC TFs in upregulated DEGs at Mars gravity level, which could suggest a transcriptional adaptive response to the new environment.

4. Blue and red light photostimulation modulate *A. thalina* seedlings´ response to microgravity and partial gravity

Red light is perceived by phytochromes, which are expressed in different zones of the root (reviewed in Mo et al., 2015). PhyA and PhyB, expressed in the root tip, are implicated in red light root phototropism and gravitropism (Kiss et al., 2003; Correll and Kiss, 2005). Red light induces root positive phototropism, which is usually masked by gravitropism but was found in agravitropic mutants (Ruppel et al., 2001) and is mediated by PhyB (Kiss et al., 2003). In space, shoot phototropism in response to

red light was discovered using the EMCS hardware in the TROPI space experiment (Millar et al., 2010). Moreover, a correlation between red light positive root phototropism and the gravity level was discovered, as a part of the SG experiment (Vandenbrink et al., 2016), where the phototropic response was increased when the gravity level decreased.

In the ground control samples, the transcriptomic analysis showed that red light photostimulation for the last two days had a positive effect on the physiological status of the seedlings compared with the seedlings that were kept in the dark (Manzano et al., 2020b). However, there was no significant difference in the quantifications of anatomic features, such as meristem and nucleolus size, between photostimulated and not photostimulated seedlings in the ground control samples (Villacampa et al., 2021a). In spaceflight, the analysis of meristem size and number of cells in the meristem row indicates red light increases both parameters in microgravity and at Mars gravity level, compared to the seedlings that were kept in the dark (Villacampa et al., 2021a). Moreover, the same tendency was found in the nucleolus size. Similar results were obtained before in simulated microgravity experiments (Valbuena et al., 2018). Even though the difference in nucleolus size was not statistically significant between red light photostimulated and samples kept in the darkness, the increased nucleolar activity in red light photostimulated seedlings was confirmed by the analysis of the nucleolar ultrastructure. The transcriptomic data also confirm that, in microgravity, red light promotes cell cycle and proliferation upregulation, which is in agreement with the known effects of red light, of promoting cell proliferation and ribosome biogenesis (Reichler et al., 2001). In conclusion, red light could help to overcome some of the previously reported deleterious effects of space environment on plant development.

On the other hand, blue light induces positive phototropism in shoots and negative phototropism in roots on Earth (Kutschera and Briggs, 2012; Liscum et al., 2014). However, as a part of the SG experiment, a blue light root positive phototropism in space was discovered (Vandenbrink et al., 2016). This phototropism did not have a correlation with the gravity level, in contrast to the red light phototropism (Vandenbrink et al., 2016), where the phototropic root growth was more pronounced when the gravity decreased. Blue light positive phototropism was clearly observed only in the samples exposed to microgravity, and it was greatly reduced at low *g* gravity level. The discovery of the blue light positive phototropism was a surprise, as blue light has usually a negative effect on root growth (Silva-Navas et al., 2015, 2016) and can be reckoned as a stress condition for root.

This influences the results presented in Vandenbrink et al., 2019 and Herranz et al., 2019. The seedlings in these studies were photostimulated with blue light. The results from the different gravity levels show that the low *g* condition had more DEGs and they were related to stress responses. One possible explanation for this enhanced stress response compared to microgravity or Moon gravity could be the lack of direction of these seedlings by either the blue light root phototropism or by gravity, given that both would be very low to activate a tropic response and they act in different directions. The number of DEGs at the Moon gravity level was similar to microgravity. In the case of the Moon gravity level the gravitropic signal is more pronounced than in microgravity or at low *g* level, even if the phototropic response is almost nonexistent.

5. Transcriptional baseline of nucleolin mutants in the SG conditions on the ground

Ground controls are an essential part of the spaceflight experiments. Comparison of the space samples to ground experiment provides a global view on the impact of the spaceflight that include not only

microgravity, but also factors such as radiation (Micco et al., 2011). Even though the EMCS hardware on the ISS allowed us to obtain a 1 *g* control in space, as in the GLDS-251 dataset, we found ground control crucial for analysis of our data.

SG experiment included two mutant lines deficient in nucleolins (*At*NUC1 and *At*NUC2), proteins involved in ribosome biogenesis among other functions (Pontvianne et al., 2007; Durut et al., 2014). NUC2 is not expressed under normal conditions, it has only been described in *nuc1-2* mutant (Durut et al., 2014) or under environmental stress (Huang et al., 2018; Cheong et al., 2021). The involvement of NUC2 in stress response is in agreement with the gene elements analysis, *NUC2* gene presents cis-acting elements related to biotic and abiotic stress responses, such as a Heat Shock Element (HSE) (Durut et al., 2019). As the first step to analyze nucleolin mutants´ response to space environment, it was important to study the response of both, *nuc1-2* and *nuc2-2* to the experimental conditions in ground control, and to determine how red light influences each of them compared to the WT.

This study has helped us in the understanding of how the two nucleolin mutants responded to red light photostimulation or a stress condition such as darkness. Red light upregulated photosynthesis, cell wall modification, drug metabolism, pathogenesis and biotic stress responses in the three genotypes (WT, *nuc1-2* and *nuc2-2)*. In addition, it downregulated different abiotic stress responses, such as temperature, hypoxia, light, ABA, oxidative stress or circadian rhythm. Some of these processes are usually upregulated in space experiments, especially hypoxia and oxidative stress (Paul et al., 2001; Correll et al., 2013; Sugimoto et al., 2014; Kwon et al., 2015; Zhang et al., 2015; Johnson et al., 2017; Choi et al., 2019; Kruse et al., 2020), which already suggests red light photostimulation can be beneficial to plants in space, as confirmed in (Villacampa et al., 2021a). These up and down regulated processes, common to all three genotypes in response to red light, suggest nucleolins are not directly involved in the seedlings' response to red light. However, a number of common GO categories were upregulated in WT and *nuc2-2* genotypes. The DEGs common for both were involved in biosynthetic processes (ketone, cutin, small molecule), photosystem II and response to cold. This suggests NUC1 is necessary for the red light activation of these processes. Interestingly, there was also a common response in WT and *nuc1-2* genotypes, which includes a downregulation of response to karritin, cold acclimation and hormone metabolism, which suggests NUC2 might be involved in this response (Pontvianne et al., 2007).

When comparing the three genotypes in the same light conditions, *nuc2-2* was similar to the WT, whereas *nuc1-2* had many differences in comparison to both WT and *nuc2-2* in the seedlings that were kept in the dark for the last two days. These differences in *nuc1-2* were reduced to half under red light photostimulation. This result suggests NUC2 protein is not able to restore NUC1 functions, but red light photostimulation partially counteracts the adverse effects of darkness and NUC1 deficiency.

When we compared the two mutants; *nuc1-2* vs *nuc2-2* photostimulated with red light, the strongest enrichment in upregulated GO categories was the ribosome biogenesis. It is important to note, that alterations in this process have been reported in space experiments (Matía et al., 2010; Ferl et al., 2015; Vandenbrink et al., 2019a; Angelos et al., 2021). Our results confirm the implication of NUC2 in ribosome biogenesis promotion during red light photostimulation. This is in agreement with the previous reports, which confirmed red light enhances cell proliferation and ribosome biogenesis (Reichler et al., 2001). Taking into account our results, we suggest the use of NUC2 overexpressing line together with exposure to red light may help seedlings to overcome some of the deleterious effects of spaceflight.

This analysis of the nucleolin mutants in the space experimental conditions is the initial step in the analysis of the implication of nucleolin in the response to spaceflight in microgravity and at Mars gravity level, as part of the Seedling Growth experiment (SG2 and SG3). In Fig. 9, we can observe a Principal Component Analysis (PCA) which includes the three genotype samples (WT (Col0), *nuc1-2* and *nuc2-2*) exposed to three gravity levels (microgravity, Mars *g* and ground control) and two light conditions: red light photostimulation or kept darkness for the last two days. We can already appreciate some interesting results, as PC1 clear separation according to light. On the other hand, genotype or gravity seem to have a lower impact on the samples. This is in agreement with the results in Manzano et al., (2020b) and Villacampa et al., (2021a).

Figure 9. Principal Component Analysis (PCA) of SG2-3 samples. PCA of WT, *nuc1-2* and *nuc2-2* in three levels of gravity (microgravity (µg), Mars *g* or ground control) and two light conditions (red light photostimulation or darkness).

6. Application and limitations of microgravity simulation

High cost and low availability highly limit real microgravity experiments and create a necessity to perform microgravity simulation experiments on Earth, in order to expand the microgravity research and simplify the logistics. There are different tools for microgravity simulation, but the 2D-clinostat is the most common and accessible simulation tool.

Clinostats have been in use since the XIX century (Knight, 1806) but up to this moment no set of rules concerning its use and the best method for microgravity simulation have been established. Previously, we created a theoretical model which considers the statocyte and the statolith sizes and statolith and cytoplasm densities, to calculate the time that takes for a statolith to travel from the center of the statocytes to the plasma membrane where gravitropic response is triggered at a given clinorotation speed (Villacampa et al., 2018). It is important to highlight that this model applies to microgravity simulation in seedlings and is based on the statolith gravity perception model (Sack et al., 1986).

Different models, based on particular gravity perception mechanisms should be developed for *in vitro* cultures or animals.

Fast clinorotation (60 rpm) is often used in experiments with seedlings (Schüler et al., 2016; Wang et al., 2016; Polinski et al., 2017). According to our theoretical model, this setting would only be valid for a very limited time or distance from the center of rotation (Villacampa et al., 2018). In the results of root growth direction presented in Villacampa et al., (2021b), all clinorotation settings were able to avoid the root growth towards the gravity vector. However, we observed that the root angle of fast clinorotated seedlings, in both vertical and horizontal clinorotation, depends on the position of the seedling in the Petri dish. This result proves the direction of the centrifugal force was perceived by the seedlings. On the other hand, slow clinorotation resulted in non-directional growth, similar to the pattern observed in real microgravity experiments (Matía et al., 2010; Paul et al., 2017). Also, a dispersed pattern of statoliths in the columella cells was observed in DIC and electron microscopy images, which reinforces slow clinorotation is more suitable for microgravity simulation. In the previous studies, researchers have determined the minimal force that caused root directional growth and set it as the limit for microgravity simulation (Hensel and Sievers, 1980; Aarrouf et al., 1999; John and Hasenstein, 2011; Wang et al., 2016). This limit was 0.0001 *g* in oats clinorotated on a horizontal clinostat (Shen-Miller et al., 1968). In lentils, in the GRAVI-1 space experiment on a centrifuge, it was 0.000014 *g* (Driss-Ecole et al., 2008), whereas in *Chara globularis* rhizoids during a parabolic flight it was 0.05 *g* (Limbach et al., 2005). In our case, at slow clinorotation (1 rpm), the centrifugal force at the limit radius (4.5 cm) was 0.00005 *g* (Fig. 10a), which is below most of the reported thresholds and did not trigger directional growth (Fig. 10a). At fast clinorotation (60 rpm), however, the force at the 4.5 cm radius was 0.18 *g* (Fig. 10b), and triggered directional root growth even at close distances from the center (1 - 2 cm, 0.04 - 0.08 *g*) (Fig. 10b).

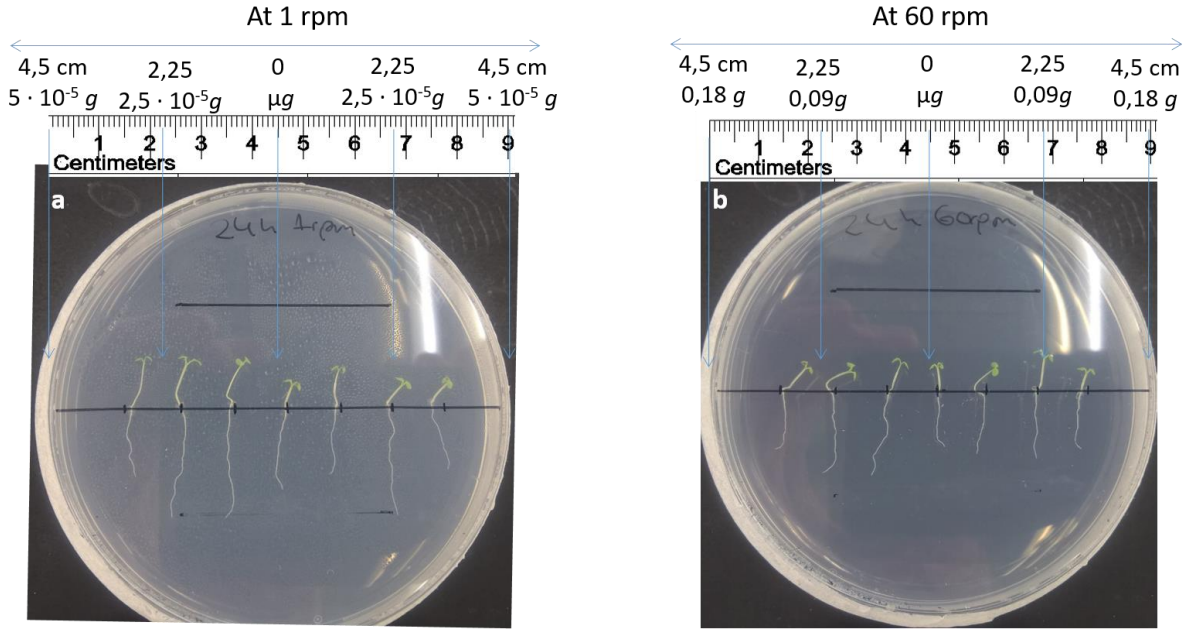

Figure 10. Theoretical forces under slow or fast clinorotation in a 2D-clinostat and real examples. a) Left, slow clinorotation at 1 rpm. Right, fast clinorotation at 60 rpm. b) Image from seedlings after 24 h of slow vertical clinorotation. c) Image from seedlings after 24 h of fast vertical clinorotation. Modified from Herranz et al., 2021 (in press).

Taking into account our model (Villacampa et al., 2018) and the lack of directional root growth (Villacampa et al., 2021b), we consider slow clinorotation is more suitable for microgravity simulation in *A. thaliana* seedlings than fast clinorotation. This is in agreement with other studies which established the range for optimal clinorotation speed for microgravity simulation between 0.33 and 2 rpm (Lyon, 1970; Dedolph and Dipert, 1971; John and Hasenstein, 2011). However, fast clinorotation is often used for cell cultures (Briegleb, 1992; Cogoli, 1992; Babbick et al., 2007; Barjaktarović et al., 2007; Aleshcheva et al., 2016; Warnke et al., 2016). In this case, fast rotation applied on cells in suspension, keeps the movement of the cells due to rotation in the range of Brownian motion. Therefore, the gravity effects on cells are practically removed (reviewed in Kiss et al., 2019). In this case, our model for seedlings would not apply.

On the other hand, researchers have reported before horizontal and vertical clinorotation produce different outcomes (Lorenzi and Perbal, 1990; John and Hasenstein, 2011). John and Hasenstein, (2011) demonstrated that horizontal slow clinorotation is less effective in nullifying gravitropic signals than vertical slow clinorotation. Lorenzi and Perbal, (1990) found the position of the nucleus was similar to real microgravity in vertical clinorotated seedlings. In our case, we observed structural alterations in statocytes and PIN2 internalization in horizontal clinorotation only, especially in the slowly clinorotated seedlings. Similar stress responses in horizontal clinorotation have been reported before (Hensel and Sievers, 1980; Smith et al., 1997, 1999; Kozeko and Kordyum, 2006). Heat shock proteins HSP70 and HSP90, were increased after 3 days of horizontal clinorotation of *P. sativum* seedlings (Kozeko and Kordyum, 2006). Ultrastructural alterations of statocytes, similar to the ones we have observed, were described in *Lepidium sativum* seedlings horizontally clinorotated for 20 h (Hensel and Sievers, 1980). Other results on 3D-clinostats, where both vertical and horizontal rotation are applied to the sample, also showed columella degradation and irregular cell walls in white clover seedlings, which was not observed in real microgravity (Olsen et al., 1984; Smith et al., 1999). In addition, the alterations in the ultrastructure of statocytes, similar to the ones we have observed, were reported for abiotic stresses (Chromium and tungsten) in *A. thaliana* and *Pisum sativum* seedlings (Eleftheriou et al., 2015; Adamakis and Eleftheriou, 2019).

The reason why horizontal clinorotation induces a stress response is not well understood. Our hypothesis is that horizontal clinorotation may induce a thigmotropic response. When seedlings are rotated vertically, the centrifugal force acts along the agar surface throughout the duration of the experiment. However, when the seedlings are rotated horizontally, the position of the Petri dish with respect to the gravity vector constantly changes, and the centrifugal force acts towards the agar, when seedlings are above the surface, or the empty side of the Petri dish, when the seedlings are below the surface, during the cycle. In result the Petri dish is tilted at different angles during the rotating cycle. Alterations in growth patterns, such as coiling, waving and skewing (Okada and Shimura, 1990; Simmons et al., 1995; Thompson and Holbrook, 2004), are observed when seedlings grow on a tilted surface. The reason for altered growth, could rely on the seedling perceiving the agar surface as an obstacle when the gravity vector acts toward that direction, which would activate the obstacle avoidance mechanism in the columella (Legué et al., 1997; Massa and Gilroy, 2003). The first bending of the root during this mechanism occurs after approximately 20 minutes of the contact with the obstacle (Lee et al., 2020). In the case of gravitropic root bending, the asymmetrical growth takes place 3 h after the stimulus (Rashotte et al., 2000; Zhang et al., 2019), which makes the thigmotropic reaction faster than the gravitropic response. This is in agreement with the more pronounced stress response in the Horizontal Slow Clinorotation (HSC) seedlings in comparison to the Horizontal Fast

Clinorotation (HFC). In HSC, each cycle (1 minute) would activate the obstacle avoidance mechanism when the agar is on lower side of the Petri dish according to the gravity vector, which would lead to an accumulation of mechanical stimuli and stress response. However, in HFC, with much shorter cycles (1 second), the mechanical stimuli could be under the limit of perception.

In conclusion, there is no perfect microgravity simulation procedure and each experiment should be adapted upon the biological material of the study. In our case of study, 2D-clinostat microgravity simulation applied on seedlings**,** it is clear different responses took place in regard with the orientation of the sample relative to the axis of rotation. The results suggest horizontal clinorotation produces higher mechanostimulation on the seedlings, independent of the seedling's response to microgravity. In addition, fast clinorotation produced a clear directional growth. Therefore, vertical slow clinorotation is the most proper microgravity simulation procedure in our system. The results presented here help to uniform the settings in 2D-clinostat studies on seedlings, which, finally, promote more reproducible and comparable results.

CONCLUSIONS

CONCLUSIONS

1. **Microgravity downregulates photosynthesis function.** Microgravity altered photosynthesis function in the two datasets included in this work (GLDS-251 and GLDS-314). The downregulation affected light harvesting antenna proteins, as well as chlorophyll biosynthesis. In the long term, this decline in the photosynthesis function could implicate an energy deficit which would affect plant development in microgravity.

2. **Microgravity disrupts nucleus-organelle communication, which results in plastid and mitochondrial genome overexpression.** In the two datasets (GLDS-251 and GLDS-314) and the three light conditions (darkness, red light or blue light photostimulation), the plastid and mitochondrial genome was overexpressed compared to the 1 *g* controls. This effect was further confirmed in other studies available in the Genelab database. The overexpression of organelle genomes implicates high energetic cost, which, together with the reduction in photosynthesis function, could affect plant development in the long-term.

3. **Mars gravity level promotes an adaptive response to the space environment not found in microgravity.** At Mars gravity level, in the GLDS-314 dataset, phytohormone signaling showed ABA, ethylene and SA pathways were activated, which, together with WRKY and NAC TFs enhanced expression at this gravity level, shows a specific response to the environment not present in microgravity. This specific response shows activation of signaling routes associated with acclimation to new environmental conditions. Moreover, the TFs expression associated with this adaptive response could be used as a possible target for the production of space adapted crop cultivation.

4. **Different gravity levels produce differential responses: very low *g*-levels (e.g. 0.09 *g*) have higher impact on transcriptome than microgravity.** In the GLDS-251 dataset, where we compared transcriptomic responses at 5 different gravity levels, the intermediate gravity level between microgravity and Moon gravity level (0.18 *g*), had the highest impact on gene expression compared to the ground control, with upregulated GO categories associated with a general stress response, such as response to chemical stimuli or response to stress.

5. **Red light facilitates adaptive response to spaceflight.** Red light photostimulation resulted in an increase in meristem and nucleolus sizes, as well as more active nucleoli, as observed by the microscopic analysis of SG3 samples. Moreover, gene expression analysis showed red light photostimulation enhanced the adaptive response at Mars gravity level. Taking all together, red light photostimulation in space helps to overcome some of the defects in plant development found in space, and it could be applied in plant cultivation for better adaptation to the environment in future missions.

6. **Nucleolin mutants respond differently to red light photostimulation. NUC2 overexpression and red light might help to overcome the ribosome biogenesis defects found in spaceflight.** The transcriptomic analysis of *nuc1-2* and *nuc2-2* mutants compared to the WT in the ground control of SG2-3 experiment showed NUC2 is involved in the response to red light. In addition, red light corrected some of the defects present in the *nuc1-2* mutant line. These results will help in the analysis of the nucleolin deficient mutant lines in space. In addition, this study highlights the importance of proper ground controls in space biology experiments.

7. **Vertical slow clinorotation is the most suitable setting for microgravity simulation applied on seedlings in a 2D-clinostat.** After testing two orientations of the sample in respect to the rotation axis (vertical and horizontal) and two speeds commonly used in the literature (1 and 60 rpm), we conclude slow vertical clinorotation is the most suitable for microgravity simulation, since fast clinorotation clearly produces directional growth towards the centrifugal force direction, and horizontal clinorotation produces a stress response which does not represent real microgravity response. Proper microgravity simulation will improve the uniformity and reproducibility between different studies and provide more reliable results.

CONCLUSIONES

CONCLUSIONES

1. **La microgravedad regula negativamente la función de la fotosíntesis**. La microgravedad alteró la función de la fotosíntesis en los dos conjuntos de datos transcriptómicos incluidos en este trabajo (GLDS-251 y GLDS-314). La bajada en la transcripción afectó a las proteínas de la antena de captación de luz, así como a la biosíntesis de clorofila. A largo plazo, esta disminución de la función de la fotosíntesis podría implicar un déficit energético que afectaría el desarrollo de las plantas en microgravedad.

2. **La microgravedad interrumpe la comunicación núcleo-orgánulo, lo que da como resultado una sobreexpresión del genoma mitocondrial y plastídico**. En los dos conjuntos de datos (GLDS-251 y GLDS-314) y las tres condiciones de luz (oscuridad, fotoestimulatión con luz roja o con luz azul), el genoma mitocondrial y del plástido se sobreexpresó en comparación con los controles 1 *g*. Este efecto se confirmó además en otros estudios disponibles en la base de datos de Genelab. La sobreexpresión de los genomas de los orgánulos implica un alto coste energético que, junto con la reducción de la función de fotosíntesis, podría afectar el desarrollo de la planta a largo plazo.

3. **El nivel de gravedad de Marte promueve una respuesta adaptativa al entorno espacial que no se encuentra en la microgravedad**. A nivel de gravedad de Marte, en el conjunto de datos GLDS-314, la señalización de fitohormonas mostró que se activaron las vías de ABA, etileno y SA, que, junto con el aumento en la expresión de los factores de transcripción WRKY y NAC, muestran una respuesta específica a la gravedad alterada que no está presente en microgravedad. Esta respuesta específica muestra la activación de rutas de señalización asociadas con la aclimatación a nuevas condiciones ambientales. Además, la expresión de TF asociada con esta respuesta adaptativa podría usarse como un posible objetivo para la producción de cultivos adaptados al espacio.

4. **Los diferentes niveles de gravedad producen respuestas diferenciales: niveles de gravedad muy bajos (por ejemplo, 0,09 *g*) tienen un mayor impacto en el transcriptoma que la microgravedad**. En el conjunto de datos GLDS-251, donde comparamos las respuestas transcriptómicas en 5 niveles de gravedad diferentes, el nivel de gravedad intermedio entre la microgravedad y el nivel de gravedad de la Luna (0,18 *g*), tuvo el mayor impacto en la expresión génica en comparación con el control terrestre, con categorías GO sobrerrepresentadas asociadas con una respuesta de estrés general, como la respuesta a estímulos químicos o la respuesta al estrés.

5. **La luz roja facilita la respuesta adaptativa a los vuelos espaciales**. La fotoestimulación con luz roja dio como resultado un aumento en los tamaños de los meristemos y nucléolos, así como nucléolos más activos, como se observó en el análisis microscópico de muestras de SG3. Además, el análisis de la expresión genética mostró que la fotoestimulación con luz roja mejoró la respuesta adaptativa en el nivel de gravedad de Marte. En conjunto, la fotoestimulación con luz roja en el espacio ayuda a superar algunos de los defectos en el

desarrollo de las plantas que se encuentran en el espacio, y podría aplicarse en el cultivo de plantas para una mejor adaptación al ambiente espacial en futuras misiones.

6. **Los mutantes de nucleolina responden de manera diferente a la fotoestimulación con luz roja**. La sobreexpresión de NUC2 y la luz roja podrían ayudar a superar los defectos de la biogénesis del ribosoma que se encuentran en las plantas cultivadas en el espacio. El análisis transcriptómico de los mutantes *nuc1-2* y *nuc2-2* en comparación con el WT en el control en Tierra del experimento SG2-3 mostró que NUC2 está involucrado en la respuesta a la luz roja. Además, la luz roja corrigió algunos de los defectos presentes en la línea mutante *nuc1-2*. Estos resultados ayudarán en el análisis de las líneas mutantes deficientes en nucleolina en el espacio. Además, este estudio destaca la importancia de los controles en Tierra en los experimentos de biología espacial.

7. **La clinorotación vertical lenta es la condición más adecuada para la simulación de microgravedad aplicada a plántulas en un clinostato 2D**. Después de probar dos orientaciones de la muestra con respecto al eje de rotación (vertical y horizontal) y dos velocidades comúnmente utilizadas en el uso del clinostato (1 y 60 rpm), concluimos que la clinorrotación vertical lenta es la más adecuada para la simulación de microgravedad, ya que la clinorrotación rápida claramente produce un crecimiento direccional hacia la dirección de la fuerza centrífuga y la clinorrotación horizontal produce una respuesta de estrés que no representa una respuesta de microgravedad real. Una simulación de microgravedad adecuada mejorará la uniformidad y la reproducibilidad entre diferentes estudios y proporcionará resultados más fiables.

ACRONYMS AND ABBREVIATIONS

Acronyms and abbreviations

ABA: Abscisic acid

AOBS: Acousto Optical Beam Splitter

APH: Advanced Plant Habitat

BRIC: Biological Research in Canisters

BSA: Bovine serum albumin

DAPI: 2-(4-amidinophenyl)-1H -indole-6-carboxamidine

DEG: Differentially Expressed Gene

DFC: Dense Fibrillar Component

DIC: Differential Interference Contrast microscopy

DIC1: Dicarboxylate Carrier 1

DIC2: Dicarboxylate Carrier 2

DOC: Deoxycholic acid

EMCS: European Module Cultivation System

ER: Endoplasmic Reticulum

FA: formaldehyde

FC: Fibrillar Center

GA: glutaraldehyde

GC: Granular Component

GFP: Green Fluorescence Protein

GLDS: Genelab Dataset

GO: Gene Ontology

GUS: β-glucuronidase

HFC: Horizontal Fast Clinorotation

HSC: Horizontal Slow Clinorotation

HSP: Heat Shock Protein

ISS: International Space Station

JA: Jasmonic acid

KEGG: Kyoto Encyclopedia of Genes and Genomes

LED: light-emitting diode

LHCB: light-harvesting chlorophyll a/b-binding

MELFI: Minus Eighty Degree Laboratory Freezer

MTSB: Microtubule Stabilization Buffer

NAC: ATAF1/2 CUC2 (cup-shaped cotyledon)

N-USOC: Norwegian User Support and Operations Center

OM66: Outer Mitochondrial membrane protein of 66 kDa

PBS: Phosphate-buffered saline

PCA: Principal Component Analysis

PCD: Programmed Cell Death

RLD: RCC1-like domain protein

RPM: Random Positioning Machine

ROS: Reactive Oxygen Species

RT: Room Temperature

SA: Salicylic acid

SG: Seedling Growth

SIB1: Sigma factor binding protein

Sig1R: sigma-1 receptor

TF: Transcription Factor

TOAST: Test of Arabidopsis Space Transcriptome

UNOOSA: United Nations Office for Outer Space Affairs

ZGIP: Zero-Gravity Instrument Project

REFERENCES

REFERENCES

Aarrouf J, Darbelley N, Demandre C, Razafindramboa N, Perbal G (1999) Effect of horizontal clinorotation on the root system development and on lipid breakdown in rapeseed (*Brassica napus*) seedlings. Plant Cell Physiol, 40, 396–405. https://doi.org/10.1093/oxfordjournals.pcp.a029555

Abas L, Benjamins R, Malenica N, Paciorek T, Wišniewska J, Moulinier–Anzola JC, Sieberer T, Friml J, Luschnig C (2006) Intracellular trafficking and proteolysis of the *Arabidopsis* auxin-efflux facilitator PIN2 are involved in root gravitropism. Nat Cell Biol, 8, 249–256. https://doi.org/10.1038/ncb1369

Adamakis IDS, Eleftheriou EP (2019) Structural evidence of programmed cell death induction by tungsten in root tip cells of *Pisum sativum*. Plants, 8. https://doi.org/10.3390/plants8030062

Adamchuk NI (1998) Ultrastructural and functional changes of photosynthetic apparatus of *Arabidopsis thaliana* (L.) Heynh induced by clinorotation. Adv Sp Res, 177, 1131–1134. https://doi.org/10.1016/S0273-1177(97)00201-9

Afgan E, Baker D, Beek M Van Den, Bouvier D, Chilton J, Clements D, Coraor N, Guerler A, Hillman-jackson J, Hiltemann S, Jalili V, Rasche H, Soranzo N, Goecks J, Taylor J, Nekrutenko A, Blankenberg D (2018) The Galaxy platform for accessible , reproducible and collaborative biomedical analyses : 2018 update. 46, 537–544. https://doi.org/10.1093/nar/gky379

van Aken O, de Clercq I, Ivanova A, Law SR, van Breusegem F, Millar AH, Whelan J (2016) Mitochondrial and chloroplast stress responses are modulated in distinct touch and chemical inhibition phases. Plant Physiol, 171, 2150–2165. https://doi.org/10.1104/pp.16.00273

Van Aken O, Zhang B, Law S, Narsai R, Whelan J (2013) *At*WRKY40 and *At*WRKY63 modulate the expression of stress-responsive nuclear genes encoding mitochondrial and chloroplast proteins. Plant Physiol, 162, 254–271. https://doi.org/10.1104/pp.113.215996

Aleshcheva G, Bauer J, Hemmersbach R, Slumstrup L, Wehland M, Infanger M, Grimm D (2016) Scaffold-free Tissue Formation Under Real and Simulated Microgravity Conditions. Basic Clin Pharmacol Toxicol, 119, 26–33. https://doi.org/10.1111/bcpt.12561

Anders S, Huber W (2010) Differential expression analysis for sequence count data. Genome Biol, 11, R106. https://doi.org/10.1186/gb-2010-11-10-r106

Angelos E, Ko DK, Zemelis-Durfee S, Brandizzi F (2021) Relevance of the Unfolded Protein Response to Spaceflight-Induced Transcriptional Reprogramming in *Arabidopsis*. Astrobiology, 21, 367–380. https://doi.org/10.1089/ast.2020.2313

Babbick M, Dijkstra C, Larkin OJ, Anthony P, Davey MR, Power JB, Lowe KC, Cogoli-Greuter M, Hampp R (2007) Expression of transcription factors after short-term exposure of *Arabidopsis thaliana* cell cultures to hypergravity and simulated microgravity (2-D/3-D clinorotation, magnetic levitation). Adv Sp Res, 39, 1182–1189. https://doi.org/10.1016/j.asr.2007.01.001

Ban Y, Kobayashi Y, Hara T, Hamada T, Hashimoto T, Takeda S, Hattori T (2013) A-Tubulin is rapidly phosphorylated in response to hyperosmotic stress in rice and *Arabidopsis*. Plant Cell Physiol, 54, 848–858. https://doi.org/10.1093/pcp/pct065

Bardou P, Mariette J, Escudié F, Djemiel C, Klopp C (2014) Jvenn: An interactive Venn diagram viewer. BMC Bioinformatics, 15, 1–7. https://doi.org/10.1186/1471-2105-15-293

Barjaktarović Ž, Nordheim A, Lamkemeyer T, Fladerer C, Madlung J, Hampp R (2007) Time-course of changes in amounts of specific proteins upon exposure to hyper-g, 2-D clinorotation, and 3-D random positioning of *Arabidopsis* cell cultures. J Exp Bot, 58, 4357–4363. https://doi.org/10.1093/jxb/erm302

Barker R, Lombardino J, Rasmussen K, Gilroy S (2020) Test of *Arabidopsis* Space Transcriptome: A

Discovery Environment to Explore Multiple Plant Biology Spaceflight Experiments. Front Plant Sci, 11, 1–20. https://doi.org/10.3389/fpls.2020.00147

Baserga R, Baserga R (2007) Is cell size important? Cell Cycle, 6, 814–816. https://doi.org/10.4161/cc.6.7.4049

Basu P, Kruse CPS, Luesse DR, Wyatt SE (2017) Growth in spaceflight hardware results in alterations to the transcriptome and proteome. Life Sci Sp Res, 15, 88–96. https://doi.org/10.1016/j.lssr.2017.09.001

Baum SF, Rost TL (1996) Root apical oragnization in *Arabidopsis thaliana*. Protoplasma, 192, 178–188. https://doi.org/10.1007/BF01273890

Blancaflor EB, Fasano JM, Gilroy S (1998) Mapping the functional roles of cap cells in the response of *Arabidopsis* primary roots to gravity. Plant Physiol, 116, 213–222. https://doi.org/10.1104/pp.116.1.213

Böhmer M, Schleiff E (2019) Microgravity research in plants. EMBO Rep, 20, 1–6. https://doi.org/10.15252/embr.201948541

Bolger AM, Lohse M, Usadel B (2014) Trimmomatic: A flexible trimmer for Illumina sequence data. Bioinformatics, 30, 2114–2120. https://doi.org/10.1093/bioinformatics/btu170

Boucheron-Dubuisson E, Manzano AI, Le Disquet I, Matia I, Saez-Vasquez J, van Loon JJWA, Herranz R, Carnero-Diaz E, Medina FJ (2016) Functional alterations of root meristematic cells of *Arabidopsis thaliana* induced by a simulated microgravity environment. J Plant Physiol, 207, 30–41. https://doi.org/10.1016/j.jplph.2016.09.011

Braam J (2005) In touch: Plant responses to mechanical stimuli. New Phytol, 165, 373–389. https://doi.org/10.1111/j.1469-8137.2004.01263.x

Briegleb W (1992) Some qualitative and quantitative aspects of the fast-rotating clinostat as a research tool. ASGSB Bull Publ Am Soc Gravitational Sp Biol, 5, 23–30

Briggs W, Christie JM (2002) Phototropins 1 and 2 : versatile plant blue-light receptors. Trends Plant Sci, 7, 201–210. https://doi.org/10.1016/S1360-1385(02)02245-8

Brinckmann E (2005) ESA hardware for plant research on the International Space Station. Adv Sp Res, 36, 1162–1166. https://doi.org/10.1016/j.asr.2005.02.019

Brown BA, Jenkins GI (2008) UV-B signaling pathways with different fluence-rate response profiles are distinguished in mature *Arabidopsis* leaf tissue by requirement for UVR8, HY5, and HYH. Plant Physiol, 146, 576–588. https://doi.org/10.1104/pp.107.108456

Brunoud G, Wells DM, Oliva M, Larrieu A, Mirabet V, Burrow AH, Beeckman T, Kepinski S, Traas J, Bennett MJ, Vernoux T (2012) A novel sensor to map auxin response and distribution at high spatio-temporal resolution. Nature, 482, 103–6. https://doi.org/10.1038/nature10791

Califar B, Sng NJ, Zupanska A, Paul A, Ferl RJ, Medina FJ, Paul A (2020) Root Skewing-Associated Genes Impact the Spaceflight Response of *Arabidopsis thaliana*. Front Plant Sci, 11, 1–25. https://doi.org/10.3389/fpls.2020.00239

Canamero RC, Bakrim N, Garay A, Dudkin EE, Habricot Y, Ahmad M (2006) Cryptochrome photoreceptors cry1 and cry2 antagonistically regulate primary root elongation in *Arabidopsis thaliana*. Planta, 224, 995–1003. https://doi.org/10.1007/s00425-006-0280-6

Cashmore AR, Jarillo JA, Wu YJ, Liu D (1999) Cryptochromes: Blue light receptors for plants and animals. Science (80-), 284, 760–765. https://doi.org/10.1126/science.284.5415.760

Chen B, Zhang A, Lu Q, Kuang T, Lu C, Wen X (2013) Characterization of photosystem i in rice (*Oryza sativa L.*) seedlings upon exposure to random positioning machine. Photosynth Res, 116, 93–105. https://doi.org/10.1007/s11120-013-9908-0

Cheong BE, Golovchuk OB, Gorka M, Wing W, Ho H, Seidel FM, Augusto A, Firmino P, Skirycz A (2021) *Arabidopsis* REI - LIKE proteins activate ribosome biogenesis during cold acclimation. Sci Rep, 11, 1–25. https://doi.org/10.1038/s41598-021-81610-z

Choi W-G, Barker RJ, Kim S-H, Swanson SJ, Gilroy S (2019) Variation in the transcriptome of different ecotypes of *Arabidopsis thaliana* reveals signatures of oxidative stress in plant responses to spaceflight. Am J Bot, 106, 123–136. https://doi.org/10.1002/ajb2.1223

Cogoli M (1992) The fast rotating clinostat: a history of its use in gravitational biology and a comparison of ground-based and flight experiment results. ASGSB Bull Publ Am Soc Gravitational Sp Biol, 5, 59–67

Colla G, Rouphael Y, Cardarelli M, Mazzucato A, Olimpieri I (2007) Growth, yield and reproduction of dwarf tomato grown under simulated microgravity conditions. Plant Biosyst, 141, 75–81. https://doi.org/10.1080/11263500601153735

Correll MJ, Kiss JZ (2005) The roles of phytochromes in elongation and gravitropism of roots. Plant Cell Physiol, 46, 317–323. https://doi.org/10.1093/pcp/pci038

Correll MJ, Pyle TP, Millar KDL, Sun Y, Yao J, Edelmann RE, Kiss JZ (2013) Transcriptome analyses of *Arabidopsis thaliana* seedlings grown in space: implications for gravity-responsive genes. Planta, 238, 519–533. https://doi.org/10.1007/s00425-013-1909-x

D'Ario M, Sablowski R (2019) Cell Size Control in Plants. Annu Rev Genet, 53, 45–65. https://doi.org/10.1146/annurev-genet-112618-043602

Dedolph RR, Dipert MH (1971) The Physical Basis of Gravity Stimulus Nullification by Clinostat Rotation. Plant Physiol, 47, 756–764. https://doi.org/10.1104/pp.47.6.756

Deng C, Wang T, Wu J, Xu W, Li H, Liu M, Wu L, Lu J, Bian P (2017) Effect of modeled microgravity on radiation-induced adaptive response of root growth in *Arabidopsis thaliana*. Mutat Res - Fundam Mol Mech Mutagen, 796, 20–28. https://doi.org/10.1016/j.mrfmmm.2017.02.002

Dobin A, Davis CA, Schlesinger F, Drenkow J, Zaleski C, Jha S, Batut P, Chaisson M, Gingeras TR (2013) STAR: Ultrafast universal RNA-seq aligner. Bioinformatics, 29, 15–21. https://doi.org/10.1093/bioinformatics/bts635

Driss-Ecole D, Legué V, Carnero-Diaz E, Perbal G (2008) Gravisensitivity and automorphogenesis of lentil seedling roots grown on board the International Space Station. Physiol Plant, 134, 191–201. https://doi.org/10.1111/j.1399-3054.2008.01121.x

NUCLEOLIN: Similar and Antagonistic Roles in *Arabidopsis thaliana* (2019, s.l.). 2019. Ed. Durut N, Abou-Ellail M, Comella P, Jobet E, de Bures A, Saez-Vasquez J. s.l., 150 p.

Durut N, Abou-Ellail M, Pontvianne F, Das S, Kojima H, Ukai S, de Bures A, Comella P, Nidelet S, Rialle S, Merret R, Echeverria M, Bouvet P, Nakamura K, Saez-Vasquez J (2014) A Duplicated NUCLEOLIN Gene with Antagonistic Activity Is Required for Chromatin Organization of Silent 45S rDNA in *Arabidopsis*. Plant Cell, 26, 1330–1344. https://doi.org/10.1105/tpc.114.123893

Eichler GS, Huang S, Ingber DE (2003) Gene Expression Dynamics Inspector (GEDI): For integrative analysis of expression profiles. Bioinformatics, 19, 2321–2322. https://doi.org/10.1093/bioinformatics/btg307

Eleftheriou EP, Adamakis IDS, Panteris E, Fatsiou M (2015) Chromium-induced ultrastructural changes

and oxidative stress in roots of *Arabidopsis thaliana*. Int J Mol Sci, 16, 15852–15871. https://doi.org/10.3390/ijms160715852

Fankhauser C, Staiger D (2002) Photoreceptors in *Arabidopsis thaliana*: light perception , signal transduction and entrainment of the endogenous clock. Planta, 216, 1–16. https://doi.org/10.1007/s00425-002-0831-4

Ferl RJ, Koh J, Denison F, Paul A-L (2014) Spaceflight Induces Specific Alterations in the Proteomes of *Arabidopsis*. Astrobiology, 15, 32–56. https://doi.org/10.1089/ast.2014.1210

Ferl RJ, Koh J, Denison F, Paul A (2015) Spaceflight Induces Specific Alterations in the Proteomes of *Arabidopsis.* Astrobiology, 1,2 1. 15, 32–56. https://doi.org/10.1089/ast.2014.1210

Ferl RJ, Paul A-L (2016) The effect of spaceflight on the gravity-sensing auxin gradient of roots: GFP reporter gene microscopy on orbit. NPJ Microgravity, 2, 15–23. https://doi.org/10.1038/npjmgrav.2015.23

Friml J, Wiśniewska J, Benková E, Mendgen K, Palme K (2002) Lateral relocation of auxin efflux regulator PIN3 mediates tropism in *Arabidopsis*. Nature, 415, 806–809. https://doi.org/10.1038/415806a

Fu Y, Li L, Xie B, Dong C, Wang M, Jia B, Shao L, Dong Y, Deng S, Liu H, Liu G, Liu B, Hu D, Liu H (2016) How to establish a bioregenerative life support system for long-term crewed missions to the moon or mars. Astrobiology, 16, 925–936. https://doi.org/10.1089/ast.2016.1477

Furutani M, Hirano Y, Nishimura T, Nakamura M, Fukao Y, Hakoshima T, Morita MT (2020) Polar recruitment of RLD by LAZY1-like protein during gravity signaling in root branch angle control. Nat Commun, 11. https://doi.org/10.1038/s41467-019-13729-7

Galen C, Rabenold JJ, Liscum E, Galen C (2006) Functional ecology of a blue light photoreceptor : effects of phototropin-1 on root growth enhance drought tolerance in *Arabidopsis thaliana*. New Phytol, 173, 91–99

Ge SX, Jung D, Jung D, Yao R (2020) ShinyGO: A graphical gene-set enrichment tool for animals and plants. Bioinformatics, 36, 2628–2629. https://doi.org/10.1093/bioinformatics/btz931

Ge SX, Son EW, Yao R (2018) iDEP: An integrated web application for differential expression and pathway analysis of RNA-Seq data. BMC Bioinformatics, 19, 1–24. https://doi.org/10.1186/s12859-018-2486-6

Ginisty H, Sicard H, Roger B, Bouvet P (1999) Structure and functions of nucleolin. J Cell Sci, 112, 761–772. https://doi.org/10.1093/emboj/17.5.1476

González-Camacho F, Medina FJ (2006) The nucleolar structure and the activity of NopA100, a nucleolin-like protein, during the cell cycle in proliferating plant cells. Histochem Cell Biol, 125, 139–153. https://doi.org/10.1007/s00418-005-0081-1

Grabov A, Ashley MK, Rigas S, Hatzopoulos P, Dolan L, Vicente-Agullo F (2005) Morphometric analysis of root shape. New Phytol, 165, 641–651. https://doi.org/10.1111/j.1469-8137.2004.01258.x

Guerrero F, De la Torre C, García-Herdugo G (1989) Control of nucleolar growth during interphase in higher plant meristem cells. Protoplasma, 152, 96–100. https://doi.org/10.1007/BF01323067

Hensel W, Sievers A (1980) Effects of prolonged omnilateral gravistimulation on the ultrastructure of statocytes and on the graviresponse of roots. Planta, 150, 338–346. https://doi.org/10.1007/BF00384664

Herranz R, Anken R, Boonstra J, Braun M, Christianen PCM, De Geest M, Hauslage J, Hilbig R, Hill RJA,

Lebert M, Javier Medina F, Vagt N, Ullrich O, Van Loon JJWA, Hemmersbach R (2013) Ground-based facilities for simulation of microgravity: Organism-specific recommendations for their use, and recommended terminology. Astrobiology, 13, 1–17. https://doi.org/10.1089/ast.2012.0876

Herranz R, Benguría A, Laván DA, López-Vidriero I, Gasset G, Javier Medina F, van Loon JJWA, Marco R (2010) Spaceflight-related suboptimal conditions can accentuate the altered gravity response of *Drosophila* transcriptome. Mol Ecol, 19, 4255–4264. https://doi.org/10.1111/j.1365-294X.2010.04795.x

Herranz R, Vandenbrink JP, Villacampa A, Manzano A, Poehlman WL, Feltus FA, Kiss JZ, Medina FJ (2019) RNAseq analysis of the response of *Arabidopsis thaliana* to fractional gravity under blue-light stimulation during spaceflight. Front Plant Sci, 10, 1–11. https://doi.org/10.3389/fpls.2019.01529

Hong JH, Chu H, Zhang C, Ghosh D, Gong X, Xu J (2015) A quantitative analysis of stem cell homeostasis in the *Arabidopsis* columella root cap. Front Plant Sci, 6, 206. https://doi.org/10.3389/fpls.2015.00206

Hoson T, Kamisaka S, Masuda Y, Yamashita M (1992) Changes in plant growth processes under microgravity conditions simulatedby a three-dimensional clinostat. Bot Mag, 105, 53–70

Hoson T, Kamisaka S, Masuda Y, Yamashita M, Buchen B (1997) Evaluation of the three-dimensional clinostat as a simulator of weightlessness. Planta, 203, 187–197. https://doi.org/10.1007/pl00008108

Huang KC, Lin WC, Cheng WH (2018) Salt hypersensitive mutant 9, a nucleolar APUM23 protein, is essential for salt sensitivity in association with the ABA signaling pathway in *Arabidopsis*. BMC Plant Biol, 18, 1–21. https://doi.org/10.1186/s12870-018-1255-z

Jiao S, Hilaire E, Paulsen AQ, Guikema JA (2004) *Brassica rapa* plants adapted to microgravity with reduced photosystem I and its photochemical activity. Physiol Plant, 2004, 281–290. https://doi.org/10.1111/j.1399-3054.2004.00400.x

John SP, Hasenstein KH (2011) Effects of mechanostimulation on gravitropism and signal persistence in flax roots. Plant Signal Behav, 6, 1365–1370. https://doi.org/10.4161/psb.6.9.16601

Johnson CM, Subramanian A, Pattathil S, Correll MJ, Kiss JZ (2017) Comparative transcriptomics indicate changes in cell wall organization and stress response in seedlings during spaceflight. Am J Bot, 104, 1219–1231. https://doi.org/10.3732/ajb.1700079

Joo JH, Bae YS, Lee JS (2001) Role of Auxin-Induced Reactive Oxygen Species in root gravitropism. Plant Physiol, 126, 1055–1060

Jordan EG (1984) Nucleolar nomenclature. J Cell Sci, 67, 217–220

Kamal KY, Herranz R, van Loon JJWA, Medina FJ (2019a) Cell cycle acceleration and changes in essential nuclear functions induced by simulated microgravity in a synchronized *Arabidopsis* cell culture. Plant Cell Environ, 42, 480–494. https://doi.org/10.1111/pce.13422

Kamal KY, Herranz R, Loon JJWA Van, Medina FJ (2018) Simulated microgravity, Mars gravity, and 2g hypergravity affect cell cycle regulation, ribosome biogenesis, and epigenetics in *Arabidopsis* cell cultures. Sci Rep, 8, 1–16. https://doi.org/10.1038/s41598-018-24942-7

Kamal KY, van Loon JJWA, Medina FJ, Herranz R (2019b) Differential transcriptional profile through cell cycle progression in *Arabidopsis* cultures under simulated microgravity. Genomics, 111, 1956–1965. https://doi.org/10.1016/j.ygeno.2019.01.007

Kanehisa M, Sato Y (2020) KEGG Mapper for inferring cellular functions from protein sequences. no.August 2019, 28–35. https://doi.org/10.1002/pro.3711

Karoliussen I, Brinckmann E, Kittang A (2013) Will Plants Grow on Moon or Mars? Curr Biotechnol, 2,

235–243. https://doi.org/10.2174/2211550111302999019

Khodadad CLM, Hummerick ME, Spencer LE, Dixit AR, Richards JT, Romeyn MW, Smith TM, Wheeler RM, Massa GD, Gioia F Di (2020) Microbiological and Nutritional Analysis of Lettuce Crops Grown on the International Space Station. Front Plant Sci, 11, 1–15. https://doi.org/10.3389/fpls.2020.00199

Kim D, Langmead B, Salzberg SL (2015) HISAT: A fast spliced aligner with low memory requirements. Nat Methods, 12, 357–360. https://doi.org/10.1038/nmeth.3317

Kimura T, Haga K, Shimizu-Mitao Y, Takebayashi Y, Kasahara H, Hayashi KI, Kakimoto T, Sakai T (2018) Asymmetric Auxin Distribution is Not Required to Establish Root Phototropism in *Arabidopsis*. Plant Cell Physiol, 59, 823–835. https://doi.org/10.1093/pcp/pcy018

Kiss JZ (2007) Where's the water? Hydrotropism in plants. Proc Natl Acad Sci U S A, 104, 4247–4248. https://doi.org/10.1073/pnas.0700846104

Kiss JZ (2014) Plant biology in reduced gravity on the Moon and Mars. Plant Biol, 16, 12–17. https://doi.org/10.1111/plb.12031

Kiss JZ, Hertel R, Sack FD (1989) Amyloplasts are necessary for full gravitropic sensitivity in roots of *Arabidopsis thaliana*. Planta, 177, 198–206. https://doi.org/10.1007/BF00392808

Kiss JZ, Kumar P, Bowman RN, Steele MK, Eodice MT, Correll MJ, Edelmann RE (2007) Biocompatibility studies in preparation for a spaceflight experiment on plant tropisms (TROPI). Adv Sp Res, 39, 1154–1160. https://doi.org/10.1016/j.asr.2006.12.017

Kiss JZ, Millar KDL, Edelmann RE (2012) Phototropism of *Arabidopsis thaliana* in microgravity and fractional gravity on the International Space Station. Planta, 236, 635–645. https://doi.org/10.1007/s00425-012-1633-y

Kiss JZ, Mullen JL, Correll MJ, Hangarter RP (2003) Phytochromes A and B mediate red-light-induced positive phototropism in roots. Plant Physiol, 131, 1411–1417. https://doi.org/10.1104/pp.013847

Kiss JZ, Wolverton C, Wyatt SE, Hasenstein KH, van Loon JJWA (2019) Comparison of Microgravity Analogs to Spaceflight in Studies of Plant Growth and Development. Front Plant Sci, 10, 1–10. https://doi.org/10.3389/fpls.2019.01577

Kleine-Vehn J, Ding Z, Jones AR, Tasaka M, Morita MT, Friml J (2010) Gravity-induced PIN transcytosis for polarization of auxin fluxes in gravity-sensing root cells. Proc Natl Acad Sci U S A, 107, 22344–22349. https://doi.org/10.1073/pnas.1013145107

Knight (1806) On the direction of the radicle and germen during the vegetation of seeds. Philos Trans R Soc London, 96, 99–108. https://doi.org/10.1098/rstl.1806.0006

Kojima A, Yárnoz DG, Pippo S Di (2018) Access to space: A new approach by the united nations office for outer space affairs. Acta Astronautica, 152, 201–207. https://doi.org/10.1016/j.actaastro.2018.07.041

Kozeko L, Kordyum E (2006) The stress protein level under clinorotation in context of the seedling developmental program and the stress response. Microgravity Sci Technol, 18, 254–256. https://doi.org/10.1007/BF02870422

Kraft TFB, Van Loon JJWA, Kiss JZ (2000) Plastid position in *Arabidopsis* columella cells is similar in microgravity and on a random-positioning machine. Planta, 211, 415–422. https://doi.org/10.1007/s004250000302

Krieger G, Shkolnik D, Miller G, Fromm H (2016) Reactive oxygen species tune root tropic responses. Plant Physiol, 172, pp.00660.2016. https://doi.org/10.1104/pp.16.00660

Krueger F (2015) Trim galore. A wrapper tool around Cutadapt FastQC to consistently apply Qual Adapt trimming to FastQ files, 516, 517

Kruse CPS, Meyers AD, Basu P, Hutchinson S, Luesse DR, Wyatt SE (2020) Spaceflight induces novel regulatory responses in *Arabidopsis* seedling as revealed by combined proteomic and transcriptomic analyses. BMC Plant Biol, 20, 1–16. https://doi.org/10.1186/s12870-020-02392-6

Kutschera U, Briggs WR (2012) Root phototropism: From dogma to the mechanism of blue light perception. Planta, 235, 443–452. https://doi.org/10.1007/s00425-012-1597-y

Kuznetsov OA, Hasenstein KH (1996) Intracellular magnetophoresis of amyloplasts and induction of root curvature. Planta, 198, 87–94. https://doi.org/10.1007/BF00197590

Kwon T, Alan Sparks J, Nakashima J, Allen SN, Tang Y, Blancaflor EB (2015) Transcriptional response of arabidopsis seedlings during spaceflight reveals peroxidase and cell wall remodeling genes associated with root hair development. Am J Bot, 102, 21–35. https://doi.org/10.3732/ajb.1400458

Laurinavichius R, A. Yaroshyus A, Marchyukaytis D, Shvyaghdene, Mashinskiy A (1986) Metabolism of pea plants grown under space flight conditions. USSR Sp Life Scence Dig, 4, 23–25

Lee D, Polisensky DH, Braam J (2005) Genome-wide identification of touch- and darkness-regulated *Arabidopsis* genes: A focus on calmodulin-like and XTH genes. New Phytol, 165, 429–444. https://doi.org/10.1111/j.1469-8137.2004.01238.x

Lee HJ, Kim HS, Park JM, Cho HS, Jeon JH (2020) PIN-mediated polar auxin transport facilitates root−obstacle avoidance. New Phytol, 225, 1285–1296. https://doi.org/10.1111/nph.16076

Legué V, Biancaflor E, Wymer C, Perbal G, Fantin D, Gilroy S (1997) Cytoplasmic free Ca^{2+} in *Arabidopsis* roots changes in response to touch but not gravity. Plant Physiol, 114, 789–800. https://doi.org/10.1104/pp.114.3.789

Leister D, Wang L, Kleine T (2017) Organellar gene expression and acclimation of plants to environmental stress. Front Plant Sci, 8. https://doi.org/10.3389/fpls.2017.00387

Leitz G, Kang BH, Schoenwaelder MEA (2009) Statolith sedimentation kinetics and force transduction to the cortical endoplasmic reticulum in gravity-sensing *Arabidopsis* columella cells. Plant Cell, 21, 843–860. https://doi.org/10.1105/tpc.108.065052

Liao Y, Smyth GK, Shi W (2014) FeatureCounts: An efficient general purpose program for assigning sequence reads to genomic features. Bioinformatics, 30, 923–930. https://doi.org/10.1093/bioinformatics/btt656

Limbach C, Hauslage J, Schäfer C, Braun M (2005) How to activate a plant gravireceptor. Early mechanisms of gravity sensing studied in characean rhizoids during parabolic flights. Plant Physiol, 139, 1030–1040. https://doi.org/10.1104/pp.105.068106

Lin KH, Huang MY, Huang WD, Hsu MH, Yang ZW, Yang CM (2013) The effects of red, blue, and white light-emitting diodes on the growth, development, and edible quality of hydroponically grown lettuce (*Lactuca sativa L. var. capitata*). Sci Hortic (Amsterdam), 150, 86–91. https://doi.org/10.1016/j.scienta.2012.10.002

Liscum E, Askinosie SK, Leuchtman DL, Morrow J, Willenburg KT, Coats DR (2014) Phototropism: Growing towards an understanding of plant movement. Plant Cell, 26, 38–55. https://doi.org/10.1105/tpc.113.119727

van Loon JJWA (2007) Some history and use of the random positioning machine, RPM, in gravity related research. Adv Sp Res, 39, 1161–1165. https://doi.org/10.1016/j.asr.2007.02.016

Lopez-Juez E, Dillon E, Magyar Z, Khan S, Hazeldine S, de Jager SM, Murray JAH, Beemster GTS, Bogre L, Shanahan H (2008) Distinct Light-Initiated Gene Expression and Cell Cycle Programs in the Shoot Apex and Cotyledons of Arabidopsis. Plant Cell Online, 20, 947–968. https://doi.org/10.1105/tpc.107.057075

Lorenzi G, Perbal G (1990) Root growth and statocyte polarity in lentil seedling roots grown in microgravity or on a slowly rotating clinostat. Physiol Plant, 78, 532–537. https://doi.org/10.1111/j.1399-3054.1990.tb05238.x

Luschnig C, Gaxiola RA, Grisafi P, Fink GR (1998) EIR1, a root-specific protein involved in auxin transport, is required for gravitropism in *Arabidopsis thaliana*. Genes Dev, 12, 2175–2187. https://doi.org/10.1101/gad.12.14.2175

Lyon CJ (1970) Choice of rotation rate for the horizontal clinostat. Plant Physiol, 46, 355–358. https://doi.org/10.1104/pp.46.3.355

Madrigal P, Gabel A, Villacampa A, Manzano A, Deane CS, Bezdan D, Carnero-Diaz E, Medina FJ, Hardiman G, Grosse I, Szewczyk N, Weging S, Giacomello S, Harridge SDR, Morris-Paterson T, Cahill T, da Silveira WA, Herranz R (2020) Revamping Space-omics in Europe. Cell Syst, Nov. 2020. https://doi.org/10.1016/j.cels.2020.10.006

Maere S, Heymans K, Kuiper M (2005) BiNGO: A Cytoscape plugin to assess overrepresentation of Gene Ontology categories in Biological Networks. Bioinformatics, 21, 3448–3449. https://doi.org/10.1093/bioinformatics/bti551

Manzano A, Creus E, Tomás A, Valbuena MA, Villacampa A, Ciska M, Edelmann RE, Kiss JZ, Medina FJ, Herranz R (2020a) The FixBox: Hardware to provide on-orbit fixation capabilities to the EMCS on the ISS. Microgravity Sci Technol, 32, 1105–1120. https://doi.org/10.1007/s12217-020-09837-5

Manzano A, Herranz R, Den Toom LA, Te Slaa S, Borst G, Visser M, Medina FJ, van Loon JJWA (2018) Novel, Moon and Mars, partial gravity simulation paradigms and their effects on the balance between cell growth and cell proliferation during early plant development. npj Microgravity, 4, 1–11. https://doi.org/10.1038/s41526-018-0041-4

Manzano A, Villacampa A, Sáez-Vásquez J, Kiss JZ, Medina FJ, Herranz R (2020b) The importance of Earth reference controls in spaceflight –omics research: Characterization of nucleolin mutants from the Seedling Growth experiments. iScience, 2020, 101686. https://doi.org/10.1016/j.isci.2020.101686

Manzano AI, Larkin OJ, Dijkstra CE, Anthony P, Davey MR, Eaves L, Hill RJA, Herranz R, Medina FJ (2013) Meristematic cell proliferation and ribosome biogenesis are decoupled in diamagnetically levitated *Arabidopsis* seedlings. BMC Plant Biol, 13, 124. https://doi.org/10.1186/1471-2229-13-124

Manzano AI, van Loon JJWA, Christianen PCM, Gonzalez-Rubio JM, Medina FJ, Herranz R (2012) Gravitational and magnetic field variations synergize to cause subtle variations in the global transcriptional state of *Arabidopsis* in vitro callus cultures. BMC Genomics, 13, 105. https://doi.org/10.1186/1471-2164-13-105

Manzano C, Pallero-baena M, Casimiro I, Rybel B De, Orman-ligeza B, Isterdael G Van, Beeckman T, Draye X, Casero P, Pozo JC (2014) The Emerging Role of Reactive Oxygen Species Signaling during Lateral Root Development. Plant Physiol, 165, 1105–1119. https://doi.org/10.1104/pp.114.238873

Mao K, Jiang L, Bo W, Xu F, Wu R (2014) Cloning of the Cryptochrome-Encoding PeCRY1 Gene from Populus euphratica and Functional Analysis in *Arabidopsis*. PLoS One, 9, 1–23. https://doi.org/10.1371/journal.pone.0115201

Massa GD, Dufour NF, Carver JA, Hummerick ME, Wheeler RM, Morrow RC, Smith TM (2017) VEG-01: Veggie hardware validation testing on the international space station. Open Agric, 2, 33–41.

https://doi.org/10.1515/opag-2017-0003

Massa GD, Gilroy S (2003) Touch modulates gravity sensing to regulate the growth of primary roots of *Arabidopsis thaliana*. Plant J, 33, 435–445. https://doi.org/10.1046/j.1365-313x.2003.01637.x

Massa GD, Wheeler RM, Morrow RC, Levine HG (2016) Growth chambers on the International Space Station for large plants. Acta Hortic, 1134, 215–222. https://doi.org/10.17660/ActaHortic.2016.1134.29

Matía I, González-Camacho F, Herranz R, Kiss JZ, Gasset G, van Loon JJWA, Marco R, Medina FJ (2010) Plant cell proliferation and growth are altered by microgravity conditions in spaceflight. J Plant Physiol, 167, 184–193. https://doi.org/10.1016/j.jplph.2009.08.012

Matía I, González-Camacho F, Marco R, Kiss JZ, Gasset G, Medina FJ (2005) Nucleolar structure and proliferation activity of Arabidopsis root cells from seedlings germinated on the International Space Station. Adv Sp Res, 36, 1244–1253. https://doi.org/10.1016/j.asr.2005.01.068

Medina FJ (2021) Space explorers need to be space farmers. Metod sience Stud J, 11, 55–62

Meng X, Li L, Narsai R, De Clercq I, Whelan J, Berkowitz O (2020) Mitochondrial signalling is critical for acclimation and adaptation to flooding in *Arabidopsis thaliana*. Plant J, 103, 227–247. https://doi.org/10.1111/tpj.14724

Menges M, Murray JAH (2002) Synchronous *Arabidopsis* suspension cultures for analysis of cell-cycle gene activity. Plant J, 30, 203–212. https://doi.org/10.1046/j.1365-313X.2002.01274.x

Mi H, Muruganujan A, Huang X, Ebert D, Mills C, Guo X, Thomas PD (2019) Protocol Update for large-scale genome and gene function analysis with the PANTHER classification system (v.14.0). Nat Protoc, 14, 703–721. https://doi.org/10.1038/s41596-019-0128-8

Micco V De, Arena C, Pignalosa D, Durante M (2011) Effects of sparsely and densely ionizing radiation on plants. Acta Astronaut, 50, 1–19. https://doi.org/10.1007/s00411-010-0343-8

Migliaccio F, Piconese S (2001) Spiralizations and tropisms in *Arabidopsis* roots. Trends Plant Sci, 6, 561–565. https://doi.org/10.1016/S1360-1385(01)02152-5

Mikhaylenko NF, Sytnik SK, Zolotareva EK (2001) Effects of slow clinorotation on lipid contents and proton permeability of thylakoid membranes of pea chloroplasts. Adv Sp Res, 27, 1007–1010. https://doi.org/10.1016/S0273-1177(01)00193-4

Millar KDL, Kumar P, Correll MJ, Mullen JL, Hangarter RP, Edelmann RE, Kiss JZ (2010) A novel phototropic response to red light is revealed in microgravity. New Phytol, 186, 648–656. https://doi.org/10.1111/j.1469-8137.2010.03211.x

Mizukami Y (2001) A matter of size: developmental control of organ size in plants. Curr Opin Plant Biol, 4, 533–539. https://doi.org/10.1016/s1369-5266(00)00212-0

Mo M, Yokawa K, Wan Y, Baluška F (2015) How and why do root apices sense light under the soil surface? Front Plant Sci, 6, 1–8. https://doi.org/10.3389/fpls.2015.00775

Mohammed B, Farahi Bilooei S, Doczi R, Grove E, Railo S, Palme K, Ditengou FA, Bögre L, Lopez-Juez E (2018) Converging Light , Energy and Hormonal Signaling Control Meristem Activity, Leaf Initiation, and Growth. Plant Physiol, 176, 1365–1381. https://doi.org/10.1104/pp.17.01730

Moni A, Lee A-Y, Briggs WR, Han I-S (2015) The blue light receptor Phototropin 1 suppresses lateral root growth by controlling cell elongation. Plant Biol (Stuttg), 17, 34–40. https://doi.org/10.1111/plb.12187

Monje O, Richards JT, Carver JA, Dimapilis DI, Levine HG, Dufour NF, Onate BG, Graham T, Medina FJ (2020) Hardware Validation of the Advanced Plant Habitat on ISS: Canopy Photosynthesis in Reduced Gravity. Front Plant Sci, 11, 1–15. https://doi.org/10.3389/fpls.2020.00673

Monshausen GB, Miller ND, Murphy AS, Gilroy S, Lafayette W (2011) Dynamics of auxin-dependent Ca^{2+} and pH signaling in root growth revealed by integrating high-resolution imaging with automated computer vision-based analysis. Plant J, 65, 309–318. https://doi.org/10.1111/j.1365-313X.2010.04423.x

Montojo J, Zuberi K, Rodriguez H, Kazi F, Wright G, Donaldson SL, Morris Q, Bader GD (2010) GeneMANIA cytoscape plugin: Fast gene function predictions on the desktop. Bioinformatics, 26, 2927–2928. https://doi.org/10.1093/bioinformatics/btq562

Morita MT (2010) Directional gravity sensing in gravitropism. Annu Rev Plant Biol, 61, 705–20. https://doi.org/10.1146/annurev.arplant.043008.092042

Morohashi K, Okamoto M, Yamazaki C, Fujii N, Miyazawa Y, Kamada M, Kasahara H, Osada I, Shimazu T, Fusejima Y, Higashibata A, Yamazaki T, Ishioka N, Kobayashi A, Takahashi H (2017) Gravitropism interferes with hydrotropism via counteracting auxin dynamics in cucumber roots: clinorotation and spaceflight experiments. 2017. https://doi.org/10.1111/nph.14689

Musielak TJ, Schenkel L, Kolb M, Henschen A, Bayer M (2015) A simple and versatile cell wall staining protocol to study plant reproduction. Plant Reprod, 28, 161–169. https://doi.org/10.1007/s00497-015-0267-1

Muthert LWF, Izzo LG, van Zanten M, Aronne G (2020) Root tropisms: Investigations on Earth and in space to unravel plant growth direction. Front Plant Sci, 10, 1–22. https://doi.org/10.3389/fpls.2019.01807

Nakamura M, Nishimura T, Morita MT (2019) Bridging the gap between amyloplasts and directional auxin transport in plant gravitropism. Curr Opin Plant Biol, 52, 54–60. https://doi.org/10.1016/j.pbi.2019.07.005

Okada K, Shimura Y (1990) Reversible root tip rotation in *Arabidopsis* seedlings induced by obstacle-touching stimulus. Science (80-), 250, 274–276. https://doi.org/10.1126/science.250.4978.274

Oliva M, Dunand C (2007) Waving and skewing: how gravity and the surface of growth media affect root development in *Arabidopsis*. New Phytol, 176, 37–43. https://doi.org/10.1111/j.1469-8137.2007.02184.x

Olsen GM, Mirza JI, Maher EP, Iversen T -H (1984) Ultrastructure and movements of cell organelles in the root cap of agravitropic mutants and normal seedlings of *Arabidopsis thaliana*. Physiol Plant, 60, 523–531. https://doi.org/10.1111/j.1399-3054.1984.tb04921.x

Ottenschläger I, Wolff P, Wolverton C, Bhalerao RP, Sandberg G, Ishikawa H, Evans M, Palme K (2003) Gravity-regulated differential auxin transport from columella to lateral root cap cells. Proc Natl Acad Sci U S A, 100, 2987–2991. https://doi.org/10.1073/pnas.0437936100

Passaia G, Queval G, Bai J, Margis-pinheiro M, Foyer CH (2014) The effects of redox controls mediated by glutathione peroxidases on root architecture in *Arabidopsis thaliana*. J Exp Bot, 65, 1403–1413. https://doi.org/10.1093/jxb/ert486

Pasternak T, Tietz O, Rapp K, Begheldo M, Nitschke R, Ruperti B, Palme K (2015) Protocol: An improved and universal procedure for whole-mount immunolocalization in plants. Plant Methods, 11, 1–10. https://doi.org/10.1186/s13007-015-0094-2

Paul AL, Daugherty CJ, Bihn EA, Chapman DK, Norwood KLL, Ferl RJ (2001) Transgene expression

patterns indicate that spaceflight affects stress signal perception and transduction in *Arabidopsis*. Plant Physiol, 126, 613–621. https://doi.org/10.1104/pp.126.2.613

Paul AL, Sng NJ, Zupanska AK, Krishnamurthy A, Schultz ER, Ferl RJ (2017) Genetic dissection of the *Arabidopsis* spaceflight transcriptome: Are some responses dispensable for the physiological adaptation of plants to spaceflight? PLoS One, 12, 1–24. https://doi.org/10.1371/journal.pone.0180186

Phukan UJ, Jeena GS, Shukla RK (2016) WRKY transcription factors: Molecular regulation and stress responses in plants. Front Plant Sci, 7, 1–14. https://doi.org/10.3389/fpls.2016.00760

Pletser V (2016) European aircraft parabolic flights for microgravity research, applications and exploration: A review. REACH, 1, 11–19. https://doi.org/10.1016/j.reach.2016.05.002

Polinski E, Schueler O, Krause L, Wimmer MA, Hemmersbach R, Goldbach HE (2017) 2-D clinorotation alters the uptake of some nutrients in *Arabidopsis thaliana*. J Plant Physiol, 212, 54–57. https://doi.org/10.1016/j.jplph.2017.01.011

Pontvianne F, Abou-Ellail M, Douet J, Comella P, Matia I, Chandrasekhara C, DeBures A, Blevins T, Cooke R, Medina FJ, Tourmente S, Pikaard CS, Sáez-Vásquez J (2010) Nucleolin is required for DNA methylation state and the expression of rRNA gene variants in *Arabidopsis thaliana*. PLoS Genet, 6, 1–13. https://doi.org/10.1371/journal.pgen.1001225

Pontvianne F, Matía I, Douet J, Tourmente S, Medina FJ, Echevarria M, Sáez-Vásquez J (2007) Characterization of *At*NUC-L1 Reveals a Central Role of Nucelolin in Nucelolus Organization and Silencing of *At*NUC-L2 Gene in *Arabidopsis*. Mol Biol Cell, 18, 369–379. https://doi.org/10.1091/mbc.E06

Quail PH (2002) Phytochrome photosensory siganlling networks. Mol Cell Biol, 3, 85–93. https://doi.org/10.1038/nrm728

Rashotte AM, Brady SR, Reed RC, Ante SJ, Muday GK (2000) Basipetal auxin transport is required for gravitropism in roots of *Arabidopsis*. Plant Physiol, 122, 481–490. https://doi.org/10.1104/pp.104.900172

Ray S, Gebre S, Fogle H, Berrios DC, Tran PB, Galazka JM, Costes S V. (2019) GeneLab: Omics database for spaceflight experiments. Bioinformatics, 35, 1753–1759. https://doi.org/10.1093/bioinformatics/bty884

Reichler SA, Balk J, Brown ME, Woodruff K, Clark GB, Roux SJ (2001) Light differentially regulates cell division and the MRNA abundance of pea nucleolin during de-etiolation. Plant Physiol, 125, 339–350. https://doi.org/10.1104/pp.125.1.339

Risueño MC, Medina FJ (1986) The nucleolar structure in plant cells. Cell Biol Rev, 7, 1–154

Rizzini L, Favory JJ, Cloix C, Faggionato D, O'Hara A, Kaiserli E, Baumeister R, Schäfer E, Nagy F, Jenkins GI, Ulm R (2011) Perception of UV-B by the *Arabidopsis* UVR8 protein. Science (80-), 332, 103–106. https://doi.org/10.1126/science.1200660

Robert HS, Grunewald W, Sauer M, Cannoot B, Soriano M, Swarup R, Weijers D, Bennett M, Boutilier K, Friml J (2015) Plant embryogenesis requires aux/lax-mediated auxin influx. Dev, 142, 702–711. https://doi.org/10.1242/dev.115832

Roger B, Moisand A, Amalric F, Bouvet P (2003) Nucleolin provides a link between RNA polymerase I transcription and pre-ribosome assembly. Chromosoma, 111, 399–407. https://doi.org/10.1007/s00412-002-0221-5

Rumyantseva V, Mashinsky, Merzlyak A, Nechitailo G (1990) The effect of space-flight factors on the

pigment and lipid-composition of wheat plants. Kosm Biol Aviakosm Med, 23, 53–55

Ruppel NJ, Hangarter RP, Kiss JZ (2001) Red-light-induced positive phototropism in *Arabidopsis* roots. Planta, 212, 424–430

Sablowski R, Dornelas MC (2014) Interplay between cell growth and cell cycle in plants. J Exp Bot, 65, 2703–2714. https://doi.org/10.1093/jxb/ert354

Sack FD (1991) Plant gravity sensing. Int Rev Cytol, 127, 193–252. https://doi.org/10.1016/S0074-7696(08)60695-6

Sack FD, Suyemoto M. M, Leopold A. C (1986) Amyloplast sedimentation and organelle saltation in living corn columella cells. Am J Bot, 73, 1692–1698. https://doi.org/10.1002/j.1537-2197.1986.tb09700.x

Sáez-Vásquez J, Medina FJ (2008) The Plant Nucleolus. Adv Bot Res, 47, 1–46. https://doi.org/10.1016/S0065-2296(08)00001-3

Sato EM, Hijazi H, Bennett MJ, Vissenberg K, Swarup R (2015) New insights into root gravitropic signalling. J Exp Bot, 66, 2155–2165. https://doi.org/10.1093/jxb/eru515

Schluttenhofer C, Pattanaik S, Patra B, Yuan L (2014) Analyses of *Catharanthus roseus* and *Arabidopsis thaliana* WRKY transcription factors reveal involvement in jasmonate signaling. BMC Genomics, 15, 1–20

Schmidt W (2010) Gravity induced absorption changes in phycomyces blakesleanus and coleoptiles of zea mays as measured on the drop tower in Bremen (FRG). Microgravity Sci Technol, 22, 79–85. https://doi.org/10.1007/s12217-009-9113-0

Schüler O, Krause L, Görög M, Hauslage J, Kesseler L, Böhmer M, Hemmersbach R (2016) ARADISH - Development of a standardized plant growth chamber for experiments in gravitational biology using ground based facilities. Microgravity Sci Technol, 28, 297–305. https://doi.org/10.1007/s12217-015-9454-9

Schultz ER, Zupanska AK, Sng NJ, Paul A, Ferl RJ (2017) Skewing in *Arabidopsis* roots involves disparate environmental signaling pathways. BMC Plant Biol, 17, 1–16. https://doi.org/10.1186/s12870-017-0975-9

Shen-Miller J, Hinchman R, Gordon SA (1968) Thresholds for georesponse to acceleration in gravity-compensated avena seedlings. Plant Physiol, 43, 338–344. https://doi.org/10.1104/pp.43.3.338

Shen H, Liu C, Zhang Y, Meng X, Zhou X, Chu C, Wang X (2012) *Os*WRKY30 is activated by MAP kinases to confer drought tolerance in rice. Plant Mol Biol, 80, 241–253. https://doi.org/10.1007/s11103-012-9941-y

Silva-Navas J, Moreno-Risueno MA, Manzano C, Pallero-Baena M, Navarro-Neila S, T??llez-Robledo B, Garcia-Mina JM, Baigorri R, Gallego FJ, Del Pozo JC (2015) D-Root: A system for cultivating plants with the roots in darkness or under different light conditions. Plant J, 84, 244–255. https://doi.org/10.1111/tpj.12998

Silva-Navas J, Moreno-Risueno MA, Manzano C, Téllez-Robledo B, Navarro-Neila S, Carrasco V, Pollmann S, Gallego FJ, Del Pozo JC (2016) Flavonols mediate root phototropism and growth through regulation of proliferation-to-differentiation transition. Plant Cell, 28, 1372–1387. https://doi.org/10.1105/tpc.15.00857

Silveira WA, Fazelinia H, Rosenthal SB, Mason CE, Costes S V (2020) Comprehensive multi-omics analysis reveals mitochondrial stress as a central biological hub for spaceflight impact. Cell, 183, 1185-1201.e20. https://doi.org/10.1016/j.cell.2020.11.002

Simmons C, Migliaccio F, Masson P, Caspar T, Söll D (1995) A novel root gravitropism mutant of *Arabidopsis thaliana* exhibiting altered auxin physiology. Physiol Plant, 93, 790–798. https://doi.org/10.1111/j.1399-3054.1995.tb05133.x

Smith JD, Staehelin LA, Todd P (1999) Early root cap development and graviresponse in white clover (*Trifolium repens*) grown in space and on a two-axis clinostat. J Plant Physiol, 155, 543–550. https://doi.org/10.1016/S0176-1617(99)80052-2

Smith JD, Todd P, Andrew Staehelin L (1997) Modulation of statolith mass and grouping in white clover (*Trifolium repens*) grown in 1-g, microgravity and on the clinostat. Plant J, 12, 1361–1373. https://doi.org/10.1046/j.1365-313x.1997.12061361.x

Somers DE, Quail PH (1995a) Phytochrome-Mediated Light Regulation of PHYA- and PHYB-CUS Transgenes in Arabidopsis thaljana Seedlings. Plant Physiol, 107, 523–534

Somers DE, Quail PH (1995b) Temporal and spatial expression patterns of PHYA and PHYB genes in *Arabidopsis*. Plant J, 7, 413–427. https://doi.org/10.1046/j.1365-313X.1995.7030413.x

Staneloni RJ, Rodriguez-Batiller MJ, Casal JJ (2008) Abscisic acid, high-light, and oxidative stress down-regulate a photosynthetic gene via a promoter motif not involved in phytochrome-mediated transcriptional regulation. Mol Plant, 1, 75–83. https://doi.org/10.1093/mp/ssm007

Staves MP, Wayne R, Leopold AC (1992) Hydrostatic pressure mimics gravitational pressure in characean cells. 1992, 141–152

Stutte GW, Monje O, Hatfield RD, Paul AL, Ferl RJ, Simone CG (2006) Microgravity effects on leaf morphology, cell structure, carbon metabolism and mRNA expression of dwarf wheat. Planta, 224, 1038–1049. https://doi.org/10.1007/s00425-006-0290-4

Sugimoto M, Oono Y, Gusev O, Matsumoto T, Yazawa T, Levinskikh MA, Sychev VN, Bingham GE, Wheeler R, Hummerick M (2014) Genome-wide expression analysis of reactive oxygen species gene network in *Mizuna* plants grown in long-term spaceflight. BMC Plant Biol, 14, 1–11. https://doi.org/10.1186/1471-2229-14-4

Sullivan JA, Deng XW (2003) From seed to seed: The role of photoreceptors in *Arabidopsis* development. Dev Biol, 260, 289–297. https://doi.org/10.1016/S0012-1606(03)00212-4

Swarup R, Bennett MJ (2018) Root Gravitropism. Annu Plant Rev online, Apr. 2018, 157–174. https://doi.org/doi:10.1002/9781119312994.apr0401

Swarup R, Kramer EM, Perry P, Knox K, Leyser HMO, Haseloff J, Beemster GTS, Bhalerao R, Bennett MJ (2005) Root gravitropism requires lateral root cap and epidermal cells for transport and response to a mobile auxin signal. Nat Cell Biol, 7, 1057–1065. https://doi.org/10.1038/ncb1316

Szklarczyk D, Gable AL, Lyon D, Junge A, Wyder S, Huerta-Cepas J, Simonovic M, Doncheva NT, Morris JH, Bork P, Jensen LJ, Von Mering C (2019) STRING v11: Protein-protein association networks with increased coverage, supporting functional discovery in genome-wide experimental datasets. Nucleic Acids Res, 47, D607–D613. https://doi.org/10.1093/nar/gky1131

Takahashi H, Mizuno H, Kamada M, Fujii N, Higashitani A, Kamigaichi S, Aizawa S, Mukai C, Shimazu T, Fukui K, Yamashita M (1999) A spaceflight experiment for the study of gravimorphogenesis and hydrotropism in cucumber seedlings. J Plant Res, 112, 497–505. https://doi.org/10.1007/pl00013906

Taniguchi M, Furutani M, Nishimura T, Nakamura M, Fushita T, Iijima K, Baba K, Tanaka H, Toyota M, Tasaka M, Morita MT (2017) The *Arabidopsis* LAZY1 family plays a key role in gravity signaling within statocytes and in branch angle control of roots and shoots. Plant Cell, 29, 1984–1999. https://doi.org/10.1105/tpc.16.00575

Thompson M V., Holbrook NM (2004) Root-gel interactions and the root waving behavior of *Arabidopsis*. Plant Physiol, 135, 1822–1837. https://doi.org/10.1104/pp.104.040881

Toyota M, Ikeda N, Sawai-Toyota S, Kato T, Gilroy S, Tasaka M, Morita MT (2013) Amyloplast displacement is necessary for gravisensing in *Arabidopsis* shoots as revealed by a centrifuge microscope. Plant J, 76, 648–660. https://doi.org/10.1111/tpj.12324

Tsukagoshi H, Busch W, Benfey PN (2010) Transcriptional Regulation of ROS Controls Transition from Proliferation to Differentiation in the Root. Cell, 143, 606–616. https://doi.org/10.1016/j.cell.2010.10.020

Ulmasov T, Murfett J, Hagen G, Guilfoyle TJ (1997) Aux/IAA proteins repress expression of reporter genes containing natural and highly active synthetic auxin response elements. Plant Cell, 9, 1963–1971. https://doi.org/10.1105/tpc.9.11.1963

Unseld M, Marienfeld JR, Brandt P, Brennicke A (1997) The mitochondrial genome of *Arabidopsis thaliana* contains 57 genes in 366,924 nucleotides. Nat Genet, 15, 1–5

Valbuena MA, Manzano A, Vandenbrink JP, Pereda-Loth V, Carnero-Diaz E, Edelmann RE, Kiss JZ, Herranz R, Medina FJ (2018) The combined effects of real or simulated microgravity and red-light photoactivation on plant root meristematic cells. Planta, 248, 691–704. https://doi.org/10.1007/s00425-018-2930-x

Vandenbrink JP, Herranz R, Medina FJ, Edelmann RE, Kiss JZ (2016) A novel blue-light phototropic response is revealed in roots of *Arabidopsis thaliana* in microgravity. Planta, 244, 1201–1215. https://doi.org/10.1007/s00425-016-2581-8

Vandenbrink JP, Herranz R, Poehlman WL, Alex Feltus F, Villacampa A, Ciska M, Medina FJ, Kiss JZ (2019) RNA-seq analyses of *Arabidopsis thaliana* seedlings after exposure to blue-light phototropic stimuli in microgravity. Am J Bot, 106, 1466–1476. https://doi.org/10.1002/ajb2.1384

Vandenbrink JP, Kiss JZ (2016) Space, the final frontier: A critical review of recent experiments performed in microgravity. Plant Sci, 243, 115–119. https://doi.org/10.1016/j.plantsci.2015.11.004

Vandenbrink JP, Kiss JZ (2019) Preparation of a spaceflight experiment to study tropisms in *Arabidopsis* seedlings on the International Space Station. Methods Mol Biol, 1924, 207–214. https://doi.org/10.1007/978-1-4939-9015-3_17

Vanlerberghe GC (2013) Alternative oxidase: A mitochondrial respiratory pathway to maintain metabolic and signaling homeostasis during abiotic and biotic stress in plants. Int J Mol Sci, 14, 6805–6847. https://doi.org/10.3390/ijms14046805

Villacampa A, Ciska M, Manzano A, Vandenbrink JP, Kiss JZ, Herranz R, Medina FJ (2021a) From Spaceflight to Mars g -Levels: Adaptive response of *A. thaliana* seedlings in a reduced gravity environment is enhanced by red-light photostimulation. Int J Mol Sci, 22, 899. https://doi.org/10.3390/ijms22020899

Villacampa A, Sora L, Herranz R, Medina FJ, Ciska M (2021b) Analysis of graviresponse and biological effects of vertical and horizontal clinorotation in *Arabidopsis thaliana* root tip. Plants, 10, 1–20. https://doi.org/10.3390/plants10040734

Villacampa A, Sora L, Javier Medina F, Ciska M (2018) Optimal clinorotation settings for microgravity simulation in *A. thaliana* seedlings. Proc Int Astronaut Congr IAC, 2018

Wang H, Li X, Krause L, Görög M, Schüler O, Hauslage J, Hemmersbach R, Kircher S, Lasok H, Haser T, Rapp K, Schmidt J, Yu X, Pasternak T, Aubry-Hivet D, Tietz O, Dovzhenko A, Palme K, Ditengou FA (2016) 2-D Clinostat for simulated microgravity experiments with *Arabidopsis* seedlings. Microgravity Sci

Technol, 28, 59–66. https://doi.org/10.1007/s12217-015-9478-1

Warnke E, Kopp S, Wehland M, Hemmersbach R, Bauer J, Pietsch J, Infanger M, Grimm D (2016) Thyroid Cells Exposed to Simulated Microgravity Conditions – Comparison of the Fast Rotating Clinostat and the Random Positioning Machine. Microgravity Sci Technol, 28, 247–260. https://doi.org/10.1007/s12217-015-9456-7

Wayne R, Staves MP, Leopold AC (1990) Gravity-dependent polarity of cytoplasmic streaming in *Nitellopsis*. Protoplasma, 155, 43–57. https://doi.org/10.1007/BF01322614

Wicke S, Schneeweiss GM, dePamphilis CW, Müller KF, Quandt D (2011) The evolution of the plastid chromosome in land plants: Gene content, gene order, gene function. Plant Mol Biol, 76, 273–297. https://doi.org/10.1007/s11103-011-9762-4

Xie G, Zhang Y, Yang J, Yu D, Ren M (2021) Adaptation to real 1 / 6 g moon gravity contributes to plant development and expeditious acclimation to super-freezing. Res Sq, 2021

Xu J, Scheres B (2005) Dissection of *Arabidopsis* ADP-RIBOSYLATION FACTOR 1 Function in Epidermal Cell Polarity. 17, 525–536. https://doi.org/10.1105/tpc.104.028449.1

Xu Y, Liu R, Yan L, Liu Z, Jiang S, Shen Y (2012) Light-harvesting chlorophyll a / b -binding proteins are required for stomatal response to abscisic acid in *Arabidopsis*. J Exp Bot, 63, 1095–1106. https://doi.org/10.1093/jxb/err315

Yamburenko M V., Zubo YO, Vanková R, Kusnetsov V V., Kulaeva ON, Börner T (2013) Abscisic acid represses the transcription of chloroplast genes. J Exp Bot, 64, 4491–4502. https://doi.org/10.1093/jxb/ert258

Yokawa K, Fasano R, Kagenishi T, Baluška F (2014) Light as stress factor to plant roots – case of root halotropism. Front Plant Sci, 5, 1–9. https://doi.org/10.3389/fpls.2014.00718

Yoshihara T, Spalding EP (2017) LAZY genes mediate the effects of gravity on auxin gradients and plant architecture. Plant Physiol, 175, 959–969. https://doi.org/10.1104/pp.17.00942

Zabel P, Bamsey M, Schubert D, Tajmar M (2016) Review and analysis of over 40 years of space plant growth systems. Life Sci Sp Res, 10, 1–16. https://doi.org/10.1016/j.lssr.2016.06.004

Zhang J, Vanneste S, Brewer PB, Michniewicz M, Grones P, Kleine-Vehn J, Löfke C, Teichmann T, Bielach A, Cannoot B, Hoyerová K, Chen X, Xue HW, Benková E, Zažímalová E, Friml J (2011) Inositol trisphosphate-induced ca2+ signaling modulates auxin transport and pin polarity. Dev Cell, 20, 855–866. https://doi.org/10.1016/j.devcel.2011.05.013

Zhang KX, Xu HH, Yuan TT, Zhang L, Lu YT (2013) Blue-light-induced PIN3 polarization for root negative phototropic response in *Arabidopsis*. Plant J, 76, 308–321. https://doi.org/10.1111/tpj.12298

Zhang S, Li C, Wang R, Chen Y, Shu S, Huang R, Zhang D, Li J, Xiao S, Yao N, Yang C (2017) The *Arabidopsis* Mitochondrial Protease FtSH4 Is Involved in Leaf Senescence via Regulation of WRKY-Dependent Salicylic Acid Accumulation and Signaling. Plant Physiol, 173, 2294–2307. https://doi.org/10.1104/pp.16.00008

Zhang Y, Wang L, Xie J, Zheng H (2015) Differential protein expression profiling of *Arabidopsis thaliana* callus under microgravity on board the Chinese SZ-8 spacecraft. Planta, 241, 475–488. https://doi.org/10.1007/s00425-014-2196-x

Zhang Y, Xiao G, Wang X, Zhang X, Friml J (2019) Evolution of fast root gravitropism in seed plants. Nat Commun, 10, 4–13. https://doi.org/10.1038/s41467-019-11471-8

Zhou Y, Zhou B, Pache L, Chang M, Khodabakhshi AH, Tanaseichuk O, Benner C, Chanda SK (2019)

Metascape provides a biologist-oriented resource for the analysis of systems-level datasets. Nat Commun, 10. https://doi.org/10.1038/s41467-019-09234-6

Zupanska AK, Denison FC, Ferl RJ, Paul AL (2013) Spaceflight engages heat shock protein and other molecular chaperone genes in tissue culture cells of *Arabidopsis thaliana*. Am J Bot, 100, 235–248. https://doi.org/10.3732/ajb.1200343